Dissertation
submitted to the
Combined Faculties for the Natural Sciences and for Mathematics
of the Ruperto-Carola University of Heidelberg, Germany
for the degree of
Doctor of Natural Sciences

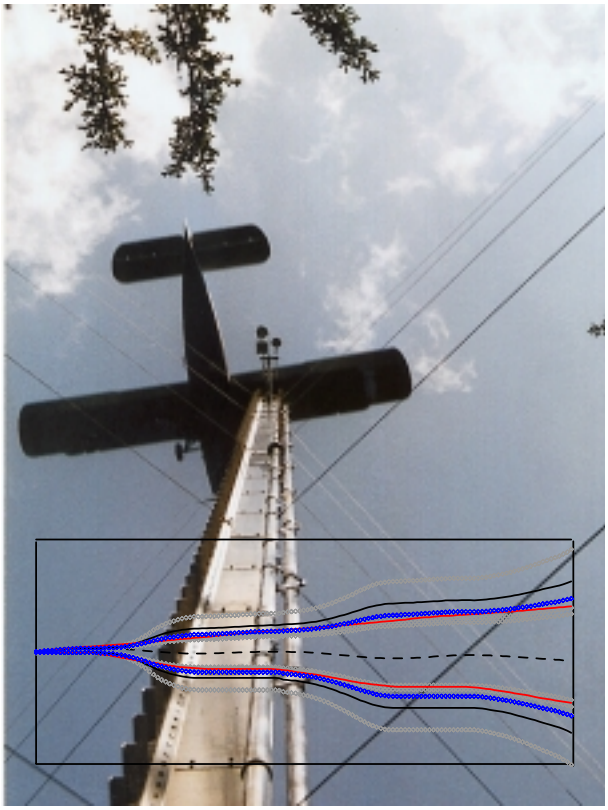

presented by

Diplom-Physicist:	Uwe Langendörfer
born in:	Karlsruhe

Oral examination: 18th July, 2001

Oxygen isotopes as a tracer of biospheric CO_2 gross fluxes - a local feasibility study -

Referees: Priv.-Doz. Dr. Ingeborg Levin
Prof. Dr. Konrad Mauersberger

Abstract

Oxygen isotopes as a tracer of biospheric CO_2 gross fluxes - a local feasibility study -

Quantitative knowledge of gross biospheric CO_2 fluxes is crucial in atmospheric carbon cycle budgeting, especially in view of unknown biospheric feedback mechanisms to an increasing atmospheric CO_2 mixing ratio or to temperature changes. The $^{18}O/^{16}O$ ratio of CO_2 has the potential to separate respiration and assimilation fluxes because of their characteristic isotopic signatures derived from equilibration with respective water reservoirs (i.e. soil and leaf water). The associated processes were investigated here on a local scale during three intensive measurement campaigns in a natural boreal forest reserve in Russia. Diurnal cycles of atmospheric CO_2 and its stable isotope ratios, of the $^{18}O/^{16}O$ ratio of atmospheric water vapour, leaf and soil water were measured. The data sets were then quantitatively interpreted in a ^{222}Radon-transport-calibrated 1-D canopy box model. On the basis of observations and plant physiological parameterisations, for the first time, the feasibility to separate gross ecosystem CO_2 fluxes could be demonstrated. Reasonable agreement with classical local scale methods could be achieved, whereby the model results are most sensitive to the parameterisation of leaf internal CO_2 gradients. Concurrent year-round aircraft CO_2 and stable isotope observations showed that the biospheric ecosystem ^{18}O signals are effectively transferred into the free troposphere. Provided that adequate parameterisations on the leaf scale can be achieved, this gives the perspective to successfully use the $^{18}O/^{16}O$ ratio in atmospheric CO_2 within coupled mesoscale or even global biosphere-atmosphere models of the carbon cycle.

Zusammenfassung

Sauerstoffisotope als Indikator für biosphärische CO_2 Bruttoflüsse - eine lokale Machbarkeitsstudie -

Die Bestimmung der biosphärischen Brutto-CO_2-Flüsse ist notwendig zur quantitativen Bilanzierung des atmosphärischen CO_2-Mischungsverhältnisses, insbesondere im Hinblick auf mögliche biosphärische Rückkopplungen auf den globalen atmosphärischen CO_2-Anstieg oder auch Klimaveränderungen. Das $^{18}O/^{16}O$-Verhältnis im atmosphärischen CO_2 erlaubt es potentiell, die Assimilations- und Respirationsflüsse zu separieren, aufgrund ihrer charakteristischen Isotopensignaturen, welche durch Äqulilibrierungsprozesse mit den zugehörigen Wasserreservoiren (Blatt- und Bodenwasser) zustande kommen. Im Rahmen dieser Arbeit wurden diese Prozesse während dreier intensiver Feldkampagnen in einem natürlichen borealen Wald in Rußland untersucht. Es wurden Tagesgänge von CO_2 und seinen stabilen Isotopenverhältnissen, der ^{18}O-Isotopie des Luftwasserdampfs sowie des Blatt- und Bodenwassers gemessen. Die Messungen wurden mit Hilfe eines eindimensionalen, mit ^{222}Radon transportkalibrierten, Ökosystemmodells untersucht. Auf der Basis der Messungen und mit Hilfe von pflanzenphysiologischen Parametern konnte zum ersten Mal gezeigt werden, daß es möglich ist, die CO_2-Ökosystembruttoflüsse zu separieren. Das Modell liefert Ergebnisse, die sich gut mit klassischen lokalen Methoden vergleichen, es zeigt jedoch eine starke Abhängigkeit der Flüsse von der Parameterisierung des blattinternen CO_2-Gradienten. Parallele, quasikontinuierliche Flugzeugmessungen von CO_2 und seinen stabilen Isotopenverhältnissen zeigen darüber hinaus, daß sich die kleinskaligen biosphärischen ^{18}O-Signale in der freien Troposphäre abbilden. Dies eröffnet die Möglichkeit, das $^{18}O/^{16}O$-Verhältnis im CO_2 in gekoppelten mesoskaligen oder sogar globalen Biosphäre-Atmosphäre-Modellen zu nutzen, wenn eine adäquate Parameterisierung auf der Blattebene gefunden werden kann.

Contents

Chapter 1

Introduction

"As early as at the beginning of this century, the great french physicists Fourier and Pouillet had established a theory according to which the atmosphere acts extremely favourably for raising the temperature of the earth's surface. They suggested that the atmosphere functioned like the glass in the frame of a hotbed."..."The main components of the air, oxygen and nitrogen, do not absorb heat to any appreciable extent, however the opposite is true to a high degree for the aqueous vapour and carbonic acid in the air although they are present in very small quantities. And these substances have the peculiarity that to a great extent they absorb the heat radiated by the earth's surface while they have little effect on the incoming heat from the sun.

If now the quantity of carbonic acid in the air is increased, the temperature of the earth's surface increases." [1]

Svante Arrhenius principal predictions on the increase of the earth's surface temperature linked to the simultaneous increase of carbon dioxide (the atmospheric precursor of carbonic acid mentioned by Arrhenius) still hold true after the modern scientific perceptions achieved in the last hundred years. He was the first to quantify the potential temperature changes due to an increasing CO_2 concentration in the atmosphere, which again was explained by a colleague of Arrhenius, Arvid Högbom (1857-1940), to originate from anthropogenic coal burning. While calculating this so called "green house effect" he also recovered a relevant accompanying feedback process, namely the increases of atmospheric water vapour: *"This also causes some increase in the amount of aqueous vapour in the air, resulting in a slight intensification of the effect."* [1] Therefore, he indirectly stated the present day finding that atmospheric interactions and variabilities behave highly non-linearly.

Besides the other major greenhouse gases methane, nitrous oxide and the halocarbons, carbon dioxide provides the largest individual contribution of 1.46 Wm^{-2} (about 60 %) to the overall radiative forcing due to changes from pre-industrial to present day conditions [IPCC, 2001]. Therefore, the understanding of the carbon cycling processes and the predictability of the atmospheric CO_2 concentration development - under prescribed emission scenarios - are framing the potential of political decision making with the intention to stabilize future atmospheric CO_2 concentration.

As Arrhenius and Högbom were formulating their scientific interest with the focus on long time scales, mainly directed towards exploring the extension and effects of the last glaciation, present-day scientific questions are asked within the context of the public, and more and more political "global change" debate:

[1] Excerpts of notes from a lecture "Nature's heat storage" given by Prof. Svante Arrhenius (1859-1927) at Stockholm University on third of February 1896 (printed in Swedish in Nordisk Tidskrift 14(1896), 121-1130).

- How will the atmospheric CO_2 concentration develop due to future anthropogenic CO_2 emissions ?
- What are the key feed back reactions of the oceanic and the terrestrial carbon systems on changes of the climate system ?

1.1 The Global Carbon Budget

The prerequisite to predict the future evolution of the CO_2 concentration in the atmosphere, and therewith the potential global climate impact of future elevated CO_2 in the atmosphere, is understanding of processes that control the actual carbon system. The present quantitative knowledge of the net fluxes between the three major carbon reservoirs, the atmosphere, the oceans and the terrestrial biosphere, is summarized in Table 1.1. Fluxes are given in PgC yr^{-1} [2]. The determination of the annual *net* fluxes is a general (measurement) problem, if

Table 1.1: *Global atmospheric carbon balance based on CO_2 and O_2 budgets [Heimann, 2000] (fluxes in PgC yr^{-1}).*

	1980 to 1989	1990 to 1999
Atmospheric increase	3.3 ± 0.1	3.2 ± 0.1
Emissions(fossil fuel, cement)	5.4 ± 0.3	6.3 ± 0.4
Ocean-atmosphere flux	-2.0 ± 0.6	-1.8 ± 0.6
Land-atmosphere flux*	-0.2 ± 0.7	-1.4 ± 0.7
*Partitioned during 1980 to 1989 as follows (range of uncertainty given in parenthesis):		
Land-use change	1.6 (0.5 to 2.4)	
Residual terrestrial sink	-1.8 (-3.7 to 0.4)	

one bears in mind the numbers of the annual *gross* fluxes between the reservoirs given in Table 1.2. Here small differences, the net fluxes, between large numbers, the gross fluxes, are particularly hard to determine precisely as the net fluxes are about two orders of magnitude smaller than the 'one-way' gross fluxes. The gross fluxes given in Table 1.2 represent mean

Table 1.2: *Gross fluxes (PgC yr^{-1}) between the reservoirs and inventory (PgC) of the reservoirs within the global carbon cycle over the period 1980 to 1989 [Houghton* et al.*, 1996].*

Carbon reservoir	Content (PgC)	Gross flux to atmosphere (PgC yr^{-1})	Gross flux from atmosphere (PgC yr^{-1})
Ocean	39000	90	-92
Land biosphere	2200	60	-61.4
Atmosphere	750	-	-

values, and are itself afflicted with uncertainties in the order of 30 % for the lands biosphere

[2] 1 Pg = 10^{15} g = 1 Gigaton

and of about 15 % for the ocean fluxes. Furthermore, the uncertainties of the fluxes between the reservoirs given in Tables 1.1 and 1.2 illustrate another principal problem of balancing the global carbon cycle: the possible scientific accessibility of each reservoir and flux, respectively. The most precise value of the determined inventories within the global carbon cycle is the change of the atmospheric CO_2 inventory with an uncertainty of about ±4 %. This is due to the fact, that the atmosphere is a relatively well mixed system. Furthermore the atmosphere is accessible easily by measurements, which is done worldwide [Francey *et al.,* 1990; Levin *et al.,* 1995; Nakazawa *et al.,* 1997]. The largest monitoring network is operated by NOAA/CMDL (National Oceanic & Atmospheric Administration / Climate Monitoring & Diagnostics Laboratory) since 1967 with stations shown in Figure 1.1 [Conway *et al.*, 1994]. The first station that started long term observation of CO_2 mixing ratios was initiated in the middle of the Pacific ocean at Mauna Loa, Hawaii, by C.D. Keeling in 1958 [Keeling, 1958].

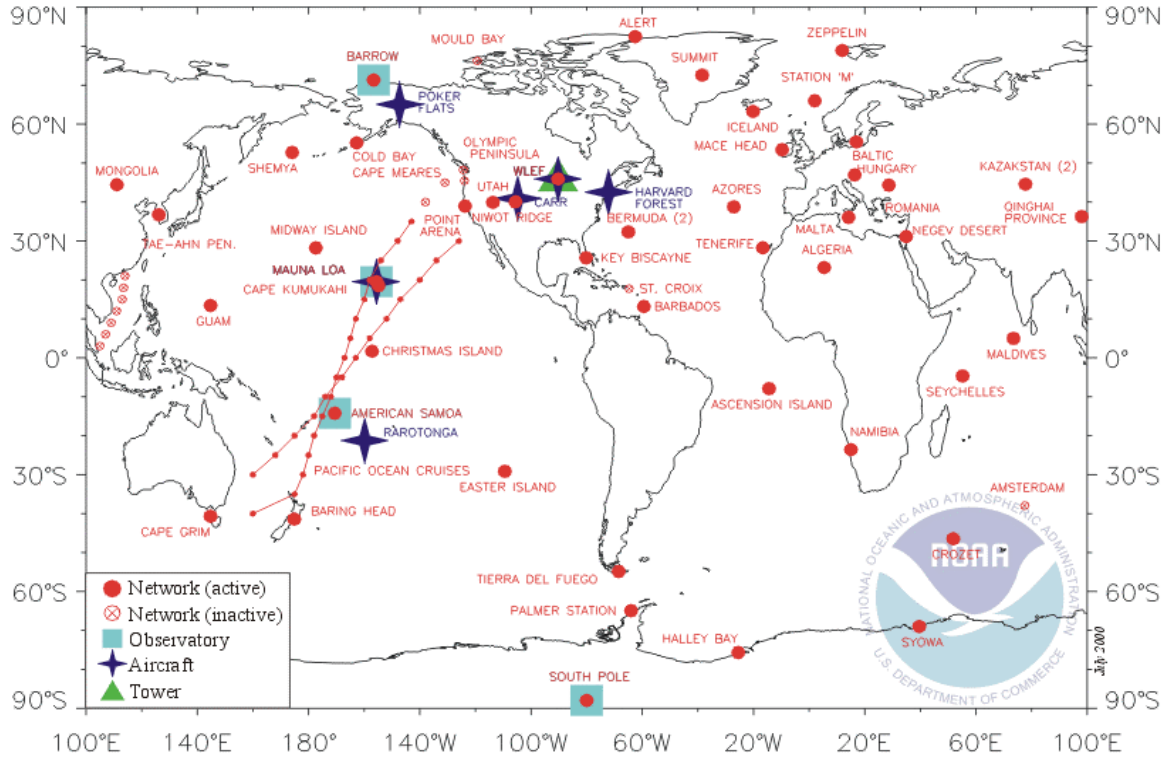

Figure 1.1: *The NOAA/CMDL monitoring station network [Pieter Tans, NOAA, http://www.cmdl.noaa.gov]*

According to Table 1.1 the emission flux of anthropogenic carbon is the second best known value in the budget with an uncertainty of about 7 %. These data are derived from global fossil fuel burning and cement production emission statistics including the information of the spatial distribution of the emissions [Marland and Boden, 1997]. The observed rise in atmospheric CO_2 amounts to only about 50 to 60 % of the anthropogenic emissions, which implies that the residual carbon has to be stored in the oceans and/or the terrestrial biosphere. Whereas the net ocean-atmosphere flux (via uptake of CO_2 through air-sea exchange) can be determined as an atmospheric sink with a circa 30 % accuracy, the land-atmosphere fluxes (via the gross fluxes resulting from photosynthesis as an atmospheric sink and ecosystem respiration as an atmospheric source) net direction from 1980 to 1989 can not even unequivocally be stated.

For the period from 1990 to 1999, however, a significant net sink flux from the atmosphere to the land biosphere could be detected. The principal problem in determining the fluxes between the land biosphere and the atmosphere is twofold: First, the net flux has to be separated into two components as shown in Table 1.1. Changes in land use cause a net source for atmospheric CO_2 due to deforestation, a process that is believed to be counterparted by a residual terrestrial CO_2 sink. The second principal problem is caused by the heterogeneity of the terrestrial biosphere itself. The global biosphere consists of a large number of different ecosystems that may also variably react on climatic conditions. Furthermore, it is well known, that the biospheric exchange does not only act on a daily or seasonal timescale but also on a long term scale, a fact that complicates future predictions. As the net CO_2 emission flux of land use change is determined with an accuracy of only about 50 %, the error of the estimated residual terrestrial sink is about 100 %. For this reason, the accurate quantification of regional biospheric surface fluxes of CO_2 is essential to minimize the lack of information on larger scales by (model) extrapolation up to the global scale.

1.2 Temporal and Spatial Evolution of CO_2 in the Atmosphere

1.2.1 CO_2 Mixing Ratio

Besides the investigation of the actual processes that control the exchange of carbon between the respective pools, the past status of the atmosphere and the global climate yield basic information to explore the global climate system. The inspection of the anthropogenically undisturbed system should provide the natural amplitudes of the relevant climate signals. Therefore, the significance of the recent changes including the anthropogenic influence can largely benefit from the assessment of past variations.

Although the degree and chronology of change observed in climate archives may differ from actual and future variations, they provide an important insight into the system. The most valuable perception is the strong association between CO_2 and temperature changes during glacial-interglacial transitions gained from ice core measurements. Figure 1.2 presents the early results of the Vostok ice core, drilled in Antarctica [Jouzel *et al.*, 1993].

After the recent extension of this ice core back to the past 420,000 years, four glacial-interglacial cycles are covered by this record. The main result of these extensive studies are [Jouzel *et al.,* 1993; Petit *et al.,* 1999]:

- The present-day high atmospheric load of the two major greenhouse gases, CO_2 and CH_4, seems to be unique and has never been observed in the last 420,000 years. CO_2 mixing ratios in the atmosphere varied between 180 to 200 ppm[3] during glacial and 280 to 300 ppm during warm periods. These values are to be compared with recent annual mean atmospheric CO_2 mixing ratios in Antarctica of about 368.2 ppm; $\sim$ 21 % more than the highest values detected in the Vostok core (on the basis of latest data at the Neumayer station, Antarctica, with an annual mean CO_2 mixing ratio of 365.22 ppm [Schmidt *et al.*, 2001], assuming a CO_2 growth rate of about 1.5 ppm per year for 2000 and 2001).

- There is a strong correlation between the changes in temperature[4] and the greenhouse gases; the succession of the changes through the climate periods was similar.

[3] 1 ppm = 1 part per million, mol fraction

[4] The temperature anomalies relative to the present temperature are derived from δD $(H_2O)_{ice}$ variations [Petit *et al.*, 1999].

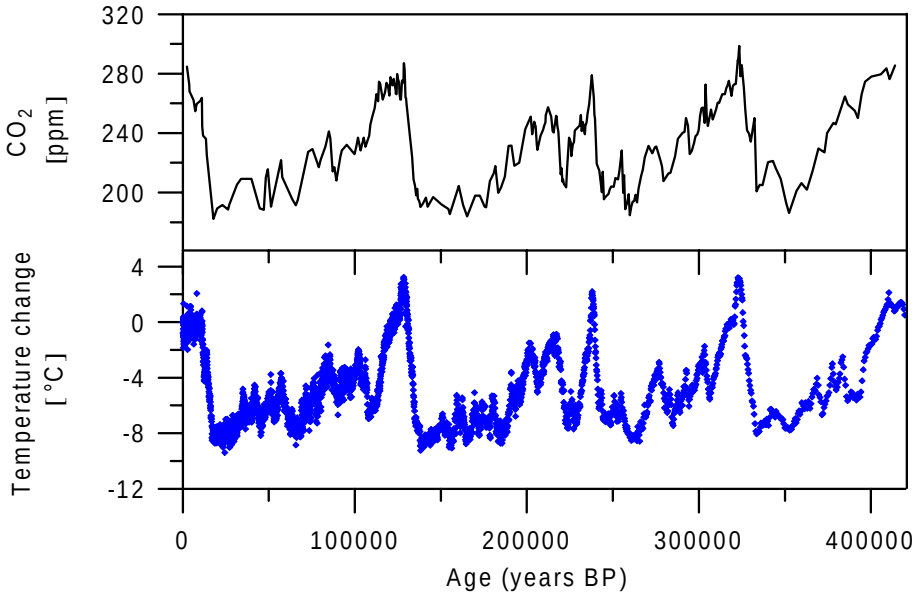

Figure 1.2: *The Vostok (Antarctica) ice core record over the past 420,000 years [Jouzel et al., 1993; Petit et al., 1999]. Top: CO_2 concentration, bottom: temperature anomalies relative to present temperature.*

Still the remaining open question and matter of debate left from these studies is: What are the driving forces of natural climate changes? The Vostok ice core temperature, CO_2 and CH_4 increase more or less in phase during terminations [Petit *et al.*, 1999]. The time, and therefore depth resolution of an ice core is restricted by the ubiquitous uncertainty in gas-age/ice-age differences. Petit *et al.,* [1999] state this uncertainty to be well over $\pm$ 1 kyr. For that reason, they could not detect any significant phase shift between the changes in temperature and the greenhouse gases. Any statements on a potential principle of cause and effect of climate changes are thus still impossible. However, in a recent study, Fischer *et al.,* [1999] investigated parts of the Vostok core and the Taylor Dome core (also Antarctica) around the last three glacial terminations in high time resolution. They found that CO_2 mixing ratios increased by 80 to 100 ppm 600 $\pm$ 400 years *after* the warming of the last three deglaciations. CO_2 concentrations were also observed to stay high for several thousands of years during glaciations. These results are based on an assumed gas-age/ice-age uncertainty of 100 to 1000 years [Fischer *et al.*, 1999]. They could imply that temperature variations are driving the burden of greenhouse gases in the atmosphere due to their effect on the ocean-atmosphere carbon transfer (increasing with temperature), the control of land ice coverage and the build-up of the terrestrial biosphere. But the identification of a time lag between temperature and CO_2 changes smaller than 1000 years of Fischer *et al.,* [1999] takes the present knowledge of ice core signals to a limit and is therefore critizised [Staufer *et al.,* 1993; Petit *et al.,* 1999].

Still the discussion on the uncertainty of gas-age/ice-age and the possible interpretation of ice core records is ongoing and the question of what is the hen and what is the egg in natural climate change remains unanswered. Especially the reaction of the global climate to the anthropogenic emissions of greenhouse gases since the industrialisation can not be evaluated. Therefore, the scientific focus is largely directed towards the interpretation of recent measurements performed worldwide (Figure 1.1).

CO_2 measurements at the Pacific Mauna Loa station since 1958 constitute the longest continuous record of direct atmospheric CO_2 concentrations available in the world. The Mauna Loa site is considered one of the most favorable locations for measuring undisturbed air because possible local influences of vegetation or human activities on atmospheric CO_2 concentrations are minimal and any influences from volcanic events can be excluded from the records. The Mauna Loa record (Figure 1.3) shows a 16.6 % increase in the mean annual mixing ratio, from 315.83 ppm of dry air in 1959 to 368.37 ppm in 1999 [Keeling and Whorf, 2000].

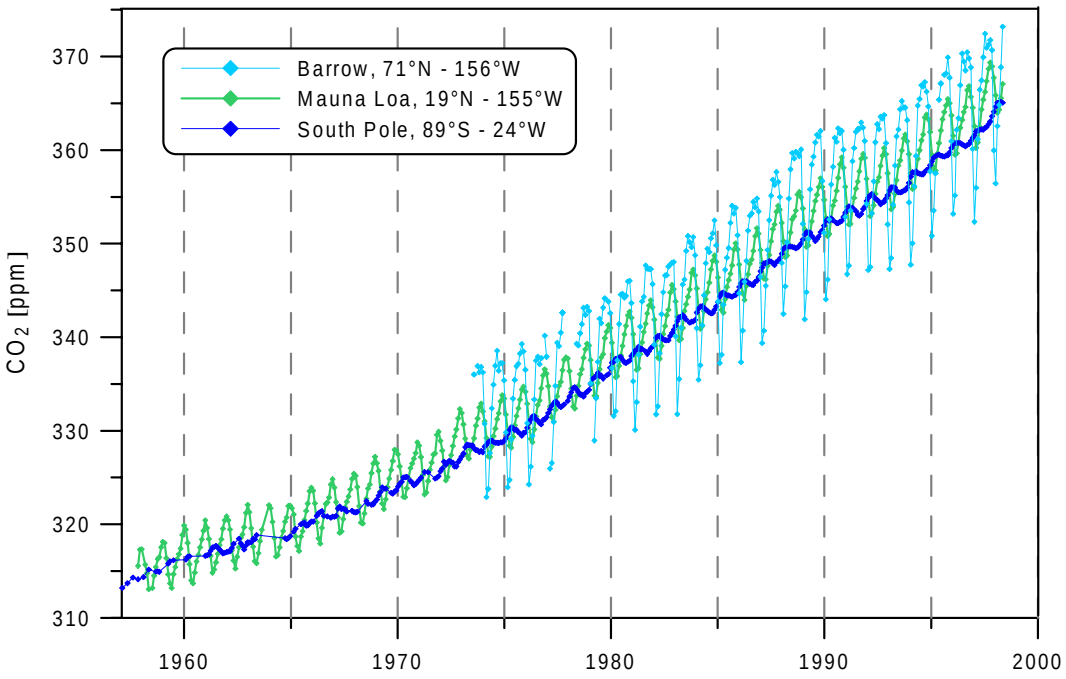

Figure 1.3: *The SIO (Scripps Institution of Oceanography) atmospheric CO_2 records from Barrow (Alaska), Mauna Loa (Hawaii) and the South Pole (Antarctica) [Keeling and Whorf, 2000].*

Detailed analysis of the Mauna Loa record and the comparison with other time series at Barrow and at the South Pole delivers significant temporal and spatial differences of the CO_2 concentration variabilities:

- There is a growing difference in annual mean CO_2 concentration between the Northern and Southern Hemisphere ($[CO_2]_{MaunaLoa}$ - $[CO_2]_{SouthPole}$: changing from ∼0.5 ppm in 1958 to ∼2.5 ppm in 1994). Furthermore, this difference is observed to scale linearly with fossil fuel CO_2 emissions from 1959 to 1992 [Keeling *et al.,* 1989; Heimann, 1999].

- The peak-to-peak amplitudes of the seasonal cycles are increasing northward from about 1 ppm at the South Pole to about 15 ppm in the boreal forest zone of the Northern Hemisphere (55 to 65 °N). This cycle is mainly caused by the seasonal uptake and release of atmospheric CO_2 by the terrestrial biosphere and to a small portion by oceanic processes [Heimann *et al.,* 1989b; Keeling *et al.,* 1995]. The amplitude is observed to increase with time (e.g. from 5.2 ppm from the beginning of the Mauna Loa record in 1958 to 5.8 ppm in the 1980s). As this increase is not well correlated with the CO_2

concentration increase, a more or less significant evidence for CO_2 fertilization of the terrestrial vegetation is discussed by several authors [Enting, 1987; Manning, 1993; Idso and Kimball, 1993; Heimann *et al.,* 1996]. However, the changes in biological activity of the terrestrial biosphere can not necessarily be causally connected to increased photosynthetic storage [Houghton *et al.*, 1996].

- The growth rate of 2.9 ppm yr^{-1} of the Mauna Loa record between 1997-98 represents the largest single yearly jump since the Mauna Loa record began in 1958 [Keeling and Whorf, 2000]. Since 1975 the average increase is 1.5 ppm yr^{-1}, with a minimum of 0.5 ppm yr^{-1} between 1991-92 and maximum growth rates of 2.0 ppm yr^{-1} from 1988-89. Because fossil fuel emissions after 1985 increased quite linearly at a rate of 0.1 to 0.2 PgC yr^{-1} [Boden *et al.*, 1994] the variability of the growth rate must be due to variations in the source/sink behaviour of the terrestrial biosphere and the ocean, respectively.

These findings demonstrate that there must be strong sink/source variabilities currently absorbing/respiring CO_2 at the Earths surface, whereby both, the ocean and the terrestrial biosphere may contribute. As the budgeting of the global carbon cycle with the aid of atmospheric CO_2 concentration observation and ocean global circulation modelling is limited, further CO_2 inert tracers are essential to distinguish between land-atmosphere and ocean-atmosphere fluxes.

1.2.2 $^{13}C/^{12}C$ Isotope Ratio of CO_2

The CO_2 molecule consists of one carbon and two oxygen atoms. The element carbon is found to exist naturally as the stable isotopes ^{12}C and ^{13}C and as a radioactive isotope ^{14}C (half-life: 5730 years). Oxygen is an element that naturally exists as three stable isotopes ^{16}O, ^{17}O and ^{18}O. In the following considerations and the work presented here the focus will be on the processes in which the stable isotope ratios $^{13}C/^{12}C$ and $^{18}O/^{16}O$ are involved.

Isotopic ratios are usually reported in the standard δ-notation:

$$\delta E_{rare} = \left(\frac{R_{sample}}{R_{standard}} - 1 \right) \cdot 1000 \; [‰] \tag{1.1}$$

with e.g.

$$R = \left(\frac{[E_{rare}]}{[E_{main}]} \right)$$

and

R_{sample} : isotopic ratio of the sample
$R_{standard}$: isotopic ratio of the standard
E_{main} : main isotope of the element "E" (e.g. ^{12}C, ^{16}O)
E_{rare} : rare isotope of the element "E" (e.g. ^{13}C, ^{18}O)

The reference standard is Vienna Pee Dee Belimnite (VPDB) (discussed in Allison *et al.,* [1995]), a virtual material related to the original Pee Dee Belimnite (PDB) [Craig, 1957]. The $^{13}C/^{12}C$ ratio of VPDB is taken from the PDB ($^{13}C/^{12}C$ (PDB) = 1.1237 $\times 10^{-2}$). The $^{18}O/^{16}O$ ratio is related to the isotopic ratio of Vienna Standard Mean Ocean Water (VSMOW) and the $\delta^{18}O$ value of VPDB on the SMOW scale ($^{18}O/^{16}O$ (SMOW) = 2.0088 $\times 10^{-3}$, for details see Allison *et al.*, [1995], Gonfiantini *et al.*, [1995] and Neubert [1998]). The reference materials are distributed by the International Atomic Energy Agency (IAEA) in Vienna.

A fractionation associated with a CO_2 flux from a reservoir A to a reservoir B is generally defined with a fractionation factor α as

$$\alpha_{A\rightarrow B} = \frac{R_A}{R_B} \tag{1.2}$$

with e.g.

$$R = \frac{^{13}C}{^{12}C}$$

If α >1, reservoir B is referred to as isotopically depleted with respect to reservoir A, and vice versa if α <1, reservoir B is referred to as isotopically enriched. Furthermore, the fractionation ϵ is defined as

$$\epsilon = (\alpha - 1) \times 1000\ [‰]$$

Generally speaking, the $^{13}C/^{12}C$ isotope ratio in atmospheric CO_2 gets modified during exchange between CO_2 reservoirs. Therefore, the isotope ratio of CO_2 is a potential tracer of the global partitioning between the fluxes of atmospheric CO_2 to the oceans and the land biosphere, respectively. This is due to the fact that plant CO_2 uptake via photosynthesis strongly discriminates against ^{13}C which causes the $^{13}C/^{12}C$ ratio of plant tissues to be smaller (also referred to as isotopically depleted) than the $^{13}C/^{12}C$ ratio of atmospheric CO_2. The repatriation of CO_2 to the atmosphere via plant respiration is not observed to change the isotopic composition of CO_2, CO_2 from this source is, therefore, also depleted in ^{13}C. The degree of depletion is specific to the plant's genome and varies from about ϵ=17 to 19 ‰ for C3 plants to about 4 to 5 ‰ for C4 plants [Vogel 1980; Farquhar et al., 1989]. Discrimination also depends on plant physiological parameters, which will be discussed in more detail in chapter 2.2.1. As the uptake of CO_2 in the ocean is associated with a smaller depletion of only about ϵ=1 ‰ [Mook, 1994] the isotopic signatures of the ocean-atmosphere CO_2 flux and the land-atmosphere CO_2 flux differ significantly.

The ^{13}C signature of fossil fuel CO_2 emissions is also depleted due to the biological origin of fossil energy sources. There is a dependence of the ^{13}C signature on the type of fuel and its specific region of origin. The $^{13}C/^{12}C$ ratio of oil ranges from $\delta^{13}C$ = -30 ‰ to -26.4 ‰, natural gas carries a signature of about $\delta^{13}C$ = -44 ‰, and coal of about $\delta^{13}C$ = -24.1 ‰ [Andres *et al.*, 1999]. The global mean value of the ^{13}C signature of fossil fuel CO_2 is determined to -28.4 ‰ in the period from 1990 to 1992 [Andres *et al.*, 1993] and changed to -29.4 ± 1.8 ‰ in 1995 (personal communication with R. J. Andres in [Battle *et al.*, 2000]). The shift in time to a lower ^{13}C content coincides with a pro rata displacement from coal towards natural gas burning. This trend could directly be observed via atmospheric measurements on a regional scale in Heidelberg, Germany. Schmidt [1999] found a change of the fossil CO_2 $\delta^{13}C$ source signature from $\delta^{13}C$ = -28.6 ± 0.6 ‰ in 1982/83 to $\delta^{13}C$ = -38.5 ± 1 ‰ in 1996.

As a consequence of the input of fossil fuel CO_2 into the atmosphere, with a recent $\delta^{13}C$ signature of -7.9 ‰, the ^{13}C content of atmospheric CO_2 is decreasing with time. Figure 1.4 illustrates, that the decrease of the $^{13}C/^{12}C$ ratio of atmospheric CO_2 is anticorrelated to the increase of the atmospheric CO_2 concentration. The CO_2 and $\delta^{13}C$ data presented in Figure 1.4 are gained from ice core measurements (Law Dome, Antarctica), which could be chronologically linked to recent atmospheric measurements at Cape Grim, Antarctica.

The observed increase in the atmospheric CO_2 mixing ratio from about 280 ppm to 350 ppm within the last 1000 years is accompanied with a decreasing $\delta^{13}C$ signature from about -6.4 ‰ to -7.8 ‰. The trend in the atmospheric ^{13}C signal is, however, also a function of the changing land use. As the global net storage of carbon in the biosphere translates directly in an isotopic enrichment of the atmospheric ^{13}C signal, a net source behaviour of the land's

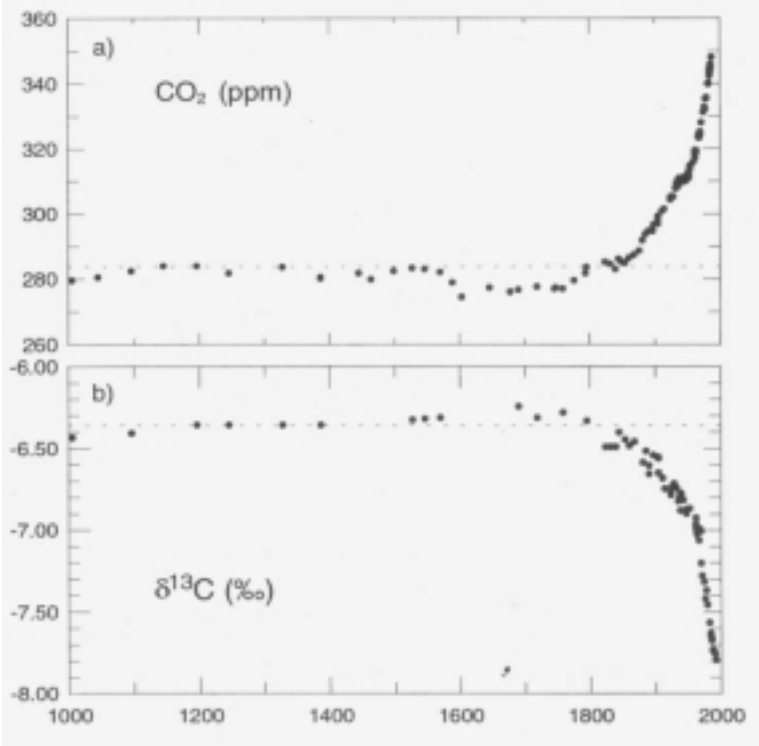

Figure 1.4: *Law Dome (Antarctica) ice core CO_2 record (a) [Etheridge* et al.*, 1996] and $\delta^{13}C$ record (b) [Francey* et al.*, 1999] (from [Trudinger* et al.*, 1999]).*

biosphere leads to an isotopic depletion of the atmospheric ^{13}C signal. Since there is no, or only a negligible, fractionation occurring during the combustion and respiration of fossil, plant or soil carbon, both, industrial and land use changes cause similar changes in the atmospheric ^{13}C signal.

Figure 1.5 illustrates the present global latitudinal distribution of the $^{13}C/^{12}C$ ratio of carbon dioxide in the marine boundary layer. The Northern Hemisphere CO_2 is depleted in ^{13}C with respect to the Southern Hemisphere CO_2. The North Pole minus South Pole gradient in $\delta^{13}C$ is about -0.3 ‰ [Trolier *et al.*, 1996]. This is interpreted as a direct consequence of the predominant emissions of fossil fuel CO_2 in the Northern Hemisphere, which can also be manifested in the actual north-south gradient of CO_2 mixing ratios of about 3 ppm (see also Figure 1.3). The correlated behaviour of CO_2 and the $\delta^{13}C$ signature is also observed in the differences of the amplitudes of the seasonal $\delta^{13}C$ cycles between the hemispheres. The growing impact of biospheric activity, principally increasing from South to North, results in higher amplitudes in the $\delta^{13}C$ (CO_2) in northern latitudes.

There have been several global modelling studies which also include the ^{13}C signature of atmospheric CO_2 simulating the carbon exchange within the ocean-land-atmosphere system [i. e. Francey *et al.,*1995; Keeling *et al.,*1995; Ciais *et al.,*1995b]. In principal, these studies allow one to distinguish between ocean-atmosphere and land-atmosphere fluxes using the strongly different ^{13}C fractionation factors mentioned above. The most recent study concludes, that there was a strong terrestrial biospheric sink in the mid 1990s in contrast to a more or less neutral biosphere in the 1980s [Battle *et al.*, 2000]. Via an inverse modelling approach Ciais et al. [1995a] located a large terrestrial sink in the temperate latitudes of the Northern Hemisphere for the years 1992 and 1993, that reached roughly half of the mag-

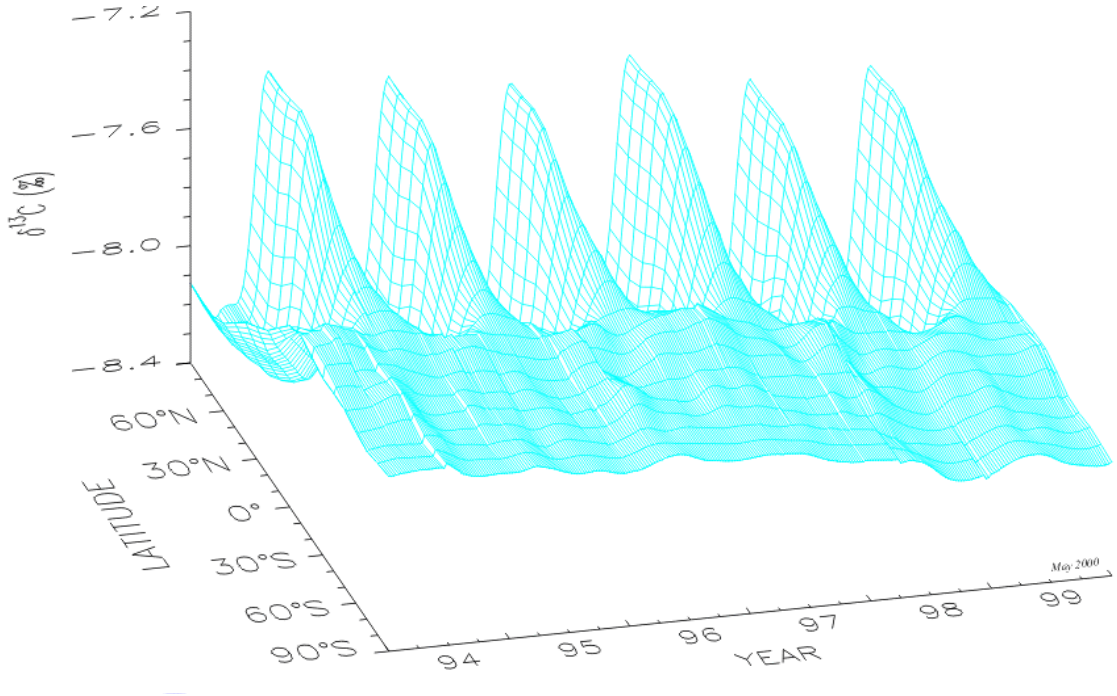

Figure 1.5: *3-dimensional global latitudinal distribution of $\delta^{13}C$ in atmospheric CO_2 in the marine boundary layer. The surface represents data smoothed in space and latitude. [Jim White, NOAA, http://www.cmdl.noaa.gov]*

nitude of fossil fuel emissions. Moreover these studies show a highly variable behaviour of the partitioning between ocean-atmosphere and land-atmosphere fluxes in space as well as in time. Whereas the total net flux in the latitudinal band from 30°N to 90°N from atmosphere to land and ocean was calculated to 4.6 $PgCyr^{-1}$ in 1992, it decreased to 3.7 $PgCyr^{-1}$ in 1993. Even more did the partitioning ratio of the fluxes atmosphere-land/atmosphere-ocean change for the same latitudinal band: from 13.1 in 1992 to 4.6 in 1993. [Ciais *et al.*, 1995a]. The uncertainties of this approach illustrate the process dependency of the CO_2 exchange and may also explain the high temporal variabilities via unknown feedback mechanisms. The process based uncertainties are principally threefold:

- The calculation of the discrimination of ^{13}C by plant photosynthesis in biosphere models is a function of the CO_2 partial pressure in the chloroplasts and other plant physiological parameters. The uncertainty of the ^{13}C discrimination is in the order of $\delta = 1\,‰$, which contributes about 7 % to the uncertainty of the global atmosphere-land flux.

- The 'isotopic disequilibrium' of the soil CO_2 flux: As the ^{13}C content of atmospheric CO_2 is decreasing with time due to fossil fuel emissions, organic carbon in soils contained less depleted ^{13}C in the past than today. Or in other words: carbon that is respired is isotopically enriched compared to carbon that is fixed photosynthetically at the same time. This is due to the time lag between carbon fixation via photosynthesis and the respiration of soil carbon because of the residence time (in the order of 30 to 100 years) of carbon in the biosphere (discussed by Ciais *et al.*, [1999]). This uncertainty is about 30 %, which contributes about 4 % to the uncertainty of the global atmosphere-land net

flux.

- The 'isotopic disequilibrium' of the ocean CO_2 flux, in principle the same mechanism as the soil disequilibrium, causes an uncertainty of about 30 %, which contributes about 25 % to the uncertainty of the global atmosphere-ocean flux.

These uncertainties illustrate the strong dependency of the models on an accurate knowledge of the controlling processes of carbon exchange between the atmosphere and the terrestrial biosphere and the oceans. Beyond that, however, the use of time series of $^{13}C/^{12}C$ to determine a global CO_2 budget is also seriously limited by the measurement precision of the atmospheric $^{13}C/^{12}C$ CO_2 ratio and the density of the global monitoring network. At present, model calculations determine net source/sink fluxes with an uncertainty, which has the same order of magnitude as the fluxes themselves [Ciais *et al.,* 1995b; Ciais and Meijer, 1998]. Therefore, a strong effort is undertaken at present to intercompare the different monitoring networks and to reach the required measurement precision of 0.01 ‰ for $\delta^{13}C$. Despite this, the status quo of the ^{13}C modelling approaches after all permits a reasonable detection of atmosphere-land-ocean fluxes on a regional scale.

1.2.3 $^{18}O/^{16}O$ Isotope Ratio of CO_2

In principle, the $^{18}O/^{16}O$ ratio of atmospheric CO_2 gets modified in the same way as the $^{13}C/^{12}C$ ratio during CO_2 exchange processes between the respective carbon reservoirs. However, the basic difference between the observed $^{13}C/^{12}C$ and $^{18}O/^{16}O$ ratios of atmospheric CO_2 is due to the fact that gaseous CO_2 may exchange an ^{18}O atom with water according to the isotopic equilibrium reaction:

$$H_2\,{}^{18}O_{(l)} + C^{16}O^{16}O \leftrightarrow H^+ + [HC^{16}O^{16}O^{18}O]^-_{(aq)} \leftrightarrow H_2^{16}O_{(l)} + C^{16}O^{18}O_{(g)} \qquad (1.3)$$

The equilibrium fractionation, ϵ_{eq-CO_2}, between the oxygen in water and CO_2 is dependent on temperature according to:

$$\epsilon_{eq-CO_2}(T) = 17604/T - 17.93 \qquad (1.4)$$

with T in °K and $d\epsilon_{eq-CO_2}/dT$=-0.20 ‰/ °C, resulting for example in ϵ_{eq-CO_2}= + 41.11 ‰ at a temperature of 20°C [Brenninkmeijer *et al.*, 1983].

In the atmosphere, the prominent feature of the global meridional $\delta^{18}O$ (CO_2) distribution is a huge North-South gradient of almost -2 ‰ [Mook *et al.,* 1983; Francey and Tans, 1987; Ciais and Meijer, 1998]. Figure 1.6 presents the $\delta^{18}O$ (CO_2) records from the the Scripps (Scripps Institution of Oceanography, La Jolla) and CIO (Centrum voor IsotopenOnderzoek, Groningen)[Mook *et al.,* 1983; and in Ciais and Meijer, 1998]. The $\delta^{18}O$ becomes depleted going from South to North, and the seasonal cycle amplitudes of the $\delta^{18}O$ CO_2 signal increase significantly from about 0.3 ‰ at the South Pole to about 1.3 ‰ at Point Barrow. Compared to the observed $\delta^{13}C$ meridional gradient, the North-South gradient of $\delta^{18}O$ is larger by one order of magnitude. This behaviour suggests very strong $C^{16}O^{18}O$ fluxes opposing any active meridional atmospheric mixing. The seasonal cycles of $\delta^{18}O$ behave similar to those of $\delta^{13}C$. There is, however, a phase shift observed in the Northern Hemisphere between the seasonal cycles of $\delta^{13}C$ together with CO_2 concentrations and the $\delta^{18}O$ signal. This phase shift is in the order of several months. There seems to be a trend in the $\delta^{18}O$ record of Point Barrow in Figure 1.6. Within the period from 1982 to 1989 the autumn minima of $\delta^{18}O$ at Point Barrow seem to decrease slightly by about 0.2 ‰. The $\delta^{18}O$ time series at the South Pole and at Mauna Loa also seem to trend towards more depleted values for the same time period, even though not as significant as at Point Barrow.

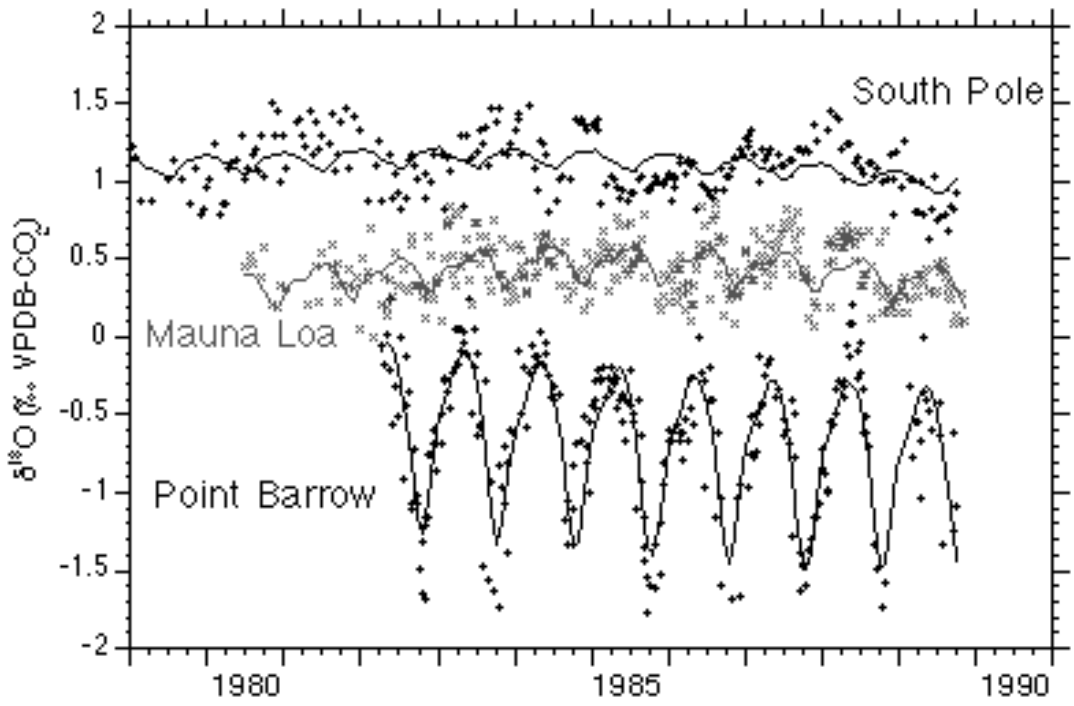

Figure 1.6: *$\delta^{18}O$ (CO_2) measurements of the Scripps (Scripps Institution of Oceanography, La Jolla)/CIO (Centrum voor IsotopenOnderzoek, Groningen) cooperation at Point Barrow (71.3°N), Mauna Loa (19.5°N) and the South Pole (90.0°S)(from Ciais and Meijer, 1998).*

As described in Reaction 1.3, water must be in the liquid phase for the CO_2 hydration reaction to occur. Direct isotopic exchange between CO_2 and atmospheric water vapour is excluded due to the slow rate of hydration which demands several minutes. Furthermore, only a very small portion of CO_2 is dissolved in the small liquid water fraction of clouds (about 1 %) at any time [Francey and Tans, 1987], so that the ^{18}O equilibration process is very unlikely to occur in the atmosphere.

Since the isotopic composition of water vapour is successively depleted via the rain-out of clouds travelling northward and into the continents, the precipitation water also gets successively depleted. The isotopic difference of evaporating ocean water ($\delta^{18}O$ about 0 ‰ SMOW) and the precipitation in polar regions ($\delta^{18}O$ of about -25 ‰ SMOW) [Mook, 1994] delivers a depleted water pool for CO_2 isotopic equilibration in northern continental regions. The same Raleigh-condensation effect leads to a progressively depleted $\delta^{18}O$ of precipitation in direction of continental interiors [Sonntag *et al.*, 1983].

Assuming a 10 ‰ lower overall water equilibration pool in the Northern Hemisphere, Francey and Tans [1987] showed by means of an order of magnitude calculation, that a CO_2 flux of about 200 PgC yr^{-1} is needed for the Northern Hemisphere only to explain the strong $\delta^{18}O$ CO_2 meridional gradient. But such enormous fluxes are not observed (see Table 1.2. For comparison, the global gross fluxes of the ocean and the terrestrial biosphere to the atmosphere together are about the same value [Houghton *et al.*, 1996].

Another explanation for the observed gradient could be the combustion of fossil fuel CO_2 carrying a -17 ‰ source signature for $\delta^{18}O$. Francey and Tans [1987] showed that fos-

sil fuel emissions can explain an interhemispheric gradient of about 0.3‰ only. There is also no exchange of CO_2 with atmospheric O_2 except in the upper stratosphere with ozone molecules [Thiemens *et al.*, 1995]. It was first observed by Mauersberger [1981] that stratospheric ozone is enriched in ^{18}O beyond that expected from theory. $\delta^{18}O$ measurements of stratospheric CO_2 showed a 3‰ enrichment in the lower stratosphere [Gamo *et al.*, 1989]. Yung *et al.* [1991] suggested that this ^{18}O ozone enrichment could be transferred to CO_2 via the isotopic exchange between $O(^1D)$, produced from ozone photolysis, and CO_2. As there is no stratospheric loss of CO_2, the stratospheric enrichments are lost only at the earth's surface by isotopic reactions with water reservoirs. As the stratosphere-troposphere annual CO_2 exchange flux is about one third or less of the total ocean-biosphere-troposphere flux [Boaz *et al.*, 1999], the tropospheric ^{18}O signal in CO_2 should be controlled by processes at the Earth's surface.

The summary of the basic differences between the features of $\delta^{18}O$ and $\delta^{13}C$ in atmospheric CO_2 is as follows:

Feature	$\delta^{13}C$ (CO_2)	$\delta^{18}O$ (CO_2)
Formation of the atmospheric signal	By fractionation processes during exchange between reservoirs, $\delta^{13}C$ values of different reservoirs influence each other	By ^{18}O exchange in oceanic and meteoric water via Equation 1.3 and by fractionation processes
North-South gradient	North-South gradient mainly controlled by the uneven distribution of fossil fuel combustion	North-South gradient mainly controlled by the unequal distribution of ocean and land between the hemispheres and the entirely different $\delta^{18}O$ of oceanic and meteoric H_2O
Association with CO_2 concentration changes	All variations in some way associated	Not all variations are associated, as the $\delta^{18}O$ of CO_2 is also determined via the isotopic exchange with water

After several years of research on this phenomena it was learnt from plant physiologists that during the plant uptake of CO_2 via photosynthesis much more CO_2 than expected gets in contact with leaf (chloroplast) water without being irreversibly fixed by the plant. About one-third of the CO_2 diffusing into the leaves is fixed and the remaining two-thirds are diffuse back to the atmosphere after ^{18}O equilibration with leaf water. The dissolution of CO_2 in leaf water is catalysed with the enzyme CA (carbonic anhydrase), which is ubiquitous in plant tissues, and therefore the isotopic equilibrium Reaction 1.3 in leaf water takes place quasi instantaneously [Francey and Tans, 1987; Farquhar *et al.*, 1993a; Ciais *et al.*, 1997a]. This huge retrodiffusive flux has therefore no influence either on the atmospheric CO_2 concentration or on the $^{13}C/^{12}C$ ratio of atmospheric CO_2, but controls only the atmospheric $\delta^{18}O(CO_2)$ signal.

Farquhar et al. [1993] combined the global information on the $\delta^{18}O$ of precipitation and ground water, a description of leaf water enrichment and the oxygen exchange process within the leaf and a global biosphere model. Leaf exchange is enriching the $\delta^{18}O$ isotopic composition of atmospheric CO_2 because leaf water gets enriched during plant evapotranspiration [Craig and Gordon, 1965] with respect to the source water. The results of the investigation of Farquhar et al. [1993] showed a satisfying agreement with the observed averages of the global atmospheric $\delta^{18}O(CO_2)$ observations. Deeper insight into the latitudinal differences and the seasonal cycles of $\delta^{18}O$ in CO_2 was obtained by the work of Ciais *et al.* [1997a,b]. The major

outcome of this modelling study was the finding that the isotopic exchange with soils induces a large isotopic depletion of the $\delta^{18}O$ (CO_2) signal over the Northern Hemisphere continents which is larger than the opposite effect of isotopic enrichment due to leaf exchange. Furthermore, they concluded a relatively minor influence of the ocean fluxes and the anthropogenic CO_2 emissions on the atmospheric $\delta^{18}O$ seasonal cycle compared to the impact of the land biosphere fluxes.

There is a number of additional novel characteristics that make $\delta^{18}O$ in atmospheric CO_2 an important new tool in global carbon cycle studies. First, as mentioned above, the seasonal cycle in $\delta^{18}O$ shows a phase shift of up to several months from both CO_2 and $\delta^{13}C$ of atmospheric CO_2 . While the seasonal cycle amplitude is of the same magnitude, the latitudinal gradient in $\delta^{18}O$ is almost 10 times larger than that of $\delta^{13}C$. These characteristics illustrate that the mechanisms controlling the $^{18}O/^{16}O$ ratio of atmospheric CO_2 are almost completely independent from those of $^{13}C/^{12}C$. The terrestrial biosphere exerts major control over the ^{18}O signal. Furthermore, it is the gross one-way fluxes, photosynthesis and total respiration, in terrestrial ecosystems that cause changes in the $\delta^{18}O$ composition of atmospheric CO_2 . While affected by gross photosynthesis and total respiration, the ^{18}O signal is controlled by the isotope ratio of the water pool in plant leaves (assimilation) and soils (respiration). Water in plant leaves has a very different oxygen isotope composition than that of water in soils, which induces different ^{18}O signals when CO_2 exchanges with leaves and soils, respectively. In this manner, the respective one-way fluxes associated with photosynthesis and soil respiration can potentially be separated and studied directly. $\delta^{18}O$ in atmospheric CO_2, therefore, carries the potential to determine biospheric gross fluxes. Since the processes controlling the ^{13}C composition of atmospheric CO_2 are almost completely independent from those affecting the ^{18}O composition, measurements of both isotopes can be used to provide independent information about large scale CO_2 exchange processes. Consequently, the use of the ^{18}O signal is potentially large but it requires a detailed understanding of hydrological processes that influence the ^{18}O content of water in plant leaves and soils. In this context, more knowledge is required on the fractionation processes that occur during CO_2 - H_2O exchange. Even with the uncertainties, however, soil-respired CO_2 should largely reflect $\delta^{18}O$ depleted soil water. In comparison to that depleted signature, the photosynthetic assimilation leaf CO_2 exchange will reflect the large enrichment of leaf water. Due to that difference of the resulting isotopic composition of $\delta^{18}O$ in atmospheric CO_2 it should be potentially possible to distinguish between individual photosynthetic and respiratory gross fluxes of an ecosystem. Therefore, $\delta^{18}O$ in atmospheric CO_2 represents a unique tool, because it is sensitive to different fluxes and pools within an terrestrial ecosystem.

1.3 Summary

As discussed before, the role of the terrestrial biosphere is a major subject of debate within the global carbon cycle research. Estimates of fossil fuel emissions and measurements of the spatial and temporal distribution of CO_2 and $\delta^{13}C$ showed evidence for an actual strong terrestrial carbon sink [Ciais *et al.,* 1995a; Ciais *et al.,* 1995b; Francey *et al.,* 1995; Enting *et al.,* 1995]. The $^{18}O/^{16}O$ ratio in atmospheric CO_2 has been identified as a unique tracer with the potential to constrain separately the gross uptake (photosynthesis) and release (respiration) of carbon by terrestrial biota. CO_2 can exchange an ^{18}O atom with two isotopically distinct water reservoirs: evaporating leaf water during photosynthesis and soil moisture during respiration. Thus, the $^{18}O/^{16}O$ isotopic composition of CO_2 is controlled indirectly by the $^{18}O/^{16}O$ ratio of water in the biosphere, and thus is linked to the global water cycle. The use of stable CO_2 isotopes, however, requires the precise knowledge of the controlling processes

which determine the ^{13}C and ^{18}O composition during the biospheric CO_2 exchange.

Therefore, knowing the $\delta^{13}C$ and $\delta^{18}O$ values of CO_2 as it enters and leaves terrestrial ecosystems is extremely important for interpreting global CO_2 observations. It is precisely this kind of information that allows to interpret the source and sink strength of different carbon-compartments (ocean versus land) and should be applicable to understand which ecosystems are active in gas exchange (C3 versus C4, forest versus grassland, etc.). Especially one would like to apply a tool to control the reaction of global biospheric activity in the context of rising atmospheric CO_2 mixing ratios in terms of gross fluxes. However, the global information of $\delta^{18}O$ in atmospheric CO_2 can not be used yet to quantitatively determine the global terrestrial gross fluxes of CO_2. That is, besides model-intrinsic problems like e.g. the validation of sensitivity tests, due to the fact that several processes are poorly understood and need to be investigated:

- More realistic values for the isotope fractionation during CO_2 exchange with leaves and soils need to be determined.
- The characterisation of the isotopic composition of the different H_2O pools (leaf water, soil water and water vapour) of an ecosystem has to be improved.
- The formulation of the leaf water enrichment has to be validated on the ecosystem scale.

At present the understanding of the isotopic gas exchange of land surfaces is still in its infancy. In pursuing and improving the monitoring of atmospheric CO_2 and its isotopic composition, there is a crucial need to augment the coverage of poorly known continental areas, thus improving our ability to characterise and quantify carbon fluxes on the continents via local scale investigations.

Chapter 2

Terrestrial Biospheric CO_2 Exchange

In order to assign the characteristic biospheric CO_2 mixing ratio and CO_2 stable isotope variabilities to the respective processes, the mechanisms of biospheric CO_2 exchange have to be investigated. As the observable atmospheric variation of CO_2 is always a potpourri of reservoir exchange processes and atmospheric transport, the local scale micro-meteorology has to be characterised as well.

2.1 CO_2 Mixing Ratio

The terrestrial biosphere, like the global carbon cycle, can be subdivided into carbon fluxes and reservoirs and fluxes between them. In the following, the processes controlling these fluxes and the nomenclature of these fluxes within a biospheric ecosystem will be defined and specified, respectively. The scheme of the respective CO_2 carbon reservoirs and fluxes, illustrated in Figure 2.1, shows the basic flow of carbon. Beginning in the atmosphere, the very first step of interaction between the atmosphere and plants is the conversion of atmospheric CO_2 into carbohydrate compounds in the plant via photosynthesis (PS):

$$CO_2 + H_2O + h\nu \rightarrow CH_2O + O_2 + chemical\ energy \tag{2.1}$$

It is this mechanism that converts light energy from the sun into chemical energy used by all other forms of life on earth and it produces oxygen which is needed for cellular metabolisms of many other organisms. Therefore, photosynthesis is undoubtedly one of the most important chemical reactions on our planet. The synthesis reaction 2.1 reduces CO_2 to carbohydrates in a rather complex set of reactions. Electrons for this reduction reaction ultimately come from water, which is then converted to oxygen and protons. Energy for this process is provided by light, which is absorbed by pigments, primarily chlorophylls. Chlorophylls absorb blue and red light that, by the way, makes the tree itself look virtually green. The initial CO_2 fixation reaction involves the enzyme Ribulose-1,5-Bisphosphate Carboxylase/Oxygenase (RuBisCO), which can react with either oxygen (leading to a process named photorespiration not resulting in carbon fixation) or with CO_2. Non-photosynthetic organisms as well as photosynthetic organisms need to crack complex organic bonds like carbohydrates during darkness to produce energy while respiring CO_2. Therefore, photosynthesis and respiration (R) are antagonistic processes, that change energy forms and keep water and carbon in the biospheric cycle [Lawlor, 1990].

$$CH_2O + O_2 \rightarrow CO_2 + H_2O + energy \tag{2.2}$$

In a biospheric ecosystem one has to distinguish between two different forms of respiration, both respiring CO_2 basically following reaction 2.2. Plant or autotrophic respiration (R_a) corresponds to the loss of carbon due to respiration by the living biomass of the vegetation. Soil or heterotrophic respiration (R_h) is the carbon released to the atmosphere by heterotrophs (bacteria) in the soil from breakdown of litter and organic compounds.

Following Schulze et al. [2000] the definition of the CO_2 fluxes given in Figure 2.1 classifies

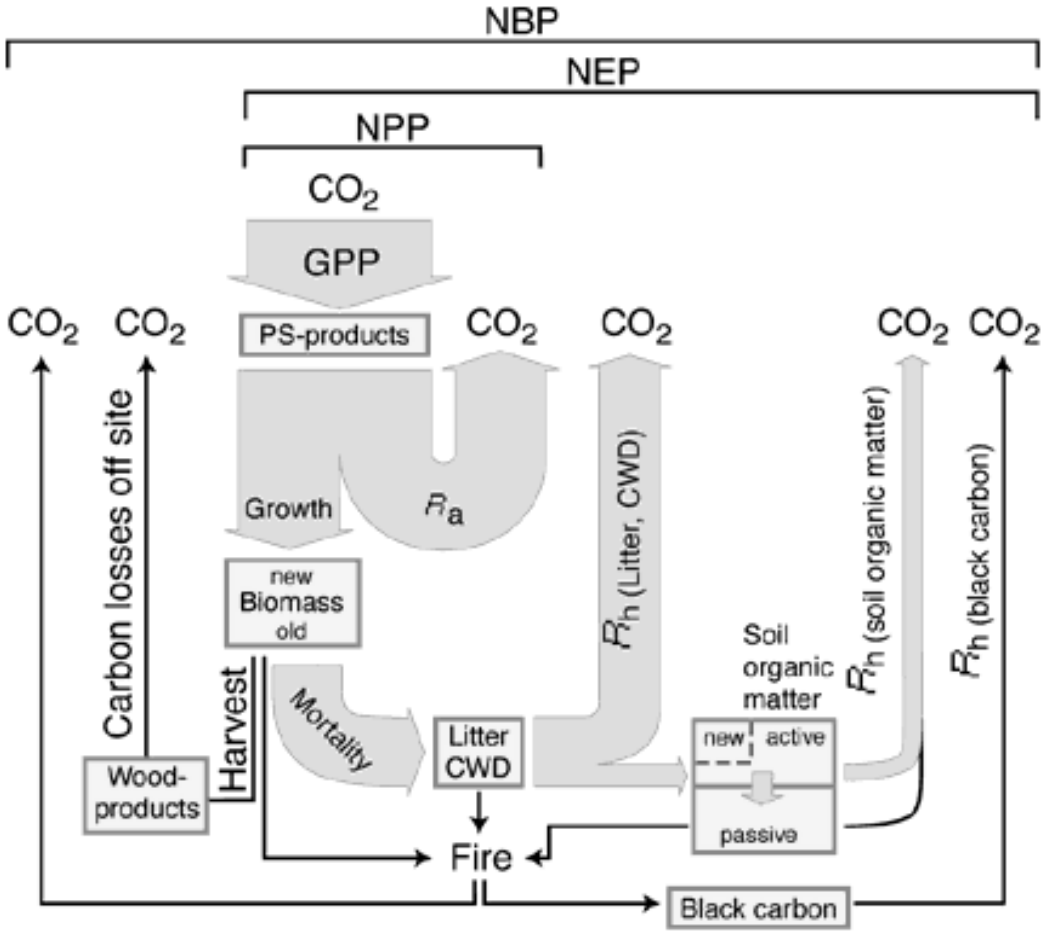

Figure 2.1: *Scheme of the terrestrial carbon cycle. Fluxes are indicated by arrows; reservoirs are indicated by boxes. CWD: coarse wood debris; PS: Photosynthesis; R_h: heterotrophic respiration by soil organisms; R_a: autotrophic plant respiration [Schulze* et al.*, 2000].*

the carbon cycle fluxes of a terrestrial ecosystem as follows:

- GPP: Gross Primary Production, represents the total carbon uptake via photosynthesis.
- NPP: Net Primary Production (= GPP - R_a), represents the fraction of GPP resulting in plant growth when plant autotrophic respiration, R_a, is subtracted.
- NEP: Net Ecosystem Production (= NPP - R_h), represents the fraction of NPP when the heterotrophic respiration of soil organisms, R_h, is taken into account. NEP describes the local, site-specific carbon balance. (Furthermore NEE: Net Ecosystem Exchange (NEE = - NEP in case of NPP $<$ R_h).
- NBP: Net Biome Production (= NPP -(R_h+ disturbance), takes nonrespiratory losses such as fire and harvest into account.

GPP and NPP are based on an annual budget and fluxes into the biosphere are well defined via the increase in biomass. As there are intermediate pools in the biosphere that differ in their carbon turnover time, the terrestrial carbon cycle is a highly non-linear and dynamical system. The carbohydrate pools produced via photosynthesis turn over on a daily basis whereas leaves may stay for several seasons in the form of litter on the top soil floor. Soil organic matter and living wood may survive for several thousand years, depending on the species and environment. Disturbances like fire may emit carbon instantaneously but on the other hand produce extremely long living black carbon [Schulze *et al.*, 2000]. Therefore, a long term prediction of the net carbon exchange (NBP) between the atmosphere and the (even undisturbed) terrestrial biosphere is highly complex. The NEP (= GPP - R_a- R_h), however, is a flux that can be determined on an individual local scale even on a daily basis. It covers all changes in ecosystem carbon stocks resulting from the balance of physiological processes of both, plants and dead organic matter.

When setting up a mass balance to formally describe the respective fluxes it is useful to consider a column of air expanded from the soil surface to a height h within or above the canopy. The mass balance of CO_2 in such a column of air within an ecosystem canopy, in case of no horizontal advection of CO_2, is given by[1]

$$M\frac{\mathrm{d}c}{\mathrm{d}t} = R - A + F_{ae} - F_{ea} \tag{2.3}$$

with

M=$h\ \rho$:	number of moles of air of density ρ in the column with height h per unit ground area [mol(air) m^{-2}]
c :	average mol fraction of CO_2 within the column [mol(CO_2) (mol air)$^{-1}$]
R :	CO_2 respiration flux from soil and stems (and foliage at night) within the column [mol(CO_2) m^{-2} s^{-1}]
A :	net CO_2 assimilation flux by the foliage within the column [mol(CO_2) m^{-2} s^{-1}]
F_{ae} :	one-way flux of CO_2 into the ecosystem canopy from the atmosphere above [mol(CO_2) m^{-2} s^{-1}]
F_{ea} :	one-way flux of CO_2 out of the ecosystem canopy to the atmosphere above [mol (CO_2) m^{-2} s^{-1}]

Within a canopy it is a priori not the case, and in fact never observed in reality, that there is no gradient of CO_2 concentration within a column of air from a height h to a height $h + \triangle h$. Depending on the canopy structure and meteorological conditions there is usually a typical, strong night time gradient of up to 100 ppm between bottom and top due to suppressed vertical mixing. Therefore, the average concentration

$$\overline{c} = \frac{1}{h_{max} - h_{min}} \int_{h_{min}}^{h_{max}} c\,(h)\ \mathrm{d}h \tag{2.4}$$

should be calculated vertical profile measurements. Otherwise a possible term of "CO_2 storage" during a certain time interval would be neglected in equation 2.3.

In the following the exchange process terms assimilation and respiration as well as the transport terms in equation 2.3 will be discussed in more detail.

[1]The convention for the algebraic signs are: inward fluxes (into the canopy column) are calculated positively, outward fluxes negatively.

2.1.1 Assimilation

The gross assimilation flux is the amount of CO_2 that is fixed by photosynthesis and stored in the plant tissue. Formally, the assimilation term A in equation 2.3 represents the net assimilation, which is the difference of GPP and the leave respiration

$$A = GPP - R_{a_{leaves}} \tag{2.5}$$

Therefore, the gross assimilation equals GPP. Furthermore, NPP includes the overall autotrophic respiration flux of the plant including the branches, stems and roots. This definition directly indicates, that an ecosystem is in equilibrium if the total respiratory loss R (the sum of above-ground autotrophic respiration except leaf respiration and the below-ground autotrophic root respiration and the heterotrophic soil respiration) equals the net assimilation flux A.

At the leaf level the net assimilation A drives the CO_2 gradient between the ecosystem atmosphere (c_e) and the chloroplast (c_c), where CO_2 is consumed by the carboxylation reaction. During assimilative activity there is a stepwise decline of CO_2 concentration via the turbulent air leaf surface layer (c_{sur}), the stomatal or inner-cellular air spaces (c_i), the mesophyll cell walls (c_{mw}) to the CO_2 carboxylation sink at the chloroplasts (c_c). During day time it can

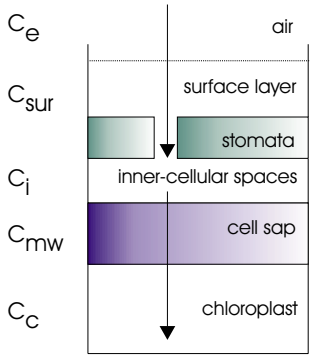

Figure 2.2: *Scheme of the flow of CO_2 during the assimilation gas diffusion process*

be assumed that the CO_2 concentration at the turbulent air leaf surface layer (c_{sur}) is only about a few % lower than the ambient ecosystem CO_2 concentration (c_e). Particularly in nature, the environmental conditions at the leaf surface vary, from CO_2 values close to ambient atmospheric concentrations, in case of relatively high wind speeds and a well mixed surface layer, to depleted values in case of lower wind speeds and photosynthetic activity [Ball, 1987]. Leaf-scale measurements of the CO_2 concentration in the substomata cavities (c_i) indicate a further CO_2 concentration draw-down to the chloroplasts. This decline is estimated to range from $(c_i\text{-}c_c)/c_e \approx 0.1$ [Farquhar *et al.*, 1993a], $(c_i\text{-}c_c)/c_e \approx 0.15$ [Raven and Glidewell, 1981] to $(c_i\text{-}c_c)/c_e \approx 0.2$ [Lloyd *et al.*, 1992]. Furthermore, it was also observed that there is a decline in CO_2 concentration from the substomata cavities (c_i) to the mesophyll cell walls of less than 20 ppm [Farquhar and Rashke, 1978].

At this stage, the formulation of the diffusion path neglects the different respective conductances, see Figure 2.2. There is a formulation simplifying the assimilation process by defining an overall "stomatal conductance" g [in mol air m^{-2} s^{-1}] as [Ball, 1987]

$$g = \frac{A}{(c_e - c_c)} \tag{2.6}$$

This formulation of Ohm's law has been reasonably useful for the description of the diffusive transport of CO_2 into the leaves and it is correct in the first approximation [Ball, 1987].

As I will not directly deal with plant-intrinsic physiological terminations within this thesis, the major parameters controlling assimilation will be described only qualitatively. However, the characterization of the isotope effects during the diffusion processes in section 2.2.1 and 2.2.2 will show that the assumption of only one overall conductance is insufficient in that case. For CO_2 the overall controlling and limiting parameters for the rate of assimilation are [Lawlor, 1990]:

- Photosynthetic Active Radiation (PAR): controls the photochemical process.
- Temperature
- Availability of nutrients: mainly nitrogen and phosphate, essential for the buildup of enzymes needed for the biochemical photosynthesis processes.
- Availability of water: directly needed for photosynthesis process, controls diffusion conductance via stomata aperture.
- Availability of CO_2: drives the gradient $c_e - c_i$.

The exchange of CO_2 constantly follows the change of these factors which determine the rate of photochemical and biochemical processes involved in the overall assimilation. Basically there are two types of photosynthetic progressions:

First, there are progressions where the rate of assimilation increases with an increasing supply and then reaches a saturation point after a while, despite a further increase in supply. This behaviour is typically observed for increasing PAR or CO_2 concentration in the atmosphere, while all other factors are sufficiently available. The saturation point is reached when the respective parameter no longer dominates the rate of assimilation.

Second, there are progressions that are characterized by the search of an assimilation optimum. They are always accompanied by an over- and/or under-supply of some controlling factors. For example in case of "water stress" (under-supply of water) the plant tries to protect itself by closing the stomata to avoid running dry. The closure of the stomata on the other hand enlarges the diffusion resistance for CO_2. Following an economic principle of an optimum between too much water loss and too low CO_2 diffusive input, the plant behaves like a healthy, ideal free-market economy. (A detailed plant physiological photosynthesis model is given by Farquhar *et al.*, [1980] describing the complex biochemical interactions and the combination of the limiting factors controlling the assimilation flux.)

2.1.2 Respiration

The respiratory fluxes of an ecosystem occur as two types of respiration, the autotrophic respiration and the respiration of heterotrophs in the soil and the litter. Furthermore, one can distinguish between above-ground and below-ground respiratory fluxes. On an overall respiratory basis, there are studies suggesting a rather stable R_a/GPP ratio of 0.53 ± 0.04 for forests ecosystems [Waring *et al.*, 1998]. On the other hand there is data that suggests R_a/GPP to a range between 0.5 and 0.7 [Amthor and Baldocchi, 1998; Ryan *et al.,* 1997].

Above-ground, there is usually night time respiration of the foliage, but it is found that there might also be a respiratory activity of plants in light. The day-light respiration varies between 25 and 100 % of the dark respiratory activity [Kromer, 1995]. Furthermore, there is also autotrophic respiration from the stem and the branches above-ground.

Below-ground, soil CO_2 is produced by microbiological decomposition of soil organic matter (heterotrophic) and by root respiration (autotrophic). There are several studies which estimated the ratio of both processes within the overall respiration flux. Various authors assessed the contribution of root respiration to the overall soil flux to be 30 to 60 % in forests and pastures [Reich and Schlesinger, 1992; Trumbore *et al.,* 1995]. Via ^{14}C measurements in soil air,

Dörr and Münnich [1987] estimated the fraction of root respiration to 40 to 50 % for a mixed beech-spruce forest on sandy soil and about 10 % for a grass-covered, uncultivated soil. For agricultural ecosystems root-respiration seems to be smaller, for example maize cultivation shows a contribution of 16 to 20 % and winter wheat of about 20 % [Schüßler *et al.,* 2000; Dörr and Münnich, 1980]. The biogenic activity, which apart from total amount of organic carbon in the soil, drives the heterotrophic soil CO_2 emission, is mainly temperature controlled and increases with increasing temperature. Therefore, the annual cycle of soil CO_2 production is also mainly controlled by temperature. But also the degree of soil moisture influences the soil emission CO_2 flux. In years with high soil humidity, the soil CO_2 production is reduced and the temperature dependency of the emission flux is weakened. The temperature dependency of the soil flux is parameterized with an exponential temperature dependency, where Q_{10} is the relative change of CO_2 production due to a temperature change of 10 degrees (usual values: 1.5 to 2). It was found that in years with more rain (about 20 % over average) and about the same annual mean temperature, soil CO_2 production is reduced and Q_{10} values decrease to nearly half of the "normal" value [Dörr and Münnich, 1987].

2.1.3 Boundary Layer and Canopy Meteorology

The quantitative determination of the biological terrestrial source and sink processes in equation 2.3 simultaneously requires a precise description of the air exchange flux between the atmosphere and the canopy. Therefore, the transport CO_2 flux terms in Equation 2.3 from the atmosphere to the column of air in the ecosystem canopy (F_{ae}) and vice versa (F_{ea}) have to be determined.

The free troposphere, the lower part of the atmosphere reaching from about 0.5 to 2 km height up to a height of 8-12 km (depending on the season), is usually bordered at the lower limit by the atmospheric boundary layer (ABL). In contrast to the free troposphere, the ABL is characterized by strong interaction with the surface, namely via radiative heating and cooling, friction and the presence of sources and sinks of trace gases. These interactions between the surface and the ABL usually occur on time scales of less than a day and are transported by turbulent motions with a size up to the entire depth of the ABL. In case of strong surface solar heating, thermal instability is produced by convection of large plumes. Therefore, the boundary layer is named convective boundary layer (CBL) and shows a diurnal variability. The night time ABL is characterized by suppressed vertical mixing due to the absence of surface solar heating and called nocturnal boundary layer (NBL). The height of the ABL is not only controlled by radiative convection but also by surface roughness (canopy height and stock density) and horizontal wind speed. A reasonable mean value of the ABL height is circa 1000 m with diurnal variations between some 100 m and some 1000 m [Stull, 1988].

The characterization of the atmospheric boundary layer follows the dominating physical processes in the respective height regime that determine the dynamics of exchange [Roedel, 1994; Etling, 1996]:

- Directly above the earths surface the dynamics are determined only by diffusive molecular transport processes. Within this molecular boundary layer with a height of only a few millimeters there is no turbulent transport because eddies larger than a few millimeters will dissipate near the ground.
- The lower part (about 10 %) of the ABL is called surface or Prandtl layer. The dynamics are only controlled by dissipative forces. The dominating characteristics of this layer are the negligible influence of large scale pressure fields and the earth rotation as well as the constancy of vertical fluxes with height.

- Adjacent to the Prandtl layer is the so called Ekmann layer, which is characterized by the rotation and increase of the wind vector with height. This is a consequence of the balance between the increasing impact of the coriolis force, the pressure gradient force and the decreasing impact of dissipating forces.

In case of a thermally neutral stratification ($d\theta/dh$=0, θ: potential temperature), the definition of the Prandtl layer states that the friction velocity

$$u_* = \sqrt{|\frac{\tau_{xz}}{\varrho}|} \tag{2.7}$$

is constant in height (ϱ: air density). This directly implies the assumption that the shear stress, τ_{xz}, which is the vertical flux of horizontal momentum, is constant with height. Considering the dimensions, the evolution of the vertical wind profile is then given by [Monin and Obukov, 1954]

$$v_x(h) = \int \frac{1}{\kappa}\frac{u_*}{h} = \frac{u_*}{\kappa}\ ln\frac{h}{H_0} \tag{2.8}$$

The integration constant H_0 is termed roughness length and has finally to be determined via the measurement of the vertical wind profile as the height at which the horizontal wind would tend to be zero ($v_x(h)$=0) and $\kappa = 0.4$ is the universal von Kármán constant. The roughness length H_0 varies between 3 and 10 % of the respective surface roughness height (e.g. for forests between 0.5 and 3 m) [Roedel, 1994].

Furthermore, the logarithmic wind profile 2.8 in the Prandtl layer changes if, for example, a forest canopy or other course surface structures are ventilated near the surface. Then, an upward shift of the logarithmic wind profile is observed and Equation 2.8 becomes

$$v_x(h) = \frac{u_*}{\kappa}\ ln\frac{h-d}{H_0} \tag{2.9}$$

The magnitude of the shift, d, is termed a zero-plane-displacement and there is no universally valid law for the extent of d. As an estimate for the zero-plane-displacement, values between 65 % and 80 % of the canopy height are observed to be reasonable [Thom, 1975; Panofsky and Dutton, 1984].

Within the canopy, the profiles of micro-meteorological properties can no longer be described with the simple logarithmic approach. As illustrated in Figure 2.3, a second wind

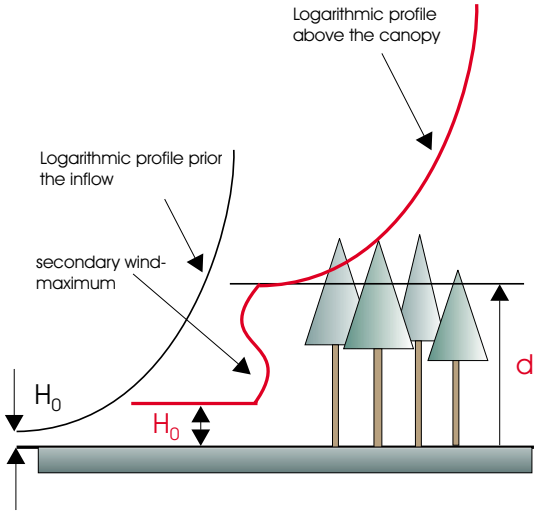

Figure 2.3: *Scheme of the changing properties during the flow through and above a forest canopy for a thermally neutral stratification exemplified by the horizontal wind velocity (from [Nützmann, 1999]).*

maximum or an even more complex vertical structure is usually generated mainly due to

- a lateral, sidewise inflow into the forest canopy. There is a higher aerodynamic resistance in the top of the canopy compared to the stem area. This results in higher horizontal wind velocities near the stem area. But also other, site specific effects like the thermal stratification within the canopy and the magnitude of the horizontal wind influences the profile within the canopy;

- the inflow of large eddies into the canopy. While large eddies with a size in the order of the canopy height itself or larger, can transfer momentum directly to the stem area due to their large inertia, smaller eddies will dissipate in the top leaf area of the canopy. Large eddies are, therefore, able to transfer momentum directly from the Prandtl layer to the soil surface of a forest and can produce fluxes against meteorological or trace gas gradients, so called "counter-gradient" fluxes.

In analogy to Fick's first law, a vertical flux F of a trace gas under turbulent conditions can be formulated as

$$F = -K(h)\frac{\mathrm{d}c(h)}{\mathrm{d}h} \tag{2.10}$$

with *K(h)*: turbulent diffusion coefficient [in $\mathrm{m}^2\ \mathrm{s}^{-1}$] and *c(h)*: concentration of the trace gas at a height h. Assuming thermally neutral stratification, it can be shown that the diffusion coefficient is a function of height [Roedel, 1994]:

$$K(h) = u_*\kappa h \tag{2.11}$$

To describe the transport within and above a forest canopy (i.e.F_{ae} and F_{ea}), it is, therefore, necessary to obtain a parameterization of the vertical structure of the diffusion coefficient as well as a concentration profile of the trace gas in a reasonable spatial and temporal resolution.

A possibility to directly measure the flux of a trace gas is the simultaneous measurement of the respective fluctuations of the vertical wind velocity and the concentration of a trace gas [Baldocchi *et al.*, 1988]. A flux F can be expressed as the product of a concentration c and a transfer-velocity w. To obtain the fluctuations, c and w are separated into their mean values ($\bar{c}$ and $\bar{w}$) and fluctuations (c´and w´)

$$\begin{aligned} F &= c\ w \\ &= (\overline{c} + c')\ (\overline{w} + w') \\ &= \overline{c}\ \overline{w} + \overline{c}\ w' + c'\ \overline{w} + c'\ w' \end{aligned}$$

Averaging in time yields

$$\begin{aligned} F &= \overline{\overline{c}\ \overline{w}} + \overline{\overline{c}\ w'} + \overline{c'\ \overline{w}} + \overline{c'\ w'} \\ &= \overline{c}\ \overline{w} + \overline{c}\ \overline{w'} + \overline{c'}\ \overline{w} + \overline{c'\ w'} \\ &\quad \overbrace{\qquad\qquad}^{advective\ transport} \\ &= \overbrace{\overline{c}\ \overline{w}} + \underbrace{\overline{c'\ w'}}_{turbulent\ transport} \end{aligned} \tag{2.12}$$

As the averaged mean value of a fluctuation is zero the final flux term has two components. The first term in Equation 2.12 describes the advective mean flux as the product of the mean values and the second describes the turbulent flux as the mean of a product of fluctuations. The turbulent term in Equation 2.12 will disappear if the fluctuations of c and w are not correlated. Therefore this approach is named "eddy correlation" method and is a tool to directly measure turbulent fluxes. The realisation of the measurement, however, is limited by the response time of the sensors measuring the wind fluctuations and the fluctuations of

the trace gas concentration. Therefore, very fast Doppler-anemometers are used to determine even small eddies and CO_2 concentrations are measured online via fast IRGA (Infrared Gas Analyzer) absorption spectroscopy.

2.2 CO_2 Isotope Ratios

Combined measurements of CO_2 concentration and stable isotope ratios in principle allow the identification and contribution of respective CO_2 fluxes to the overall ecosystem exchange with the atmosphere. Even ecosystem compartment contributions (e. g. soil, plants) can potentially be distinguished due to their different isotopic signatures.

If one assumes that the atmospheric CO_2 concentration within an ecosystem (c_e) is a mixture of some (constant) background air concentration (c_a) and CO_2 that is added or removed by sources and sinks (c_s) within the ecosystem, the concentration within the ecosystem is given by

$$c_e = c_a + c_s \tag{2.13}$$

This two-component mixing approach can be extended to balance the respective isotopes of the compartments via the (approximated) mass balance equation [Mook, 1994]

$$\delta_e \; c_e = \delta_a \; c_a + \delta_s \; c_s \tag{2.14}$$

were δ_e, δ_a and δ_s represent the isotopic composition of the measured ecosystem air, the atmospheric background air and the source CO_2 . Combining Equations 2.13 and 2.14 yields

$$\delta_e = \frac{c_a(\delta_a - \delta_s)}{c_e} + \delta_s \tag{2.15}$$

This is a linear relationship between δ_e and $\frac{1}{c_e}$ with a slope of $c_a(\delta_a - \delta_s)$ and an intercept at δ_s for $c_e \to \infty$. Here, it is important to note that this so called Keeling plot [Keeling, 1958] can only be applied on a timescale where the characteristic isotopic composition of the sources do not change. On the other hand, the Keeling plot delivers an overall isotopic source signature information even if the ecosystem source/sink consists of several different sub-sources/sinks, as long as the contribution of each sub-component does not change in time. The Keeling approach was used first to identify the contributions of different sources to increasing CO_2 concentrations at a regional scale. More recently, the identification of the isotopic composition of sources/sinks was also performed within terrestrial ecosystems [Yakir and Sternberg, 2000].

2.2.1 $^{13}C/^{12}C$

The isotope ratio of ambient CO_2 within a forest canopy like the CO_2 concentration is determined by the photosynthetic, respirative and transport CO_2 fluxes. However, the isotopic composition of the different reservoirs has to be considered as well as the potential change of the isotopic composition during transfer from one reservoir to the other. Following Lloyd *et al.* [1996], the mass balance for CO_2 (2.3) can be written for ^{13}C as

$$M\frac{\mathrm{d}(R_e\, c)}{\mathrm{d}t} = R \cdot R_R + A \; \frac{R_e}{1 + {}^{13}\Delta_{leaves}} + F_{ae}R_a - F_{ea}R_e \tag{2.16}$$

with

$R_{e,R,a}$: average $^{13}CO_2/^{12}CO_2$ ratio of CO_2 within the ecosystem, of respired CO_2 and of atmospheric CO_2 above the canopy

$^{13}\Delta_{leaves}$: discrimination against $^{13}CO_2$ during assimilation

using

$$Mc\frac{\mathrm{d}R_e}{\mathrm{d}t} = M\frac{\mathrm{d}(R_e c)}{\mathrm{d}t} - MR_e\frac{\mathrm{d}c}{\mathrm{d}t}$$

and replacing the isotope ratios R_i by the δ notation

$$\delta_i = \left(\frac{R_i}{R_{VPDB}} - 1\right)$$

and furthermore ignoring terms in Δ^2, after a few algebraic conversions Lloyd *et al.* [1996] showed, that the mass balance for $^{13}CO_2$ can be written as

$$Mc\frac{\mathrm{d}\delta_e}{\mathrm{d}t} = R(\delta_R - \delta_e) + A\ {}^{13}\Delta_{leaves} + F_{ae}(\delta_a - \delta_e) \tag{2.17}$$

The general assumption in determining δ_R in Equation 2.17 is that there is no fractionation during the respiration process [Lin and Ehleringer, 1997]. Compared to respiration CO_2, CO_2 in soil air is enriched in ^{13}C due to diffusional fractionation by $\epsilon_{CO_2-diff} = 4.4\,‰$. However, under steady state conditions δ_R equals the $\delta^{13}C$ of CO_2 respired within the soil. In that case, the soil CO_2 leaving the soil during respiration gets depleted by -4.4 ‰ and therefore δ_R converges to the ^{13}C signature of the mixture of both, source organic matter and root respiration [Dörr and Münnich, 1987]. As already mentioned in Chapter 1.2.2, there is a small difference between the ^{13}C values of soil respiration CO_2 and the ^{13}C values of the actual biomass production via photosynthesis. This isotopic disequilibrium arises when soil organic matter that was produced several years before decomposition contributes to soil respiration. Due to long term decrease in atmospheric $\delta^{13}C(CO_2)$, this delay between production and decomposition (in the range of one year to several tens of years) is responsible for an enriched organic respiration source compared to the organic material that is actually produced [Enting *et al.,* 1995; Buchmann and Ehleringer, 1998].

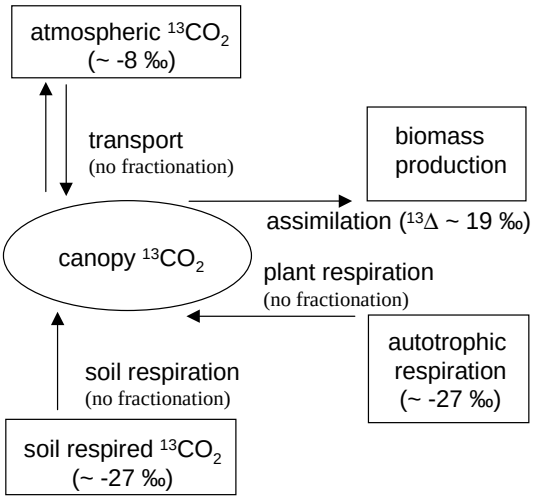

Figure 2.4: *Scheme of the basic $^{13}CO_2$ flow within a canopy*

The total discrimination against $^{13}CO_2$ during assimilation, $^{13}\Delta_{leaves}$, is the sum of the respective fractionation processes occurring during the overall assimilation process. Recalling Figure 2.2, the respective steps of the diffusive path from the atmosphere to the sites

of carboxylation are associated with different isotopic fractionation. In principle, these fractionations must be weighted by the respective diffusion resistances. The fractionation during molecular diffusion in free air is -4.4‰ [Craig, 1953] and diffusion through the surface layer of the leaves fractionates with -2.9‰ [Farquhar, 1983]. The equilibrium fractionation for the solution of CO_2 in the cell sap H_2O is -1.1‰ [Mook *et al.*, 1974] and the molecular CO_2 diffusion in aqueous solution is -0.7‰ [O'Leary, 1984]. The final step of the overall discrimination is the fractionation during the enzymatic fixation by RuBisCo. Plants applying the so called Calvin pathway reaction are referred to as C3 plants[2]. For example, all trees belong to this C3 genome applying the Calvin reaction. There have been a number of investigations which determined this fractionation to 29 to 30 ‰ [O'Leary, 1993]. However, it was learned that the carboxylation mechanism by phosphoenolpyruvate (PEPC) has to be taken also into account. The effective C3 carboxylation fractionation can vary between 26.4 and 30‰ at 25°C (a detailed summary of the fractionation processes is given by Lloyd *et al.,* [1996]).

The often used approximate equation for isotope discrimination is given by Farquhar *et al.,* [1982]:

$$^{13}\Delta_{leaves} = a + (b - a)\frac{c_i}{c_e} \tag{2.18}$$

with

- c_i : inner cellular CO_2 partial pressure
- c_e : CO_2 partial pressure of the air surrounding the leave within the ecosystem canopy
- a : fractionation during diffusion in free air: 4.4‰
- b : effective C3 carboxylation fractionation: about 29‰

Equation 2.18 ignores the fractionation associated with the diffusion through the leaf surface layer and simplifies the respective CO_2 gradients between each assimilation step to the total gradient between the CO_2 concentration of the surrounding air and the site of carboxylation. However, this equation describes the overall process in a reasonable way and is therefore widely used.

The photosynthetic impact on the $\delta^{13}C$ values of ambient CO_2 discriminates against ^{13}C, therefore, the remaining atmospheric CO_2 reservoir will be enriched in ^{13}C [Langendörfer *et al.*, 2001]. The extent of this impact on ambient CO_2 enrichment depends on the ratio of C3 to C4 plants in an ecosystem and on the rate of photosynthesis in relation to vertical mixing with the atmosphere above the canopy (see Figure 2.4).

Finally, the last term in Equation 2.17 is the transport term, that describes mixing of ecosystem air with CBL. The change of ecosystem ^{13}C composition is directly proportional to the exchange CO_2 flux and the difference between the ^{13}C isotopic composition of atmospheric and ecosystem CO_2.

2.2.2 $^{18}O/^{16}O$

Contrary to the carbon isotopic composition of ambient ecosystem CO_2, the $\delta^{18}O$ value is controlled by the isotopic equilibration (see reaction 1.3 in chapter 1.2.3) with different water reservoirs within the ecosystem. The mass balance for $\delta^{18}O$ can again be written as the sum of respiration, assimilation and transport terms

$$Mc\frac{\mathrm{d}\delta_e}{\mathrm{d}t} = R_{soil}(\delta_{soil} - \delta_e + \epsilon_{soil}) + R_a(\delta_{stem} - \delta_e + \epsilon_{stem}) + A\ ^{18}\Delta_{leaves} + F_{ae}(\delta_a - \delta_e) \tag{2.19}$$

with

[2] C4 plants (mainly grasses) use a different carboxylation reaction (carboxylation by phosphoenolpyruvate (PEPC), Hatch-Slack pathway) and the discrimination is about -5.7‰.

ϵ_{soil} : effective fractionation of $C^{16}O^{18}O$ diffusing through the soil to the atmosphere beginning at the location of isotopic equilibration with soil water
ϵ_{stem} : effective fractionation of $C^{16}O^{18}O$ diffusing from chloroplast to the atmosphere
δ_{soil} : $C^{16}O^{16}O$ /$C^{16}O^{18}O$ ratio of soil respired CO_2 in equilibrium with soil water
δ_{stem} : $C^{16}O^{16}O$ /$C^{16}O^{18}O$ ratio of stem respired CO_2 in equilibrium with stem water
${}^{18}\Delta_{leaves}$: discrimination against $C^{16}O^{18}O$ during assimilation

The $\delta^{18}O$ respiration flux of the soils can be described as the product of the soil respiration CO_2 flux, R_{soil}, with the difference between the $\delta^{18}O(CO_2)$ in isotopic equilibrium with soil water, δ_{soil}, which is depleted by the effective diffusive fractionation of CO_2, ϵ_{soil}, and the ecosystem $\delta^{18}O$ of CO_2, δ_e. Isotopic equilibration of soil CO_2 with soil water is temperature dependent and follows Equation 1.4. Ciais et al. [1997a] estimate a diffusion length for this equilibration reaction occurring in the soil of about 4 cm. During diffusion through the soil there is kinetic fractionation of the diffusing CO_2 molecules, which is theoretically limited to ϵ_{soil} = -8.8 ‰. However, as turbulent diffusion does not fractionate and the top few cm of the soil are exposed to turbulences of the atmosphere, effective fractionation is adjusted somewhere between 0 ‰ and the maximum value of -8.8 ‰. Still no parameterisation of ϵ_{soil}, for example dependent of the wind velocity near the soil surface, could be found. There are global estimates of ϵ_{soil} given by Farquhar et al. [1993a] resulting in ϵ_{soil} = -7.6 ‰ and in an assessment by Ciais et al. [1997ab] leading to -5 ‰. Miller et al. [1999] investigated the soil fractionation using direct, small scale measurements suggesting an ϵ_{soil} of -7.0 ‰. The $\delta^{18}O$ of atmospheric CO_2 is also influenced by invasion of atmospheric CO_2 into the soil. During this process CO_2 diffuses into and out of the soil again and is potentially subject to the isotopic equilibrium reaction [Tans, 1998; Miller et al., 1999]. This process may be important if the soil moisture at the top layer of the soil is high. Consideration of the invasion effect is difficult due to missing information on the presence of "carbonic anhydrase" in the soil and the parameterisation of the turbulent characteristics of the atmospheric soil surface layer.

Similarly, the impact of the above-ground autotrophic respiration of the stems and branches, R_a, on the change of $\delta^{18}O$ in ecosystem CO_2 is formulated. The $\delta^{18}O$-flux of the stems and branches can be described as the product of the autotrophic stem and branch respiration CO_2 flux, R_a, with the difference between the $\delta^{18}O(CO_2)$ in isotopic equilibrium with stem and branch water, δ_{stem}, which is depleted by the effective diffusive fractionation of CO_2, ϵ_{stem}, and the ecosystem $\delta^{18}O$ of CO_2, δ_e. As the stems and branches respiration apertures do not allow turbulent eddies to interfere in the diffusion process of respirative CO_2, maximum diffusive fractionation of -8.8 ‰ is assumed for the value of ϵ_{stem} [T. Bariac, personal communication].

The quantitative description of the discrimination against $CO^{18}O$ during the assimilation process, ${}^{18}\Delta_{leaves}$, can be derived from Equation 2.6. As about one-third of the CO_2 diffusing into the leaves is irreversibly fixed by carboxylation and the remaining two-thirds are diffusing back to the atmosphere after ^{18}O equilibration with leaf water, the assimilation term is the sum of two opposing fluxes. By defining the fluxes from the ecosystem atmosphere to the leaf (F_{el}) and vice versa (F_{le}), the net assimilation discrimination against $CO^{18}O$ can be formulated as [Farquhar and Lloyd, 1993]:

$$ {}^{18}\Delta_{leaves} = -\epsilon_{leaf} + \frac{c_c}{c_e - c_c} \, (\delta_{leaf} - \delta_e) \tag{2.20} $$

with

ϵ_{leaf}: mean diffusional fractionation of $C^{16}O^{18}O$ (surface layer to stomata): -7.4 ‰ [Farquhar *et al.*, 1993a].
δ_{leaf}: $\delta^{18}O$ of leaf CO_2 in full isotopic equilibrium with leaf H_2O (see reaction 1.3).

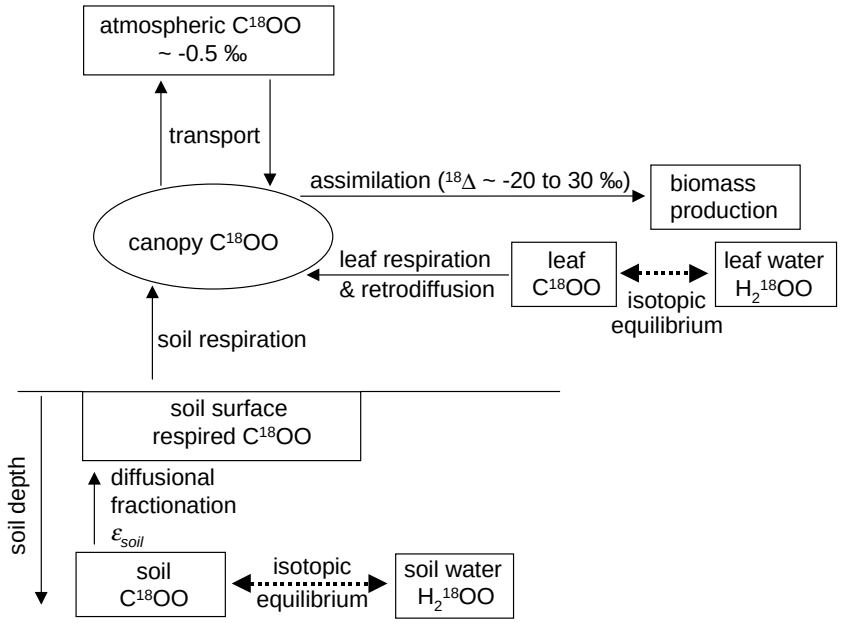

Figure 2.5: *Scheme of the basic $CO^{18}O$ flow within a canopy*

On a regional scale, there are variations in temperature, the isotopic composition of the source water, relative humidity and c_c/c_e. These changes cause ${}^{18}\Delta_{leaves}$ to vary from -20 ‰ in the arctic tundra to +32 ‰ in the dry steppes of Kazakhstan and Ukraine [Farquhar *et al.*, 1993a].

As CO_2 has a mean residence time in the stomata of the leaves of about 0.2 s [Ciais *et al.*, 1997a] and hydration of CO_2 in water needs approximately 3 min at 10°C, it is not obvious, that CO_2 must be in isotopic equilibrium with the leaf water. However, due to the ubiquitous presence of the enzyme "carbonic anhydrase" in plant tissues, the hydration reaction 1.3 is accelerated by a factor of 10^7 [Stryer, 1981]. Therefore it is widely assumed that leaf CO_2 is in isotopic equilibrium with leaf water. The quantity of water involved in the equilibration reaction 1.3 is orders of magnitude larger than that of CO_2, so equilibrated CO_2 will take the oxygen isotope ratio of the water in which it is dissolved with a temperature dependence following Equation 1.4, regardless of its original $\delta^{18}O$ composition [Yakir and Sternberg, 2000]. However, on the basis of leaf scale measurements Gillon and Yakir [2000; 2001] showed, that the generally assumed isotopic equilibration during photosynthesis between oxygen in CO_2 and oxygen in H_2O needs not be complete. They detected large differences in the activity of carbonic anhydrase among major plant groups. They estimate a global value of 80 % isotopic equilibration as a mean. However, there is a characteristic difference between C3 and C4 plants. Whereas C3 plants equilibrate nearly complete (93 %), C4 grasses equilibrate only by about 50 % [Gillon and Yakir, 2000; 2001].

Much of the variation in ${}^{18}\Delta_{leaves}$ is controlled by the variation of the leaf water ${}^{18}O$ isotopic composition. It is widely assumed that CO_2 reaches equilibrium with water evaporating from the mesophyll cells [Farquhar *et al.*, 1993a]. However, Yakir et al. [1994] suggest that CO_2 is not equilibrating with evaporating leaf water but with a mixture of less enriched source water supplying the leaf and the enriched water at the evaporation zone. The process of water evaporation tends to enrich the leaf water ${}^{18}O$ isotopic composition [Jacob, 1982;

Farquar *et al.*,1993]. Under steady state conditions, the $^{18}O/^{16}O$ ratio of evaporating leaf water is given by [Craig and Gordon, 1965]

$$\delta_{leaf}^{H_2O} = \epsilon_{liq-vap} + (1-h)\cdot(\delta_{root}^{H_2O} - \epsilon_{kin}) + h\cdot\delta_{vap} \tag{2.21}$$

with

h:	relative humidity at the leaf surface [%]
$\delta_{root}^{H_2O}$:	$\delta^{18}O$ of root H_2O, taken up from the soil water
δ_{vap}:	$\delta^{18}O$ of water vapour outside the leaf
$\epsilon_{liq-vap}$:	equilibrium fractionation factor of $H_2^{18}O$ for the liquid-vapour phase transition
ϵ_{kin}:	kinetic fractionation factor of $H_2^{18}O$ for the diffusion of water vapour across the stomatal cavity and the leaf boundary layer

Bariac et al. [1994b] found no isotopic fractionation during root uptake of soil water. Therefore, δ_{root} should be equal to δ_{soil}. The equilibrium fractionation factor of $H_2^{18}O$ during the phase transition of water from the liquid phase to the vapour phase, $\epsilon_{liq-vap}$, is temperature dependent and is calculated following Majube [1971] using a simplified 1/T adjustment

$$\epsilon_{liq-vap} = 7356/T + 15.38 \tag{2.22}$$

with T in °K and $d\epsilon_{liq-vap}/dT$ $\sim$0.10‰/°C resulting for example in $\epsilon_{liq-vap}$= + 9.7‰ at a temperature of 20°C. The kinetic fractionation factor ϵ_{kin} for the diffusion of water vapour across the stomatal cavity to the leaf boundary layer is a much more variable parameter and depends on the turbulent boundary conditions at the leaf surface layer. The value for ϵ_{kin} is greater for molecular diffusion (film model) than for a mixed layer at the leaf surface (surface renewal model) and values between -15 to -28.5‰ are therefore possible [Deacon, 1977; Merlivat, 1978; Merlivat and Jouzel, 1979]. This value is also species specific [White, 1983] and depends also on the turbulence conditions, i.e. wind velocity at the leaf surface [Förstel *et al.*, 1975].

Besides the value of the leaf water isotopic composition, δ_{leaf}, the mean diffusional fractionation of $C^{16}O^{18}O$ from the leaf surface layer to the site of carboxylation, ϵ_{leaf}, in Equation 2.20 determines the value of the overall discrimination against $C^{16}O^{18}O$. The value given in Equation 2.20 (-7.4‰) is an average, weighted over the different diffusive steps from the leaf surface to the stomata. Farquhar and Lloyd [1993] give an expression for the weighted average discrimination down to the leaf interior to the site of carboxylation as

$$\epsilon_{leaf} = \frac{(c_e - c_{sur})\epsilon_b + (c_{sur} - c_{mw})\epsilon_d + (c_{mw} - c_c)\epsilon_w}{c_e - c_c} \tag{2.23}$$

with

ϵ_d:	fractionation for molecular diffusion through the stomata: - 8.8‰
ϵ_b:	fractionation for diffusion through the leaf boundary layer: - 5.8‰ (molecular diffusion to the 2/3 power [Kays, 1966])
ϵ_w:	fractionation summarising an equilibrium dissolution effect and diffusion fractionation in solution at the mesophyll cell walls: - 0.8‰

[Vogel *et al.*, 1970; O'Leary, 1984; Jähne *et al.*, 1987]. Considering the drop-down of the respective CO_2 concentrations from the ecosystem to the chloroplasts (see Chapter 2.1.1, page 21) and the diurnal variation of the meteorological and plant physiological parameters, it is obvious that this diffusion fractionation is also likely to vary.

2.3 Open Questions and Motivation for this Work

The main objective of the present thesis is to investigate the CO_2, $\delta^{13}C$ and $\delta^{18}O$ variabilities of the relevant reservoirs within a local ecosystem during their exchange with the atmosphere. The perspective is, to examine the feasibility of exploiting $\delta^{18}O$ as a tracer to separate between the biospheric gross fluxes assimilation and respiration, respectively.

In theory, the knowledge of the discussed terms should allow to investigate the characteristic ecosystem fluxes. To characterise the observable CO_2 concentration and CO_2 stable isotope ratio variabilities within an ecosystem canopy, basically, three controlling categories have to be determined:

- the turbulent exchange within the canopy and with the atmosphere above,
- the isotope ratios of the respective CO_2 and H_2O compartments,
- and the isotope fractionations and discriminations, respectively, that occur during the gas exchange between the reservoirs.

The determination of net ecosystem CO_2 exchange, as a controlling parameter of the total CO_2 efflux at the biosphere-troposphere interface, is essential. To determine short term variations of the isotopic composition of ambient air, an adequate time resolution of the measurement and sampling, respectively, is required. In order to account for the vegetational variability, besides the time resolution, the investigation of the spatial heterogeneity is important. On the basis of what is learned from plant-physiological studies with regard to micro-scale isotopic fractionation processes, the system should be reasonably determined.

Up to now, there is no experience, whether it is possible to quantitatively describe the processes in a well parameterised, closed ecosystem. The main problem of verifying the theory, is to accurately separate between atmospheric transport processes and pure biospheric source/sink processes. The question therefore is: are the characteristic isotopic imprints of biospheric exchange processes on the ambient air quantitatively accessible in terms of their mass fluxes ? In this context, of course, the micro-scale plant physiological parameterisations have to be validated within their known uncertainties and within their species dependent characteristics. Within this joint project, therefore, the design and the strategy of the measurements in Russia was aligned on the basis of these theoretical assumptions.

The progressing perspective of this study is to test the $\delta^{18}O$ potential for its appliance in global transport models. Up to know, global modelling efforts to reproduce atmospheric $\delta^{18}O$ variations deliver fairly well results. However, these forward mode simulations are not yet able to predict characteristic longitudinal variations [Peylin *et al.,* 1999; Cuntz *et al.,* 2001].

Up to know, tropospheric CO_2 mixing ratio and CO_2 stable isotope records over the Euro-Siberian area are rare, but they are strongly needed to gain insight in biospheric carbon cycling. The Euro-Siberian area is furthermore suitable to investigate the biospheric impact, due to extensive vegetational areas. Within the framework of the EUROSIBERIAN-CARBONFLUX project, during intensive field campaigns, the large scale impact of the lands biota on tropospheric CO_2 mixing ratio and CO_2 stable isotope variabilities is investigated by aircraft observations.

Chapter 3

Experimental

The measurement program in Russia consists basically of two categories: (1) three intensive, local scale campaigns within a *picea abies* forest were performed, and (2) continuous year-round aircraft flasks at the top of the CBL were sampled.

3.1 The Areas of Investigation

The intensive campaigns were performed within the large scale territory of the Tver region, about 300 km northwestern of Moscow. The territory of about 70.000 km^2 area is located within the temperate continental climate zone in the central part of European Russia, the Southwest part of the Valdai upland of the Russian Plain (see Figure 3.1). Fluctuation of the altitude is from 50-70 m to 250-300 m above sea level. The upper level of the soils are represented by loess-like loams, medium-heavy loams, sands and peat. The percentage of forestland is about 50 %. Different types of bogs represent about 15 % of the territory. The forest is dominated by small-leaved (birch, aspen) and piny trees. The store of carbon in vegetation above-and below-ground and mortmass is 309 million tons, and 115 million tons of carbon are stored in peat. The soils of the territory are represented by podsolic, sod-podsol and gley-podsol as well as bogs. The store of carbon in soils equals 245 million tons. The basic atmospheric pollutants, that could influence the Tver region are located in St.-Petersburg, Moscow and Tver [M. Puzachenko, personal communication].

During the EUROSIBERIAN CARBONFLUX project, three intensive campaigns took place: from July 23 to July 31, 1998, from July 27 to August 1, 1999, and from October 21 to October 26, 1999. The measurements were performed within a natural *picea abies* forest in the 'Central Reserve' (CR) at Fyodorovskoye near Nelidovo (56°27'N, 32°55'E) as short-term intensive campaigns. The predominant native woody species (49 % of the total CR area) is spruce (*picea abies*), the CR was not actively used by man before 1931 and after 1960.

Local vegetation (1km × 1km) is represented by southern taiga biota that penetrated into broad-leaved forests of the central part of the Russian Plain. The forest type near the measurement location is dominated by 36 % birch and 20 % spruce stocks, 30 % consists of a mixture of birch and spruce, 12 % is pine and the residual forest consists of alder and deciduous trees [D. Kozlov, personal communication]. The small scale vegetation cover pattern and characteristics are controlled primarily by their location in a watershed. The soil profile consist of humus on the top 50 cm followed by a coarse loamy soil to a depth of about 1 m. Bogs cover in total 4 % of the CR area. The age of the spruces is 181 ± 35 years

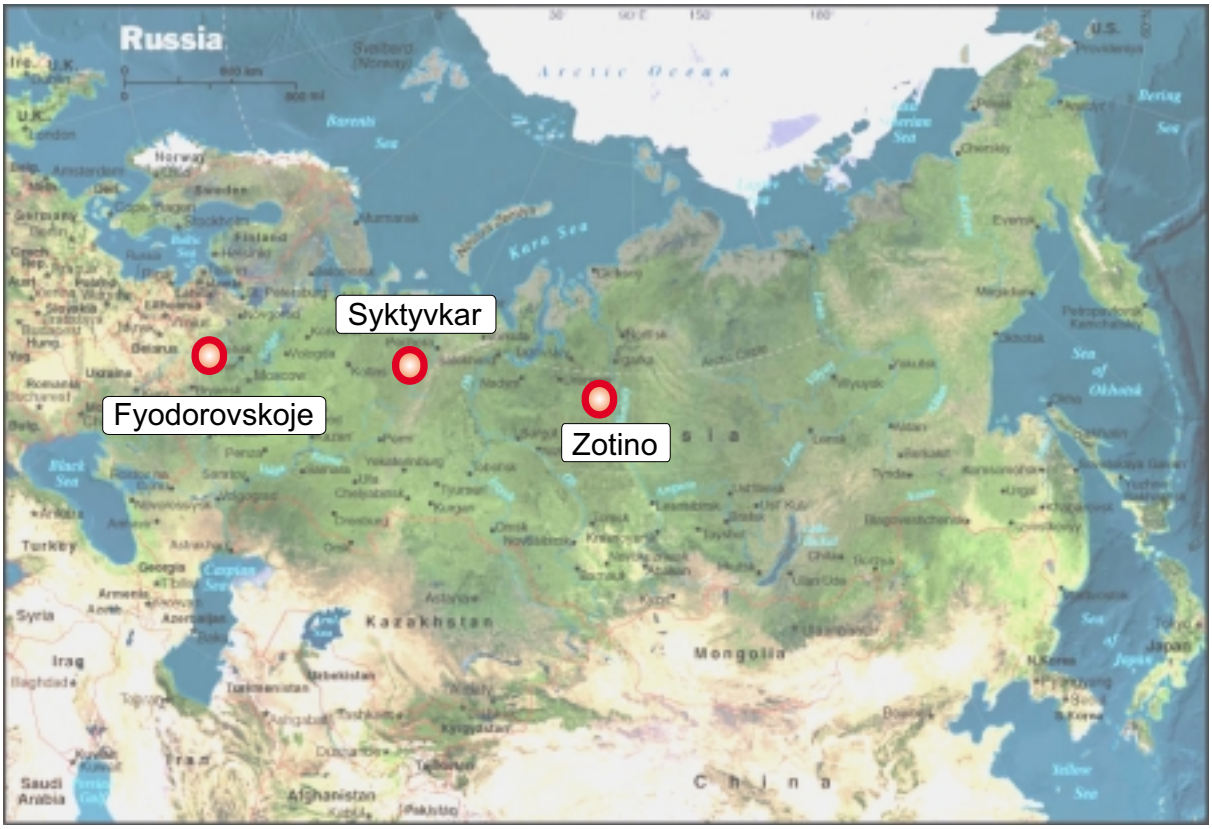

Figure 3.1: *EUROSIBERIAN CARBONFLUX observation stations*

with an average height of about 27 m (LAI[1] = 4.3), the understory small shrub and moss layers, are dominated by blueberry (*vaccinium myrtillus*) and moss (*sphagnum girgensohnii*), respectively.

The continuous year round aircraft flask sampling at the top of the CBL was performed at Syktyvkar, west of the Ural mountains (see Figure 3.1). The Syktyvkar aircraft program is run by IPEE[2] in close co-operation with MPI-BGC[3]. The flight location for Syktyvkar is at 51°E, 62°N over the north European taiga about 400 km west of the Ural mountains. Vertical profiles of continuous CO_2 NDIR measurements as well as virtual temperature and relative humidity are measured every 2 to 4 weeks. Duplicate flasks are collected at 2000 m, 2500 m and 3000 m a.s.l. Flask samples have been analysed in Heidelberg for CO_2 and stable isotope ratios of CO_2 as well as for CH_4, N_2O and SF_6 mixing ratios.

[1]Leaf area index. Unit: m^2/m^2. Half the total green leaf area (one-sided area for broad leaves) in the plant canopy per unit ground area. Globally, it varies from less than 1 to above 10 but also exhibits significant variation within biomes at regional, landscape and local levels [Chen and Black, 1992].

[2]Severtsov Institute of Evolution and Ecology Problems, Russian Academy of Sciences, V.N. Sukatschev's Laboratory of Biogeocenology, Moscow, Russia

[3]Max-Planck-Institut für Biogeochemie, Jena, Germany

3.2 Measurements

In order to characterise the change of CO_2 concentration and CO_2 stable isotope ratios in time and space within the ecosystem canopy, ambient flask air sampling at a tower (31 m height) was performed. During the very first campaign in summer 1998, flasks were collected at 15.3 m above ground and flushed in series to verify the sampling quality. To obtain the vertical gradient within the canopy, during the intensive campaigns in 1999 the flasks were sampled from two heights, 26.3 m and 1.8 m (tubing: Decabon furon 1300). During all intensive campaign periods, a time resolution of 2 hours for flask sampling was performed. Two

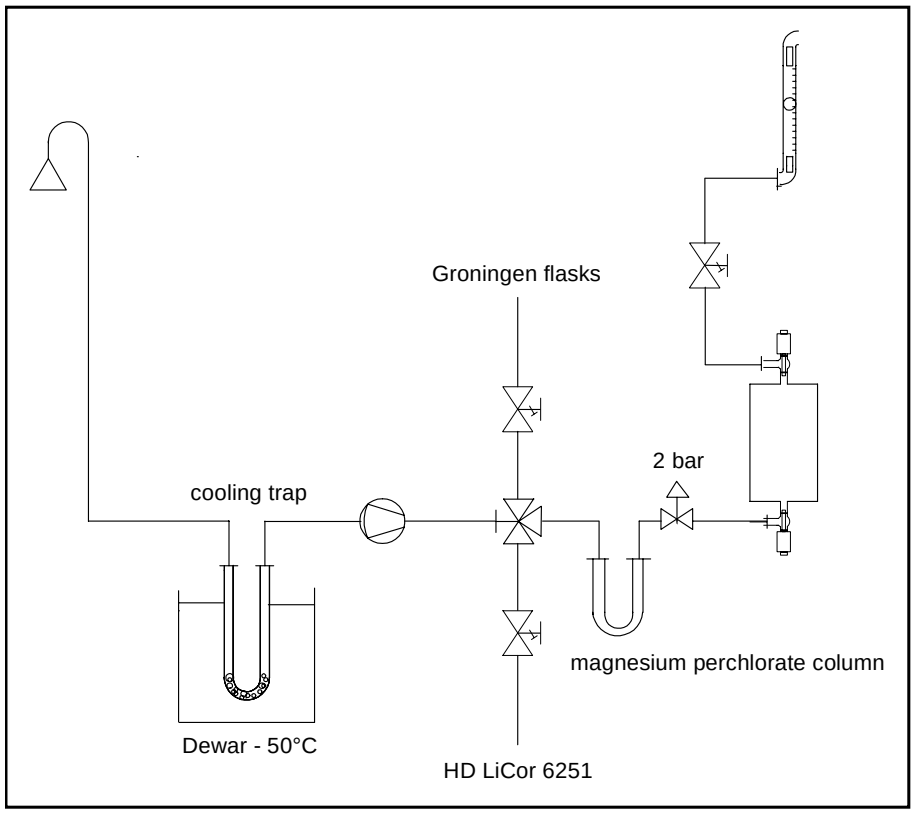

Figure 3.2: *Flask sampling set-up at the canopy tower during the intensive campaigns*

preconditioned glass flasks (1.2 liter volume each) were flushed (air flow about 2 l/min, pump: KNF Neuberger PM 16029, 24V) with atmospheric air for about 30 minutes and finally pressurised to 2 bar (Figure 3.2). The stable isotopes of the canopy air flask samples were analysed in the Heidelberg laboratory with a Finnigan MAT 252 mass spectrometer, combined with a multiport trapping box for CO_2 extraction [Neubert, 1998]. Typical reproducibilities for flask CO_2 stable isotopes are (1 σ) are $\pm$ 0.015 ‰ for $\delta^{13}C(CO_2)$ and $\pm$ 0.03 ‰ for $\delta^{18}O(CO_2)$. CO_2 mixing ratios were measured with an automated HP 5890 series II gas chromatograph equipped with a flame ionisation detector (FID) for detection of CO_2 [Bräunlich, 1996]. The reproducibility of the CO_2 concentration analysis (1σ) is $\pm$ 0.1 ppm.

A combined sampling set-up was designed to allow flushing of the 1.2 l flasks and 2 l flasks and the continuous LiCor CO_2 detector (see below). The 2 l flasks were sampled by the Groningen group in order to perform O_2/N_2 measurements. Condensation of water vapour within the flask can lead to an isotopic change of the sampled $\delta^{18}O$ signal via the exchange of

oxygen atoms between water and carbon dioxide [Gemery *et al.*, 1996]. A cryo-cooling system prior to a chemical drying column (magnesium perchlorate) was implemented in the 26.3 m and 1.8 m sampling lines which reduced the vapour pressure of the air streams to a dewpoint of less than -40°C. The cryo-cooling system consisted of a commercial cryocooler (NESLAB

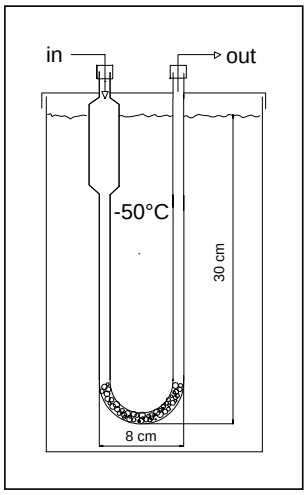

Figure 3.3: *Design of the cold trap for water vapour sampling*

CC-65) combined with specially designed cooling traps (Figure 3.3). As the ^{18}O signature of water vapour is an important component of the total ^{18}O balance at the tower site, the water vapour samples from cryogenic drying of the ambient air were used for $^{18}O(H_2O)$ analysis (time resolution of integrated samples: 4 hours). To increase the interacting surface between the airstream and the cold trap, glass spheres (4mm diameter) were filled into the bottom of the cold trap. Additional factors, that decrease sampling efficiency, is the relaxation length of the water vapour diffusion to the walls of the cold trap and the systematic loss of water vapour due to the finite water vapour partial pressure. The loss due to the relaxation length was minimised by the design of the cold trap and the overall loss of water vapour was determined not to change the $\delta^{18}O$ signature by more than $+0.4‰$. For ambient dew points between 10 and 25°C the cooling traps yield an H_2O sampling efficiency of more than 99.8 %. The typical reproducibility of the $H_2^{18}O$ isotope analysis (Finnigan MAT 252) is $\pm$ 0.02‰.

Within the Diploma Thesis framework of Tobias Naegler continuous CO_2 concentration was measured with NDIR (Non-Dispersive Infrared Spectroscopy, LiCor 6251) at the same heights, where flask samples were taken [Naegler, 1999]. The basic idea of these measurements was to correlate CO_2 variations with simultaneously measured ^{222}Radon activity changes. ^{222}Radon is a radioactive noble gas (half life: 3.8 days) and a decay product of the ^{238}Uranium decay sequence. The only source for atmospheric ^{222}Radon is the soil, where it diffuses from the soil air to the atmosphere after the production via the decay of ^{226}Radium. As ^{222}Radon has the same transport characteristics in the atmosphere as CO_2, ^{222}Radon activity can be exploited as a transport tracer. With the Heidelberg Radon Monitor, atmospheric ^{222}Radon activity was measured with the static filter method at the same heights where flasks were taken with a time resolution of 30 minutes [Levin *et al.*, 2001]. Via correlation of the CO_2 and ^{222}Radon variability, nocturnal CO_2 fluxes can be estimated [Naegler, 1999; Naegler *et al.,* 2001].

As input for this so called "Radon-tracer-method" the ^{222}Radon soil exhalation flux has to be determined via the closed chamber method for the catchment area around the measurement tower. Soil flux measurements of CO_2 and ^{222}Radon were performed via the

so-called "Lundegardh chamber method", where a closed diffusion chamber (with one open end) is placed air tight onto the soil. Here a method developed by Dörr and Münnich [1990] is performed. Trace gases, that diffusive out of the soil following a concentration gradient between the soil air and the atmosphere, accumulate within the chamber volume. Following Dörr [1984], the associated soil flux of a trace gas, F_{gas}, is given by:

$$j_{gas} = (h + \Delta z) \cdot \frac{c_{gas}(t_0 + \Delta t) - c_{gas}(t_0)}{\Delta t} \tag{3.1}$$

with

h :	height of the chamber (here about 30 cm)
$c_{gas}(t)$:	concentration (or activitity in case of ^{222}Radon) of the observed gas at a time t.
Δt:	time difference between two samples, collected at t_0 and t, respectively
Δz:	term to correct for the change of the concentration gradient between the soil air and the air in the chamber volume ($\Delta z < 4$ % for $\Delta t < 1$ hour) [Dörr, 1984]

Immediately after closing the chamber at the sampling site, circa 300 ml of air are sucked out of the chamber volume via a syringe into a 500 ml aluminium bag, to determine $c_{gas}(t_0)$. The exhaling soil gases were then accumulated for about one hour and a final sample was subsequently collected to determine $c_{gas}(t_0+\Delta t)$. After fast transportation back to Heidelberg the CO_2 concentration was analysed via gas chromatography [Greschner, 1995] and ^{222}Radon activity via slow-pulse ionisation chambers [Fischer, 1976]. As the soil ^{222}Radon exhalation flux is mainly controlled by the water content of the soil [Dörr and Münnich, 1987], soil flux measurements were regularly performed along a hydrological transect during the intensive campaign periods [Levin *et al.*, 2001].

To link the vegetation driven CO_2 variability with the concentrations in the CBL, aircraft flight flask sampling was performed three times a day during early morning, midday and afternoon. However, the Antonov-AN2 could not always fly, due to low visibility and bad weather conditions. Vertical aircraft profiling for flask sampling was performed with local Antonov-

Figure 3.4: *Fyodorvskoye forest tower along with flying Antonov II during the intensive campaign in summer 1999*

AN2 bi-plane aircraft. Separate air intake lines (6 mm Decabon tubing) for continuous LiCor

6152 CO_2 measurements and for flask sampling systems were installed in the wings of the Antonov-AN2 aircraft. Whole air samples were collected into 1-liter cylindrical flasks made of Pyrex glass and PFA o-ring valves (Glass Expansion, Australia) at both ends. Drying of the air was performed with magnesium perchlorate. Flasks were flushed for more than 5 minutes at a flow rate of ca. 4 l per min, and pressurised to 1 atm above ambient pressure at final filling (pump: KNF-Neuberger, N86KNDC with neoprene membrane). The samples were taken at heights of 100, 200, 300, 500, 700, 1000, 1500, 2000, 2500 and 3000 meter above ground, and analysed for CO_2 concentration and CO_2 stable isotopes at LSCE[4] [Ramonet *et al.*, 2001]. The interfacing of the canopy tower measurements and the Antonov-AN2 CBL profiling is illustrated in Figure 3.4.

Net ecosystem exchange (NEE) of CO_2 was measured continuously via eddy correlation in addition to the meteorological parameters at the top of the forest tower [Milukova *et al.*, 2001].

To characterise the ^{13}C and ^{18}O isotopic composition of CO_2 exchanged with the leaves and the soils, leaves and soil material was sampled over the course of the intensive campaigns. The sampling frequency was 4 hours and was synchronised with the tower and aircraft sampling schedule. Deciduous tree leaves and coniferous tree needles have been sampled at two levels (about 10 m and 22 m above ground) as well as moss and blueberry leaves and stems with the same time resolution. Furthermore, once per day (around midday) a trunk wood core of the deciduous and of the coniferous tree was sampled, and a soil core (60 cm depth with a 10 cm vertical resolution) underneath each tree. Vegetation samples were analysed for $\delta^{18}O$ of bulk water and $\delta^{13}C$ of the organic material at the Laboratoire de Biogéochimie Isotopique, Université Pierre et Marie Curie in Paris, using vacuum distillation prior to the isotopic analysis of the plant H_2O [Bariac *et al.,* 1990; Bariac *et al.,* 1994b].

[4]Laboratoire des Sciences du Climat et de l'Environnement, Saclay, France.

Chapter 4

Results of the Field Campaigns in Russia

4.1 Hydrological Characterisation

To characterise the basic seasonal patterns of the regional biospheric activity within the observed ecosystem at the Fyodorovskoye forest, the knowledge of the water input via precipitation is important. As soil CO_2 fluxes vary with temperature and soil water content and soil ^{222}Radon fluxes vary with soil water content, their seasonal variation can be interpreted together with the seasonal variation of temperature and precipitation. Furthermore, the investigation of $\delta^{18}O$ in atmospheric CO_2 requires the knowledge of the $\delta^{18}O(H_2O)$ of the respective interacting water pools. Precipitation water builds up in the soil, where it is integrated in time. The soil water isotopic composition in turn is the reference for the variation of $\delta^{18}O(H_2O)$ within the plants.

At the Fyodorovskoye forest site, both, monthly mean temperature and monthly cumulated precipitation, show a strong seasonal cycle from June 1998 to December 1999 (see Figure 4.1). Average temperature for this period is 5.95 °C with the coldest month in January 1999 with -9.7 °C and the warmest in June 1999 with 21°C. Temperature and precipitation both show a similar seasonality. During winter between January 1999 and April 1999 there was no detectable rain, whereas during summer, monthly cumulative rain peaks were as high as 400 mm/month in September 1999. Annual precipitation from June 1998 to June 1999 was 577 mm, which is comparable with the long term mean of 549 mm. The mean seasonal cycles of precipitation water $\delta^{18}O$ and $\delta^{2}H$ stable isotope signatures at the GNIP station Kalinin (Figure 4.1) also show a strong seasonal cycle with enriched values of about -8 ‰ in $\delta^{18}O$ and -60 ‰ in $\delta^{2}H$ during summer-time and most depleted values of -17 ‰ / -140 ‰ during winter-time. This cycle is the well known consequence of the temperature dependent fractionation during the rain-out of clouds. The lower the condensation temperature, the lower the number of rare isotopes ^{18}O and ^{2}H is in the precipitation. However, the isotopic signature does not only carry the temperature information of the condensation process prior to the rain-out, but also the temperature information of the region of evaporation. Basically, both processes, condensation and evaporation, show more depleted values with decreasing temperatures [Mook, 1994]. However, precipitation samples taken during the intensive campaigns and irregularly during the project period, show significantly different values compared to the long term mean. Especially during summer 1998 a shift to more depleted $\delta^{18}O(H_2O)$ values from about -2 ‰ to -16 ‰ is observed within nearly three weeks alone. During this rain intensive summer the mean $\delta^{18}O$ changed significantly from -5.5 ± 1.2 ‰ between July 24 and

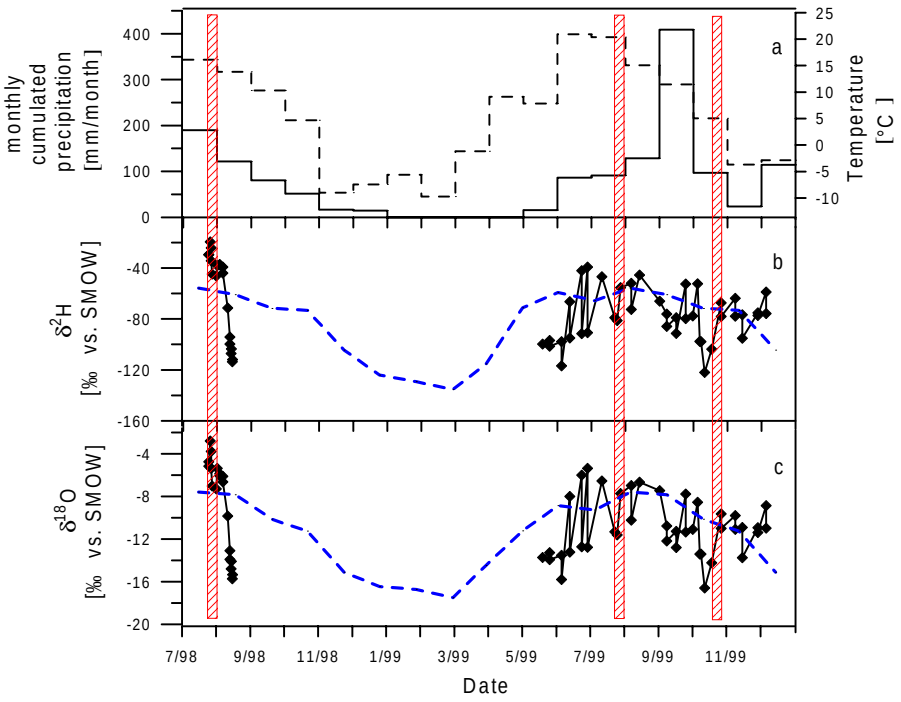

Figure 4.1: *Seasonal cycles of monthly cumulated precipitation (solid line) and monthly mean temperatures (dashed line) (a), $\delta^2 H$ (b) and $\delta^{18} O$ (c) in precipitation water at the Fyodorovskoje forest station. The dashed blue lines in (b) and (c) represent the mean seasonal cycle of precipitation water isotopes at the GNIP (Global Network for Isotopes in Precipitation) station Kalinin (the former Soviet Union name of Tver, 56°54'N, 35°54'E) of the years 1981 to 1988 [IAEA/WMO, 1998]. The shaded areas symbolise the periods of the intensive campaigns.*

August 4 to -13.8 ± 1.8 ‰ between August 8 to August 12. These short term changes may be due to the changing origin of the condensing water vapour from southern to colder northern condensation sites. Comparable deviations of the precipitation sample isotopic signatures and the long term mean are also observed for the period from spring 1999 to end of 1999.

4.2 Summer 1998

In order to test all measurement and sampling systems for the very first intensive campaign during the EUROSIB project, the summer 1998 campaign started for one day on July 24 in 1998. After three days measurement and sampling break, four consecutive days of intensive sampling and measurements were performed between July 27 and August 1.

4.2.1 Meteorology

Unfortunately, during the first campaign test day the data logger assimilation broke down, therefore no meteorological data is available (Figure 4.2). From July 26 onwards the temperature measured on top of the forest tower at about 30 m showed a clear diurnal cycle with maximum values of about 20°C between July 26 and July 28 during day-time and minimum values of about 12°C during night-time. From July 27 to July 29 temperature generally in-

creased up to 27°C during day and to 18°C during night. Heavy rain started in the evening of July 29 for about 24 hours and due to an extremely cloudy sky, July 30 was relatively cold throughout the day with about 18°C. The whole summer 1998, and especially July 1998, was characterised by an untypically high amount of precipitation (see Figure 4.1). These wet conditions were directly translated into a nearly waterlogged soil floor and into very high relative humidity values within the forest canopy. Relative humidity showed, temperature anti-correlated, maximum values of about 90 % during night-time and minimum values of about 50 % during day-time. During the extreme rainfall from July 29 to July 30 relative humidity reached saturation with 100 %.

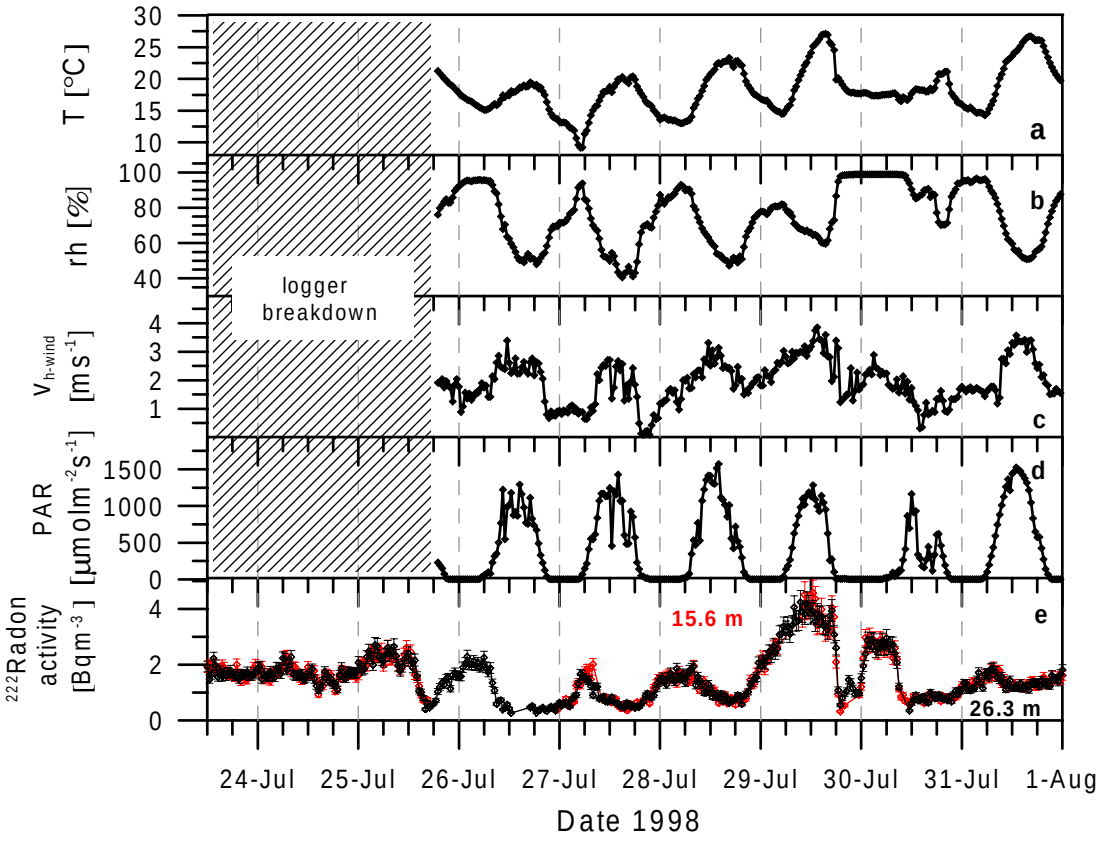

Figure 4.2: *Meteorological parameters observed during the intensive summer campaign 1998: (a) temperature, (b) relative humidity, (c) horizontal windspeed, (d) photosynthetically active radiation (PAR) as well as (e) ^{222}Radon activity at two heights (26.3 m and 15.6 m, error bars indicate 10% statistical counting error).*

Horizontal wind speed as a proxy of turbulent mixing also showed clear diurnal variations from July 25 to July 28 with day-time values of about 2.5 ms^{-1} and night-time values of about 1 ms^{-1}. From the evening of July 28 onwards, wind speed generally increased by about 1 ms^{-1} to calm down again on July 30. Photosynthetically active radiation (PAR) exhibits a pronounced diurnal cycle with maximum day-time radiation of about 1300 μmol m^{-2}s^{-1}, except for July 30, where clouds shielded solar radiation. PAR gets zero between 22:30 pm and 4:30 am. The atmospheric ^{222}Radon activity shows diurnal variations for both heights, mostly with no significant vertical gradient within the statistical counting error between 15.6 and 26.3 m above the ground. Due to the high soil water table in the forest,

namely a nearly waterlogged soil surface, the soil ^{222}Radon exhalation flux is expected to be very low [Dörr and Münnich, 1987]. The mean ^{222}Radon soil source strength of all 6 sampling sites for the catchment area of the tower site is determined to 4.7 ± 2.2 Bq m^{-2}h^{-1} [Naegler *et al.*, 2001].

4.2.2 CO_2 Mixing Ratio and Stable Isotopes

During this first intensive campaign flask sampling was performed directly beneath the forest tower, without any roofing. The flask sampling was performed only at one height, at 15.6 m, but two flasks were sampled in order to test the reproducibility of the sampled flasks. Due to an unstable 220 Volt power supply (regular and irregular, daily power cutoff by the power company in the order of several hours), cryogenic drying of the sampled air was impossible. Therefore, the drying of the flasks could only be performed chemically via a magnesium perchlorate column prior to the flask inlet (see Figure 3.2 in Chapter 3.2). Due to the very

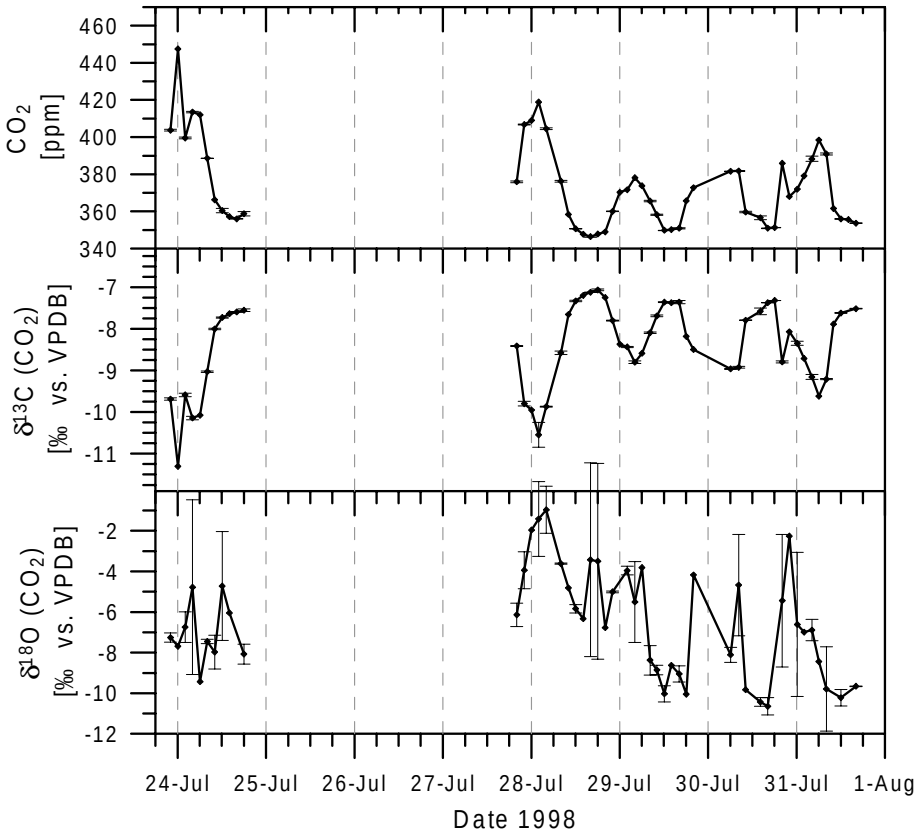

Figure 4.3: *Diurnal cycles of flask CO_2 concentration (top), $\delta^{13}C(CO_2)$(middle) and $\delta^{18}O(CO_2)$(bottom) during the summer campaign in 1998 at 15.6 meter above ground. Plotted are the mean values of a pair of flasks flushed in series. Error bars indicate the standard deviation (1 σ) of the flask pairs.*

high relative humidity and the frequent rainfall during sampling, flasks could not be sampled perfectly dry, despite the replacement of the magnesium perchlorate column after every sampling. Therefore, flasks had to be additionally dried prior to the gas chromatographic analysis at the Heidelberg laboratory, to avoid dilution of the measured air by water vapour. To determine the water vapour impact on the CO_2 mixing ratio due to dilution, the flasks

were measured twice: the first time without and the second time with additional cryogenic drying prior to the gas chromatograph. Indeed measurements show a water vapour concentration in the sampled flasks between 1 and 2%, depending on the atmospheric water vapour concentration during sampling (Figure 4.4).

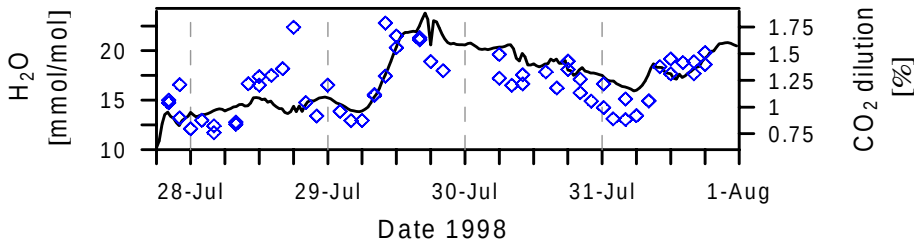

Figure 4.4: *Dilution effect on the measured CO_2 concentration of the flasks (blue) along with ambient water vapour concentration (black).*

Diurnal variations of CO_2 concentration and stable isotope ratios at 15.6 m height within the forest canopy measured on the flask samples are shown in Figure 4.3. The mean CO_2 difference between the first and the second flask flushed in series for the whole period is -0.3 ± 0.6 ppm. Depending on the meteorological conditions within the canopy, CO_2 concentration shows a strong diurnal cycle with maximum concentrations in the morning and minimum values during the afternoon. During the intensive campaign period the CO_2 amplitude of this diurnal cycle at 15.6 m varied between 35 and about 70 ppm. The variation in night-time amplitudes is due to different night-time inversion strengths. As can be seen in Figure 4.2, the horizontal wind speed at the top of the canopy is relatively high during nights with small night-time CO_2 values. The respirative source CO_2 signal at 15.6 m is considerably diluted by the mixing of CBL air during day-time, whereas there is higher variability during night-time inversion build up. The mean difference between the first and the second flask flushed in series for $\delta^{13}C(CO_2)$ during the whole period is 0.004 ± 0.08 ‰. The $\delta^{13}C(CO_2)$ variability shows a strongly anti-correlated behaviour to CO_2 concentration, with values between -11.25 ‰ to -8.8 ‰ during night-time and between -7.5 and -7.25 ‰ during day-time. Following Equation 2.14, correlation of the $\delta^{13}C(CO_2)$ against the inverse CO_2 concentration yields the apparent isotopic source signature of $\delta^{13}C$ within the ecosystem canopy. This so called "Keeling" plot

Table 4.1: *$\delta^{13}C(CO_2)$ source signatures. (day-time: 7:00 am - 7:00 pm, night-time: 9:00 pm - 5:00 am.)*

Period	$\delta^{13}C_s(CO_2)$ [‰ vs VPDB]	correlation coefficient r^2
overall	-25.96 ± 0.20	0.99
day-time	-25.33 ± 0.46	0.98
night-time	-26.04 ± 0.35	0.99

is presented in Figure 4.5(a). The apparent $\delta^{13}C$ source signature for the overall campaign period is calculated to -25.96 ± 0.20 ‰. However, there is a significant difference between the separately calculated day-time (CO_2 concentration decrease) and night-time (CO_2 concentration increase) source signatures: whereas during night the source shows a mean value of -26.04 ± 0.35 ‰, the day-time signature is more enriched with -25.33 ± 0.46 ‰. This difference of

0.71 ‰ is just significant within the 1 σ confidence level. The day-time enrichment of the source signature illustrates the slight enrichment of photosynthetic assimilation compared to soil respiration.

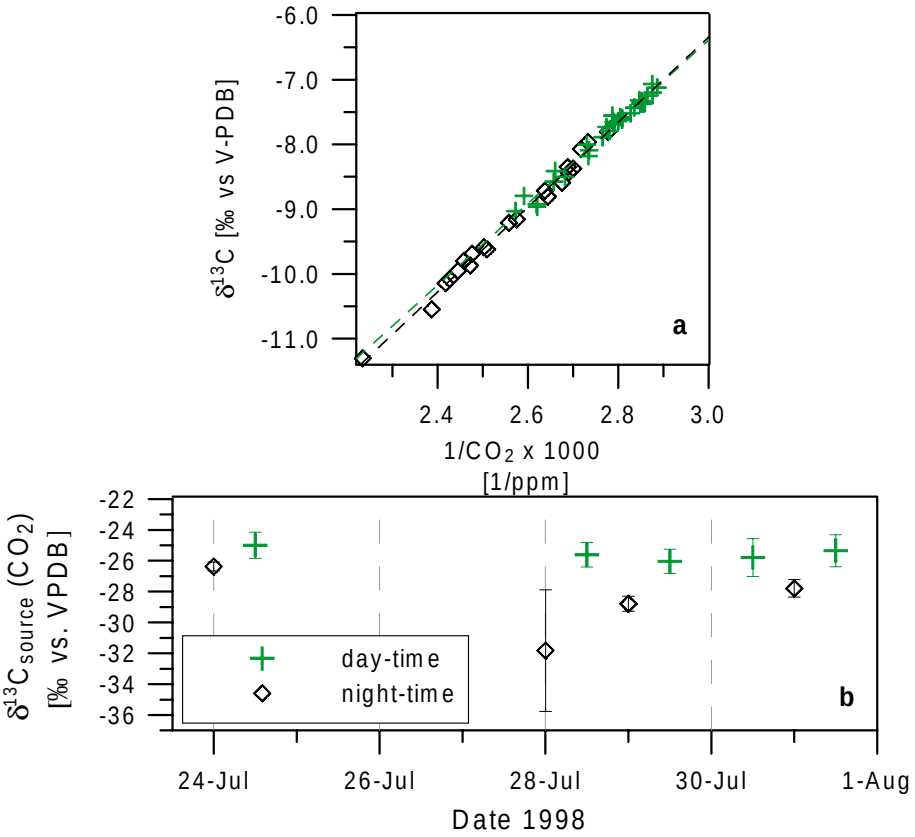

Figure 4.5: *"Keeling plot" of $\delta^{13}C(CO_2)$ for day and night time values (a, day-time: 7:00 am - 7:00 pm, night-time: 9:00 pm - 5:00 am.). Panel (b) presents the apparent $\delta^{13}C$ source signatures calculated for the respective single days and nights.*

Further inspection of the δ^{13}C source signature daily variability is presented in Figure 4.5(b), where the source signatures are calculated for every single day and night. Here, the day to night difference is even more pronounced with a mean value of -25.56 ± 0.36 (n=5) for the day-time correlations and -27.65 ± 0.99 (n=3) for night-time correlations, where the value of the night of July 28 is excluded, due to its poor correlation coefficient (r^2=0.93).
In principle, the correlation between CO_2 and $\delta^{18}O(CO_2)$ should be the same like the correlation between CO_2 and $\delta^{18}O(CO_2)$. As described in Chapter 2.2.2, the respiration δ^{18}O signal is expected to be depleted and the photosynthetic assimilation impact is expected to be enriched in ^{18}O. In the context of the Keeling approach, the basic difference between δ^{18}O and δ^{13}C is, that $\delta^{18}O(CO_2)$ observed in the atmosphere is not a two- but a multiple component mixing. The mechanisms controlling the $\delta^{18}O(CO_2)$ correlation to CO_2 are schematically presented in Figure 4.6. The mixing line is a simple straight line intersecting the values of only two sources of the ambient $\delta^{18}O(CO_2)$ mixture. That is the respiration δ^{18}O signal, assumed to be depleted due to the interconnection to soil water, and the free tropospheric values, representing continental background conditions. If the effect of photosynthetic assimilation or ambient CO_2 equilibration with water surfaces within the canopy is absent or negligible, then the Keeling two component mixing should provide

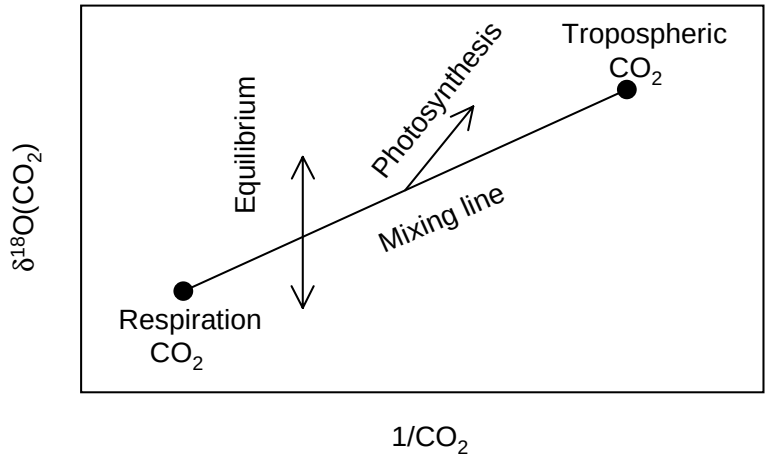

Figure 4.6: *Hypothetical relationship between $\delta^{18}O$ and the inverse CO_2 mixing ratio within a canopy.*

the straight mixing line. However, as discussed before, photosynthetic activity has the potential to change ecosystem ambient $\delta^{18}O(CO_2)$ without changing ambient CO_2 in the same relationship. This is due to the partly compensating retrodiffusive CO_2 flux out of the leaves; the ambient ecosystem $\delta^{18}O(CO_2)$ is "washed" to enriched values by the leaves. The other factor leading to a deviation from the two-component mixing line, is the equilibration of ecosystem ambient CO_2 with wet surfaces in condensed water droplets. The impact of both potential deviations from the two-component mixing line on ambient $\delta^{18}O(CO_2)$ gets larger if the amount of turbulent mixing between the ecosystem and the troposphere is low. During this summer 1998 campaign the forest represented an enormous surface of liquid water. The soil was largely waterlogged and the leaf and plant surfaces were permanently wet. Therefore, a reasonable analysis of the ecosystem $\delta^{18}O(CO_2)$ variations via the Keeling two-component mixing approach is not possible and any potential change in the apparent source composition would misslead the interpretation of the $\delta^{18}O$ source signature. The same, but not as wet conditions, were present during the following campaigns in summer and autumn 1999.

Due to the hight water vapour content in the sampled flasks, the $\delta^{18}O(CO_2)$ canopy variations are difficult to interpret, as possible isotopic exchange between condensed water at the flasks surfaces and CO_2 in the flask may have changed the $\delta^{18}O(CO_2)$ of the sample [Gemery *et al.*, 1996]. Ecosystem $\delta^{18}O(CO_2)$ was observed to vary between -11 ‰ and -1 ‰ without any significant diurnal cycle, except for the night from July 27 to July 28. Here, $\delta^{18}O(CO_2)$ is getting enriched in correlation with the nocturnal CO_2 mixing ratio increase, qualitatively indicating an enriched $\delta^{18}O(CO_2)$ source, which does absolutely not agree with theory. Also a possible equilibration with soil/surface water can not explain this enriched value, as the soil water isotopic composition suggest an equilibrated $\delta^{18}O(CO_2)$ of about -10 ‰ (see Chapter 4.2.3). The same $\delta^{18}O(CO_2)$ "puzzle" continues, if one investigates the aircraft profiles in the CBL in Figure 4.7 (right panel). Here, the variability of $\delta^{18}O(CO_2)$ also shows large scatter between -13 ‰ and 0 ‰. The most striking feature of the $\delta^{18}O(CO_2)$ profiles, if compared with the profiles of CO_2 mixing ratio and $\delta^{13}C(CO_2)$ is, that there is no significant difference between the early morning profiles (crosses in Figure 4.7) and the day-time profiles. The early morning profiles were sampled as early as possible

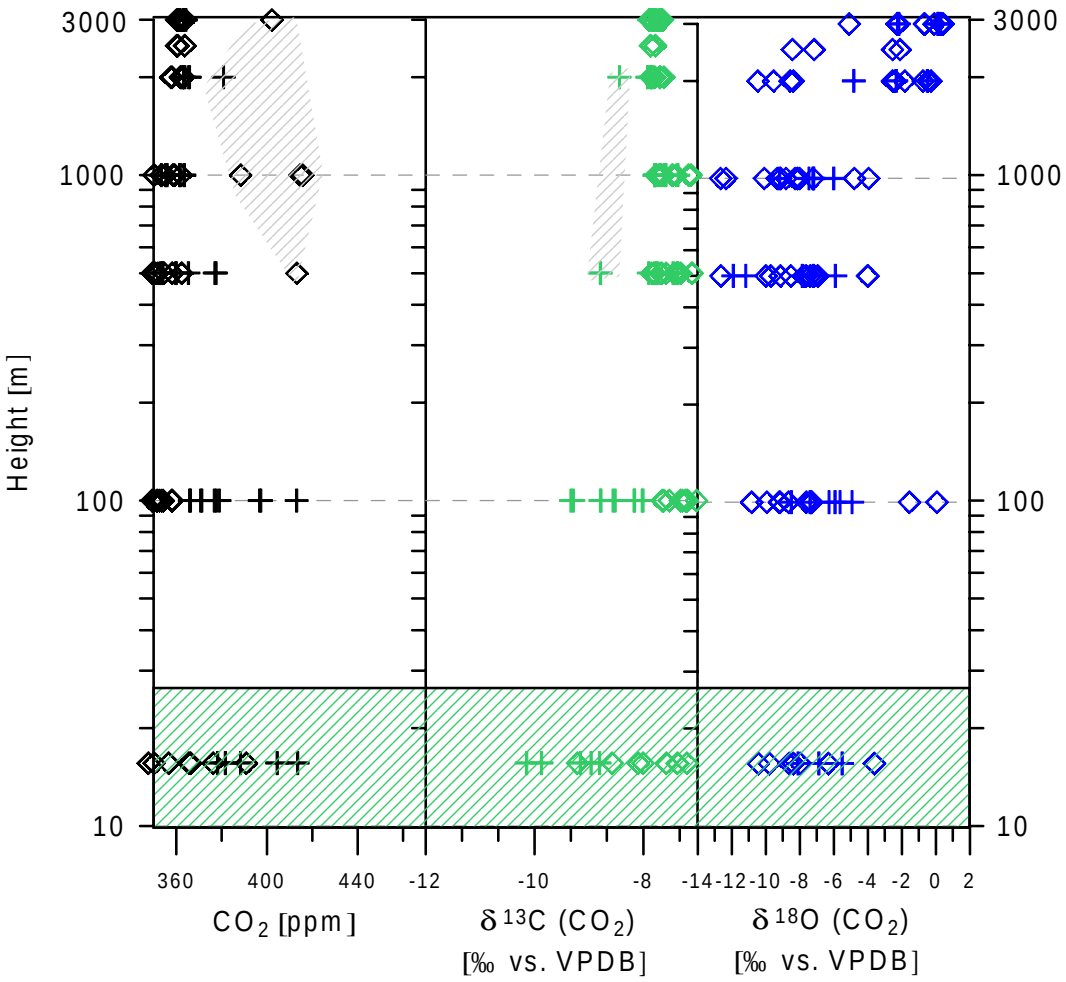

Figure 4.7: *Aircraft profiles along with the simultaneous canopy data (shaded green area). The crosses refer to the first profile in the early morning.[Ramonet* et al.*, 2001]*

around 6 am (unfortunately, for the Antonov-II, there is no way to fly during darkness) and they should represent the night-time respiration situation, connected with typical night-time vertical inversion situation. The day-time flights took place in the morning around 10 am and again in the afternoon around 3 pm. Therefore, the day-time profiles should provide information on the mixed condition of the CBL in connection to the ecosystem canopy. The CO_2 mixing ratio as well as the $\delta^{13}C(CO_2)$ profiles clearly show this pattern. The early morning profiles show a significant vertical gradient if compared to the mixed situation during day-time. There is a increase in CO_2 due to the ecosystem respiration source to values grater than 400 ppm during early morning, whereas the day-time profiles tend to smaller values. Analog is the variation of $\delta^{13}C(CO_2)$, where depleted values are observed during the early-morning situation, due to the influx of depleted respiratory $\delta^{13}C(CO_2)$. However, there are some samples from 1500 to 3000 m height, that show higher CO_2 concentration, that may represent contamination of the samples by fossil sources (shaded grey area in Figure 4.7). For $\delta^{18}O(CO_2)$, there is no difference between the day and early morning profiles and the scatter roughly shows the same behaviour from the canopy up top 3000 m height. As one would expect values for $\delta^{18}O(CO_2)$ of around 0‰ in the upper CBL, it is quite possible, that the aircraft flasks were also not sampled perfectly dry and $\delta^{18}O(CO_2)$ values vary due

to isotopic exchange with condensed water in the flasks. After "learning the hard way" under this unexpected wet conditions in 1998, the flask drying was improved for the following campaigns by adding the cryocooling system to the canopy sampling system. The french colleagues, who were responsible for the profiling, added additional magnesium perchlorate columns to improve drying efficiency of the aircraft flask sampling system.

4.2.3 $H_2^{16}O/H_2^{18}O$ of Plant Tissue

As mentioned before, the summer 1998 campaign was characterised by untypically high amounts of precipitation for this region. Compared to July 1999 with 91.3 mm precipitation, during July 1998 190 mm rain accumulated at the Fyodorovskoye forest site. Therefore, the easiest samples to take in 1998 were soil surface water samples of the waterlogged soil. Figure 4.8(a) presents the $\delta^{18}O(H_2O)$ variations of the different vegetation water pools and the $\delta^{18}O$ of the surface water. Despite the fact that the mean $\delta^{18}O(H_2O)$ of precipitation

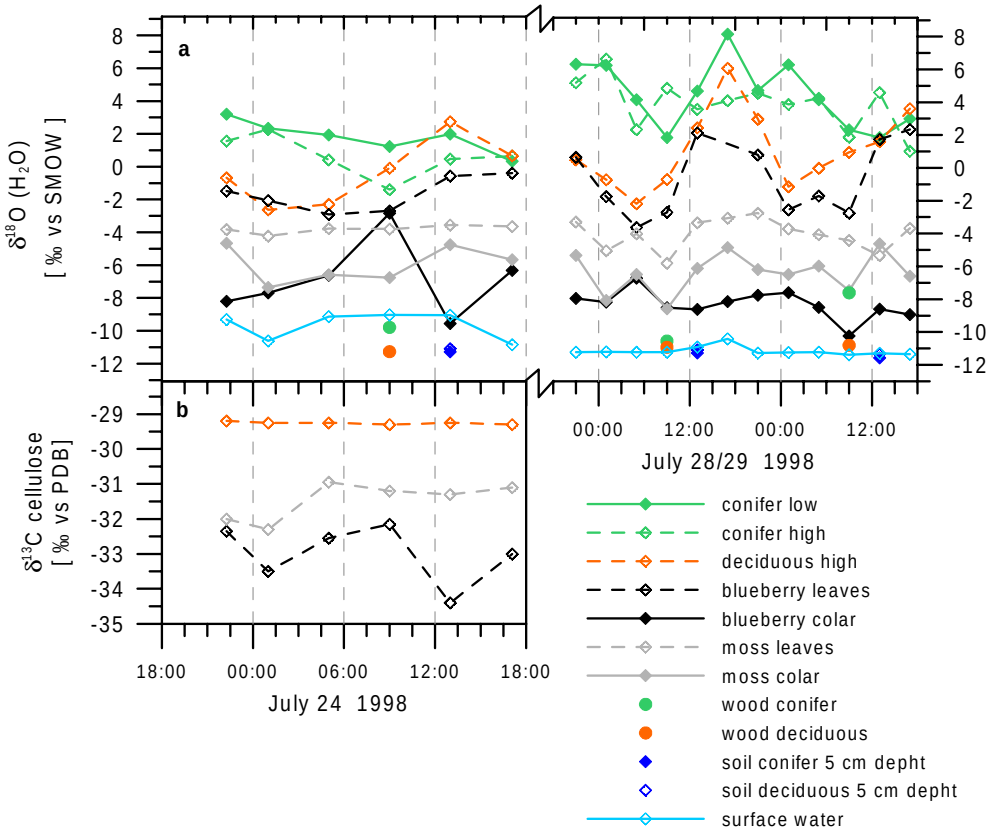

Figure 4.8: *Diurnal $\delta^{18}O(H_2O)$ variations of the different vegetation water pools along with soil and trunk $\delta^{18}O(H_2O)$ (a) and diurnal $\delta^{13}C$ variations of plant tissue material (b).*

between July 23 and July 24 is -4.2 ‰, the soil surface water shows relatively heterogeneous values between -9 and -11 ‰. During July 28/29 the mean precipitation got more depleted to -5.7 ‰ and the soil surface water stayed relatively stable at -11 ‰. Interesting is the comparison between the soil surface water $\delta^{18}O$ and the $\delta^{18}O$ of the conifer and deciduous stem wood water and the soil water at the top 5 cm layer, respectively. The conifer and the deciduous stem wood water, which represents the long term soil water input to the plants, as well as the soil top layer water, show slightly depleted values compared to the soil surface water. This

situation is again different between July 28 and July 29, where all reservoirs show comparable values of about -11 ‰. The point to make is, that the input of enriched precipitation water could be observed on July 24, whereas slow mixing of surface water with depleted soil water leads to a homogeneous distribution of the soil surface water isotopic composition. Apart from short term variation of precipitation δ^{18}O, a constant δ^{18}O(H_2O) of the top soil layer is observed. The same is true for the deciduous wood water. However the conifer stem wood water shows values from -7.5 to -10.5 ‰. To get a principal idea of the spatial heterogeneity within the vegetation δ^{18}O of the different classes, duplicate samples were taken and analysed. Table 4.2 presents the mean differences between the duplicates. Investigation of the

Table 4.2: *Mean $\delta^{18}O(H_2O)$ differences for analysed water (along with the standard deviations) and vegetation duplicate samples*

Sample	mean difference of duplicates [‰ vs VPDB]	n
conifer high	0.38 ± 1.08	17
conifer low	0.63 ± 1.77	17
deciduous high	0.31 ± 1.73	18
blueberry leaves	0.37 ± 1.25	18
blueberry colar	0.12 ± 1.33	17
moss leaves	0.37 ± 1.04	18
moss colar	0.17 ± 1.25	18
soil water	0.23 ± 0.26	4
surface water	0.01 ± 0.24	12

δ^{18}O water pools within the plants in vertically upward direction exhibits the striking overall feature of a general enrichment of the δ^{18}O from bottom to top of the canopy ecosystem vegetation. Moss and blueberry collar show values between -10 to -5 ‰ with an overall mean value of -6.9 ± 1.6 ‰ (standard deviation) during the campaign period. Whereas the moss leaves stay quite stable between -6 and -3 ‰, the blueberry leaves show higher variation in time with δ^{18}O values between -4 to 2.2 ‰. The overall mean for the understory leaf regime is -2.5 ± 2.0 ‰. Moving further upward to the tree leaves, the deciduous high level (about 23 m above ground) leaves vary between -2 and 6 ‰. Two levels for the coniferous tree, the low level (about 12 m above ground) as well as the high level, again show a generally increased enrichment with values between -1 and 8 ‰. The tree leaf regime shows an overall mean δ^{18}O of 2.34 ± 2.46 ‰. Summarizing the general vertical gradient behaviour of δ^{18}O within the ecosystem, vertical enrichment can be classified via the mean (± standard deviation)

soil water: -11.33 ± 0.33 ‰
stem tree water: -9.98 ± 1.37 ‰
understory colar water: -6.92 ± 1.56 ‰
understory leaf water: -2.52 ± 2.0 ‰
tree leaf water: 2.34 ± 2.46 ‰

Further inspection of the diurnal variation of the respective water pools exhibits strong diurnal cycles for the blueberry leaves and the deciduous leaves with significantly enriched δ^{18}O during day-time and amplitudes of up to 6 ‰.

4.3 Summer 1999

4.3.1 Meteorology

With more than 100 % less precipitation compared to July 1998, the soil surface was not waterlogged and the soil water table depths at around 10 cm. Also, there was no need to wear rubber boots during fieldwork in the intensive summer campaign in July 1999, the most significant indicator for drier conditions in 1999. During the 5 day measurement period the overall meteorological conditions were characterised by periodic, solar driven diurnal cycles. As shown in Figure 4.9 air temperature varied between 12°C during night and maximum values of 24°C during day, accompanied by anti-correlated variation of the relative humidity ranging between 85 % during night and day-time values of about 30 to 40 %. Also the horizontal wind, measured on top of the canopy, shows significant diurnal cycles with night-time windspeeds between 1 to 2 m s^{-1} up to 4 m s^{-1} during day. Inspection of photosynthetically

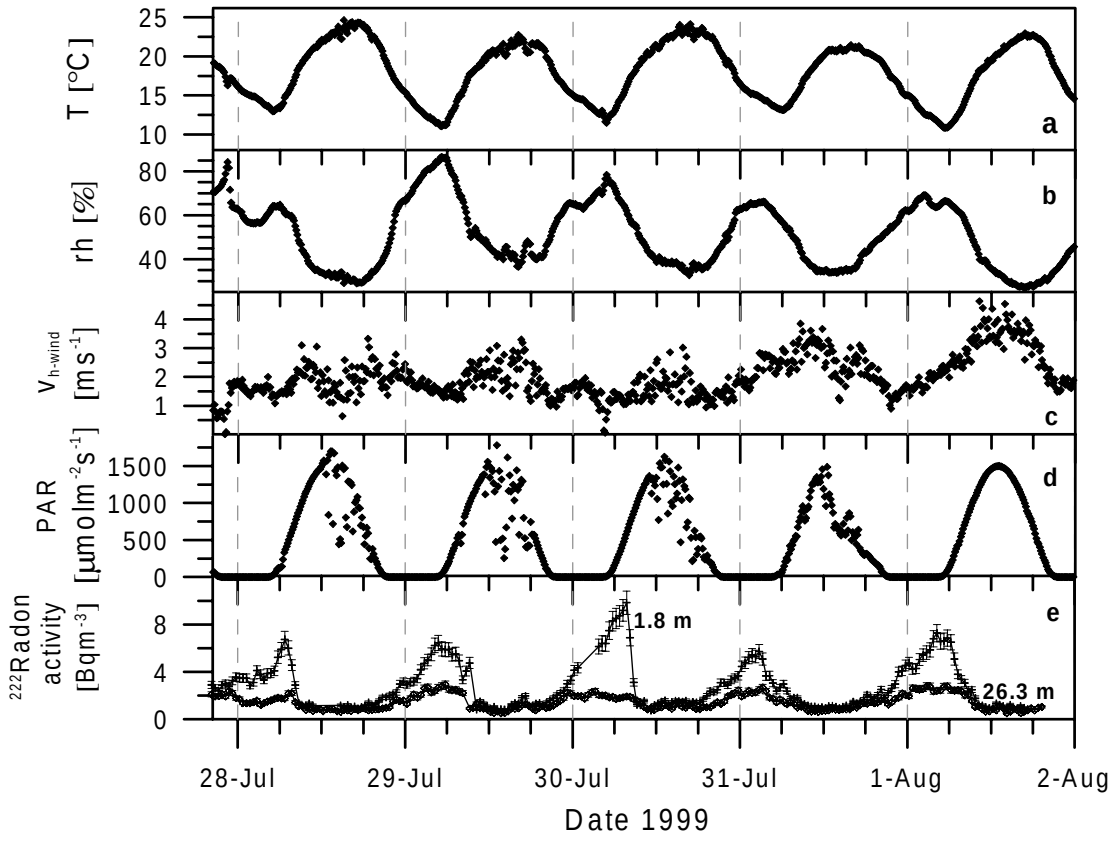

Figure 4.9: *Meteorological parameters observed during the intensive summer campaign 1999: (a) temperature, (b) relative humidity, (c) horizontal windspeed, (d) photosynthetically active radiation (PAR) as well as (e) ^{222}Radon activity at two heights (26.3 m and 1.8 m, error bars indicate 10% statistical counting error).*

active radiation (PAR) clearly exhibits the solar radiation controlled behaviour of the canopy micrometeorology. PAR gets zero between 9:40 pm and 4:20 am (local winter time) and reaches maximum radiation values of about 1500 μmol $m^{-2}s^{-1}$ around 1 pm. The observed ^{222}Radon activity variabilities presented in Figure 4.9(e) underlies this diurnal, periodic mete-

orological pattern. In order to detect vertical gradients for all components within the canopy, sampling and measurements were performed at two heights (1.8 and 26.3 m above ground). Compared to 1998, where no significant vertical gradient between 15.6 and 26.3 m could be detected, a strong vertical gradient in ^{222}Radon activity between 1.8 and 26.3 m was observed. This inversion buildup of a night-time vertical gradient ranges between 4 and 8 Bq m^{-3}. Due to dryer soil conditions, the ^{222}Radon soil exhalation rate was higher than in 1998, which consequently also resulted in a larger vertical gradient under comparable meteorological conditions. Indeed, the mean ^{222}Radon soil source strength of all 6 sampling sites for the catchment area of the tower site is determined to 24 ± 9.7 Bq $m^{-2}h^{-1}$, nearly a factor 5 larger than in 1998. Nevertheless, ^{222}Radon soil exhalation fluxes showed a large variability along the hydrological measurement transect which is due to the dramatically changing water table depth [Levin *et al.*, 2001]. After sunrise radiative heating initiates convective turbulence, that rapidly destroys the accumulated vertical gradient. During day-time both heights reach similar values, suggesting the canopy to be well mixed with the convective boundary layer (CBL).

4.3.2 CO_2 Mixing Ratio and Stable Isotopes

During this intensive summer campaign 1999 the flask sampling setup was installed within a small wooden hut, approximately 15 m away from the forest tower. To obtain vertical gradients of CO_2 and CO_2 stable isotopes single flasks at two heights were sampled (1.8 m and 26.3 m above ground) at a time resolution of 2 hours. As the power supply in 1999 was quite stable, the drying of the air prior to the flask inlet could be performed cryogenically as described in Chapter 3.2. Applying this set-up, the flasks could be sampled almost perfectly dry. Diurnal variations of CO_2 concentration and stable isotope ratios at 2 heights within the forest canopy measured on the flask samples are shown in Figure 4.10.

Comparison of the flask CO_2 concentration values with simultaneous, continuous measurement of CO_2 by NDIR [Naegler et al, 2001] (LiCor LI-6251) yields a mean difference (LiCor minus flasks) of -0.27 ± 0.38 ppm for the 26 m level and -0.65 ± 6.34 ppm for the 1.8 m level, respectively. Depending on the meteorological conditions within the canopy, the CO_2 concentration shows a strong diurnal variability with maximum concentrations in the morning and minimum values during the afternoon. During the intensive campaign period the CO_2 amplitude of this diurnal cycle at 1.8 m of 70 to 120 ppm shows much more variability than the amplitude at 26.3 m, which is only about 20 ppm. The respirative source CO_2 signal at 26.3 m is considerably smoothed by the mixing of CBL air whereas the 1.8 m measurements detect the respirative soil flux to a much greater quota especially when vertical mixing is suppressed during the build up of night-time inversions. The stable

Table 4.3: *Source signatures of the $\delta^{13}C(CO_2)$ stable isotope ratios, δ_s. (Accepted linear correlation coefficient r^2 used for the mean values: $\delta^{13}C_s(CO_2)$: $r^2 > 0.95$, day-time: 7:00 am - 7:00 pm, night-time: 9:00 pm - 5:00 am.)*

$\delta^{13}C_s(CO_2)$ [‰ vs VPDB]		
Period	1.8 m height	26.3 m height
overall	-25.94 ± 0.1	-25.68 ± 0.4
day-time	-24.79 ± 0.5	-24.73 ± 0.4
night-time	-26.39 ± 0.4	-26.82 ± 1.5

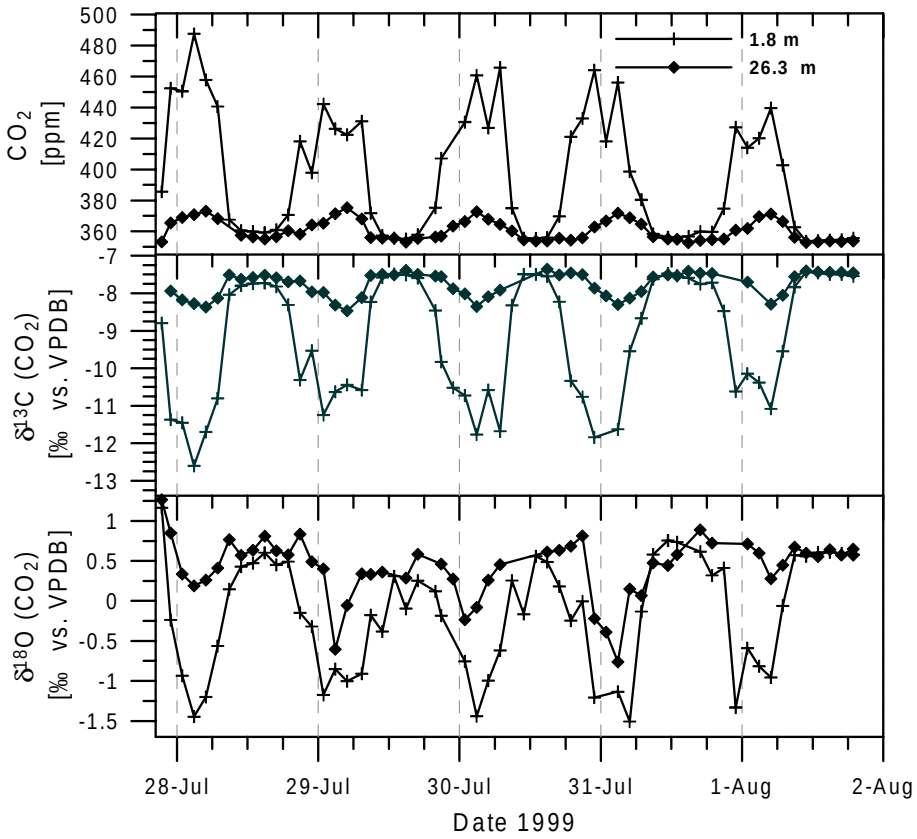

Figure 4.10: *Diurnal cycles of flask CO_2 concentration (top), $\delta^{13}C(CO_2)$(middle) and $\delta^{18}O(CO_2)$(bottom) during the summer campaign in 1999 at two sampling heights, 26.3 and 1.8 meter above ground.*

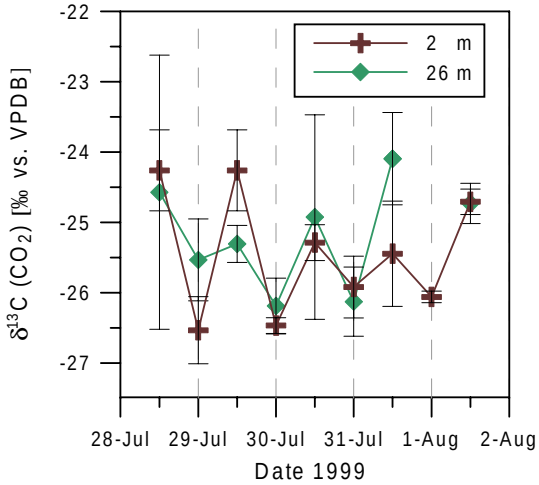

Figure 4.11: *Apparent $\delta^{13}C$ source signatures calculated for the respective single days and nights.*

isotope diurnal cycles show an anticorrelated behaviour to the CO_2 concentration variations which is expected for both, $\delta^{13}C(CO_2)$ and $\delta^{18}O(CO_2)$. The mean $\delta^{13}C(CO_2)$ source signatures derived from the correlation with the inverse CO_2 concentration for both heights - distinguished between day-time (concentration decrease) and night-time (concentration increase) - are given in Table 4.3. The two component mixing approach yields a consistent picture for the source signature diurnal variability of $\delta^{13}C(CO_2)$ within the ecosystem. For both heights the same source signature values of about -24.8 ‰ within 1 σ were detected during day-time, during night-time the source gets depleted by about 1.8 ‰ to -26.6 ‰. This enrichment of the $\delta^{13}C(CO_2)$ day-time source of 1.8 ‰ illustrates the strong assimilation discrimination influence on the ecosystem CO_2.

The connection of the canopy CO_2 variabilities to the CBL via the aircraft profiles is presented in Figure 4.12.

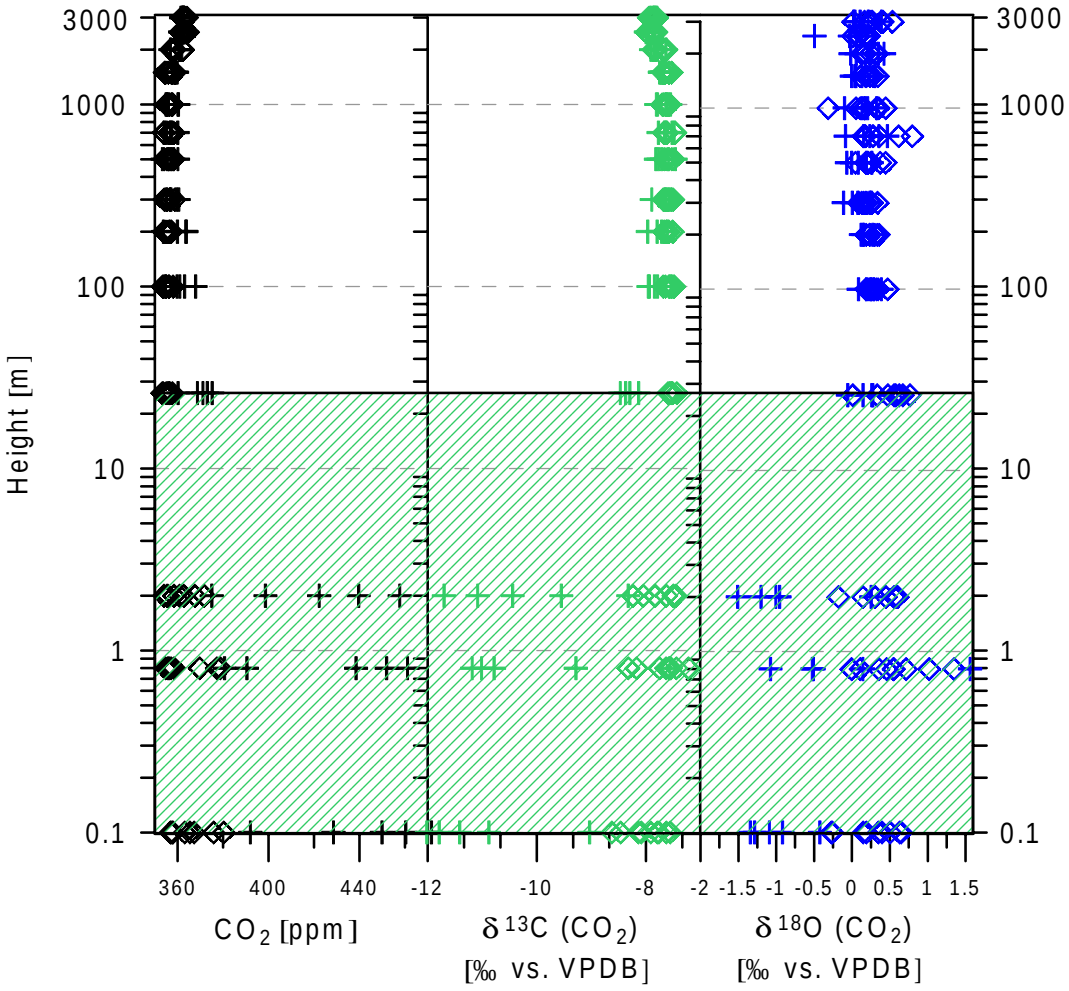

Figure 4.12: *Aircraft profiles along with the simultaneous canopy data (green shaded area). The crosses refer to the first profile in the early morning.[Ramonet* et al.*, 2001]*

The basic features, as observed for the summer 1998 campaign, were again observed during summer 1999. The improvement of the drying procedures of both, the canopy ground sampling and the flying device, now allowed to obtain reliable $\delta^{18}O(CO_2)$ values. The $\delta^{18}O(CO_2)$ pro-

files show a behaviour corresponding to the expected scenario. Depleted values were observed during the early morning profiles near the soil surface, representing the depleted respiration source. However, this respirative signal in $\delta^{18}O(CO_2)$ already vanishes at a height of 100 m, whereas the CO_2 mixing ratio as well as the $\delta^{13}C(CO_2)$ signature seem to retain the respirative signal up to larger heights. From 100 m upwards, the $\delta^{18}O(CO_2)$ signal shows values largely varying between 0 and +0.8 ‰, values that are expected for the lower troposphere.

There is a significant difference between the summer 1998 and summer 1999 profile data. During 1999 all CO_2 values higher than 2500 m show always - during day and early morning - higher CO_2 mixing ratios than the lower heights. This characteristic pattern was not as significant in 1998. The interpretation of this structure is the existence of a net CO_2 biospheric sink. The predominance of gross assimilation over gross respiration during the course of 24 hours, leads to a net CO_2 influx into the biosphere. Therefore, the night-time respiration flux into the CBL is not large enough to increase the lower CBL CO_2 mixing ratios up to 2000 m to the values observed above 2500 m. Then, in principle, the area between a typical day-time profile and a night-time profile should allow to estimate the net sink flux of the biosphere. However, applying this properly, it is not only subtracting profiles, but also regarding advection fluxes, that become more important with increasing altitude, and also regarding the CO_2 exchange between the CBL and the troposphere above. The CBL budgeting method, therefore, requires a detailed inspection of vertical stability parameters like temperature and relative humidity. A detailed description on the theory of CBL budgeting is given by Raupach *et al.* [1992].

4.3.3 $H_2^{16}O/H_2^{18}O$ of Plant Tissue and Water Vapour

Two major schemes of the spatial and temporal evolution of the $\delta^{18}O(H_2O)$ composition of the vegetation and soil water pools are shown in Figure 4.13. First, in principle there is an obvious vertical enrichment of the $^{18}O/^{16}O$ ratio towards the top of the ecosystem water pools, which was also observed during summer 1998. The soil water on the top layer of the soil (5 cm depth) has a $\delta^{18}O(H_2O)$ value of -11.25 ‰ vs SMOW (mean between soil under coniferous and deciduous dominated areas), whereby the soil water gets depleted to about -12.2 ‰ at a depth of 40 cm to stay nearly constant down to 60 cm depths. The mean (coniferous and deciduous) stem water $^{18}O/^{16}O$ ratio of -9.8 ‰ is enriched compared to the soil water by about 2 ‰. For the night time with no assimilation activity the enrichment can further be observed via the understory vegetation (mosses collar, leaves and grass collar) with an $^{18}O/^{16}O$ ratio from about -5 ‰ to -2 ‰, followed by the grass leaves and the deciduous low level leaves with an $^{18}O/^{16}O$ ratio around 0 ‰. Highest values for $\delta^{18}O(H_2O)$ during night-time between 0 ‰ and + 4 ‰ can be observed for the high and low levels of the coniferous and the deciduous high level leaves. The second dominant pattern of the ^{18}O signature in the water pools is the difference in their diurnal cycles. Basically the vertical gradient is maintained, but except for the grass and moss collar and the moss leaves, a strong enrichment of about 10 ‰ during day-time is detected for all other leaf compartments within the vegetation. This is also a significant difference compared to the wet summer in 1998, where day-time enrichment within the diurnal cycle was not as pronounced as in summer 1999

The variation of the 4 hour integral water vapour $\delta^{18}O$ within the canopy is presented in Figure 4.14. Regarding the measurement uncertainty of about 0.4 ‰, there is a huge diurnal cycle and vertical gradient observed. Compared to the 1.8 m level, at 26.3 m $\delta^{18}O$ of water vapour is always more depleted with a diurnal cycle between -19.5 and -22 ‰. The 1.8 m level shows a larger diurnal cycle with most depleted values during day of about -20 ‰ and

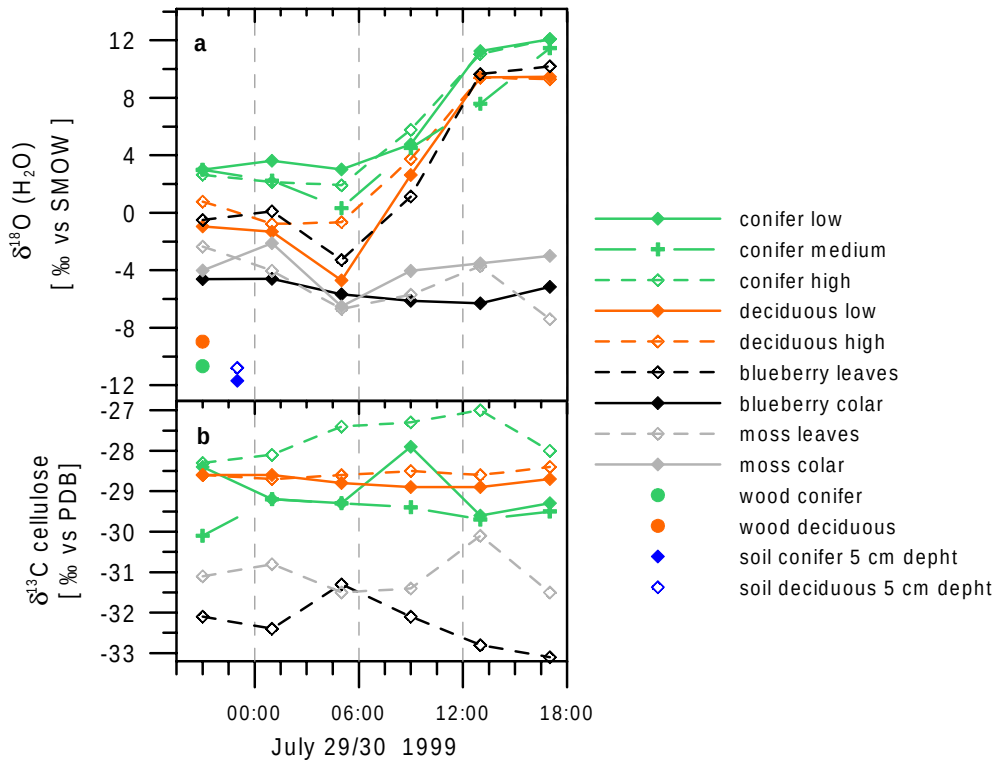

Figure 4.13: *Diurnal $\delta^{18}O(H_2O)$ variations of the different vegetation water pools along with soil and trunk $\delta^{18}O(H_2O)$ (a) and diurnal $\delta^{13}C$ variations of plant tissue material (b).*

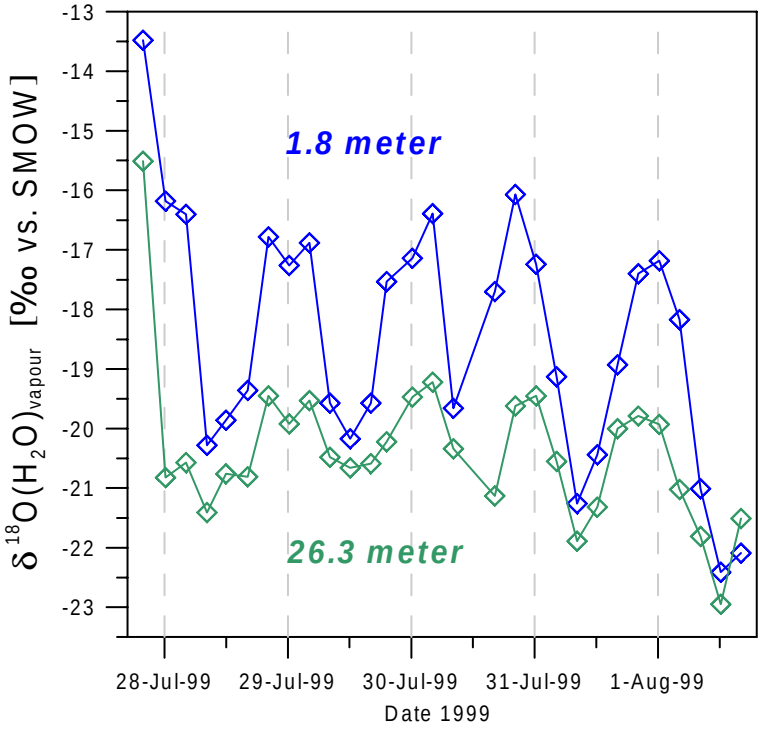

Figure 4.14: *$\delta^{18}O$ water vapour variations within the canopy.*

enriched values during night of about -17 ‰. This diurnal cycle as well as the vertical profile can be interpreted as the mixture of evaporating soil and leaf water and tropospheric water vapour being significantly depleted compared to the evaporating water. As the evaporating soil water (δ^{18}O about -11 ‰) should result in a water vapour δ^{18}O of about -21 ‰, due to evaporation fractionation, a large portion of the evaporating water must origin from enriched reservoirs, i.e. from the leaves or condensed surface water of the plants.

4.4 Autumn 1999

4.4.1 Meteorology

Due to the extensive rainfalls during September 1999 with 400 mm precipitation, the soil was again nearly saturated with water. During the intensive campaign period between October 21 and October 26 the accumulated rainfall was about 14 mm. Temperature varied between -3°C during the night and 3°C during day until October 24 and from there on temperatures increased nearly continuously up to 9°C. Relative humidity shows values around 60 and 90 %, but also increases from October 24 up to 100 %. Also the horizontal wind velocity increases from quite constant values of around 1 ms^{-1} to 3 ms^{-1} during October 24, without any strong diurnal cycles. PAR shows maximum values of between 50 and 380 μmol $m^{-2}s^{-1}$, a factor 7 smaller than during the summer season. Also the duration of daylight is reduced from 18 hours during summer to only 9 hours during autumn. The ^{222}Radon variability of both heights shown in Figure 4.15(e) illustrates the meteorological conditions within the canopy during this campaign. Compared to the summer intensive campaign in 1999 (see Figure 4.15) no strong vertical gradients and regular diurnal cycles could be observed. The mean ^{222}Radon soil source strength of all 6 sampling sites for the catchment area of the tower site is determined to 6.2 ± 4.5 Bq $m^{-2}h^{-1}$. This value is comparable with the mean source strength of 4.7 ± 2.2 Bq $m^{-2}h^{-1}$ of the wet summer campaign in 1998. Within the statistical counting error of the ^{222}Radon monitoring, no vertical gradient between 1.8 and 26.3 m could be detected. This vertical atmospheric ^{222}Radon distribution suggests a well mixed meteorological situation during the overall campaign period, which is also supported by the horizontal wind speed as a proxy of vertical mixing. Beginning from the evening of October 23, a trend of increasing ^{222}Radon activities was observed accompanied by permanently increasing wind velocities, which can be interpreted as a general air mass change transporting air masses with higher ^{222}Radon activities to the Fyodorovskoye forest site.

4.4.2 CO_2 Mixing Ratio and Stable Isotopes

Following the meteorology and the seasonal cycle of biospheric activity, CO_2 concentration and stable isotopes also show less significant diurnal cycles compared to the summer period (Figure 4.16). Thereby both, the peak-to-peak amplitude and the shape of the diurnal cycle are less pronounced compared to the summer in 1999. This is a consequence of three basic seasonal differences: first, the shorter night-time duration leads to lower night-time inversion strengths, which are furthermore less stable due to higher night-time turbulences during the campaign. Second, temperature controlled reduced soil respiration lowers the CO_2 influx to the canopy and third very low assimilative activity leads to significantly higher day-time CO_2 concentrations within the canopy during day-time. Compared to a mean CO_2 peak-to-peak amplitude at 26.3 m of about 25 ppm in July 1999, during autumn only about 15 ppm were observed. The diurnal cycles completely vanish on October 24 when wind velocities increase and the origin of air obviously changes. Comparison of the flask CO_2 concentration values

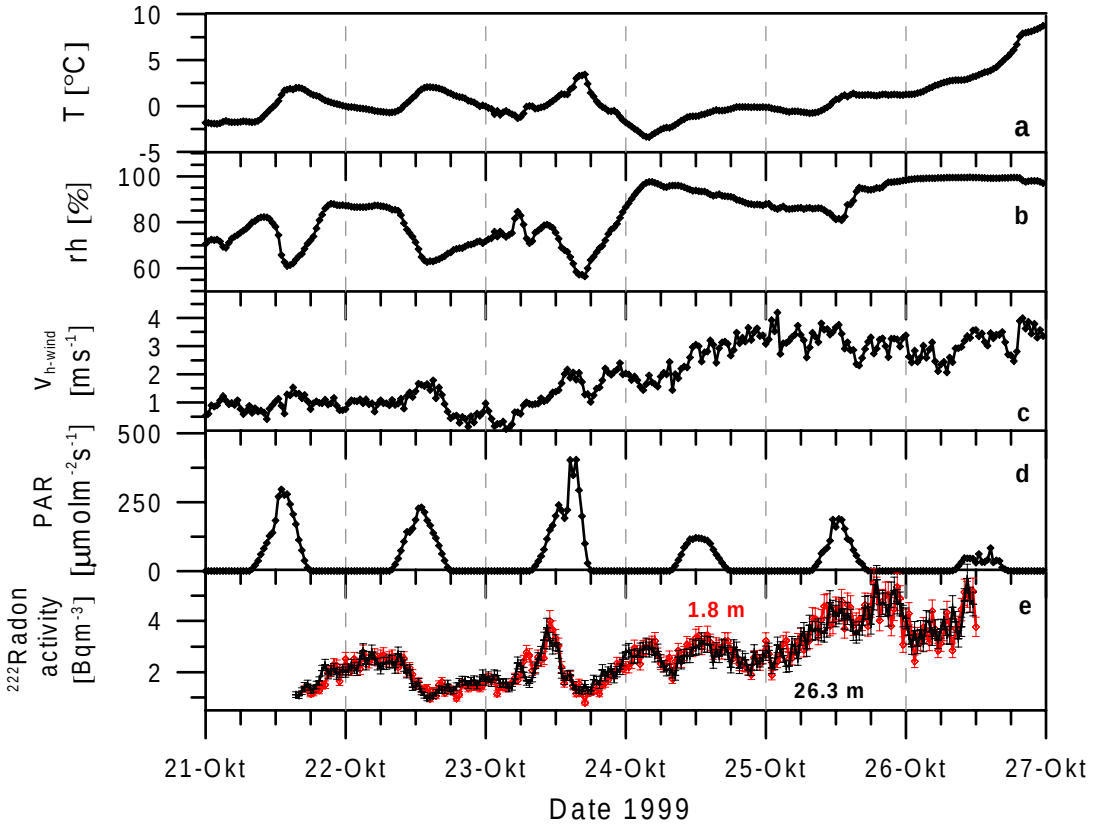

Figure 4.15: *Meteorological parameters observed during the intensive autumn campaign 1999: (a) temperature, (b) relative humidity, (c) horizontal windspeed, (d) photosynthetically active radiation (PAR) as well as (e) ^{222}Radon activity of two heights (26.3 m and 1.8 m, error bars indicate 10% statistical counting error).*

with continuous CO_2 measurements by NDIR (Li-Cor LI-6251) yields a mean difference (Li-Cor minus flasks) of -0.31 $\pm$ 0.29 ppm for the 26.3 m level, which agrees well with the value of -0.27 $\pm$ 0.38 ppm for the summer campaign in 1999.

The seasonality of the biospheric CO_2 signals observed at the Fyodorovskoye forest site are summarised in Table 4.4. From August to end of October 1999 the mean CO_2 concentration at the top of the canopy (at 26.3 m height) increased by about 15 ppm which is accompanied by a decrease of the mean $\delta^{13}C(CO_2)$ by about 0.7 ‰. Both changes are expected, due to a generally decreasing assimilation activity in the northern hemisphere during this time of the year. Lower biospheric activity can also clearly be observed in decreasing diurnal peak to peak amplitudes and in a decrease of the $\delta^{13}C(CO_2)$ source signature by about 2 ‰. A significant drop of the mean atmospheric $\delta^{18}O(CO_2)$ by about 1.5 ‰ was observed; a decrease that is also found in the seasonal cycle of the free troposphere at Syktyvkar for the same time period (see Figure 6.1 in Chapter 6). The driving force of this behaviour, is assumed to be the commonly observed depletion of the $\delta^{18}O(H_2O)$ signature in precipitation from autumn to winter (see Figure 4.1), that is transferred into the vegetational water pools and therefore again depletes the $\delta^{18}O$ signature of atmospheric CO_2. The depletion in the water reservoirs is also observed in depleted water vapour $\delta^{18}O$ values within the canopy (Figure 4.19).

The seasonal change of biospheric activity is also manifested in the shape of the vertical

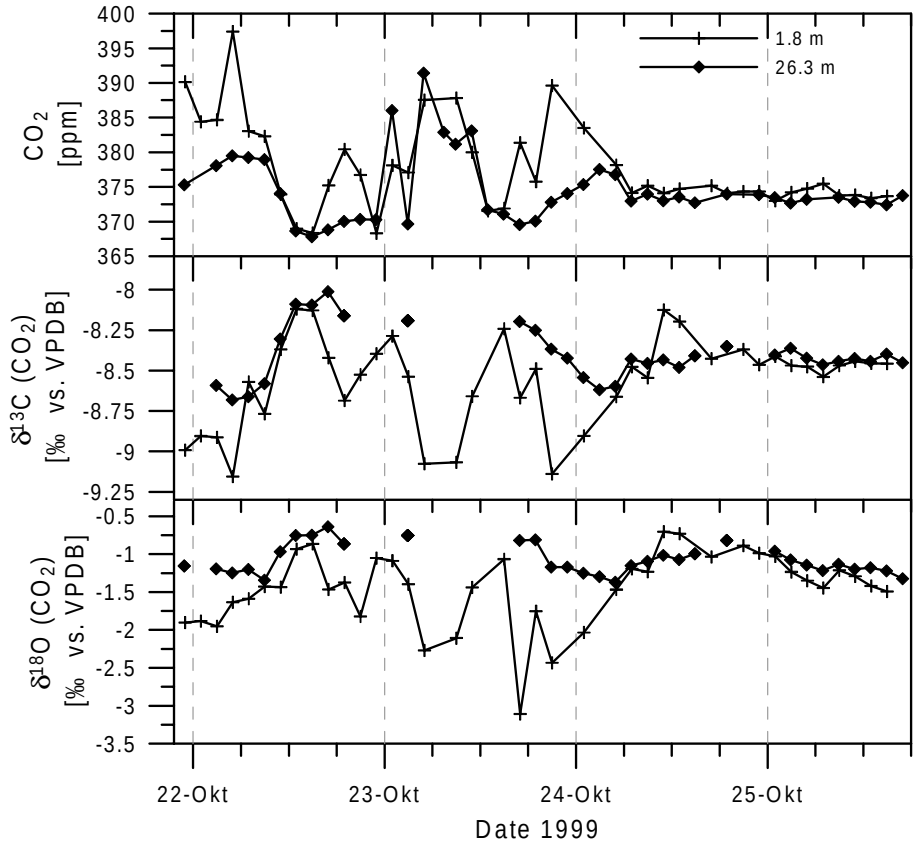

Figure 4.16: *Diurnal cycles of flask CO_2 concentration (top), $\delta^{13}C(CO_2)$(middle) and $\delta^{18}O(CO_2)$(bottom) during the autumn campaign in 1999 at two sampling heights, 26.3 and 1.8 meter above ground.*

Table 4.4: *Comparison of the summer and autumn campaign in 1999: Mean values of CO_2 concentrations [ppm], stable isotope ratios [‰ vs VPDB], typical diurnal peak to peak amplitudes (ppa in [ppm]) and the overall isotope source signature of $\delta^{13}C(CO_2)$ at the top of the canopy at 26.3 m height.*

Campaign overall mean values (at 26.3 m)	Summer 1999 (July 27 to August 1)	Autumn 1999 (October 21 to October 25)
CO_2	359.71 ± 6.68	374.59 ± 4.85
$\delta^{13}C(CO_2)$	-7.72 ± 0.32	-8.39 ± 0.16
$\delta^{18}O(CO_2)$	0.39 ± 0.37	-1.07 ± 0.19
ppa CO_2	∼ 25	∼ 15
ppa $\delta^{13}C(CO_2)$	∼ 1	∼ 0.6
ppa $\delta^{18}O(CO_2)$	∼ 1.5	∼ 0.7
$\delta_{source}{}^{13}C(CO_2)$	-25.68 ± 0.4	-27.72 ± 1.27

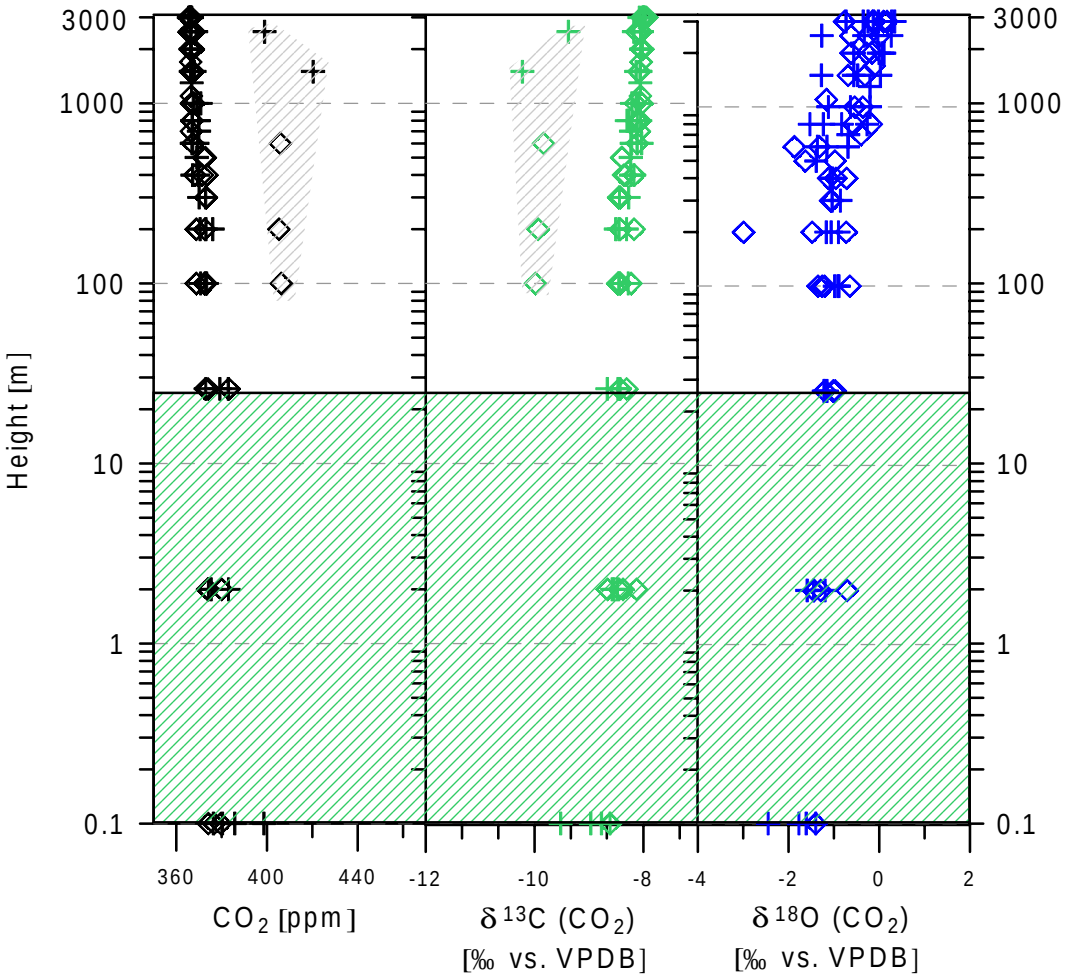

Figure 4.17: *Aircraft profiles along with the simultaneous canopy data (shaded green area). The crosses refer to the first profile in the early morning.[Ramonet* et al.*, 2001]*

profiles of CO_2 and CO_2 stable isotopes (Figure 4.17). Except for the five outliers above 100 m (shaded grey areas), which may be due to fossil fuel emission contamination by the aircraft exhaust, the profiles show decreasing CO_2 mixing ratios in upward direction. Therefore, as the CBL mixing was quite strong, compared to the summer campaigns with lower windspeeds, the biosphere must have been a net respiration source to the CBL. The corresponding behaviour is observed in $\delta^{13}C(CO_2)$, and the $\delta^{18}O(CO_2)$ profile in total is about 1 ‰ shifted to more depleted values, if compared with the summer 1999 profiles.

4.4.3 $H_2^{16}O/H_2^{18}O$ of Plant Tissue and Water Vapour

Comparison of the vegetational water pools during October 1999 with the previous summer campaigns displays generally less enriched $\delta^{18}O(H_2O)$ values for all water pools. As the precipitation $\delta^{18}O$ input at this time of the year ranges between -8 and -16 ‰, the soil water and therefore the plant supply source water should also get more depleted. Soil water and stem wood water range from -10.5 to -11.5 ‰. However, all understory vegetation water samples tend to be even more depleted, partly down to -15 ‰. This may indicate a very heterogeneous distribution of soil water, that is taken up by the respective understory vegetation. The

deciduous tree leaves show comparable values to the soil water for both, the high and the low level, with δ^{18}O values between -9 and -11 ‰. Only the conifer tree leaves are significantly enriched by about 9 ‰ compared to the soil water. This is due to the fact, that coniferous trees also assimilate at very low temperatures. No significant diurnal cycles are observed for the respective categories. Basically this overall pattern can be interpreted by very low to zero assimilative activity of the broad leaved plants ecosystem. As the transpiration rate of the plants also gets lower, fractionation of ^{18}O by transpiration gets a lower impact on the δ^{18}O composition of the plant water reservoirs.

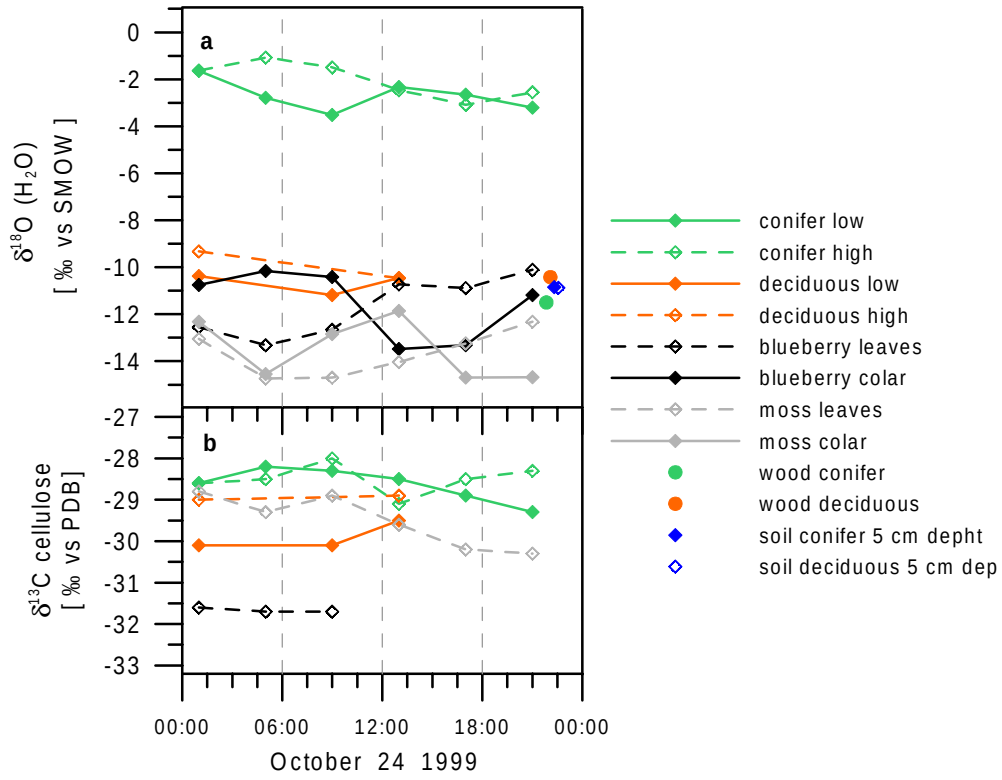

Figure 4.18: Diurnal δ^{18}O(H_2O) variations of the different vegetation water pools along with soil and trunk δ^{18}O(H_2O) (a) and diurnal δ^{13}C variations of plant tissue material (b).

The well mixed situation during the autumn 1999 campaign is also illustrated in the δ^{18}O of water vapour. There is nearly no vertical gradient between the bottom and top of the canopy, whereas during summer a permanent vertical gradient, from enriched values at the canopy floor to more depleted values towards the top of the canopy, was observed. Furthermore, there is, also in comparison to the more stable atmospheric conditions during summer, no diurnal cycle in δ^{18}O of the water vapour. The main difference to summer is, however, the overall depletion in δ^{18}O of the water vapour, with values between -22 and -25.7 ‰. As turbulent exchange with the CBL was comparatively high, the water vapour observed in the canopy should largely reflect large scale variations in atmospheric water vapour.

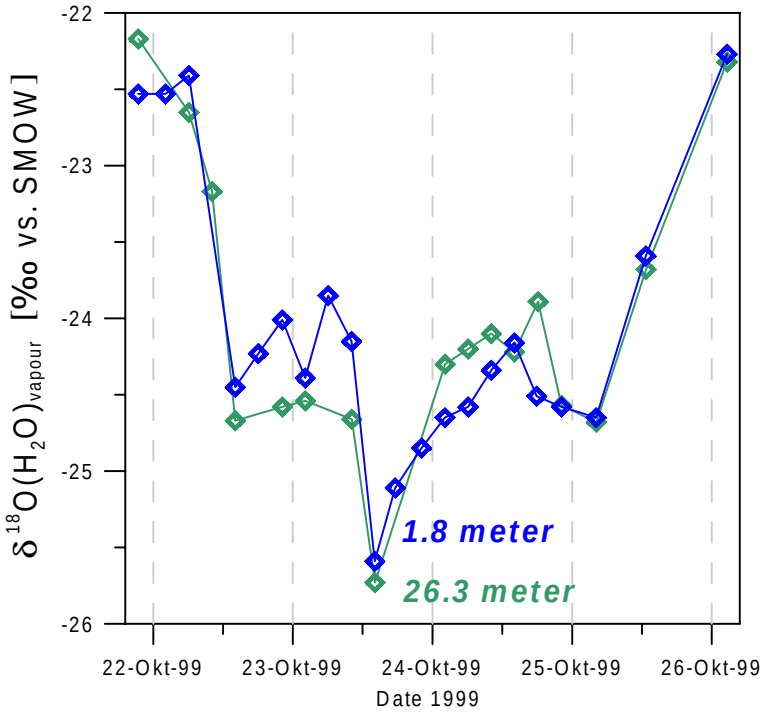

Figure 4.19: *$\delta^{18}O$ water vapour variations within the canopy.*

4.5 Summary of Experimental Findings and Conclusion

During the three intensive campaigns in summer 1998, summer 1999 and in autumn 1999, the observations of CO_2 mixing ratio and stable isotope variations were observed to be characteristic with respect to seasonality, meteorological as well as to hydrological conditions. The summer 1998 $\delta^{13}C(CO_2)$ overall day-time source signature with -25.55 $\pm$ 0.46 ‰ is significantly depleted if compared to the summer 1999 signature with -24.73 $\pm$ 0.4 ‰. This higher day-time enrichment of ambient ecosystem air in 1999, suggest higher assimilation rates during 1999, due to a increased impact of assimilation discrimination against $^{13}CO_2$. High resolved flask sampling showed, that there is large short time variation of the overall $\delta^{13}C(CO_2)$ signature that is transferred into the atmosphere. Therefore, assuming a constant $\delta^{13}C(CO_2)$ source signature for example in mesoscale models or as a tracer for CBL bugets, may lead to serious problems.

Differences in assimilation activity of the biosphere can also be derived from the shape of the vertical profiles sampled during the campaigns. During summer 1999 the top CBL values were always higher in CO_2 concentration than the lower values towards the ground, implying the biosphere to be a net sink of CO_2 to the atmosphere. Even more significant were the differences from summer to the autumn campaign, where CO_2 mixing ratios steadily increased from bottom to top - a situation where the biosphere is interpreted as a net source of CO_2 to the atmosphere. The differences between the years as well as the seasonality, in terms of biospheric activity, can also be investigated by the cumulative net ecosystem exchange (NEE) fluxes, measured by eddy correlation (Figure 4.20, from Milukova *et al.*, [2001]). Measurements of NEE started in May 1998 and unfortunately broke down towards winter. For 1999, measurements could be performed over the whole year. However, the differences between both years can clearly be seen: 1998 assimilation exceeded respiration to a much

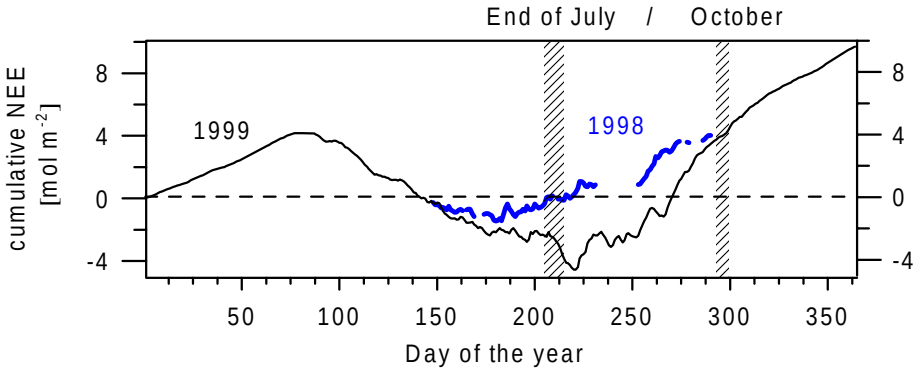

Figure 4.20: *Cumulated Net Ecosystem Production (NEE) for the years 1998 and 1999*

lower extent than in 1999. Whereas during the in summer 1998 campaign the biosphere behaved nearly neutral, during summer 1999 strong assimilation clearly exceeded respiration and the biosphere acted as a net CO_2 sink to the atmosphere.

The quantitative interpretation of the respective ^{18}O in CO_2 and the water pools, is a nebulous business. Not even an evaluation via the two-component mixing approach is applicable, as ambient $\delta^{18}O(CO_2)$ is a mixture of more than two processes. Therefore, to use the potential of atmospheric $\delta^{18}O(CO_2)$ as a tracer for biospheric gross fluxes in a real ecosystem, a parameterisation of the respective processes is necessary. As discussed above, the vegetational imprint on ambient ecosystem $\delta^{18}O(CO_2)$, is most easily to detect under low turbulent conditions. Furthermore, a strong diurnal variation in leaf water enhances the assimilation impact on ambient $\delta^{18}O(CO_2)$. Therefore, the parameterisation of the ^{18}O processes is performed for the summer 1999 campaign, where periodic, strong diurnal cycles were observed, assimilation was comparably high and, after the experience from 1998, reliable $\delta^{18}O(CO_2)$ values were obtained.

Chapter 5

1-D ^{222}Radon Calibrated Canopy Model

The main objective of the modelling approach is to investigate the potential of the ^{18}O isotopic composition of combined carbon dioxide and water to determine the gross CO_2 fluxes of an ecosystem. As the observable $\delta^{18}O(CO_2)$ variability within the forest canopy is controlled by both, transport driven exchange of canopy CO_2 with the CBL and process related biospheric activity impact, the model has to be well parameterised with respect to transport prior to the investigation of the biological processes. As only during the summer 1999 intensive campaign the observed vertical profiles of CO_2 and ^{222}Radon as well as of the vegetational water pools were significant, this data set was used for the modelling approach.

5.1 Model Set-up

A 1-dimensional box-model set-up was chosen to differentiate between the respective carbon and water pools, whereby three boxes with quasi-logarithmic height scaling from bottom to top are investigated for their turbulent transport and assimilative and respirative exchange fluxes (see Figure 5.1). The lowest box (box 1, from soil surface to 4 m height) represents the interface with the soil and the understory vegetation regime. The change of CO_2 concentration in box 1 is controlled by the input of CO_2 via the soil respiration flux, $R_{soil}(CO_2)$, and the autotrophic plant respiration of the understory vegetation, $R_{a1}(CO_2)$ as well as by CO_2 sinks for box 1: the assimilation flux, A_1, and the transport of CO_2 from box 1 to box 2 via turbulent exchange, $F_{1\rightarrow 2}(CO_2)$. Furthermore, the change of ^{222}Radon activity in box 1 is determined by the input via soil exhalation, $F_{soil}(Rn)$, and turbulent transport of ^{222}Radon from box 1 to box 2, $F_{1\rightarrow 2}(Rn)$. The second box (box 2, 4 m to 26 m height) represents the deciduous and coniferous tree activity within the canopy. CO_2 concentration change in box 2 is determined by the exchange fluxes with box 1, $F_{1\rightarrow 2}(CO_2)$, and box 3, $F_{2\rightarrow 3}(CO_2)$, the autotrophic plant respiration of the upper tree vegetation, $R_{a2}(CO_2)$, and the assimilation flux, A_2. Convention for the fluxes are, that fluxes into a box are calculated positive and outward fluxes are calculated negative.

5.2 Turbulent Vertical Transport

In order to parameterise the intra-canopy transport, we exploited soil-borne ^{222}Radon. The ^{222}Radon flux from the lowermost canopy box, box 1, to the adjacent canopy box 2 can be calculated using the mean measured soil ^{222}Radon exhalation rate $F_{soil}(Rn)$, assumed to be

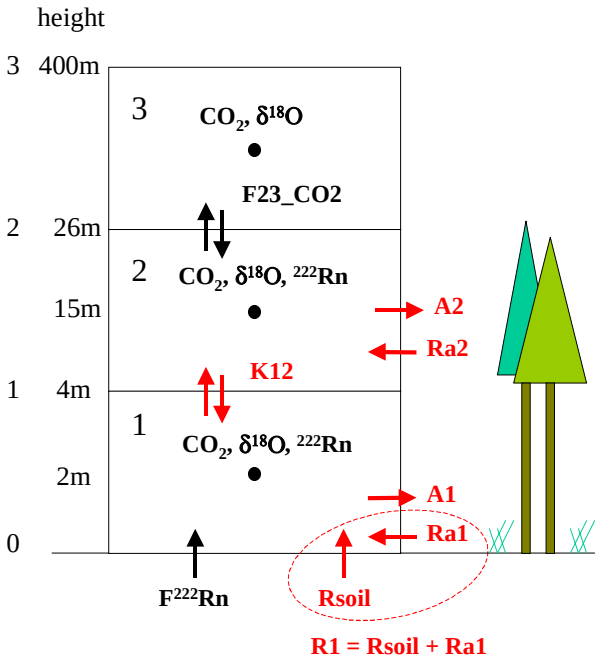

Figure 5.1: *Scheme of the canopy box model set-up: the measured input values are marked in black, the calculated model output values are marked in red.*

constant in time, and the atmospheric ^{222}Radon change with time in box 1.

$$H_1 \times \frac{\mathrm{d}Rn_1}{\mathrm{d}t} = F_{soil}(Rn) - F_{1\rightarrow 2}(Rn)(t) \tag{5.1}$$

In analogy to Fick's first law (Equation 2.10), the turbulent diffusion coefficient, $K_{1\rightarrow 2}$, can be formulated via the measured vertical ^{222}Radon gradient between box 1 and box 2 and the distance between the box centres Δ h with

$$K_{1\rightarrow 2}(t) = \frac{F_{1\rightarrow 2}(Rn)(t) \times \Delta h}{\overline{[^{222}Rn_1(t)]} - \overline{[^{222}Rn_2(t)]}} \tag{5.2}$$

To parameterise the intra-canopy turbulent transport of CO_2 between box 1 and box 2, it is assumed that CO_2 has the same transport characteristics as soil-borne atmospheric ^{222}Radon. The radioactive decay of ^{222}Radon can be neglected, as the half-life time of 3.8 days is orders of magnitude higher than the time resolution of the observed variation (30 minutes) and as, after the breakup of the inversion layer each morning, the ^{222}Radon activity is reset to background values, due to increasing vertical exchange. Mean ^{222}Radon activity and CO_2 concentration values for each box are calculated by integration of the measured CO_2 tower profile, assuming similarity between ^{222}Radon and CO_2 following Equation 2.4. The CO_2 flask concentrations and ^{222}Radon activities, which are both measured at heights h=1.8 and h=26.3 m, respectively, are subsequently scaled to their mean value by assuming

$$\overline{[CO_{2flasks}]}_i = \frac{\overline{[CO_{2profile}]}_i}{\overline{[CO_{2profile}(h)]}} \times [CO_{2flasks}(h)] \tag{5.3}$$

and

$$\overline{[^{222}Rn]}_i = \frac{\overline{[CO_{2profile}]}_i}{\overline{[CO_{2profile}(h)]}} \times [^{222}Rn(h)] \tag{5.4}$$

The CO_2 flux between box 1 and box 2 is then calculated using the ^{222}Radon derived $K_{1\rightarrow 2}$(t) via (see Equation 5.2)

$$F_{1\rightarrow 2}(CO_2) = K_{1\rightarrow 2} \times \frac{[CO_2]_1 - [CO_2]_2}{\Delta h \times V_{mol}} \tag{5.5}$$

In the majority of the situations, there is a negative gradient in ^{222}Radon activity between bottom and top of the canopy (Figure 4.9(e)). Only during day-time, when the canopy is well mixed with the CBL above, both heights show similar values. Therefore, the model introduces a minimum gradient of 0.2 Bq m^{-3} during the rare situations during day, when $[^{222}Rn]_1 < [^{222}Rn]_2$. This forces the exchange coefficient $K_{1\rightarrow 2}$ to be always positive as long as there is a positive flux $F_{1\rightarrow 2}$(Rn) in Equation 5.2. The CO_2 flux from box 2 to box 3, $F_{2\rightarrow 3}(CO_2)$, is taken from the measured eddy covariance flux at the top of the canopy.

5.3 Parameterisation

Considering a box i of air within the canopy extending over a height, H_i, a mass balance to formally describe the respective CO_2 fluxes can be set-up. The mass balance of CO_2 in such an air column within an ecosystem canopy, in case of no horizontal advection of CO_2, is given by Equation 5.6 (the convention for the algebraic signs is: inward fluxes (into the canopy column) are calculated positively, outward fluxes negatively):

$$\frac{H_i}{V_{mol}} \times \frac{\mathrm{d}[CO_2]_i}{\mathrm{d}t} = -A_i + R_i + F_{a\rightarrow e} \tag{5.6}$$

with

V_{mol} :	Molar volume of the air [m^3 mol(air)$^{-1}$]
H_i :	Height of the canopy box i [m]
$[CO_2]_i$:	Average mol fraction of CO_2 within the column [mol(CO_2) mol(air)$^{-1}$]
A_i :	net CO_2 assimilation flux by the foliage within the column [mol(CO_2) m^{-2} s^{-1}]
R_i :	CO_2 respective respiration flux within the column [mol(CO_2) m^{-2} s^{-1}]
F_{ae} :	flux of CO_2 between the ecosystem canopy and the atmosphere above [mol(CO_2) m^{-2} s^{-1}]

The average CO_2 concentration for $[CO_2]_i$ is calculated following Equation 5.3 to avoid a possible CO_2 storage term to be missing in Equation 5.6.

The CO_2 mass balance equations for box 1 and box 2, respectively, then can be written as

$$\frac{H_1}{V_{mol}} \times \frac{\mathrm{d}[CO_2]_1}{\mathrm{d}t} = -A_1 + R_{soil} + R_{a1} - F_{1\rightarrow 2}(CO_2) \tag{5.7}$$

$$\frac{H_2}{V_{mol}} \times \frac{\mathrm{d}[CO_2]_2}{\mathrm{d}t} = -A_2 + R_{a2} + F_{1\rightarrow 2}(CO_2) - F_{2\rightarrow 3}(CO_2) \tag{5.8}$$

Equations 5.7 and 5.8 contain 5 unknowns, namely the assimilation terms in each box, A_1 and A_2, the autotrophic plant respiration terms in each box, R_{a1} and R_{a2}, and the soil respiration term in box 1, R_{soil}. To determine the unknowns, more equations have to be introduced. Therefore, the ^{18}O/^{16}O ratio of the canopy air CO_2 and of CO_2 isotopically equilibrated with

vegetation water pools are introduced, along with the respective isotope discriminations:

$$\frac{H_1[CO_2]_1}{V_{mol}} \times \frac{\mathrm{d}\delta^{18}O_1}{\mathrm{d}t} = -A_1\ {}^{18}\Delta_{leaves1} + R_{soil}(\delta^{18}O_{soil} - \delta^{18}O_1 + \epsilon_{soil}) + R_{a1}(\delta^{18}O_{stem1} - \delta^{18}O_1 + \epsilon_{stem}) - F_{1\rightarrow2}(CO_2)(\delta^{18}O_1 - \delta^{18}O_2) \quad (5.9)$$

$$\frac{H_2[CO_2]_2}{V_{mol}} \times \frac{\mathrm{d}\delta^{18}O_2}{\mathrm{d}t} = -A_2\ {}^{18}\Delta_{leaves2} + R_{a2}(\delta^{18}O_{stem2} - \delta^{18}O_2 + \epsilon_{stem}) + F_{1\rightarrow2}(CO_2)(\delta^{18}O_1 - \delta^{18}O_2) - F_{2\rightarrow3}(CO_2)(\delta^{18}O_2 - \delta^{18}O_3) \quad (5.10)$$

with

${}^{18}\Delta_{leaves}$:	leaf discrimination against $C^{16}O^{18}O$ in the respective box [‰]
$\delta^{18}O_{soil}$:	isotopic composition of soil CO_2 in isotopic equilibrium with soil water [‰]
$\delta^{18}O_{stem}$:	isotopic composition of stem CO_2 in isotopic equilibrium with stem water [‰]
$\delta^{18}O_{1,2,3}$:	isotopic composition atmospheric CO_2 in the respective box [‰]
ϵ_{soil} :	effective soil fractionation during diffusion, -7.2 ‰ [Miller *et al.*, 1999]
ϵ_{stem} :	effective stem fractionation during diffusion, -8.8 ‰ [T. Bariac, personal communication]

Combining equations 5.7 to 5.10 yields a system with four equations and five unknowns. Therefore, to solve this system of differential equations, it is assumed that the ratio of R_{a1}/ R_{soil}=β in box 1 is about 1/3, i.e. autotrophic stem respiration is about 30 % of the overall respirative flux of the understory vegetation in box 1 [Milukova *et al.*, 2001]. Therefore only one overall respirative flux R_1 is calculated for box 1 with $R_1 = R_{soil} + R_{a1}$ and Equation 5.7 gets to

$$\frac{H_1}{V_{mol}} \times \frac{\mathrm{d}[CO_2]_1}{\mathrm{d}t} = -A_1 + R_1 - F_{1\rightarrow2}(CO_2) \quad (5.11)$$

and Equation 5.9 can be written as

$$\frac{H_1[CO_2]_1}{V_{mol}} \times \frac{\mathrm{d}\delta^{18}O_1}{\mathrm{d}t} = -A_1\ {}^{18}\Delta_{leaves1} + R_1 \cdot [(1-\beta) \cdot (\delta^{18}O_{soil} - \delta^{18}O_1 + \epsilon_{soil}) + \beta \cdot (\delta^{18}O_{stem1} - \delta^{18}O_1 + \epsilon_{stem})] - F_{1\rightarrow2}(CO_2)(\delta^{18}O_1 - \delta^{18}O_2) \quad (5.12)$$

The system of four differential equations 5.8, 5.10, 5.11 and 5.12 is now determined and can be solved for the respective assimilation terms, A_1 and A_2 and for the respiration fluxes R_1 and R_{a2}. During night it is reasonable to set the assimilation fluxes to zero, which is triggered in the model via PAR < 150 μmol $m^{-2}s^{-1}$.

The left hand terms in Equations 5.8, 5.10, 5.11 and 5.12 contain the change in time of the measured mean CO_2 concentrations and $\delta^{18}O$ isotopic composition of the respective box. Here, the high time resolution of 2 hours allows the stepwise calculation of the change of CO_2 concentration and $\delta^{18}O$ with time. The molar volume of the air, V_{mol}, as well as the height of the boxes are constants (see Table 5.3 and Figure 5.1). The overall discrimination against

Table 5.1: *Notation of model values*

Constants	Description	Value [Units]
V_{mol}	molar volume of air	0.0224 [m^3/mol(air)]
a	fractionation of diffusion of $^{13}CO_2$ in air	4.4 [‰]
b	fractionation during C3 carboxylation of $^{13}CO_2$	29 [‰]
h_i	top of box i	m
H_i	height of box i(h_i-h_{i-1})	m
Fractionations	**Description**	**Value [Units]**
ϵ_{leaf}	fractionation of diffusion of CO_2 stomata-air	-7.4 [‰]
ϵ_{soil}	fractionation of diffusion of CO_2 soil-air	-7.2 [‰]
ϵ_{stem}	fractionation of diffusion of CO_2 stem-air	-8.8 [‰]
ϵ_{kin}	kinetic fractionation of diffusion of water vapour diffusion of $H_2^{18}O$ from inside the leaf to the air	-26.3 [‰]
ϵ_{li-vap}	fractionation of $H_2^{18}O$ with respect to the liquid phase during the liquid to vapour transition	-9.39 [‰] (at 25°C)
Variables	**Description**	**Units**
$^{222}Rn_i$	activity of ^{222}Radon in box i	Bq m^{-3}
$[CO_2]_i$	atmospheric concentration of CO_2 in box i	ppm ($molCO_2$/mol air)
$\delta^{18}O_i$	atmospheric $\delta^{18}O$ (CO_2) in box i	‰ VPDB
$\delta^{13}C_i$	atmospheric $\delta^{13}C$ (CO_2) in box i	‰ VPDB
$\delta^{18}O_{soil}^{H_2O}$	$\delta^{18}O$ of soil water	‰ VSMOW
$\delta^{18}O_{stem}^{H_2O}$	$\delta^{18}O$ of stem water	‰ VSMOW
$\delta^{18}O_{leaf-i}^{H_2O}$	$\delta^{18}O$ of leaf water in box i	‰ VSMOW
$\delta^{18}O_{soil}$	$\delta^{18}O$ of CO_2 in equilibrated with soil water	‰ VPDB
$\delta^{18}O_{stem}$	$\delta^{18}O$ of CO_2 in equilibrated with stem water	‰ VPDB
$\delta^{18}O_{leaf}$	$\delta^{18}O$ of CO_2 in equilibrated with leaf water	‰ VPDB
$\delta^{13}C_{leaf-i}$	mean $\delta^{13}C$ of leaves in box i	‰ VPDB
c_c	chloroplast CO_2 concentration in box i	ppm
c_i	inner stomatal CO_2 concentration in box i	ppm
$^{18}\Delta_{leaves}$	discrimination against $C^{16}O^{18}O$ during assimilation in box i	‰
$^{13}\Delta_{leaves}$	discrimination against $^{13}CO_2$ during assimilation in box i	‰
T_i	air temperature in box i	°C
T_{soil}	soil temperature	°C
T_{stem}	stem temperature	°C
rh_i	relative humidity in box i	%
PAR	photosynthetically active radiation	μmol $m^{-2}s^{-1}$
Fluxes	**Description**	**Unit**
$K_{i\rightarrow i+1}$	exchange coefficient from box i to i+1	m^2h^{-1}
F_{soil}(Rn)	flux of radon from soil to box 1	Bq $m^{-2}h^{-1}$
$F_{i\rightarrow i+1}$(Rn)	flux of radon from box 1 to box 2	Bq $m^{-2}h^{-1}$
$R_{soil}(CO_2)$	soil respiration CO_2 flux	mol(CO_2)$m^{-2}h^{-1}$
$F_{i\rightarrow i+1}(CO_2)$	flux of CO_2 from box 1 to box 2	mol(CO_2)$m^{-2}h^{-1}$
A_{-i}	net CO_2 assimilation flux in box i	mol(CO_2)$m^{-2}h^{-1}$
R_{a-i}	autotrophic respiration CO_2 flux in box i	mol(CO_2)$m^{-2}h^{-1}$
$F_{i\rightarrow i+1}(\delta^{18}O$)	$\delta^{18}O$ flux from box 1 to box 2	mol(CO_2)[‰]$m^{-2}h^{-1}$

δ^{18}O during assimilation in the respective box i, ${}^{18}\Delta_{leaves-i}$, is calculated following Equation 2.20

$$ {}^{18}\Delta_{leaves-i} = -\epsilon_{leaf} + \frac{c_{c-i}}{[CO_2]_{\mathrm{i}} - \mathrm{c_{c-i}}} \; (\delta_{leaf} - \delta^{18}O_i) $$

The mean leaf discrimination, ϵ_{leaf}, of -7.4 ‰ and the fractionation during diffusion from the stems to the atmosphere, ϵ_{stem}, of -8.8 ‰ were used here. The standard model calculates with the effective soil fractionation, ϵ_{soil}, of -7.2 ‰. It is furthermore assumed that there is a nearly complete isotopic equilibration between CO_2 and water of 93% before the assimilative fixation of CO_2, which was determined by Gillon and Yakir for C3 plants [Gillon and Yakir, 2000, 2001]. Mean values of the measured $\delta^{18}O_{leaf}^{H_2O}$ are calculated and the isotopic composition of leaf CO_2, δ_{leaf}, is determined subsequently following the temperature dependent equilibration given by Brenninkmeijer et al. [1983](Equation 1.4). It is quite reasonable to assume, that ambient air temperature equals the mean leaf temperature during the course of a day, and that the temperature at the forest floor is about 2°C lower than at the top of the canopy [J. Lloyd, personal communication]. The chloroplast CO_2 concentration, c_{c-i}, is estimated using the mean δ^{13}C of measured plant tissue cellulose for each box, $\delta^{13}C_{leaf-i}$, and ambient air δ^{13}C flask measurements in the respective box i via [Farquhar *et al.*, 1982]

$$ \delta^{13}C_{leaf-i} = \delta^{13}C_i - a - (b-a)\frac{c_{i-i}}{[CO_2]_{\mathrm{i}}} \tag{5.13} $$

with, a representing the fractionation of diffusion of ${}^{13}CO_2$ in air (4.4 ‰) and, b representing the fractionation during C3 carboxylation of ${}^{13}CO_2$ (29 ‰). The further CO_2 concentration draw-down from the substomata cavities, c_{i-i}, to the CO_2 chloroplast concentration, c_{c-i}, for each box is estimated via (c_{i-i} - c_{c-i})/$[CO_2]_i$ ≈0.2 [Lloyd *et al.*, 1992].

Figure 5.2 presents the basic data input fields, that drive the model for each time step. As δ^{18}O isotopic composition of the soil water, the measured values of the top soil layer were used as input data. Equilibration with CO_2 in the soil was again calculated following Brenninkmeijer et al. [1983](Equation 1.4), using the mean measured soil temperature of two sensors at 5 cm depths. The δ^{18}O of the stem water is also measured and equilibrated with CO_2 at ambient temperature + 4°C. For box 3 the aircraft flasks were used to calculate the mean of this box for both, CO_2 concentration and $\delta^{18}O(CO_2)$, with the heights at 100, 200 and 300 m. All model input data is linearly interpolated to the same time steps (30 min), and afterwards a harmonic fit is applied to the data. The harmonic curve fitting is done with the technique developed by the NOAA/CMDL carbon cycling group and is documented in Thoning et al. [1989].

Furthermore, a constant ^{222}Radon soil exhalation rate of 10 Bq m^{-3} is used as $F_{soil}(Rn)$ in equation 5.1, to complete the set of model input data.

5.4 Results

5.4.1 Standard Simulation

The standard simulation uses the parameterisation introduced in the precedent section. Figure 5.3 presents the calculated parameters of the model, which determine the equation system 5.8, 5.10, 5.11 and 5.12. The transport from box 1 to box 2 underlies a strong diurnal cycle, as illustrated by the variability of $F_{1\rightarrow2}(Rn)$ and $K_{1\rightarrow2}$. During night, vertical exchange is suppressed with an exchange coefficient $K_{1\rightarrow2}$ of about 50 m^{2}h^{-1}, that rapidly increases around noon up to values of about 500 m^{2}h^{-1}. However, the CO_2 flux from box 1 to box 2, calculated by Equation 5.5 shows a different behaviour. Despite an increasing

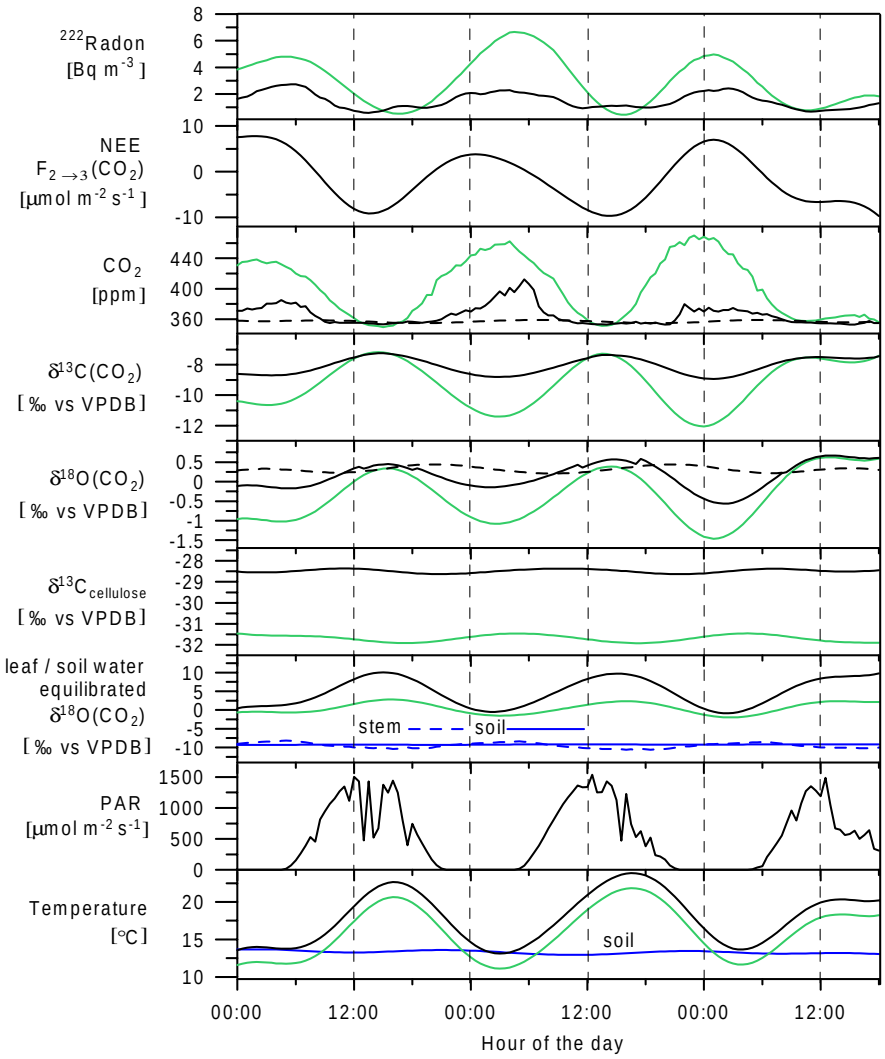

Figure 5.2: *Model input data: green lines represent box 1, black lines box 2 and dashed black lines box 3. NEE represents the CO_2 flux from box 2 to 3, $F_{2\rightarrow3}(CO_2)$.*

exchange coefficient $K_{1\rightarrow2}$ around noon, the CO_2 flux from box 1 to box 2 is nearly zero. This is due to the very small vertical CO_2 gradient between the mean CO_2 mixing ratios of both boxes. This gradient tends to zero and gets even slightly positive (box 2 higher than box 1). Therefore the model integrates a minimum vertical gradient of 0.3 ppm (twice the standard reproducibility of the flask measurement at the GC), whenever this vertical gradient gets smaller than 0.3 ppm. With the build up of the vertical CO_2 gradient during afternoon / evening, accompanied by high exchange coefficients $K_{1\rightarrow2}$, the CO_2 transport from box 1 to box 2 increases to maximum values of about 7 to 15 μmol $m^{-2}s^{-1}$. Here, the gradient box model approach obviously reaches a limit, because the Fick transport equation is highly sensitive to very small gradients. Via Equation 5.13, the ratio of inner stomatal to ecosystem CO_2 concentration, c_i/c_e, is calculated. Note here, that only the day-time values are reasonable. During night-time the inner stomatal CO_2 concentrations can reach values of several thousand ppm in reality, due to zero assimilation activity and the dominating leaf respiration. The model, however, ignores the night-time c_i/c_e ratios,

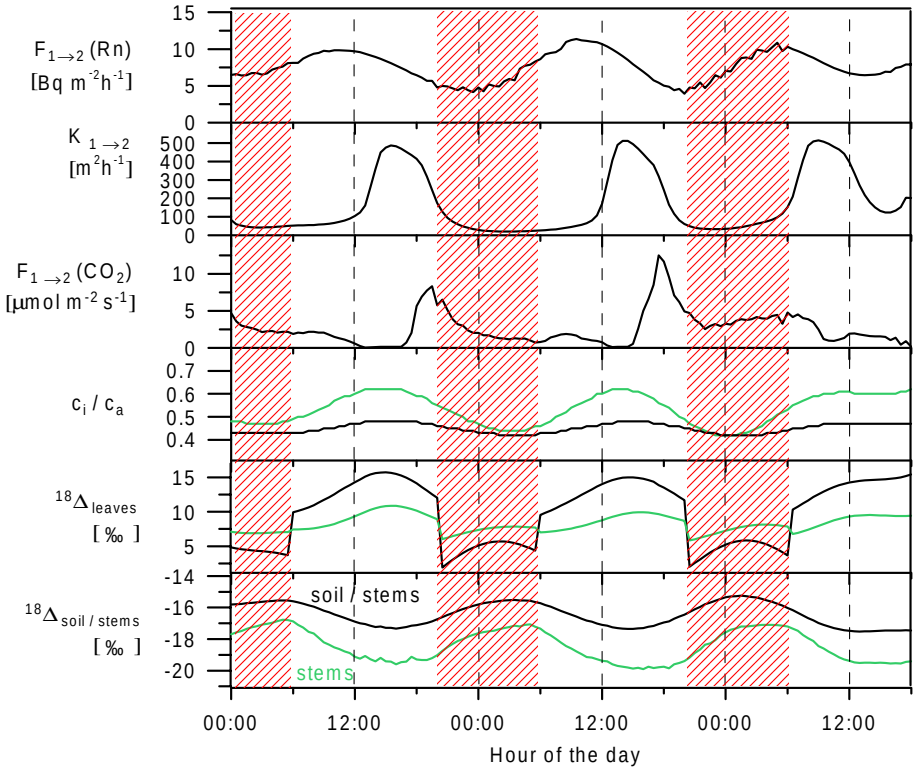

Figure 5.3: *Calculated model parameter: green lines represent box 1 and black lines box 2. Note that during night (shaded area, by definition PAR < 150 µmol $m^{-2}s^{-1}$) the assimilation flux is set to zero.*

and the assimilation flux is forced to be zero. Therefore, the calculation of the overall leaf discrimination against $C^{18}O^{16}O$, ${}^{18}\Delta_{leaves}$, which depends on c_i/c_e (Equation 2.20), is also only relevant for the flux equation system (5.8, 5.10, 5.11 and 5.12) during day-time. c_i/c_e ratios are modelled to range between 0.4 and 0.6, values that are also observed elsewhere for C3 plants [Yakir and Sternberg, 2000]. The overall leaf discrimination against $C^{18}O^{16}O$, ${}^{18}\Delta_{leaves}$, basically follows the diurnal cycle of the mean leaf water isotopic composition in the respective box (see Figure 5.2). The diurnal cycle reaches from about 7 to 10 ‰ for box 1 and from about 10 to 16 ‰ for box 2. Here, comparison of ${}^{18}\Delta_{leaves}$ with the discrimination against $C^{18}O^{16}O$ by the soil (${}^{18}\Delta_{soil}$) and the stems (${}^{18}\Delta_{stems}$), respectively, exhibits the potential of $\delta^{18}O(CO_2)$ as a unique tracer: the imprint of the soils and stem respiration, respectively, on the ecosystem $\delta^{18}O(CO_2)$ is significantly depleted by about 30 ‰, compared to the leaves. ${}^{18}\Delta_{soil}$ and ${}^{18}\Delta_{stems}$ show small temperature driven variability around -18 ‰ and -16 ‰, respectively, with a peak-to-peak amplitude of about 1 to 2 ‰.

The model output gross fluxes of the standard simulation are presented in Figure 5.4. The 1-D box model approach, combining transport and isotope vegetational processes, is able to separate between assimilation and respiration fluxes. Assimilation fluxes are modelled to direct into the canopy and they follow a diurnal cycle similar to PAR. This appears to be trivial, and of course there is no reason to wonder about assimilation being a sink flux to the atmosphere. However, this is the first approach that uses the ${}^{18}O$ interaction between CO_2 and H_2O in a closed process/transport model, resulting in reasonable numbers. There has been only one study up to know, combining isotopic processes with measured transport,

that could not even predict the correct direction of the gross fluxes [Bowling *et al.*, 1999]. They combined *NEE* measurements with flasks measurements within the canopy to derive the exchange of isotopes. The processing of the respective discriminations was basically performed with the same equations which were applied here, and with measurements of bulk leaf water. However, this study assumed the respirative isotopic signal to be constant in time, by applying the Keeling two-component approach. Furthermore, they treated the ecosystem as one box, not considering vertical gradients in leaf water δ^{18}O within the canopy.

The 1-D box model output fluxes are compared with concurrently estimated gross fluxes using the eddy correlation method (red line in Figure 5.4, Milukova *et al.* [2001]). Milukova *et al.* applied the model developed by Lloyd and Taylor [1994], using mean night-time CO_2 total ecosystem respiration fluxes and air and soil temperatures obtained on a daily basis. Basically, they extrapolate an empirical respiration function, derived from the night-time ecosystem respiration in dependence on the soil and air temperature, to the day-time. By introducing a coefficient, that allows for a joint effect of both, soil temperature and air temperature, on the ecosystem respiration rate, they partitioned the overall respiration flux into 71 % soil respiration and 29 % stem and foliar respiration (best fit). A shortcoming of the eddy covariance technique is its dependence on a sufficient turbulence strength, due to decreasing sensitivity of the anemometers with decreasing friction velocity u_*. Therefore, Milukova *et al.* recalculated all night-time fluxes for situations $u_* < 0.35$ ms^{-1} by regression. During the simulated period a mean day-time friction velocity of $u_* = 0.54 \pm 0.16$ ms^{-1} and a mean night-time friction velocity of $u_* = 0.31 \pm 0.13$ ms^{-1} was measured. Especially the second night showed very low u_* values with a mean of 0.21 ± 0.07 ms^{-1}; therefore, for this night all data was recalculated by regression and the smoothed, measured *NEE* (Figure 5.4, lowest panel) deviates from the results of Milukova *et al.*.

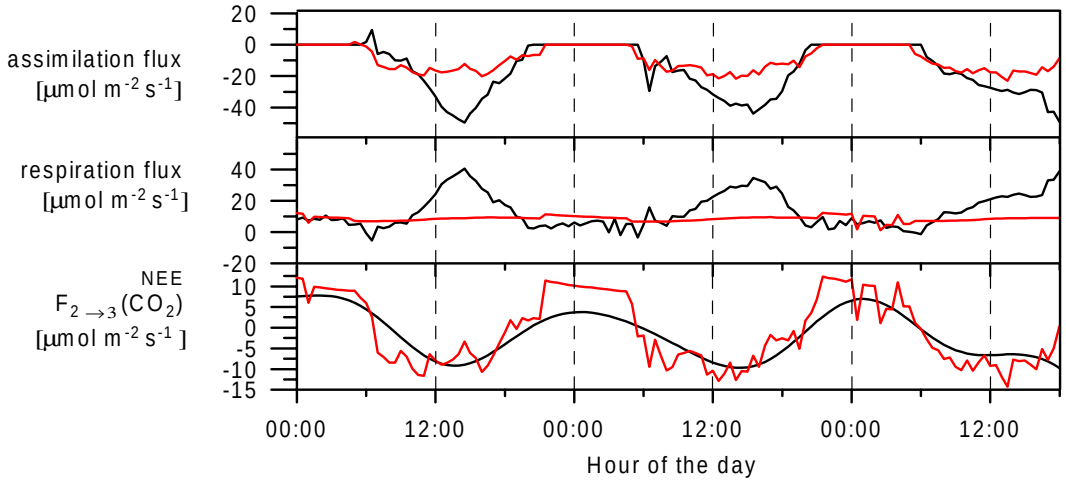

Figure 5.4: *Model output of the standard simulation (black lines): the gross fluxes (sum of box 1 and box 2), assimilation and respiration, along with the net exchange flux at the top of the canopy. The red lines present the results of the modified Lloyd and Taylor [Lloyd and Taylor, 1994] model, based on NEE measurements [Milukova* et al.*, 2001].*

To compare the 1-D box model with this approach, the same R_{a1}/ R_{soil} ratio was chosen in the parameterisation of the isotope balance in box 1 (partitioning parameter β in Equation 5.12). This implies, that at the same soil and air temperatures 71 % of night-time respiration

would be accounted by soil temperature (soil respiration) and 29 % by air temperature (stem and foliage respiration). Subsequently the continuous respiration flux, R, is subtracted from the measured *NEE*, with the residuum being the assimilation flux, A; thus $A = NEE - R$. Therefore, according to convention, *NEE* is negative when the net CO_2 flux is directed downward into the ecosystem.

During night-time, when assimilation is set to zero, the modelled respirative flux plus the gradient in each box is identical to the measured values of the eddy covariance measurements, which is a simple consequence of the conservation of mass in the model equations. During day-time the model predicts assimilation fluxes with a shape similar to PAR resulting in maximum values between 40 and 50 μmol $m^{-2}s^{-1}$ around noon. Simultaneously, to balance the mass flows, respiration is increasing up to about 30 to 40 μmol $m^{-2}s^{-1}$. The mean day-time ambient air temperature during the simulation was 19.8 $\pm$ 2.7°C and the mean night-time temperature 14.9 $\pm$ 2°C, whereas the soil temperature did not vary significantly with a mean of 13.3 $\pm$ 0.2°C. Compared to the night-time respiration flux with values of about 10 μmol $m^{-2}s^{-1}$ this would imply a Q_{10} of about 7, if related only on ambient temperature. This Q_{10} value relates to the flux weighted sum of all processes yielding ecosystem respiration, that is tree plus root respiration and soil heterotrophic respiration. Traditionally ecosystem process models used a Q_{10} of around 2 [Reich *et al.*, 1991], even though respiration studies suggest a mean Q_{10} of around 2.5 [Reich and Schlesinger, 1992]. Usually Q_{10} values are related to soil respiration only and a large variation between local site studies is observed. Besides Q_{10} values of around 2, values can range site specific from 3.5 for bulk soil in a mixed temperate forest [Boone *et al.*, 1998] to 11.7 for a floodland white spruce forest [Gulledge and Schimel, 2000]. Respiration of living cells in foliage, woody tissue and roots can consume more than 60 % of the carbon fixed in photosynthesis [Edwards *et al.*, 1980], but information on respiration rates, and especially ecosystem-level flux estimates, is sparse [Ryan *et al.*, 1994]. Leaf scale measurement of foliage respiration suggest Q_{10} values to range around 2.3 [Hubbard *et al.*, 1995].

There is a significant difference between the 1-D box model to the eddy correlation derived gross fluxes. Whereas the 1-D isotope box model predicts assimilation maxima of about 40 μmol $m^{-2}s^{-1}$, the respiration extrapolation yields maximum values of about 20 μmol $m^{-2}s^{-1}$. Table 5.2 compares the mean day- and night-time fluxes derived by the 1-D box model, the *NEE* approach and the direct soil respiration measurements.

Table 5.2: *Comparison of the mean assimilation and respiration fluxes (fluxes in μmol $m^{-2}s^{-1}$, day-time: 7:00 am - 7:00 pm, night-time: 9:00 pm - 5:00 am).*

Flux & Q_{10}	1-D box model	*NEE* derived	soil chamber
mean night-time respiration	5.7 $\pm$ 2.8	9.5 $\pm$ 2.9	6.4 $\pm$ 1.7
mean day-time respiration	19.6 $\pm$ 9.5	8.3 $\pm$ 0.9	9.4 $\pm$ 5.2
Q_{10}	6.8	$\sim$ 1	1.5
mean assimilation	26.0 $\pm$ 11.2	15.7 $\pm$ 3.2	-

The 1-D box model yields a mean night-time respiration flux of 5.7 $\pm$ 2.8 μmol $m^{-2}s^{-1}$, a factor 1.7 smaller than the *NEE* derived flux of 9.5 $\pm$ 2.9 μmol $m^{-2}s^{-1}$. However, within the 1 σ standard deviation, both, total ecosystem respiration fluxes are comparable. Comparison with direct soil chamber measurements indicates an underestimation of the 1-D box model derived respiration fluxes, because the soil chamber does not account for above-ground respiration fluxes. However, as the soil CO_2 respiration represents the major part of the overall ecosystem respiration ($\sim$70 %), the night-time respiration fluxes of all approaches are

consistent within 1 σ. Significant differences between the results of the respective day-time respiration fluxes are observed. Compared to night-time, the mean day-time respiration of the 1-D box model increases by a factor 3.4 to 19.6 $\pm$ 9.5 μmol m^{-2}s^{-1}, the *NEE* derived day-time fluxes decrease slightly by about 14 %. The chamber derived soil respiration increases by a factor 1.5 to 9.4 $\pm$ 5.2 μmol m^{-2}s^{-1}. As mentioned before, in principle, an increase of overall ecosystem respiration is expected. With an observed average air temperature increase from about 15°C during night to a day-time mean of about 20°C, this would imply Q_{10} values of 6.8 for the 1-D box model, about 1 for the *NEE* approach and 1.5 for the direct soil measurements, if related to ambient temperature. However, the direct soil flux should to a higher extent depend on the quite stable temperature of the top soil layer (minimum: 13°C, maximum: 13.7°C), and, therefore lower short term variation is expected. Here, the standard simulation of the 1-D box model tends to overestimate the temperature dependence of the overall ecosystem respiration flux.

The basic differences of the 1-D box model and the *NEE* approach can also be manifested by inspection of the cumulated fluxes for the model run of 72 hours (Figure 5.5). This

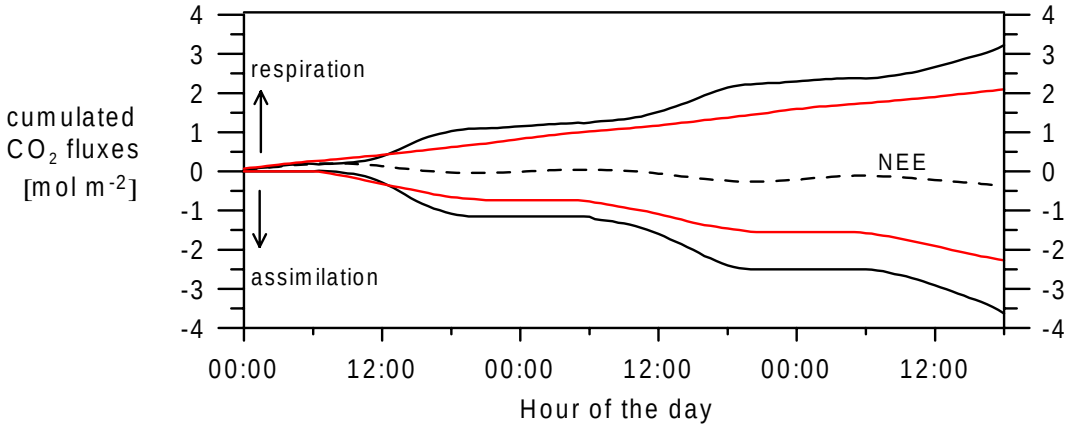

Figure 5.5: *Cumulated CO_2 fluxes. Standard simulation (black lines), Lloyd and Taylor [Lloyd and Taylor, 1994] model (red lines), along with the net ecosystem exchange (NEE) flux at the top of the canopy (black dashed line).*

Figure mirrors the cumulated gross fluxes and the net ecosystem CO_2 flux and illustrates the principal differences in the features of both approaches discussed before. The 1-D box model overall cumulative respiration slope is observed to increase during day-time, whereas the *NEE* derived cumulative respiration is increasing nearly constantly over day and night. Both cumulative assimilation curves show an increasing negative gradient with the onset of photosynthetic activity. After the 3 day model run, the differences in the cumulated assimilation fluxes end up in -3.6 mol/m^{-2} for the 1-D box model and in 2.3 mol/m^{-2} for the *NEE* derived cumulative assimilation. Due to conservation of mass, this principal difference between the approaches is also observed for the cumulative respiration fluxes.

5.4.2 Sensitivity Runs

Assessment of the 1-D isotopic box model output requires the knowledge of the sensitivity on the relevant parameters controlling the respective processes. In principle, the model depends on the parameterisation of the transport, the isotopic composition of the interacting reservoirs

and the associated fractionations and discriminations, respectively.

The only variable, that can change the model transport patterns, between the bottom canopy boxes, is the ^{222}Radon soil exhalation flux. In the model, the ^{222}Radon soil flux is assumed to be constant in time and space. As the results of the soil exhalation transect measurements show large spatial variation - correlated to soil water content [Levin *et al.*, 2001] - the mean value of 7.5 Bq m^{-2}h^{-1} needs not be the actual soil ^{222}Radon influx to box 1. Furthermore, the spatial heterogeneity of the soil ^{222}Radon flux leads to changing in-fluxes to box 1, due to changing footprint areas around the tower measurement site. The soil type directly below the tower showed a mean soil flux of 4.6 ± 0.9 Bq m^{-2}h^{-1}, whereas the overall hydrological transect mean is 24.0 ± 9.7 Bq m^{-2}h^{-1}. Therefore, the model was tested for its sensitivity to the soil influx $F_{soil}(Rn)$ in Equation 5.1 for a range from 2 to 20 Bq m^{-2}h^{-1}, assumed to be relevant for the measurement tower site. Figure 5.6 presents the results of this test via the modelled cumulated gross fluxes. Variation of $F_{soil}(Rn)$ between

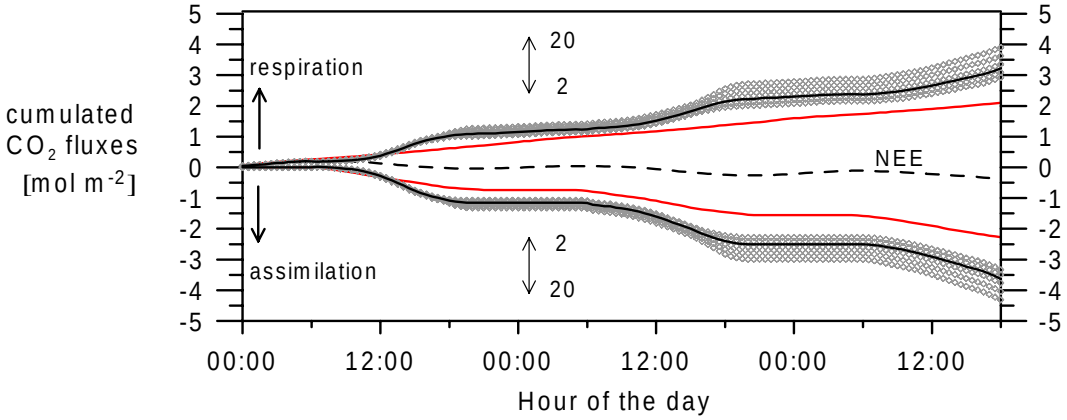

Figure 5.6: *Model output in dependence of the soil ^{222}Radon exhalation from 2 to 20 Bq m^{-2}h^{-1} (symbols). Standard simulation with $F_{soil}(Rn)$=7.5 Bq m^{-2}h^{-1} (black lines), Lloyd and Taylor model (red lines), along with the net ecosystem exchange (NEE) flux at the top of the canopy (black dashed line).*

2 to 20 Bq m^{-2}h^{-1} leads to a deviation from the standard simulation in the range between -8 % and +16 % for the resulting cumulative gross fluxes. Lower $F_{soil}(Rn)$ lead to lower gross assimilation fluxes of the system. This is due to the changing intra-canopy transport parameterisation by starting at Equation 5.1, where a lower $F_{soil}(Rn)$ directly ends up in lower exchange coefficient $K_{1\rightarrow2}$, which again lowers the CO_2 flux from box 1 to box 2, $F_{1\rightarrow2}(CO_2)$, in Equation 5.5. The answer of the equation on this changing transport is higher assimilation flux in box 1 and a lower assimilation flux in box 2. As the assimilative activity of the system is controlled by box 2, the overall assimilation flux is decreasing.

The model is also driven by the respective ^{18}O isotopic compositions of the CO_2 and H_2O reservoirs. Here, it is assumed, that the flask measurements deliver a precise characterisation of the CO_2 mixing ratio and isotopic composition of the respective box, because the model sensitivity tests within the measurement uncertainties showed no significant deviations from the standard simulation. Within the equations system (5.8, 5.10, 5.11 and 5.12) the sensitive terms are then given by the ^{18}O isotopic composition of the leaves and the soils, respectively. Together with the parameterisation of the associated fractionation and discriminations, sensitivity is tested for

- the overall leaf discrimination:

$$^{18}\Delta_{leaves} = -\epsilon_{leaf} + \frac{c_c}{[CO_2] - c_c} \, (\delta_{leaf} - \delta^{18}O)$$

(Equation 2.20) and

- the overall soil discrimination, defined as:

$$^{18}\Delta_{soil} = (1-\beta) \cdot (\delta^{18}O_{soil} - \delta^{18}O_1 + \epsilon_{soil}) + (\beta) \cdot (\delta^{18}O_{stem1} - \delta^{18}O_1) + \epsilon_{stem}).$$

(see Equation 5.12)

The overall leaf discrimination, $^{18}\Delta_{leaves}$, is itself a function of the isotopic composition of the leaf water, δ_{leaf}, ^{18}O(CO_2) diffusional fractionation from the ecosystem air to the site of carboxylation, ϵ_{leaf}, and the parameterisation of the chloroplast CO_2 concentration, c_c. Therefore, the model sensitivity on these terms is investigated. Exemplary, the basic answer of $^{18}\Delta_{leaves}$ on varying parameterisations is shown for box 2 and the overall model sensitivity is presented by the cumulated gross fluxes:

- δ_{leaf}

The leaf water isotopic compositions used in the model, are mean values of the measured bulk leaf water, that were attributed to the respective box. One can easily imagine, that these values need not be representative for all leaves in the forest, that interacted with the observed CO_2. This spatial heterogeneity in the signal is a serious problem. Obviously there is no way to get this information, without lumbering the whole forest and, therefore, destroying the experiment. Furthermore, the isotopic composition of the leaf water is also expected to be enriched at the site of evaporation and huge gradients in leaf water δ^{18}O are observed [Bariac *et al.*, 1994b]. Consequently, the measurement of the bulk leaf water may underestimate the interacting leaf water δ^{18}O. To vary δ_{leaf} in the model, the steady state leaf transpiration model of Craig and Gordon (Craig and Gordon, [1965], see Chapter 2.2.2, Equation 2.21) is used. Simultaneously, the feasibility to implement this model of Craig and Gordon into the 1-D box model, is examined. The Craig and Gordon model calculates the isotopic composition of the leaf water with

$$\delta_{leaf} = \epsilon_{liq-vap} + (1-h) \cdot (\delta_{root}^{H_2O} - \epsilon_{kin}) + h \cdot \delta_{vap}$$

Here, the relative humidity at the leaf surface, h, is assumed to be the measured ecosystem relative humidity within the ecosystem. $\delta_{root}^{H_2O}$, representing the δ^{18}O of root H_2O taken up from the soil water, was also measured, as well as the δ^{18}O of water vapour outside the leaf, δ_{vap}. The equilibrium fractionation of $H_2^{18}O$ for the liquid-vapour phase transition $\epsilon_{liq-vap}$ is well known and varies with temperature (Equation 2.22). Only the kinetic fractionation of $H_2^{18}O$ for the diffusion of water vapour across the stomatal cavity via the leaf boundary layer to the ecosystem air, ϵ_{kin}, is not well parameterised. As mentioned in Chapter 2.2.2, this value depends on the turbulent boundary conditions at the leaf surface and is varied from values for turbulent conditions, -15 ‰, to the value for molecular diffusive conditions at the leaf surface of -26 ‰. Figure 5.7 shows the results of this test and the impact on the cumulated fluxes are presented in Figure 5.8. In Figure 5.7 the isotopic δ^{18}O signature of CO_2 in isotopic equilibrium with leaf water is presented.

First of all, it is obvious, that the steady state leaf transpiration model of Craig and Gordon is applicable within the 1-D box model. The observed diurnal cycle of the leaf δ^{18}O(CO_2)

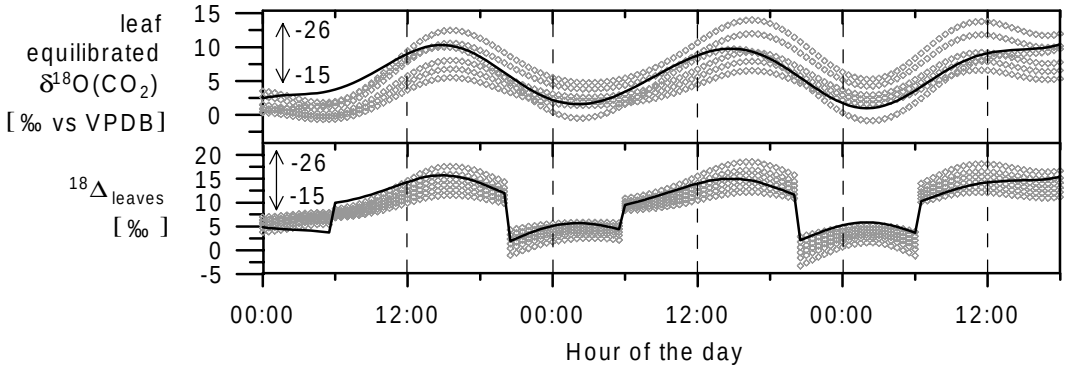

Figure 5.7: *Upper panel: δ_{leaf} values equilibrated with $\delta^{18}O^{H_2O}_{leaf}$ calculated via Craig and Gordon with varying ϵ_{kin} from -26‰ to -15‰. Lower panel: resulting variation in $^{18}\Delta_{leaves}$. Black lines: standard simulation using measured $\delta^{18}O^{H_2O}_{leaf}$, symbols: test runs. Note, that night-time values are not relevant to the model, as assimilation is set to zero.*

equilibrated with the leaf water, calculated via Craig and Gordon, shows similar variation to the measured bulk leaf water derived values. As, in the model, both are equilibrated at the same temperature, the results are comparable. Variation in ϵ_{kin} leads to the expected variation in the resulting leaf $\delta^{18}O(CO_2)$. For larger fractionations - i. e. under molecular diffusive leaf boundary conditions - the Craig and Gordon model predicts up to 5‰ more enriched leaf water $\delta^{18}O$ values, than the measured bulk derived values. Inspection of the resulting range of leaf $\delta^{18}O(CO_2)$ values in Figure 5.7 exhibits that the measured mean values are reproduced best for ϵ_{kin} between -19 and -21‰, i.e. partly turbulent conditions at the leaf surface must be relevant. However, implementation of the Craig and Gordon equation into the box model, assumes steady state transpiration conditions. These are usually not observed, especially during the strong diurnal variation of the transpiration rate. Therefore, dynamic approaches are to be developed, that parameterise the leaf water enrichment in the Craig and Gordon equation by the transpiration rate. First results show different behaviour of the diurnal cycle, with a slower enrichment slope during day-time [P. Ciais, personal communication]. However, the Craig and Gordon equation is largely controlled by the relative humidity and also influenced by the water vapour isotopic composition. Both are hard to determine on the leaf scale under natural conditions, therefore a precise determination of the leaf water ^{18}O is very difficult. But the general agreement of the measured values with the Craig and Gordon derived numbers in this 1-D box model, strongly justifies the application of the Craig and Gordon equation in global ^{18}O models. As a consequence of more enriched leaf $\delta^{18}O(CO_2)$, $^{18}\Delta_{leaves}$ also shows higher values, which can easily be seen from Equation 2.20.

Figure 5.8 shows the sensitivity of the used leaf water $\delta^{18}O$ - and the accompanied variation in $^{18}\Delta_{leaves}$ - on the overall cumulated fluxes of the model. In principle, the model output cumulated fluxes stay quite stable for smaller $^{18}\Delta_{leaves}$ discriminations, i.e. more depleted leaf water $\delta^{18}O$. The cumulated fluxes are smaller than the fluxes obtained for the standard simulation, but fit quite well with the *NEE* values. Basically, for $^{18}\Delta_{leaves}$ values exceeding the measured values of the standard simulation, the model calculates only slightly - 3‰ - larger $^{18}\Delta_{leaves}$ discriminations, and the model output diverges. This is due to the fact, that within the substitution performed in the equation system (5.8, 5.10, 5.11 and 5.12) the assimilation flux is proportional to $1/(^{18}\Delta_{leaves} +^{18} \Delta_{soil})$. With $^{18}\Delta_{soil}$ values of about

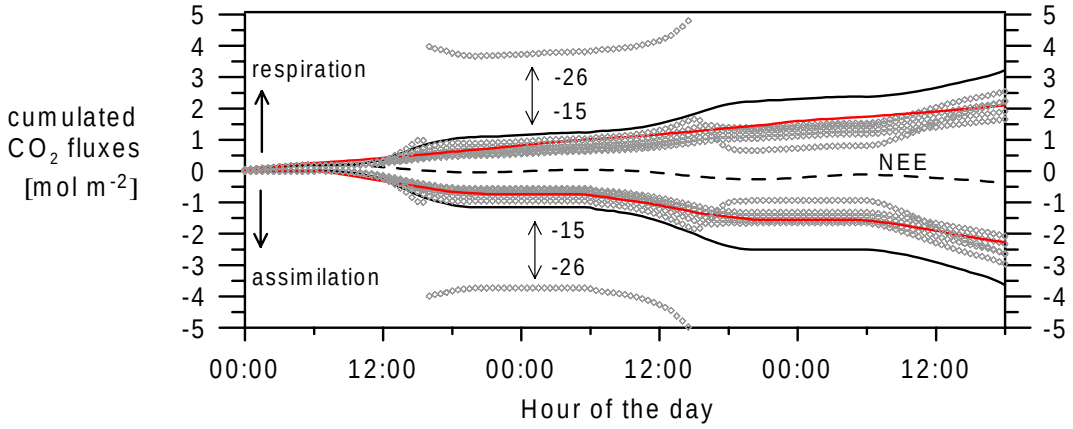

Figure 5.8: *Model output in dependence of the kinetic fractionation against $H_2{}^{18}O$, ϵ_{kin} from -15 to -26‰ (symbols). Standard simulation without using $\delta^{18}O_{leaf}^{H_2O}$ (black lines). Lloyd and Taylor model (red lines), along with the net ecosystem exchange (NEE) flux at the top of the canopy (black dashed line).*

-19‰ during day-time, increasing $^{18}\Delta_{leaves}$ values lead the denominator in the assimilation equation to converge against zero and the assimilation flux diverges immediately. Therefore, the model is highly sensitive on the parameterisation of $^{18}\Delta_{leaves}$.

- ϵ_{leaf}

The second parameter, that controls the variation in $^{18}\Delta_{leaves}$ is the $^{18}O(CO_2)$ diffusional fractionation from the ecosystem air to the site of carboxylation, ϵ_{leaf}. In the standard simulation, the effective leaf discrimination is assumed to be constant in time, using the value of -7.4‰ given by Farquhar et al. [1993]. However, as mentioned in Chapter 2.2.2, this is a mean value, averaging over three involved fractionation processes, namely the fractionation for molecular diffusion through the stomata (ϵ_d, - 8.8‰), the fractionation for diffusion through the leaf boundary layer (ϵ_b, - 5.8‰, i.e. molecular diffusion to the 2/3 power) and the fractionation summarising an equilibrium dissolution effect and diffusion fractionation in solution at the mesophyll cell walls (ϵ_w, - 0.8‰). Therefore, the model was tested for variations of ϵ_{leaf} between -8.8 and -4‰. Furthermore, a simulation run was performed, that includes the parameterisation of ϵ_{leaf} via the weighted CO_2 gradients from the ecosystem air to the site of carboxylation in the chloroplasts (Equation 2.23). Here, considering the draw-down of the respective CO_2 concentrations from the ecosystem air to the chloroplasts, the following parameterisation was chosen: c_e: measured ecosystem atmospheric CO_2 concentration, $c_{sur} = c_e$ - 0.01: CO_2 concentration at leaf surface, c_i: CO_2 concentration in the substomatal cavity (following Equation 2.18), $c_{mw} = c_i$ - 5 ppm: CO_2 concentration at mesophyll cell wall surface, $c_c = c_i$ - 0.2 c_e: CO_2 concentration in chloroplast. Figure 5.9 shows the modelled ϵ_{leaf} (blue, top panel) and the effect of variation in ϵ_{leaf} on $^{18}\Delta_{leaves}$. Calculation of ϵ_{leaf} with Equation 2.23 yields values between -5.8 and -6.1‰, which is therefore up to 1.5‰ smaller than the value for the mean fractionation factor given by Farquhar et al. [1993] of -7.4‰. This parameterisation, therefore, suggests a higher influence of the associated fractionation steps connected with smaller fractionations, that are the molecular diffusion through the leaf boundary layer and the fractionation summarising an equilibrium dissolution effect and diffusion fractionation in solution at the

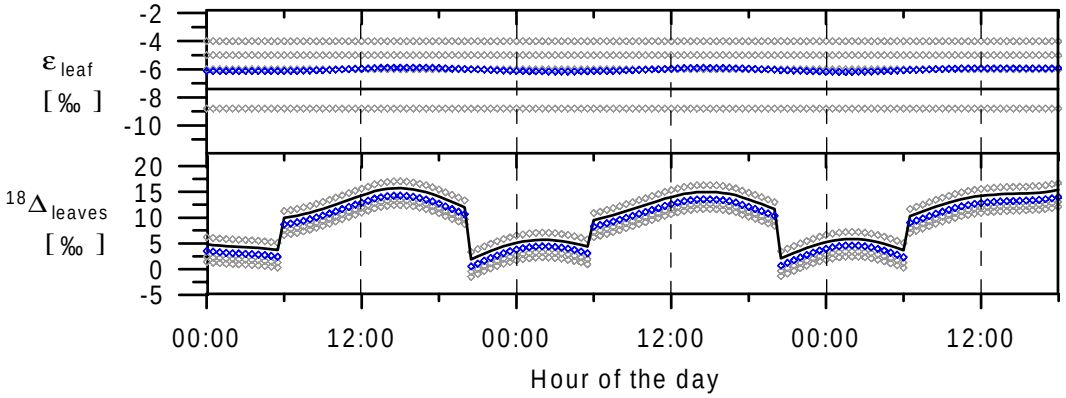

Figure 5.9: *Upper panel: ϵ_{leaf} values. Lower panel: resulting variation in $^{18}\Delta_{leaves}$. Black line: standard simulation using ϵ_{leaf} = -7.4‰, symbols: test runs with varying ϵ_{leaf} values, blue symbols: modelled ϵ_{leaf}. Note, that night-time values are not relevant to the model, as assimilation is set to zero.*

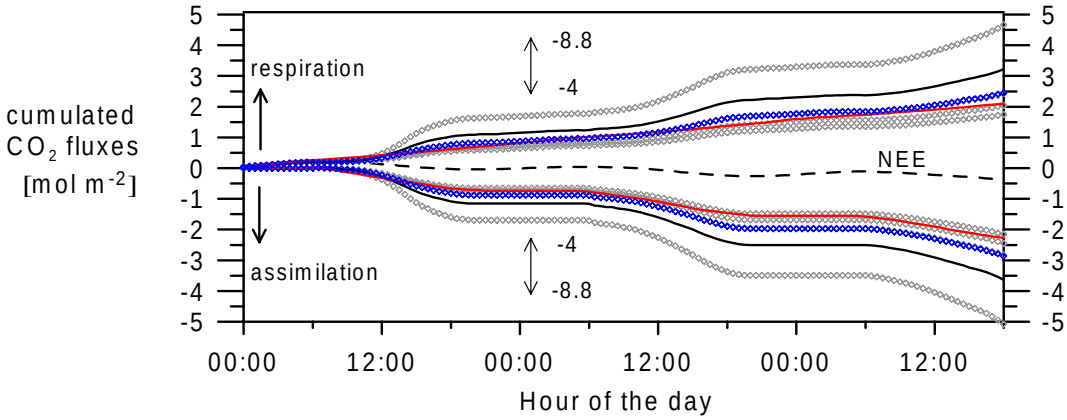

Figure 5.10: *Model output in dependence of the leaf discrimination against $C^{18}O^{16}O$ ϵ_{leaf}, from -4 to -8.8‰ (symbols). Blue: modelled ϵ_{leaf}. Standard simulation with ϵ_{leaf}=-7.4‰ (black lines), Lloyd and Taylor model (red lines), along with the net ecosystem exchange (NEE) flux at the top of the canopy (black dashed line).*

mesophyll cell walls. Just like the kinetic fractionation of water vapour in the Craig and Gordon equation, the leaf boundary conditions are likely to influence the overall ϵ_{leaf}. As the CO_2 gradients within the leaves, especially from the inner cellular spaces to the site of carboxylation, are poorly understood, the parameterisation of ϵ_w in Equation 2.23 is shaky.

The impact of smaller ϵ_{leaf} numbers (to mean the absolute value) is a decrease of $^{18}\Delta_{leaves}$. The impact of $^{18}\Delta_{leaves}$ on the resulting gross fluxes, as discussed before, is shown in Figure 5.10. Here, smaller fractionation will lead to smaller cumulative fluxes compared to the standard run. The run using the parameterised ϵ_{leaf} (blue in Figure 5.10, lower panel) shows a similar behaviour like the estimates of the *NEE* derived fluxes. Only assuming maximum diffusional fractionation of -8.8 ‰ leads to about 50 % higher gross flux results.

- c_c

The third parameter, that controls the variation in $^{18}\Delta_{leaves}$, is the parameterisation of the chloroplast CO_2 concentration, c_c. After modelling the inner stomatal CO_2 concentration c_i by using the $^{13}C/^{12}C$ ratios of ecosystem air and plant cellulose in Equation 2.18, the chloroplast CO_2 concentration has to be determined. Here, the present knowledge of how to parameterise c_c ranges from $(c_i\text{-}c_c)/c_e \approx 0.1$ [Farquhar *et al.*, 1993a], $(c_i\text{-}c_c)/c_e \approx 0.15$ [Raven and Glidewell, 1981] to $(c_i\text{-}c_c)/c_e \approx 0.2$ [Lloyd *et al.*, 1992]. Figure 5.11 shows the modelled c_c/c_e ratios in dependence of this parameterisation and the subsequent impact on $^{18}\Delta_{leaves}$.

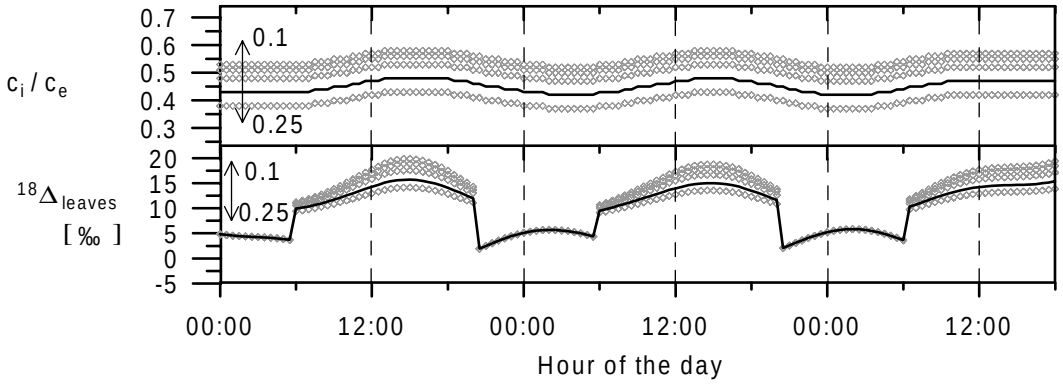

Figure 5.11: *Upper panel: modelled c_c/c_e ratios in dependence of the c_c parameterisation. Lower panel: resulting variation in $^{18}\Delta_{leaves}$. Black line: standard simulation, symbols: test runs. Note, that night-time values are not relevant to the model, as assimilation is set to zero.*

The resulting range of c_c/c_e ratios shows values between 0.4 and 0.6 in dependence of how many percent of the ambient ecosystem air are subtracted from c_i to obtain c_c in the parameterisation. Figure 5.11 illustrates, that for $c_c = c_i - 0.1 \cdot c_e$, $^{18}\Delta_{leaves}$ reaches values of about 20 ‰, which, for known reasons, delivers very high assimilation fluxes. Note here, that during night, where assimilation is set to zero and, therefore, does not influence the flux calculations, $^{18}\Delta_{leaves}$ is independent of the CO_2 gradient parameterisation. As mentioned before, during night leaf internal CO_2 concentration can increase up to several thousand ppm and the $\frac{c_c}{[CO_2]-c_c}$ term in Equation 2.20 converges against -1.

The basic features of the presented model runs in Figure 5.12 is, that estimating too low CO_2 gradients between the leaf surface and the site of carboxylation, can totally destroy the observed model output. The c_c parameterisation $c_c = c_i - 0.15 \cdot c_e$ found by Raven and Glidewell [1981], leads to about 100 % higher gross fluxes, than the setting of the standard

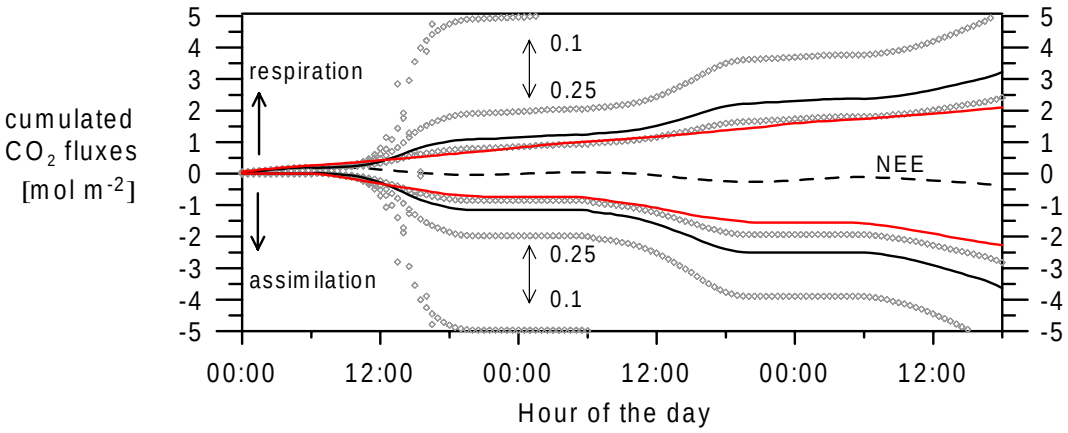

Figure 5.12: *Model output in dependence of the c_c parameterisation. Standard simulation with (c_i - c_c)/[CO_2] = 0.2 (black lines), Lloyd and Taylor model (red lines), along with the net ecosystem exchange (NEE) flux at the top of the canopy (black dashed line).*

simulation, using $c_c = c_i - 0.2 \cdot c_e$. Therefore, the knowledge of the leaf internal CO_2 concentration gradients is, besides the parameterisation of the leaf discrimination, ϵ_{leaf}, and the determination of the leaf water isotopic composition, δ_{leaves}, a limiting factor on using the potential of ^{18}O in carbon cycling studies.

As mentioned above, beside the overall leaf discrimination $^{18}\Delta_{leaves}$, the last sensitive term to discuss within the equations system 5.8, 5.10, 5.11 and 5.12, is the overall soil discrimination $^{18}\Delta_{soil}$ in box 1. The overall soil discrimination itself, is a function of the isotopic composition of the soil water, δ_{soil}, and the value of the soil ^{18}O fractionation of CO_2 diffusion from the soil to the ecosystem air, ϵ_{soil}. Therefore, the model sensitivity is investigated on these terms and the basic answer of $^{18}\Delta_{soil}$ on varying parameterisations is investigated.

- δ_{soil}

As the soil water could potentially get significantly enriched in $^{18}O(H_2O)$ near the soil surface through evaporation, the top soil layer $\delta^{18}O(H_2O)$ value of the measured top 5 cm soil water could result in an underestimation of the soil $\delta^{18}O(H_2O)$. It can also be assumed that the stem isotopic composition of the mosses and blueberries reflect the isotopic composition of the top soil layer [Jon Lloyd, personal communication]. This is due to the fact, that these understory plants are supplied by water near the surface. Furthermore, the stem isotopic composition represents an integrated value of the upper soil water in space and time. The effect of replacing the measured $\delta^{18}O_{soil}^{H_2O}$ of about -11 ‰ by the isotopic composition of the understory stems $\delta^{18}O_{stem}^{H_2O}$ of about -4 ‰, is presented in Figure 5.13. Here, the isotopic $\delta^{18}O$ signature of CO_2 in isotopic equilibrium soil water is presented. Reminding the definition of $^{18}\Delta_{soil}$ given above, shows, that $^{18}\Delta_{soil}$ is proportional to the δ_{soil} value. Therefore, more enriched soil water ^{18}O leads to higher overall soil discriminations $^{18}\Delta_{soil}$. As a consequence of the $1/(^{18}\Delta_{leaves} + ^{18}\Delta_{soil})$ term in the assimilation substitution equation, the denominator gets greater and assimilation fluxes are decreasing. The resulting gross fluxes of this test in Figure 5.14 show a good agreement with the *NEE* derived cumulated fluxes of about 2.5 mol m^{-2} assimilation after 72 hours.

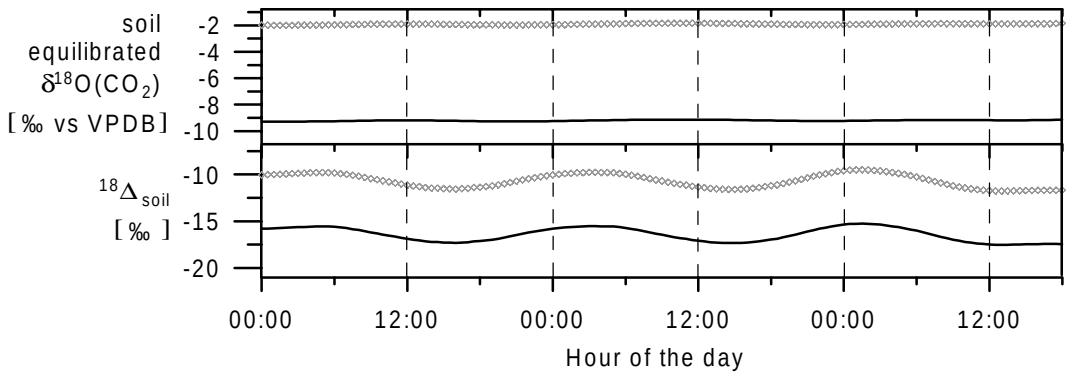

Figure 5.13: *Upper panel: δ_{soil} determined by equilibration with the measured $\delta^{18}O^{H_2O}_{stem}$ of the understory stems. Lower panel: resulting variation in $^{18}\Delta_{soil}$. Black line: standard simulation, symbols: test run.*

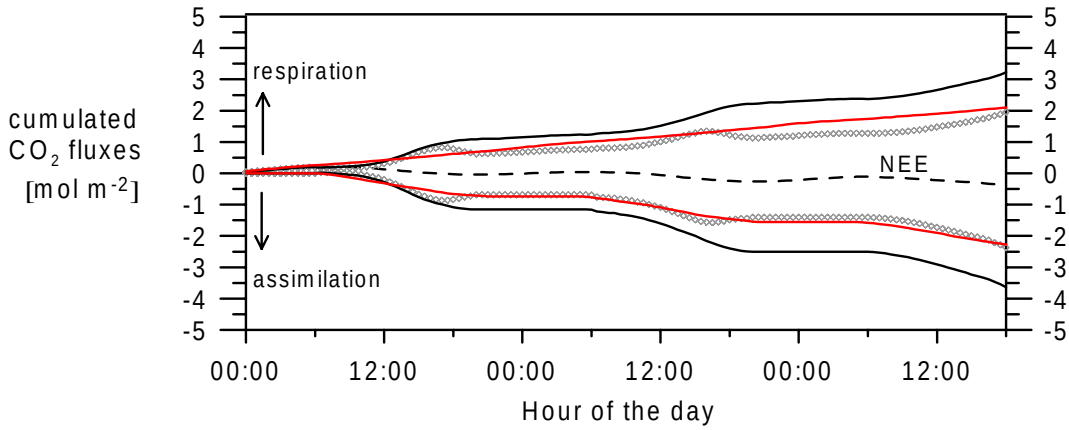

Figure 5.14: *Model output for δ_{soil} with the measured $\delta^{18}O$ of the understory stems. Standard simulation with the measured δ_{soil} (black line), Lloyd and Taylor model (red lines), along with the net ecosystem exchange (NEE) flux at the top of the canopy (black dashed line).*

- ϵ_{soil}

The second, potentially variable term, that controls the overall soil discrimination $^{18}\Delta_{soil}$ is the effective soil fractionation against $C^{18}O^{16}O$ during diffusion through the soil to the ecosystem atmosphere. As mentioned in Chapter 2.2.2, during diffusion through the soil there is kinetic fractionation of the diffusing CO_2 molecules, which is theoretically limited to a maximum ϵ_{soil} = -8.8 ‰ in case of purely molecular diffusion. However, as turbulent diffusion does not fractionate and the top few cm of the soil may be exposed to small eddy turbulences of the atmosphere, effective fractionation is varied in the sensitivity run between 0 ‰ and the maximum value of -8.8 ‰. In principle, the influence of decreasing the effective soil fractionation (by absolute value), is the same as assuming more enriched soil water in the equations. In a similar way, $^{18}\Delta_{soil}$ gets larger with the consequence of smaller resulting gross fluxes (Figures 5.15, 5.16).

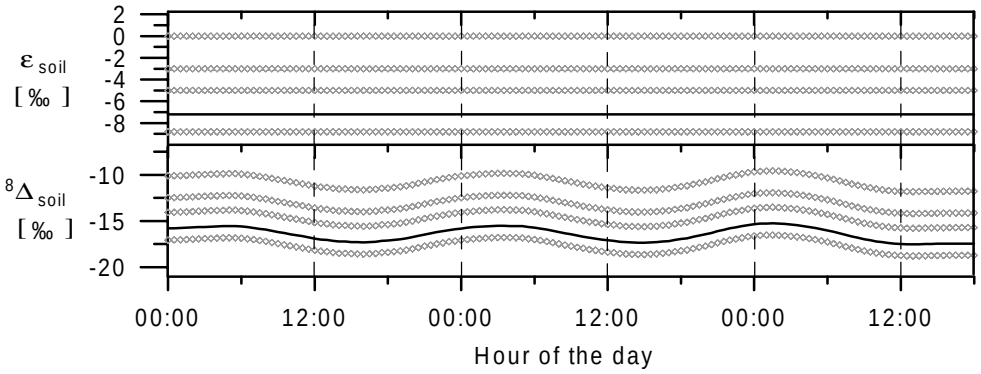

Figure 5.15: *Upper panel: variation of ϵ_{soil}. Lower panel: resulting variation in $^{18}\Delta_{soil}$. Black line: standard simulation, symbols: test runs.*

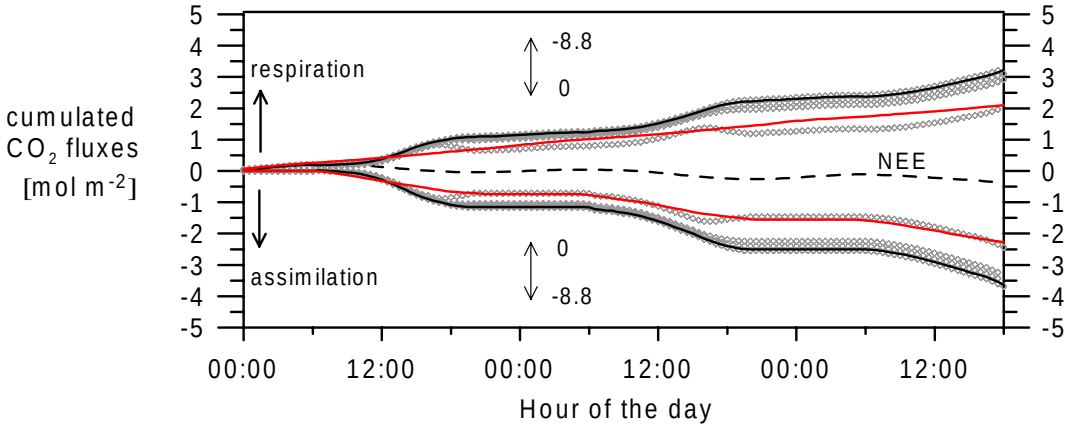

Figure 5.16: *Model output in dependence of ϵ_{soil}. Standard simulation with ϵ_{soil}=-7.2‰ (black lines), Lloyd and Taylor model (red lines), along with the net ecosystem exchange (NEE) flux at the top of the canopy (black dashed line).*

5.5 Discussion & Prospects

The 1-D isotopic box model set-up developed here is in principle capable to calculate reasonable numbers for the gross fluxes in the investigated ecosystem. It is the first approach, that combines field measurements with a closed model set-up, providing separate ecosystem CO_2 gross fluxes. In addition, with the input data set that was measured in the field, the output fluxes are comparable with concurrently estimated gross fluxes derived via the *NEE* respiration flux extrapolation method. However, the model is sensitive to the chosen parameterisation of transport, the isotopic composition of the involved reservoirs and to the associated fractionations and discriminations, respectively. Within the known range of these crucial parameters from other experiments described in the literature that were mainly obtained from small scale measurements under laboratory conditions, the model is largely stable. This is especially true with respect to the ^{222}Radon calibrated intra-canopy transport characterisation. Limiting to the model applicability, however, is the existence of adequate vertical gradients within the canopy of both, CO_2 mixing ratio and ^{222}Radon activity. As derived from the sensitivity studies, the most crucial parameter is the determination of the

overall leaf discrimination, $^{18}\Delta_{leaves}$. Here, the setting of the chloroplast CO_2 concentration exhibits the strongest control, besides the variation of $\delta^{18}O$ of leaf water. Up to know, there are only very recent studies, dealing with measurements of leaf CO_2 conductances to determine the overall leaf discrimination [Gillon and Yakir, 2000]. Therefore, effort should be invested in leaf scale investigations to properly parameterise the critical leaf internal CO_2 gradients for a wide range of different species and environmental/hydrological conditions.

Besides the respective parameterisations discussed above, the principal restriction of modelling ^{18}O in canopy ecosystems is spatial heterogeneity in the $\delta^{18}O$ signal. The model assumes horizontal homogeneity of the distribution of the isotopic signatures. Also in vertical direction, this approach assumes mean measured values to be representative for each box. Therefore, any spatial variation may seriously influence the output of the model.

In the context of global ^{18}O models, where usually monthly means of $^{18}\Delta_{leaves}$ were calculated, the parameterisation of the chloroplast concentration also is essential. Errors of the global model in the major parameters, the $\delta^{18}O$ of precipitation, leaf water ^{18}O enrichment and the overall leaf discrimination, need to be better quantified [Ciais *et al.*, 1997a; Peylin *et al.*, 1999]. However, to compare global models with local measurements is still extremely difficult (if not impossible), as the spatial resolution (horizontal: 7.5° by 7.5°, vertical: nine levels) of these global models is too coarse to detect small scale structures. Therefore, to use $\delta^{18}O$ as a CO_2 gross flux tracer in global models, the results of the presented local 1-D box model have to be tested and extended to the regional scale. Via subsequent upscaling of the models, a nested $\delta^{18}O$ model hierarchy should provide further insight to site and species specific vegetational effects.

Chapter 6

Regular Flights at Syktyvkar

After the detailed discussion of the local scale ecosystem canopy processes, the impact on the tropospheric CO_2 mixing ratio and the CO_2 isotopic composition is investigated in space and time. The objective is, to qualitatively understand tropospheric variations with respect to the biosphere-troposphere processes. Basically, that is the question of how the signals observed within the biosphere are translated into the meso- or continentalscale tropospheric signals.

6.1 Seasonality

Within the EUROSIBERIAN-CARBONFLUX project aircraft flask sampling was performed at Syktyvkar, west of the Ural mountains. Within this joint project, the responsibility for the analysis of these samples was in the Heidelberg group.
Figure 6.1 shows the two years records of CO_2 mixing ratio, $\delta^{13}C(CO_2)$ and $\delta^{18}O(CO_2)$ at the aircraft site in Syktyvkar. Very regular seasonal cycles are observed in all three components. The CO_2 and $\delta^{13}C$ amplitudes significantly decrease with height from 2000 m to 3000 m.

As expected from the local scale observations, CO_2 and $\delta^{13}C$ changes the sign of the vertical gradient from summer to winter. This is partly explained by a net ground level biospheric source of CO_2 during winter, which is depleted in $\delta^{13}C$ compared to the tropospheric background, respectively by a discriminating sink in summer (see Chapter 4.4.2). For the Syktyvkar year-round aircraft record, in a number of profiles the gradient even between 2000 and 3000 m is large enough to derive the signature of the apparent source from a two component mixing approach according to Keeling [1958; 1961] for individual profiles (Figure 6.1, lowest panel). Minimum winter time source signatures of $\delta^{13}C$ = -32 $\pm$ 3 ‰ are observed in January/February. Inspection of vertical profiles at Zotino extending from 100 up to 3000 m, also yielded winter time situations with a $\delta^{13}C(CO_2)$ source as depleted as -31.6 ‰ [Jon Lloyd, personal communication]. As the pure $\delta^{13}C$ biospheric source during winter is not observed to be as much depleted as -32 ‰, the contribution of a more depleted source (or of some sources) is needed to explain the observed source signature. Most likely is the significant contribution of from fossil fuel emissions, carrying $\delta^{13}C$ signatures between -30 ‰ (oil) to -44 ‰ (natural gas) into the troposphere. These situations could be clearly identified at Zotino as "polluted" through enhanced CO mixing ratios. However, again during the winter season, CO_2 increases in the boundary layer were frequently observed, which are not elevated in CO, and obviously caused by soil emissions of respiratory CO_2 with source signatures ranging from $\delta^{13}C$ = -26.8 to -28.9 ‰. This is the expected, solely biospheric source signature, observed during the canopy measurements in autumn 1999 of $\delta^{13}C$ = -27.72 $\pm$ 1.27 ‰.

The maximum summer sink $\delta^{13}C$ signature of -25 $\pm$ 3 ‰ corresponds to a maximum over-

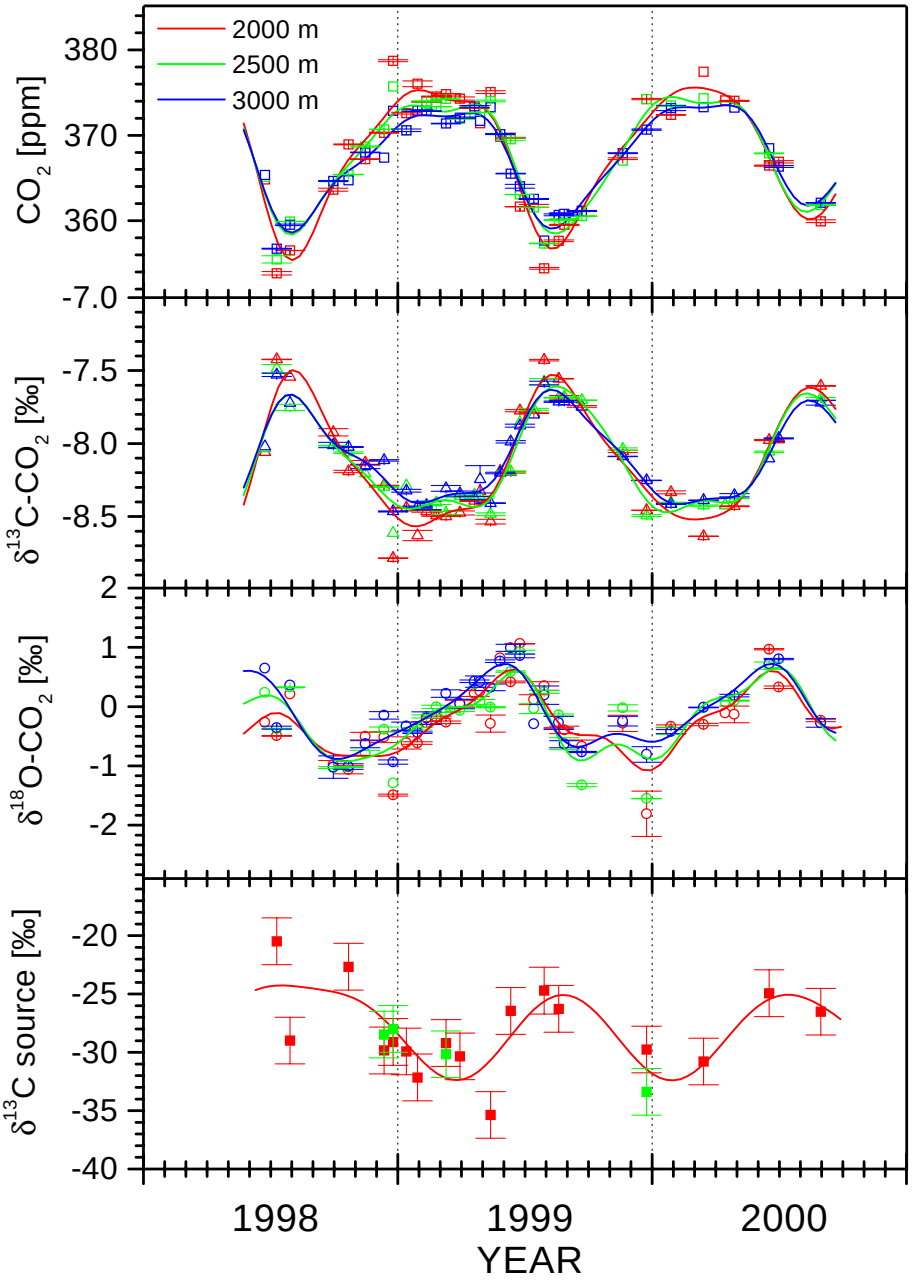

Figure 6.1: *Seasonal cycles of flask CO_2 concentration (top), $\delta^{13}C(CO_2)$(middle) and $\delta^{18}O(CO_2)$(bottom) at the Syktyvkar flight station at 3000, 2500 and 2000 meter above ground. The lowest panel presents the apparent source signature of $\delta^{13}C(CO_2)$.*

all ecosystem mean discrimination $^{13}\Delta$ of -17.5 ‰, assuming a mean summer CBL $\delta^{13}C(CO_2)$ of -7.5 ‰. As the fossil fuel emissions contribution to the CBL can be expected to be significantly smaller during summer, this CBL derived source signature corresponds very well with the values detected at the biosphere-troposphere interface. As described in Chapter 4.2.2 and 4.3.2, the observed overall mean source signatures of the canopy ecosystem during the intensive campaigns in 1998 and 1999 showed values of $\delta^{13}C$ = -25.96 ± 0.2 ‰ and $\delta^{13}C$ = -25.68 ± 0.4 ‰, respectively.

The Syktyvkar $\delta^{18}O(CO_2)$ record also shows a regular seasonality, however with a phase shift of about two months compared to $\delta^{13}C$ and CO_2 mixing ratio. The $\delta^{18}O$ maximum occurs significantly earlier in the year, namely in May instead of July/August, were the $\delta^{13}C$ reaches maximum and the CO_2 mixing ratio reaches minimum values. This $\delta^{18}O$-maximum coincides with the maximum draw down rate of CO_2 mixing ratio in the atmosphere, i.e. when the net uptake of CO_2 by plant assimilation exerts respiration fluxes [Schulze *et al.*, 1999]. The strong enrichment of $\delta^{18}O$ in leaf water observed during the summer intensive campaigns, therefore, most probably causes this $\delta^{18}O$-maximum by strong photosynthetic activity and exchange of ^{18}O with leaf water in the plants. The strong decrease of the atmospheric $\delta^{18}O(CO_2)$ signal during the remaining summer and autumn season can be interpreted as a dominating influence of soil respiration CO_2 fluxes over assimilation fluxes on the tropospheric $\delta^{18}O$ signal. The analysis of the 1-D box model exhibits, that CO_2 originating from soil respiration is depleted in $\delta^{18}O$ if compared to atmospheric CO_2 by about 5 to 15 ‰ (see Chapter 5.4).

The second principal difference of the observed tropospheric $\delta^{18}O$ signal compared with $\delta^{13}C$ and CO_2 mixing ratio, is the shape of the seasonal cycle. $\delta^{18}O$ gets slowly enriched from September onwards with a nearly linear slope until the maximum in May, whereas both, $\delta^{13}C$ and CO_2 mixing ratio, show a relatively fast increase to their maxima. This behaviour of $\delta^{18}O$ is mainly understood as a large scale equilibration process of the mixing between enriched air originating from the tropics with generally depleted air in northern Eurasia [M. Cuntz, personal communication].

Another qualitative observation is that throughout the year, $\delta^{18}O$ seems to be slightly more depleted at the lower level (2000 m) than at 3000 m, supporting the hypothesis of dominating influence from a generally depleted CO_2 source at ground level. Occasionally, mainly in autumn and early winter, very depleted $\delta^{18}O$ values are observed. If these results are not artefacts of ^{18}O exchange of CO_2 with condensed water in the flasks, they can only be explained by very strong ^{18}O equilibration processes (gross CO_2 exchange) at ground surfaces, rather than by net CO_2 emissions (i.e. from fossil fuels or net soil respiration).

6.2 Longitudinal Variation over Euro-Siberia

Besides the temporal development of the seasonal cycle, the longitudinal differences moving from west to east, are shown in Figure 6.2. Presented are results of the Orléans aircraft program, that is run by LSCE in co-operation with Meteo France since 1996. The flight location is at 3°E, 48°N, about 300 km south of Paris within an area of agricultural land and forests. Regular vertical aircraft profiles for flask sampling are performed every 2-3 weeks from 100 to 3000 m a.s.l. The Zotino aircraft program is run by IPEE and MPI-BGC. The flight location for Zotino is at 89°E, 61°N, about 600 km north of the city of Krasnoyarsk close to the small village Zotino located at the Jenisej river. The region belongs to the north Siberian taiga with the Jenisej river as the natural border between the western Siberian lowland and the Siberian highlands.

From examination of the continuous vertical profiles of CO_2 relative humidity and temperature, in most situations it is possible to determine the height of the convective boundary

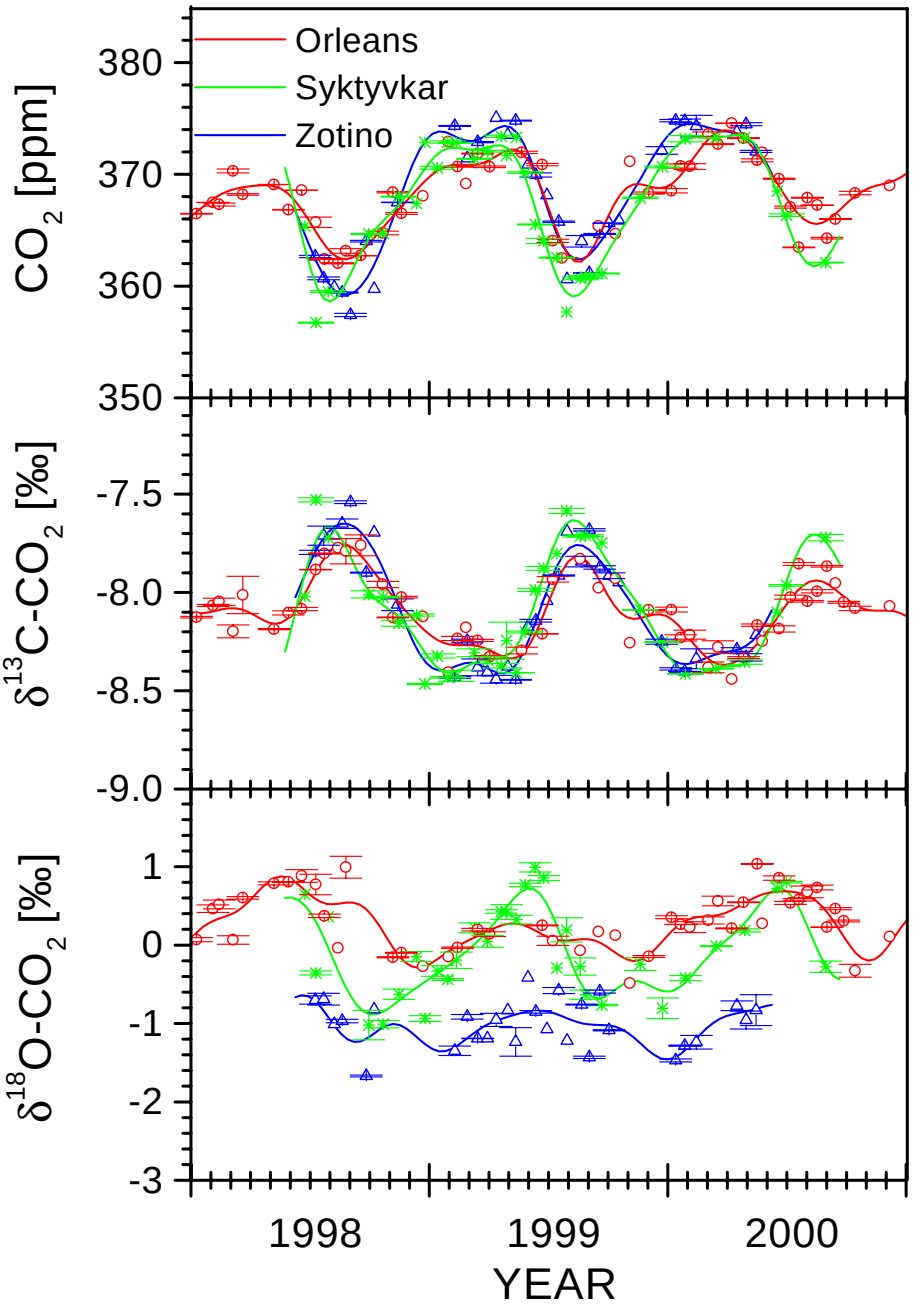

Figure 6.2: *Seasonal cycles of flask CO_2 concentration (top), $\delta^{13}C(CO_2)$(middle) and $\delta^{18}O(CO_2)$(bottom) at the Orléans (red), Syktyvkar (green) and Zotino (blue) flight station at 3000 meter above ground [Levin* et al.*, 2001].*

layer (CBL) during individual flights. Due to radiative/convective processes over the continents, this CBL height changes from 300-500 m during winter to 1500 to 2800 m in summer. Measurements within the CBL, even during the day, are still largely affected by regional short-term ground level processes while, as a first order approach, the 3000 m level represents the large scale background situation of the lower troposphere. Representative gradients over the EuroSiberian region can, therefore be derived primarily from the data at the 3000 m level.

For CO_2 mixing ratio and stable isotope ratios, Figure 6.2 shows the comparison of the observations at the three sites. Especially during summer 1999 the Zotino record exhibits a smaller summer CO_2 mixing ratio draw-down than Syktyvkar, suggesting higher assimilation activity over the western ural area. The amplitudes of the seasonal cycles in all three components increase from Orléans towards Syktyvkar and decrease again at Zotino. Comparison of all three records show a similar seasonal cycle, with an increasing peak-to-peak amplitude from Orléans towards Syktyvkar (see Table 6.1).

Table 6.1: *Peak-to-peak amplitudes (ppa) of the seasonal cycles observed in Orléans, Syktyvkar and Zotino for CO_2 concentration, $\delta^{13}C(CO_2)$ and $\delta^{18}O(CO_2)$.*

ppa/annual mean	Orléans	Syktyvkar	Zotino
ppa CO_2 [ppm]	8.29	13.28	12.43
annual mean 1999 [ppm] CO_2	368.5	367.5	369.6
ppa $\delta^{13}C(CO_2)$[‰]	0.41	0.70	0.67
annual mean 1999 $\delta^{13}C(CO_2)$[‰]	-8.13	-8.09	-8.15
ppa $\delta^{18}O(CO_2)$[‰]	0.75	1.37	1.00
annual mean 1999 $\delta^{18}O(CO_2)$[‰]	0.04	-0.10	-1.18

The yearly mean values for 1999 show a significant decrease in the annual mean CO_2 mixing ratio and a corresponding increase in $\delta^{13}C(CO_2)$ between Orléans and Syktyvkar. However, the difference in mean $\delta^{13}C(CO_2)$ is not considered as significant when taking into account still unsolved calibration biases between the laboratories involved. Between Syktyvkar and Zotino, however, the gradients observed in all three components, CO_2 mixing ratio, $\delta^{13}C(CO_2)$ and $\delta^{18}O(CO_2)$ are considered as significant. CO_2 mixing ratio and $\delta^{13}C(CO_2)$ both suggest a rather large net sink of CO_2 in 1999 in the longitude band around Syktyvkar, i.e. 50±20°E.

The most striking feature of our observations is the very large gradient of $\delta^{18}O(CO_2)$ between Syktyvkar and Zotino in the order of -1‰. A substantial gradient towards more continental longitudes within Eurasia was certainly expected from the well-known gradient of $\delta^{18}O$ in precipitation water observed [IAEA/WMO, 1998; Sonntag et al., 1983]. As a consequence of depleted precipitation, surface ground water has been modelled to show a decrease in the order of 10‰ between the longitude of Syktyvkar and the Zotino region [Farquhar et al., 1993a; Ciais et al., 1997a]. These atmospheric $\delta^{18}O(CO_2)$ observations suggest this gradient as being transferred through surface processes into the isotopic abundance of atmospheric CO_2 in the respective area.

From the observed $\delta^{18}O(CO_2)$ signal, the surface fluxes that may be involved in this process can very roughly be estimated: assuming a mean residence time of air masses reaching Zotino (hypothetically arriving from Syktyvkar) to be in the order of 2-3 days, and a well-mixed lower tropospheric air mass layer of 3000 m thickness (the observation level) which is

influenced by the surface process. If it is further assumed that, eventually, the ground water δ^{18}O gradient between Syktyvkar and Zotino of about -10 ‰ will be totally transferred to the atmospheric CO_2 our observed gradient in CO_2 of -1 ‰ suggests that 1/10 of the CO_2 inventory of the air column, about 5 moles CO_2 m^{-2} must have been ^{18}Oequilibrated at the surface. If this process was active over 3 days this corresponds to a gross exchange of about 1650 mmol CO_2 $m^{-2}day^{-1}$ or about 20 μmol $m^{-2}s^{-1}$, which is about twice the night time respiration flux in summer in this area of the globe [Schulze *et al.*, 1999] which are cycled through the biosphere. However, this interpretation of the observed atmospheric $\delta^{18}O(CO_2)$ depletion is dependent on the assumption of an airmass travelling over the continent from west to east. Recent global modelling results of Cuntz *et al.*, [2001] do not show any continental gradient in atmospheric $\delta^{18}O(CO_2)$. This model is also driven by the continental gradient of δ^{18}O in precipitation water and global atmospheric transport is calculated by the circulation model ECHAM [DKR, 1994].

Outlook

The extensive measurements performed during the intensive campaigns allowed to detect both, short-term variations in isotopic reservoir/source signatures and seasonal variability in isotopic signals, that were transferred into the convective boundary layer of the troposphere. The chosen set-up and design of the measurements allowed to quantify CO_2 gross fluxes by combined modelling of the relevant ^{18}O processes and the transport of CO_2. Currently there are efforts to install very tall towers, exceeding 250 m in height, within and above the canopy. Besides the classical components (CO_2 isotopes, etc), this will also provide the opportunity to perform continuous ^{222}Radon measurements in the lower part of the convective boundary layer, representing the top box in the presented model. This would possibly allow to parameterise the turbulent exchange between the top of the canopy and the lower part of the convective boundary layer, totally independent of eddy correlation measurements.

As a consequence of the experience with the presented 1-D isotopic box model, effort should be put into the investigation of microscale ^{18}O processes. In particular sensitive are the parameters determining the overall leaf discrimination against $C^{18}O^{16}O$, namely the leaf water isotopic composition and the leaf internal CO_2 gradients, which need better estimates.

As the number of CO_2 mixing ratio and CO_2 stable isotope records in the free troposphere over continents are rare up to now, the data presented here is extremely valuable to understand CO_2 biosphere-atmosphere interactions. In a future European Union project, the regular flights started during EUROSIBERIAN CARBONFLUX will be continued and additional sites will be taken in operation for regular flight profile sampling. The perspective is to obtain a better resolved observation network, delivering detailed information on site characteristic exchange processes.

In connection with ground-based ecosystem measurements, a nested $\delta^{18}O$ model hierarchy and ongoing microscale process investigations, there is the perspective to parameterise global $\delta^{18}O$ variability. The final goal of this efforts, namley to use $\delta^{18}O$ as a tracer for CO_2 gross fluxes on the global scale, could then be achieved.

Appendix A

Model code

The model was coded using IDL, Version 5.3 (OSF alpha), © Research Systems, Inc. Licence No. 3397, with permission of LSCE-CEA, Saclay

```
;+
;  NAME:
;       TVER
;
; PURPOSE:
;       1-D, 3-Box canopy model for Eurosib campaign
;
; CATEGORY:
;       Fully independant program.
;
; CALLING SEQUENCE:
;       MAIN
;
; INPUTS:
;       Measured data files of radon, CO2 with isotopes, leaf
;       water isotopes, etc.
;
; OPTIONAL INPUT PARAMETERS:
;       None.
;
; OUTPUTS:
;       CO2 assimilation and respiration fluxes.
;
; COMMON BLOCKS:
;       None.
;
; SIDE EFFECTS:
;       None.
;
; RESTRICTIONS:
;       A lot.
;
; EXAMPLE:
;       None.
;
; MODIFICATION HISTORY:
;       Written, Uwe Langendörfer, December 2000.
;       last modification by Uwe, 16.02.2001
;
;************************************************************
;@tver_lib @tver_lib_no_plot PRO MAIN
;;;;;;;;;;;;;;;;;;;;;;;;;;;;;;;;;;;;;;;;;;;;;;;;;;;;;;;;;;;;;;;;;;;;
;Choose approach, set switches, etc.
datapath='/home/geodata/peylin/TVER/DATA' datapath='.'
missval=-9999.       ; Missing data points in input files are
                     ; coded with this value
timeinc=30.          ; Time interval for interpolated data in
                     ; minutes, i.e. time-step of model
                     ; default = 30
approach=2           ; Approach=1 or 2
                     ; 1: Take/assume [Rn] in 3rd box for exchange coefficient
                          ;from box 2 to 3
                     ; 2: Take measured CO2 fluxes for CO2 exchange from box 2 to 3
only_conc=2          ; 1: only use CO2 data : compute resp at night
                        ; extrapolate for day time
                     ; 2: use CO2 data + isotopic data
; if only_conc=1 then choose:
assume_resp=1        ; 1: use measured soil CO2 flux, assume Ra,
                          ;calculate assimilation
                     ; 2: use measured soil CO2 flux, calculate CO2 only with
```

```
                        ; transport, calculate night-time Ra, extend it to day-time,
                        ; calculate assimilation
use_craig=0          ; 0: to use measurements for O18 of leaf
                        ; water
                     ; 1: to use Craig-Gordon equation
use_licor=2          ; 1: to use Heidelberg Licor CO2 data, 30 min mean values
                     ; 2: to use Heidelberg flask CO2 data
meanboxes=1          ; 1: intergrate mean values for Radon and CO2
                        ; for boxes via profile CO2
                     ; 2: take the measured values as mean values
assim_night=1        ; 1: assim_night = 0, get resp and disc_s1 (EPSSOIL)
                     ; 0: calculate assim with assumed EPPSOIL
file_save=1
do_harmonics=1
calculate_eps_leaf=0
running_mean_k12=1
; time interpolation
rn1timeint='linear'             ; Rn data in lower box
rn2timeint='linear'             ; Rn data in upper box
co21timeint='linear'            ; CO2 flask data in lower box
co22timeint='linear'            ; CO2 flask data in upper box
co2lictimeint='linear'          ; CO2 Heidelberg Licor data box1 and box2
c131timeint='linear'            ; 13C flask data in lower box
c132timeint='linear'            ; 13C flask data in upper box
o180_1timeint='linear'          ; 18O ampoule data at 0.1 m
o181timeint='linear'            ; 18O flask data in lower box
o182timeint='linear'            ; 18O flask data in upper box in time
co2ptimeint='linear'            ; CO2 profile data in time
co2_fluxes_26mtimeint='linear'  ; CO2 fluxes at 26 m data in time
o18vap1timeint='linear'         ; 18O water vapour data in lower box in time
o18vap2timeint='linear'         ; 18O water vapour data in upper box in time
meteo2timeint='linear'          ; meteo in upper box in time
soiltemptimeint='linear'        ; soil temp in time
o18biotimeint='linear'          ; 18O biospheric data in time
c13biotimeint='linear'          ; 13C biospheric data in time
flighttimeint='linear'          ; CO2, C13 and O18 flight flask data in time
net_fluxestimeint='linear'      ; eddy net fluxes
co2heightint='log'              ; Method of interpolation in height to obtain CO2
                                ; in 15m (for approach 2)
                                ; 'profile': uses Jena Licor tower profiles
                                ; 'log': uses logarithmic function
                                ; between flasks data at 2m and 26m
; END switches
;;;;;;;;;;;;;;;;;;;;;;;;;;;;;;;;;;;;;;;;;;;;;;;;;;;;;;;;;;;;;;;;;;;;;;;;;;;;;;;
;;;;;;;;;;;;;;;;;;;;;;;;;;;;;;;;;;;;;;;;;;;;;;;;;;;;;;;;;;;;;;;;;;;;;;;;;;;;;;;
; Set parameters, constants, fractionation factors, etc.
MOLAIR = 28.964E-3              ; mean mol mass of air in kg/mol air
MOLVOL = 22.4E-3                ; molvolume in m3/mol air
EPSLEAF = -7.4                  ; effective diffusion fractionation of the
                                ; leaves for C018O in permill, -7.4
teta = 0.93                     ; isotopic euilibrium between leaf water and
                                ; CO2 C3: 0.93 [Gillon and Yakir, 2001]
EPSSOIL = -7.2                  ; effective diffusion fractionation of soil
                                ; for C018O in permill, -7.2
EPSSTEM = -8.8                  ; effective diffusion fractionation of the
                                ; stems for C018O in permill
soil_p = 0.79                   ; percentage soil respiration in Box 1
auto_p = 0.21                   ; percentage autotrophic respiration in Box 1
EPSDIFF = -26.                  ; effective kinetic fractionation of H218O vs H216O
                                ; for water diffusion stomata via leaf boundary layer
Z11=4.          ; top of box 1, the lower box in meter, approach1
Z12=4.          ; top of box 1, the lower box in meter, approach2
Z21=48.         ; top of box 2, the upper box in meter, approach1
Z22=26.         ; top of box 2, the upper box in meter, approach2
Z31=400.        ; top of box 3, the upper box in meter, approach1
Z32=400.        ; top of box 3, the upper box in meter, approach2
EPSDIFF13C = 4.4                ; effective diffusion fractionation of
                                ; the leaves for 13CO2 in permill
EPSCARBOX13C = 29.              ; carboxylation fractionation of C3 plants
                                ; for 13CO2 in permill
FRnsoil = 7.5                   ; measured mean 222 Radon flux from soil,
                                ; assumed to be constant at first , sta 7.5
fac_rn3 = 0.9                   ; percentage of Radon activity of box 2
                                ; assumed to be in box 3
;Rn3=0.2                        ; Radon activity in Box 3, assumed to be
                                ; constant at first approximation
                                ; in Bq m-3
Rndiff_min=0.2                  ; Minimum difference in Radon activity between
                                ; 2 boxes to compute K's
```

```
co2_diff_min=0.3/1.e6           ; Minimum difference in CO2 concentration between
                                ; 2 boxes to compute F_CO2
Rsoil=10                        ; measured mean CO2 flux from soil,
                                ; assumed to be constant at first
                                ; approximation in mmol m-2 h-1
par_thresh=150                  ; PAR to switch off the light
; END Constants
;;;;;;;;;;;;;;;;;;;;;;;;;;;;;;;;;;;;;;;;;;;;;;;;;;;;;;;;;;;;;;;;;;;;;;;;;;;;;;;;;;;;;;;;;;;;;;;;;;
;;;;;;;;;;;;;;;;;;;;;;;;;;;;;;;;;;;;;;;;;;;;;;;;;;;;;;;;;;;;;;;;;;;;;;;;;;;;;;;;;;;;;;;;;;;;;;;;;;
; Define few variables (some depending on the approach)
;-- Open plot file dev='psc' file_graph='output.ps'
ccg_opendev,dev=dev,saveas=file_graph spawn,'chmod 777
'+file_graph !p.multi = 0
;--- Define Appproach specific parameters
if approach eq 1 then begin
    Z1=Z11
    Z2=Z21
    Z3=Z31
    H1=Z11                  ; height of box 1, the lower box in meter
    H2=Z21-Z11              ; height of box 2, the upper box in meter
    H3=Z31-Z21              ; height of box 3, the upper box in meter
endif else begin
    Z1=Z12
    Z2=Z22
    Z3=Z32
    H1=Z12                  ; height of box 1
    H2=Z22-Z12              ; height of box 2, the upper box in meter
    H3=Z32-Z22              ; height of box 3, the upper box in meter
endelse
; END definitions
;;;;;;;;;;;;;;;;;;;;;;;;;;;;;;;;;;;;;;;;;;;;;;;;;;;;;;;;;;;;;;;;;;;;;;;;;;;;;;;;;;
;;;;;;;;;;;;;;;;;;;;;;;;;;;;;;;;;;;;;;;;;;;;;;;;;;;;;;;;;;;;;;;;;;;;;;;;;;;;;;;;;;
 ; Read data files
print, '' print, 'READ DATA FILES FROM:'
z=0 file='radon_2m_7_99_new_rm5.prn'            ; Read Rn [Bq/m3] data from 2m height
read_data, file, rn1data, path=datapath
z=z+1
file='radon_26m_7_99_new_rm5.prn'               ; Read Rn [Bq/m3] data from 26m height
read_data, file, rn2data, path=datapath
z=z+1
file='co2_2m_7_99.prn'                          ; Read CO2 [ppm] data from 2m height
read_data, file, co21data, path=datapath
z=z+1
file='co2_26m_7_99.prn'                         ; Read CO2 [ppm] data from 26m height
read_data, file, co22data, path=datapath
z=z+1
file='co2_licor_30mean_7_99_rm3.prn'            ; Read CO2 [ppm] Heidelberg Licor data
titles_co2lic=1
read_data, file, co2licordata, path=datapath,titles=titles_co2lic
z=z+1
file='co2_profiles_7_99.prn'                    ; Read CO2 [ppm] profile data, 1st
titles_co2_profiles=1                           ; column=0.2m height
                                                ; 2=1.0m, 3=2.0m, 4=4.8m, 5=10.8m,
                                                ; 6=15.6m, 7=25.2m, 8=28.0m
read_data, file, co2pdata, path=datapath, titles=titles_co2_profiles
z=z+1
file='c13_2m_7_99.prn'                          ; Read 13C [permill PDB] data from 2m height
read_data, file, c131data, path=datapath
z=z+1
file='c13_26m_7_99.prn'                         ; Read 13C [permill PDB] data from 26m height
read_data, file, c132data, path=datapath
z=z+1
file='o18_0_1m_7_99.prn'                        ; Read 18O [permill PDB] data from 0.1m height
read_data, file, o180_1data, path=datapath
z=z+1
file='o18_2m_7_99.prn'                          ; Read 18O [permill PDB] data from 2m height
read_data, file, o181data, path=datapath
z=z+1
file='o18_26m_7_99.prn'                         ; Read 18O [permill PDB] data from 26m height
read_data, file, o182data, path=datapath
z=z+1
file='co2_fluxes_26m_7_99.prn'                  ; Read CO2 flux [ mümol m-2 s-1] data
                                                ; from 26m height
read_data, file, co2f26mdata, path=datapath
z=z+1
file='net_fluxes_irena_7_99.prn'                ; Read CO2 net fluxes [ mümol m-2 s-1]
read_data, file, net_fluxesdata, path=datapath
z=z+1
; respiration values: all nighttime values for
; u_star lower then 0.35 m/s are recalculated by regression
file='o18_vapour_2m_7_99.prn'                   ; Read 18O water vapour [permill SMOW]
```

```
                                                ; data from 2m height
read_data, file, o18vap1data, path=datapath
z=z+1
file='o18_vapour_26m_7_99.prn'                  ; Read 18O water vapour [permill SMOW]
                                                ; data from 26m height
read_data, file, o18vap2data, path=datapath
z=z+1
file='meteo_26m_7_99.prn'                       ; Read meteo data from 26m height
titles=1
read_data, file, meteo2data, path=datapath,titles=titles
z=z+1
file='soil_temp_7_99.prn'                       ; Read soil temperatures, 2 sites,
                                                ; different depths
                                                ; mean values of the 2 sites
read_data, file, soiltempdata, path=datapath,titles=titles
z=z+1
file='o18_bio_7_99_ext.prn'                     ; Read 18O of plant/soil material [permill SMOW]
titles_o18bio=1
read_data, file, o18biodata, path=datapath,titles=titles_o18bio
z=z+1
file='c13_bio_7_99_ext.prn'                     ; Read 18O of plant/soil material [permill SMOW]
titles_c13bio=1
read_data, file, c13biodata, path=datapath,titles=titles_c13bio
z=z+1
file='flight_100m_7_99.prn'               ; Read CO2, C13 and O18 from the flights [permill SMOW]
titles_flight=1
read_data, file, flightdata, path=datapath,titles=titles_flight
z=z+1
print, 'Number of read data files: ',auto_string(z)
; END read data files
;;;;;;;;;;;;;;;;;;;;;;;;;;;;;;;;;;;;;;;;;;;;;;;;;;;;;;;;;;;;;;;;;;;;;;;;;;;;;;;;;;;;;;;;;;;;;;
;;;;;;;;;;;;;;;;;;;;;;;;;;;;;;;;;;;;;;;;;;;;;;;;;;;;;;;;;;;;;;;;;;;;;;;;;;;;;;;;;;;;;;;;;;;;;;
; Interpolate data to same time structure print, '' print,
'INTERPOLATION IN TIME OF:'
z=0
rn1 = interpol_data_time(rn1data,'Radon 1',interval=timeinc,method=rn1timeint,miss=missval)
z=z+1
rn2 = interpol_data_time(rn2data,'Radon2',interval=timeinc,method=rn2timeint,miss=missval)
z=z+1
co21 = interpol_data_time(co21data,'CO21',interval=timeinc,method=co21timeint,miss=missval)
z=z+1
co22 = interpol_data_time(co22data,'CO22',interval=timeinc,method=co22timeint,miss=missval)
z=z+1
co2lic = interpol_data_time(co2licordata,'CO2licor',interval=timeinc,method=co2lictimeint,
miss=missval)
z=z+1
co2p = interpol_data_time(co2pdata,'CO2p',interval=timeinc,method=co2ptimeint,miss=missval)
z=z+1
c131 = interpol_data_time(c131data,'C131',interval=timeinc,method=c131timeint,miss=missval)
z=z+1
c132 = interpol_data_time(c132data,'C132',interval=timeinc,method=c132timeint,
miss=missval)
z=z+1
o180_1 = interpol_data_time(o180_1data,'O180.1',interval=timeinc,method=o180_1timeint,
miss=missval)
z=z+1
o181 = interpol_data_time(o181data,'O181',interval=timeinc,
method=o181timeint,miss=missval)
z=z+1
o182 = interpol_data_time(o182data,'O182',interval=timeinc,
method=o182timeint,miss=missval)
z=z+1
co2f26m = interpol_data_time(co2f26mdata,'CO2flux',interval=timeinc,
method=co2_fluxes_26mtimeint,
miss=missval)
z=z+1
netco2f = interpol_data_time(net_fluxesdata,'CO2 netflux',interval=timeinc,
method=net_fluxestimeint, miss=missval)
z=z+1
o18vap1 = interpol_data_time(o18vap1data,'O18 vap1',interval=timeinc,
method=o18vap1timeint,miss=missval)
z=z+1
o18vap2 = interpol_data_time(o18vap2data,'O18 vap2',interval=timeinc,
method=o18vap2timeint,miss=missval)
z=z+1
meteo2 = interpol_data_time(meteo2data,'Meteo2',interval=timeinc,
method=meteo2timeint,miss=missval)
z=z+1
soiltemp = interpol_data_time(soiltempdata,'Soiltemp',interval=timeinc,
method=soiltemptimeint,miss=missval)
z=z+1
o18bio = interpol_data_time(o18biodata,'O18bio',interval=timeinc,
```

```
method=o18biotimeint,miss=missval)
z=z+1
c13bio = interpol_data_time(c13biodata,'C13bio',interval=timeinc,
method=c13biotimeint,miss=missval)
z=z+1
flight = interpol_data_time(flightdata,'Flightdata',interval=timeinc,
method=flighttimeint,miss=missval)
z=z+1
print, 'Number of interpolated data files in time:
',auto_string(z) ; END time interpolation
;;;;;;;;;;;;;;;;;;;;;;;;;;;;;;;;;;;;;;;;;;;;;;;;;;;;;;;;;;;;;;;;;;;;;;;;;;;;;;;;;;;;;;;;;;;;;;;;;;
;;;;;;;;;;;;;;;;;;;;;;;;;;;;;;;;;;;;;;;;;;;;;;;;;;;;;;;;;;;;;;;;;;;;;;;;;;;;;;;;;;;;;;;;;;;;;;;;;;
; All data to same length in time
print, ''
print, 'ALL DATA FILES TO SAME LENGTH'
z=0
;--- Determine common time period to all data
temp = ['rn1(*,0)','rn2(*,0)',$
        'co21(*,0)','co22(*,0)','co2lic(*,0)','co2p(*,0)',$
        'c131(*,0)','c132(*,0)','o180_1',$
        'o181(*,0)','o182(*,0)',$
        'co2f26m(*,0)','netco2f',$
        'o18vap1(*,0)','o18vap2(*,0)',$
        'meteo2(*,0)','soiltemp(*,0)',$
        'o18bio(*,0)','c13bio(*,0)',$
        'flight(*,0)' ]
maxitime=9999.D minitime=-9999.D for n=0,n_elements(temp)-1 do
begin
    res = execute('maxi = max(' +temp(n)+ ')' )
    res = execute('mini = min(' +temp(n)+ ')' )
    maxitime = min([maxitime,maxi])
    minitime = max([minitime,mini])
endfor
;--- Truncate the data to commun period
ii=where(rn1(*,0) ge minitime and rn1(*,0) le maxitime, ntime)
date=reform(rn1[ii,0]) rn1=rn1[ii,1:*]
;moni=indgen(ntime)
;monis=1990.+moni/(3600./timeinc)
;mc_ccgvu, x=monis, y=rn1, ftn=ftn
;ftn[1,*]=rn1 rn1_o=rn1 z=z+1
ii=where(rn2(*,0) ge minitime and rn2(*,0) le maxitime, ntime)
rn2=rn2[ii,1:*] rn2_o=rn2
z=z+1
ii=where(co21(*,0) ge minitime and co21(*,0) le maxitime, ntime)
co21_h=co21[ii,1:*] co21=co21[ii,1:*]/1.e6 co21_o=co21
z=z+1
ii=where(co22(*,0) ge minitime and co22(*,0) le maxitime, ntime)
co22_h=co22[ii,1:*] co22=co22[ii,1:*]/1.e6 co22_o=co22
z=z+1
ii=where(co2lic(*,0) ge minitime and co2lic(*,0) le maxitime,
ntime) co2lic=co2lic[ii,1:*]/1.e6
z=z+1
ii=where(co2p(*,0) ge minitime and co2p(*,0) le maxitime, ntime)
co2_profiles=co2p[ii,1:8] /1.e6      ; all heights
co2p=co2p[ii,6:7] /1.e6              ; 15.6 m and 25.2 m for height
                                     ;interpol CO2 z=z+1
ii=where(c131(*,0) ge minitime and c131(*,0) le maxitime, ntime)
c131_o=c131[ii,1:*] c131=c131[ii,1:*]
z=z+1
ii=where(c132(*,0) ge minitime and c132(*,0) le maxitime, ntime)
c132_o=c132[ii,1:*] c132=c132[ii,1:*]
z=z+1
ii=where(o180_1(*,0) ge minitime and o180_1(*,0) le maxitime,ntime)
o180_1=o180_1[ii,1:*] o180_1_o=o180_1
z=z+1
ii=where(o181(*,0) ge minitime and o181(*,0) le maxitime, ntime)
o181=o181[ii,1:*] o181_o=o181
z=z+1
ii=where(o182(*,0) ge minitime and o182(*,0) le maxitime, ntime)
o182=o182[ii,1:*] o182_o=o182
z=z+1
ii=where(co2f26m(*,0) ge minitime and co2f26m(*,0) le maxitime,ntime)
co2f26m = co2f26m[ii,1:*]* 3600. / 1.e6
co2f26m_o = co2f26m* 3600. / 1.e6
z=z+1
ii=where(netco2f(*,0) ge minitime and netco2f(*,0) le maxitime,ntime)
eddy_assim = (netco2f[ii,2]* 3600. / 1.e6 )*(-1)
eddy_resp = netco2f[ii,1]* 3600. / 1.e6
```

```
z=z+1
ii=where(o18vap1(*,0) ge minitime and o18vap1(*,0) le maxitime,ntime)
o18vap1=o18vap1[ii,1:*] o18vap1_o=o18vap1
z=z+1
ii=where(o18vap2(*,0) ge minitime and o18vap2(*,0) le maxitime,ntime)
o18vap2=o18vap2[ii,1:*] o18vap2_o=o18vap2
z=z+1
ii=where(meteo2(*,0) ge minitime and meteo2(*,0) le maxitime,ntime)
meteo2=meteo2[ii,1:*]
z=z+1
ii=where(soiltemp ge minitime and soiltemp le maxitime, ntime)
soiltemp=soiltemp[ii,1:*]
z=z+1
ii=where(o18bio(*,0) ge minitime and o18bio(*,0) le maxitime,ntime)
o18bio=o18bio[ii,1:*] o18bio_o=o18bio
z=z+1
ii=where(c13bio(*,0) ge minitime and c13bio(*,0) le maxitime,ntime)
c13bio=c13bio[ii,1:*]
z=z+1
ii=where(flight(*,0) ge minitime and flight(*,0) le maxitime,ntime)
flight=flight[ii,1:*]
z=z+1
print, 'Number of cutted data: ',z
print, 'Number of time step :',ntime
print, date(0),' <-> ',date(ntime-1)
;----- Define new data from the measured data
ii = where(titles_flight eq 'co2')
co23 = flight(*,ii-1)/1.e6
co23_h=flight(*,ii-1)
co23_o = flight(*,ii-1)
ii = where(titles_flight eq 'o18')
o183 = flight(*,ii-1) o183_o =
flight(*,ii-1)
;---------------- o18 in box 1 is mean of 2m and 0.1 m value-----------------
o181 = (o181[*,0] + o180_1[*,0])/2
o181_o = (o181[*,0] + o180_1[*,0])/2
if use_licor eq 1 then begin
    print, ' '
    print, 'USE HEIDELBERG LICOR CO2 DATA'
    ii = where(titles_co2lic eq 'co21')
    co21lic_o=co2lic(*,ii-1)
    co21 = co2lic(*,ii-1)
    ii = where(titles_co2lic eq 'co22')
    co22lic_o=co2lic(*,ii-1)
    co22 = co2lic(*,ii-1)
endif else begin
    print, ' '
    print, 'USE HEIDELBERG FLASK CO2 DATA'
endelse
ii = where(titles_co2lic eq 'co21')
co21lic_o=co2lic(*,ii-1)
ii = where(titles_co2lic eq 'co22')
co22lic_o=co2lic(*,ii-1)
PAR=meteo2[*,6]
H20_conc=meteo2[*,7]               ; water vapour concentration [mmol/mol]
par_o = par v_hor=meteo2[*,5]
temp1 = meteo2[*,1] -2.
temp1_o = temp1
temp2 = meteo2[*,1]
temp2_o = temp2
soil_temp = soiltemp[*,9]
soil_temp_o = soil_temp
stem_temp = meteo2[*,1]+4
stem_temp_o = stem_temp
rh1 = -0.036 * temp1 + 1.258       ; empirical linear fit tem2/rh2 data , r^2=0.8
rh1_o = rh1
rh2 = meteo2[*,4]/100
rh2_o = rh2
;----- Radon in box 3
;----- constant value:
;rn3 = dblarr(ntime)
;for i=0,ntime-1 do begin
; rn3(i)=0.4
;endfor
;----- or percentage of Box2 rn3 = rn2 * fac_rn3
; END uniform  length
;;;;;;;;;;;;;;;;;;;;;;;;;;;;;;;;;;;;;;;;;;;;;;;;;;;;;;;;;;;;;;;;;;;;;;;;;;;;
```

```
;;;;;;;;;;;;;;;;;;;;;;;;;;;;;;;;;;;;;;;;;;;;;;;;;;;;;;;;;;;;;;;;;;;;;;;;;;;;;
; Perform harmonics print, ''
print, 'DO HARMONICS ON ATMOSPHERIC INPUT DATA'
if do_harmonics then begin
    moni=indgen(ntime)
    monis=1990.+moni/(3600./timeinc)
    mc_ccgvu, x=monis, y=rn1, ftn=ftn
    rn1=ftn[1,*]
    mc_ccgvu, x=monis, y=rn2, ftn=ftn
    rn2=ftn[1,*]
    mc_ccgvu, x=monis, y=co21_h, ftn=ftn
    co21=ftn[1,*]/1.e6
    mc_ccgvu, x=monis, y=co22_h, ftn=ftn
    co22=ftn[1,*]/1.e6
    mc_ccgvu, x=monis, y=co23_h, ftn=ftn
    co23=ftn[1,*]/1.e6
    mc_ccgvu, x=monis, y=c131, ftn=ftn
    c131=ftn[1,*]
    mc_ccgvu, x=monis, y=c132, ftn=ftn
    c132=ftn[1,*]
    mc_ccgvu, x=monis, y=o181, ftn=ftn
    o181=ftn[1,*]
    mc_ccgvu, x=monis, y=o182, ftn=ftn
    o182=ftn[1,*]
    mc_ccgvu, x=monis, y=o183, ftn=ftn
    o183=ftn[1,*]
    mc_ccgvu, x=monis, y=co2f26m, ftn=ftn
    co2f26m=ftn[1,*]
    mc_ccgvu, x=monis, y=o18vap1, ftn=ftn
    o18vap1=ftn[1,*]
    mc_ccgvu, x=monis, y=o18vap2, ftn=ftn
    o18vap2=ftn[1,*]
    mc_ccgvu, x=monis, y=temp1, ftn=ftn
    temp1=ftn[1,*]
    mc_ccgvu, x=monis, y=temp2, ftn=ftn
    temp2=ftn[1,*]
    mc_ccgvu, x=monis, y=soil_temp, ftn=ftn
    soil_temp=ftn[1,*]
    mc_ccgvu, x=monis, y=rh1, ftn=ftn
    rh1=ftn[1,*]
    mc_ccgvu, x=monis, y=rh2, ftn=ftn
    rh2=ftn[1,*]
endif
; END harmonics
;;;;;;;;;;;;;;;;;;;;;;;;;;;;;;;;;;;;;;;;;;;;;;;;;;;;;;;;;;;;;;;;;;;;;;;;;;;;
;;;;;;;;;;;;;;;;;;;;;;;;;;;;;;;;;;;;;;;;;;;;;;;;;;;;;;;;;;;;;;;;;;;;;;;;;;;;
; Interpolate height for CO2 (either logarithmic or scale with CO2
profiles), ; CO2, water vapor isotopes and Rn: logarithmic
if approach eq 2 then begin
  z=0
  print, ''
  print, 'APPROACH 2: INTERPOLATE 26M DATA TO 15M'
  rn2 = interpol_data_height(rn2,rn1,'log',missval,'Radon')
  z=z+1
  c132 = interpol_data_height(c132,c131,'log',missval,'C13')
  z=z+1
  o182 = interpol_data_height(o182,o181,'log',missval,'O18 CO2')
  z=z+1
  o18vap2 = interpol_data_height(o18vap2,o18vap1,'log',missval,'O18 vapor')
  z=z+1
  if co2heightint eq 'profile' then temp = co2p else temp=co21
  co22 = interpol_data_height(co22,temp,co2heightint,missval,'CO2')
  z=z+1
  print, 'Number of interpolated data in height: ',auto_string(z)
endif
; END height interpolation
;;;;;;;;;;;;;;;;;;;;;;;;;;;;;;;;;;;;;;;;;;;;;;;;;;;;;;;;;;;;;;;;;;;;;;;;;;;;
;;;;;;;;;;;;;;;;;;;;;;;;;;;;;;;;;;;;;;;;;;;;;;;;;;;;;;;;;;;;;;;;;;;;;;;;;;;;
; Define mean box values for CO2 and Radon via integration of CO2 profiles during night-time,
; day-time: assume boxes are well mixed and take measured values as mean box values.
if meanboxes then begin
    print, ''
    print, 'INTERGRATE MEAN BOX VALUES VIA PROFILES'
; determine mean CO2 values of the boxes via profile measurement
; Box 1:
    co21_meanprofile=dblarr(ntime)
    iip0_2m = where(titles_co2_profiles eq 'co2_0.2m')
```

```
    iip1m = where(titles_co2_profiles eq 'co2_1m')
    iip2m = where(titles_co2_profiles eq 'co2_2m')
    iip4_8m = where(titles_co2_profiles eq 'co2_4.8m')
    p0_2m=co2_profiles(*,iip0_2m-1)
    p1m=co2_profiles(*,iip1m-1)
    p2m=co2_profiles(*,iip2m-1)
    p4_8m=co2_profiles(*,iip4_8m-1)
    co21_meanprofile = (p0_2m*0.5 + p1m*1 + p2m*2.5)/4
    mean_corr1=co21_meanprofile/p2m
; calculation of mean box values
    rn1 = rn1 * mean_corr1
    co21= co21 * mean_corr1
; Box 2:
    co22_meanprofile=dblarr(ntime)
    iip4_8m = where(titles_co2_profiles eq 'co2_4.8m')
    iip10_8m = where(titles_co2_profiles eq 'co2_10.8m')
    iip15_6m = where(titles_co2_profiles eq 'co2_15.6m')
    iip25_2m = where(titles_co2_profiles eq 'co2_25.2m')
    iip28m = where(titles_co2_profiles eq 'co2_28m')
    p4_8m=co2_profiles(*,iip4_8m-1)
    p10_8m=co2_profiles(*,iip10_8m-1)
    p15_6m=co2_profiles(*,iip15_6m-1)
    p25_2m=co2_profiles(*,iip25_2m-1)
    p28m=co2_profiles(*,iip28m-1)
    if approach eq 2 then begin
        print, ''
        print, '...APPROACH 2: INTEGRATE OVER 22m IN BOX 2'
        co22_meanprofile = (p4_8m*3 +p10_8m*6 + p15_6m*8 + p25_2m*5)/22
        mean_corr2=co22_meanprofile/p25_2m
        rn2 = rn2_o * mean_corr2
        co22= co22_o * mean_corr2
    endif else begin
        print, ''
        print, '...APPROACH 1: INTEGRATE OVER 44m IN BOX 2'
        co22_meanprofile = (p4_8m*3 +p10_8m*6 + p15_6m*8 + p25_2m*5 + p28m*22)/44
        mean_corr2=co22_meanprofile/p25_2m
        rn2 = rn2_o * mean_corr2
        co22= co22_o * mean_corr2
    endelse
endif
; END define mean box values
;;;;;;;;;;;;;;;;;;;;;;;;;;;;;;;;;;;;;;;;;;;;;;;;;;;;;;;;;;;;;;;;;;;;;;;;;;;;;;
;;;;;;;;;;;;;;;;;;;;;;;;;;;;;;;;;;;;;;;;;;;;;;;;;;;;;;;;;;;;;;;;;;;;;;;;;;;;;;
; Define average values for isotopic measurements between different ; levels/species...
;---- Variables of plant C13 (mean values of the measurements)
ii2 = where(titles_c13bio eq 'c13_conif_low' or $
            titles_c13bio eq 'c13_conif_high' or $
            titles_c13bio eq 'c13_decid_low' or $
            titles_c13bio eq 'c13_decid_high', cc2 )
ii1 = where(titles_c13bio eq 'c13_grass_leaves' or $
            titles_c13bio eq 'c13_moss_leaves', cc1 )
c13_l1 = total(c13bio(*,ii1-1),2) / cc1 c13_l2 =
total(c13bio(*,ii2-1),2) / cc2
if do_harmonics then begin
    print, ''
    print, 'DO HARMONICS ON BIOSPHERIC C13 PLANT INPUT DATA'
    mc_ccgvu, x=monis, y=c13_l1, ftn=ftn
    c13_l1_o = c13_l1
    c13_l1 = ftn[1,*]
    mc_ccgvu, x=monis, y=c13_l2, ftn=ftn
    c13_l2_o = c13_l2
    c13_l2 = ftn[1,*]
endif
;---- Variables of plant O18 (mean values of the measurements)
ii2 = where(titles_o18bio eq 'o18_conif_low' or $
            titles_o18bio eq 'o18_conif_high' or $
            titles_o18bio eq 'o18_decid_low' or $
            titles_o18bio eq 'o18_decid_high' or $
            titles_o18bio eq 'o18_conif_medium', cc2 )
ii1 = where(titles_o18bio eq 'o18_grass_leaves' or $
            titles_o18bio eq 'o18_moss_leaves', cc1 )
ii1_soil_via_plant = where(titles_o18bio eq 'o18_grass_colar' or $
                           titles_o18bio eq 'o18_moss_colar', cc_soil_via_plant )
iis = where(titles_o18bio eq 'o18_soilconif_5cm' or $
```

```
            titles_o18bio eq 'o18_soildecid_5cm', ccs )
iistem = where(titles_o18bio eq 'o18_wood_conif' or $
               titles_o18bio eq 'o18_wood_decid', ccstem )
o18wat_l1 = total(o18bio(*,ii1-1),2) / cc1
o18wat_l2 = total(o18bio(*,ii2-1),2) / cc2
;  soil water is believed to be enriched in the very top soil layer:
;  therefore use mean 18O of moss colar and grass colar
;  original formulation for soil 18O:
   o18wat_soil = total(o18bio(0,iis-1),2) / ccs
;  new formulation using stems of understory vegetation for soil 18O:
;  o18wat_soil = total(o18bio(0,ii1_soil_via_plant-1),2) / cc_soil_via_plant
   o18wat_ste = total(o18bio(0,iistem-1),2) / ccstem
;--------------------extension of soil water data-----------
o18wat_s=dblarr(ntime) for n=0, ntime-2 do begin
    o18wat_s(n) = o18wat_soil
endfor
o18wat_s(ntime-1) = o18wat_s(ntime-2)
;--------------------end extension-------------------------
;--------------------extension of stem water data-----------
o18wat_stem=dblarr(ntime) for n=0, ntime-2 do begin
    o18wat_stem(n) = o18wat_ste
endfor
o18wat_stem(ntime-1) = o18wat_stem(ntime-2)
;--------------------end extension-------------------------
if do_harmonics then begin
    print, ''
    print, 'DO HARMONICS ON BIOSPHERIC O18 WATER INPUT DATA'
    mc_ccgvu, x=monis, y=o18wat_l1, ftn=ftn
    o18wat_l1_o = o18wat_l1
    o18wat_l1 = ftn[1,*]
    mc_ccgvu, x=monis, y=o18wat_l2, ftn=ftn
    o18wat_l2_o = o18wat_l2
    o18wat_l2 = ftn[1,*]
endif
; END isotopic pre-processing
;;;;;;;;;;;;;;;;;;;;;;;;;;;;;;;;;;;;;;;;;;;;;;;;;;;;;;;;;;;;;;;;;;;;;;;;;;;;;
;;;;;;;;;;;;;;;;;;;;;;;;;;;;;;;;;;;;;;;;;;;;;;;;;;;;;;;;;;;;;;;;;;;;;;;;;;;;;
; Calculation of diffusion coefficients
print, ' '
print, 'CALCULATION OF DIFFUSION COEFFICIENTS K12, K23'
K12=dblarr(ntime)
K23=dblarr(ntime)
F12_Rn=dblarr(ntime)
F23_Rn=dblarr(ntime)
grad1_rn=dblarr(ntime)
if approach eq 1 then $
  print, '  APPROACH 1: Take/assume [Rn] in 3rd box for exchange coefficient from box 2 to 3'
  print, ' '
if approach eq 2 then $
  print, '  APPROACH 2: Will take measured CO2 fluxes for CO2 exchange from box 2 to 3'
  print, ' '
for i=0,ntime-2 do begin
                                ;-- mass balance and fluxes for box 1
                                ;   and 2
    F12_Rn(i) = FRnsoil - (H1*(rn1[i+1]-rn1[i])/(timeinc/60.))
    grad1_rn[i]=(H1*(rn1[i+1]-rn1[i])/(timeinc/60.))
    F23_Rn(i) = F12_Rn(i)  - (H2*(rn2[i+1]-rn2[i])/(timeinc/60.))
                                ;-- K's assume 0.1 Bq m-3 minimum
                                ;   difference between boxes
    divisor1 = rn1[i]-rn2[i]
    divisor1 = max([divisor1,rndiff_min])
    K12(i) = F12_Rn(i) *((Z2/2)/divisor1)
    divisor2 = rn2[i]-rn3[i]
    divisor2 = max([divisor2,rndiff_min])
    K23(i)   = F23_Rn(i) * (((Z3-Z1)/2)/divisor2)
endfor
K12(ntime-1) = K12(ntime-2)
K23(ntime-1) = K23(ntime-2)
F12_Rn(ntime-1) = F12_Rn(ntime-2)
F23_Rn(ntime-1) = F23_Rn(ntime-2)
grad1_rn(ntime-1)=grad1_rn(ntime-2)
if running_mean_k12 then begin
    ; running mean (5) on K12
    for i=0,ntime-2 do begin
        if i ge 2 AND i le ntime-4 then begin
         K12[i]=(K12[i-2]+K12[i-1]+K12[i]+K12[i+1]+K12[i+2])/5
            endif else begin
         K12(i) = F12_Rn(i) *((Z2/2)/divisor1)
```

```
    endelse
endfor
K12(ntime-1) = K12(ntime-2) endif
; END calculation of diffusion coefficients
;;;;;;;;;;;;;;;;;;;;;;;;;;;;;;;;;;;;;;;;;;;;;;;;;;;;;;;;;;;;;;;;;;;;;;;;;;;
;;;;;;;;;;;;;;;;;;;;;;;;;;;;;;;;;;;;;;;;;;;;;;;;;;;;;;;;;;;;;;;;;;;;;;;;;;;
; CALCULATION OF CO2 FLUXES
print, ' '
print, 'CALCULATION OF CO2 FLUXES'
F12_co2=dblarr(ntime)
F23_co2=dblarr(ntime)
for i=0, ntime-2 do begin
multi1 = co21[i]-co22[i] multi1 = max([multi1,co2_diff_min])
multi2 = co22[i]-co23[i] multi2 = max([multi1,co2_diff_min])
F12_co2[i] = K12[i] * multi1 / ((Z2/2.) * MOLVOL)
F23_co2[i] = K23[i] * multi2 / (((Z3-Z1)/2.) * MOLVOL)
                                ;--- Use instead Olaf'Eddy flux for
                                ;    F23_co2 !!
endfor
F12_co2(ntime-1)=F12_co2(ntime-2)
F23_co2(ntime-1)=F23_co2(ntime-2)
if approach eq 2 then begin
    F23_co2 = co2f26m
endif
; END calculation of CO2 fluxes
;;;;;;;;;;;;;;;;;;;;;;;;;;;;;;;;;;;;;;;;;;;;;;;;;;;;;;;;;;;;;;;;;;;;;;;;;;
;;;;;;;;;;;;;;;;;;;;;;;;;;;;;;;;;;;;;;;;;;;;;;;;;;;;;;;;;;;;;;;;;;;;;;;;;;
; USE ONLY CO2 DATA
if only_conc then begin
print, ' '
print, 'CALCULATION OF ASSIMILATION FLUXES USING ONLY CO2'
if assume_resp eq 1 then begin
resp1 = dblarr(ntime)
resp2 = dblarr(ntime)
p1 = dblarr(ntime)
p2 = dblarr(ntime)
for i=0,ntime-2 do begin
   p1(i) = (co21[i+1] - co21[i]) / (timeinc/60.)
   p2(i) = (co22[i+1] - co22[i]) / (timeinc/60.)
   resp1[i,0] = Rsoil / 1000.
endfor
p1(ntim-1) = p1(ntime-2)
p2(ntime-1) = p2(ntime-2)
resp1(ntime-1) = resp1(ntime-2)
; Asumptions:
; resp1 = Rsoil + Ra1 ; Ra = 10 percent of Rsoil, permenantly
assim1 = resp1 - (p1 * H1/MOLVOL) - F12_co2
sumflux1 = - assim1 + resp1 - F12_co2 - (p1 * H1/MOLVOL)
assim1 = -assim1 resass1 =  assim1 + resp1
resp2 = 0.1 * resp1
assim2 = F12_co2 + resp2 - (p2 * H2/MOLVOL) - F23_co2
sumflux2 = - assim2 + resp2 + F12_co2 - (p2 * H2/MOLVOL) - F23_co2
assim2 = -assim2 resass2 =  assim2 + resp2
assim = assim1 + assim2 resp = resp1 + resp2
resass = resass1 + resass2 sumfluxes = sumflux1 + sumflux2
endif
;------------ Calculate nighttime autotrophic respiration----------------
if assume_resp eq 2 then begin
resp1 = dblarr(ntime)
resp2 = dblarr(ntime)
p1 = dblarr(ntime)
p2 = dblarr(ntime)
co2_1 = dblarr(ntime)
co2_2 = dblarr(ntime)
co2_3 = dblarr(ntime)
F12co2 = dblarr(ntime)
F23co2 = dblarr(ntime)
delta1 = dblarr(ntime)
delta2 = dblarr(ntime)
for i=0,ntime-2 do begin
   p1(i) = (co21[i+1] - co21[i]) / (timeinc/60.)
   p2(i) = (co22[i+1] - co22[i]) / (timeinc/60.)
   resp1[i,0] = Rsoil / 1000.
endfor
p1(ntime-1) = p1(ntime-2)
```

```
p2(ntime-1) = p2(ntime-2)
resp1(ntime-1) = resp1(ntime-2)
co2_1(0)= co21(0)
co2_2(0)= co22(0)
co2_3(0)= co23(0)
for i=0,ntime-2 do begin
   F12co2(i) = K12(i) * (co2_1(i) - co2_2(i)) / ((Z2/2.) * MOLVOL)
   F23co2(i) = K23(i) * (co2_2(i) - co2_3(i)) / (((Z3-Z1)/2.) * MOLVOL)
                              ;--- Use instead Olaf'Eddy flux for
                              ;    F23_co2 !!
if approach eq 2 then begin
   F23co2(i) = co2f26m(i)
endif
co2_1(i+1) = co2_1(i) +  ((resp1(i) - F12co2(i)) * (MOLVOL/H1) * (timeinc/60.))
co2_2(i+1) = co2_2(i) +  ((F12co2(i) - F23co2(i)) * (MOLVOL/H2) * (timeinc/60.))
endfor
co2_1(ntime-1) = co2_1(ntime-2)
co2_2(ntime-1) = co2_2(ntime-2)
F12co2(ntime-1) = F12co2(ntime-2)
F23co2(ntime-1) = F23co2(ntime-2)
delta1(ntime-1) = delta1(ntime-2)
delta2(ntime-1) = delta1(ntime-2)
endif
;;;;;;;;;;;;;;;;;;;;;;;;;;;;;;;;;;;;;;;;;;;;;;;;;;;;;;;;;;;;;;;;;;;;;;;;;;;;;;;
; USE ISOTOPIC MEASUREMENTS
endif else begin
;;;;;;;;;;;;;;;;;;;;;;;;;;;;;;;;;;;;;;;;;;;;;;;;;;;;;;;;;;;;;;;;;;;;;;;;;;;;;;;
; Compute CO18O fluxes
print, ' '
print, 'CALCULATION OF CO18 FLUXES'
F12_o18 = F12_co2 * (o181 - o182) F23_o18 = F23_co2 * (o182 - o183)
;;;;;;;;;;;;;;;;;;;;;;;;;;;;;;;;;;;;;;;;;;;;;;;;;;;;;;;;;;;;;;;;;;;;;;;;;;;;;;;
; CALCULATION OF CI USING C13
;(d13C_cell = d_13C_atm - a - ( b - a ) * Cc / Ca )  [Farquhar , 1982]
print, ' '
print, 'CALCULATION OF CI using C13'
a = EPSDIFF13C
b = EPSCARBOX13C
cis1=dblarr(ntime)
cis2=dblarr(ntime)
cic1=dblarr(ntime)
cic2=dblarr(ntime)
ciw1=dblarr(ntime)
ciw2=dblarr(ntime)
c_sur1=dblarr(ntime)
c_sur2=dblarr(ntime)
eps_leaf1=dblarr(ntime)
eps_leaf2=dblarr(ntime)
for i=0,ntime-2 do begin
    cis1(i)= co21(i) * ( (c131(i) - c13_l1(i) - a) / (b - a) )    ; c in substomatal cavity
; (Ci - Cc) / Ca = 0.12 , Farquhar [1993]
; (in Sternberg [1998]) or =0.2 Lloyd 1992,  c in chloroplast
    cic1(i) = cis1(i) - 0.2 * co21(i)
    cis2(i)= co22(i) * ( (c132(i) - c13_l2(i) - a) / (b - a) )    ; c in substomatal cavity
    cic2(i) = cis2(i) - 0.2 * co22(i)                             ; c in chloroplast
    c_sur1[i]=co21[i]-(0.01*co21[i])                               ; c at leaf surface
    c_sur2[i]=co22[i]-(0.01*co22[i])
    ciw1[i]= cis1[i]-(5./1.e6)                              ; c at mesophyll cell wall surface
    ciw2[i]= cis2[i]-(5./1.e6)
eps_leaf1[i]= EPSLEAF eps_leaf2[i]= EPSLEAF
if calculate_eps_leaf then begin
    eps_leaf1[i]=((co21[i]-c_sur1[i])*5.8 + (c_sur1[i]-ciw1[i])*8.8
                + (ciw1[i] - cic1[i])*0.8)/(co21[i] - cic1[i])
    eps_leaf2[i]=((co22[i]-c_sur2[i])*5.8 + (c_sur2[i]-ciw2[i])*8.8
                + (ciw2[i] - cic2[i])*0.8)/(co22[i] - cic2[i])
endif
endif
endfor
cis1(ntime-1)=cis1(ntime-2)
cis2(ntime-1)=cis2(ntime-2)
cic1(ntime-1)=cic1(ntime-2)
cic2(ntime-1)=cic2(ntime-2)
ciw1(ntime-1)=ciw1(ntime-2)
ciw2(ntime-1)=ciw2(ntime-2)
c_sur1(ntime-1)=c_sur1(ntime-2)
c_sur2(ntime-1)=c_sur2(ntime-2)
```

```
eps_leaf1(ntime-1)=eps_leaf1(ntime-2)
eps_leaf2(ntime-1)=eps_leaf2(ntime-2)
if calculate_eps_leaf then begin
    eps_leaf1=eps_leaf1*(-1.)
    eps_leaf2=eps_leaf2*(-1.)
endif
cica1 = cic1 / co21
cica2 = cic2 / co22
;;;;;;;;;;;;;;;;;;;;;;;;;;;;;;;;;;;;;;;;;;;;;;;;;;;;;;;;;;;;;;;;;;;;;;;;;;;;;;;;
; CALCULATION OF O18 OF WATER POOLS
; method : craig_gordon (sstate or dynamic), or an average from all data...
print, ' '
print, 'CALCULATION OF O18 OF WATER POOLS...'
if use_craig then begin
print, ' '
print, '...via GRAIG & GORDON EQUATION'
eps_li_va1 = dblarr(ntime)
for i=0,ntime-2 do begin
 eps_li_va1 = ((-7356 / (temp1 + 273.15)) + 15.38) * (-1)  ; [Majoube, 1971]
 eps_li_va2 = ((-7356 / (temp2 + 273.15)) + 15.38) * (-1)
 ;o18vap1(i) = -20
 ;o18vap2(i) = -20
endfor
 eps_li_va1(ntime-1) = eps_li_va1(ntime-2)
 eps_li_va2(ntime-1) = eps_li_va2(ntime-2)
 o18wat2_l1 = eps_li_va1 + (1 - rh1) * (o18wat_s - EPSDIFF) + (rh1 * o18vap1)
 o18wat2_l2 = eps_li_va2 + (1 - rh2) * (o18wat_stem - EPSDIFF) + (rh2 * o18vap2)
    ;o18wat2_l1 = compute_o18wat(o18bio)
    ;o18wat2_l2 = compute_o18wat(o18bio)
endif else begin
print, ' '
print, '...via MEASURED DATA'
    o18wat2_l1 = o18wat_l1
    o18wat2_l2 = o18wat_l2
endelse
;;;;;;;;;;;;;;;;;;;;;;;;;;;;;;;;;;;;;;;;;;;;;;;;;;;;;;;;;;;;;;;;;;;;;;;;;;;;;;
; CALCULATION OF DISCRIMINATIONS
print, ' '
print, 'CALCULATION OF DISCRIMINATIONS'
          ;--- Brenninkmeijer equilibration and conversion SMOW to PDB
o18equ_l1 = (16909./( temp1 + 273.15)) - 56.98 + o18wat2_l1
o18equ_l2 = (16909./( temp2 + 273.15)) - 56.98 + o18wat2_l2
o18equ_s = (16909./(soil_temp + 273.15))- 56.98 + o18wat_s
o18equ_stem = (16909./(stem_temp + 273.15))- 56.98 + o18wat_stem
;disc_l1 = - epsleaf + (cic1/(co21 - cic1)) * (o18equ_l1 - o181)
;disc_l2 = - epsleaf + (cic2/(co22 - cic2)) * (o18equ_l2 - o182)
;non complete isotopic equilibrium between leaf water and CO2 [Gillon, Yakir, 2001]
disc_l1 = - epsleaf + (cic1/(co21 - cic1))*((teta * (o18equ_l1 - o181))
-(((1-teta)*(- epsleaf))/((cic1/(co21 - cic1))+1)))
disc_l2 = - epsleaf + (cic2/(co22 - cic2))*((teta * (o18equ_l2 - o182))
-(((1-teta)*(- epsleaf))/((cic2/(co22 - cic2))+1)))
disc_s1 = soil_p * (epssoil + (o18equ_s - o181))
+ auto_p * (epsstem + (o18equ_stem - o181)) disc_s2 = epsstem + (o18equ_stem - o182)
;;;;;;;;;;;;;;;;;;;;;;;;;;;;;;;;;;;;;;;;;;;;;;;;;;;;;;;;;;;;;;;;;;;;;;;;;;;;;;
; SOLVING FOR THE CO2 FLUXES
print, ' '
print, 'SOLVING FOR CO2 FLUXES'
;-- Compute the time derivatives
p1 = dblarr(ntime)
p2 = dblarr(ntime)
ap1 = dblarr(ntime)
ap2 = dblarr(ntime)
pp1 = dblarr(ntime)
pp2 = dblarr(ntime)
q1 = dblarr(ntime)
q2 = dblarr(ntime)
qq1 = dblarr(ntime)
qq2 = dblarr(ntime)
assim1 = dblarr(ntime)
assim2 = dblarr(ntime)
a ss1 = dblarr(ntime)
ass2 = dblarr(ntime)
resp1 = dblarr(ntime)
```

```
resp2 = dblarr(ntime)
for i=0,ntime-2 do begin
    pp1(i) = (co21[i+1] - co21[i]) / (timeinc/60.)
    pp2(i) = (co22[i+1] - co22[i]) / (timeinc/60.)
    qq1(i) = (o181[i+1] - o181[i]) / (timeinc/60.)
    qq2(i) = (o182[i+1] - o182[i]) / (timeinc/60.)
endfor
pp1(ntime-1) = pp1(ntime-2)
pp2(ntime-1) = pp2(ntime-2)
qq1(ntime-1) = qq1(ntime-2)
qq2(ntime-1) = qq2(ntime-2)
;-- Compute the "known" terms
p1 = pp1 * H1/MOLVOL + F12_co2
p2 = pp2 * H2/MOLVOL - F12_co2 + F23_co2
q1 = qq1 * co21 * H1/MOLVOL + F12_o18
q2 = qq2 * co22 * H2/MOLVOL - F12_o18 + F23_o18
;-- Compute fluxes from substitutions
grad1 = dblarr(ntime)
grad2 = dblarr(ntime)
resass1 = dblarr(ntime)
resass2 = dblarr(ntime)
resass = dblarr(ntime)
sumflux1 = dblarr(ntime)
sumflux2 = dblarr(ntime)
sumflux = dblarr(ntime)
assim = dblarr(ntime)
resp = dblarr(ntime)
totflux = dblarr(ntime)
disc_s1 = dblarr(ntime)
disc_s2 = dblarr(ntime)
eps_soil = dblarr(ntime)
disc_l1 = dblarr(ntime)
disc_l2 = dblarr(ntime)
for i=0, ntime-2 do begin
;;;;;;;;;;;;;;;;;;;;;;;;;;;;;;;;;;;;;;;;;;;;;;;;;;;;;;;;;;;;;;;;;;;;;;;;;;;;
;  day and night- differences in respective discriminations driven by PAR
if par(i) le par_thresh then begin
;---leaf discrimination night-time
    disc_l1[i] = - eps_leaf1[i] - (o18equ_l1[i] - o181[i])
    disc_l2[i] = - eps_leaf2[i] - (o18equ_l2[i] - o182[i])
endif
if par(i) ge par_thresh then begin
;---leaf discrimination day-time
    disc_l1(i) = (- eps_leaf1[i] + (cic1(i)/(co21(i) - cic1(i))) * (o18equ_l1(i) - o181(i)))
    disc_l2(i) = (- eps_leaf2[i] + (cic2(i)/(co22(i) - cic2(i))) * (o18equ_l2(i) - o182(i)))
;non complete isotopic equilibrium between leaf water and CO2 [Gillon, Yakir, 2001]
disc_l1(i) = - eps_leaf1(i) + (cic1(i)/(co21(i) - cic1(i)))*((teta * (o18equ_l1(i) - o181(i)))-
(((1-teta)* (- eps_leaf1(i)))/((cic1(i)/(co21(i) - cic1(i)))+1)))
disc_l2(i) = - eps_leaf2(i) + (cic2(i)/(co22(i) - cic2(i)))*((teta * (o18equ_l2(i) - o182(i)))-
(((1-teta)* (- eps_leaf1(i)))/((cic2(i)/(co22(i) - cic2(i)))+1)))
endif
;;;;;;;;;;;;;;;;;;;;;;;;;;;;;;;;;;;;;;;;;;;;;;;;;;;;;;;;;;;;;;;;;;;;;;
; What will be the disc_s1, day and night ?
; 1: zero
; disc_s1(i) = 0
; 2: full equilibrium with soil/leaf water
; disc_s1(i) = o18equ_s(i) - o181(i)
; 3: soil and stem distributed, classic
disc_s1(i) = soil_p * (epssoil + (o18equ_s(i) - o181(i))) + auto_p
* (epsstem + (o18equ_stem(i) - o181(i)))
;-------------------------------- and box 2 disc_s2(i) = (epsstem + (o18equ_stem(i) - o182(i)))
;;;;;;;;;;;;;;;;;;;;;;;;;;;;;;;;;;;;;;;;;;;;;;;;;;;;;;;;;;;;;;;;;;;;;;
;-- day time scenario: get assim and resp, calculate disc_s1 (EPSSOIL)
;-----------box1
assim1(i) = (q1(i) - (p1(i) * disc_s1(i))) / (disc_l1(i) + disc_s1(i))
resp1(i) = assim1(i) + p1(i)
grad1(i) = pp1(i) * (H1/MOLVOL)
assim1(i) = -assim1(i)
;-----------box2
assim2(i) = (q2(i) - (p2(i) * disc_s2(i))) / (disc_l2(i) + disc_s2(i))
resp2(i) = assim2(i) + p2(i)
grad2(i) = pp2(i) * (H2/MOLVOL)
assim2(i) = -assim2(i)
```

```
;-----------------------------------------------------------------------
;-- night-time scenario: assim eq zero , get resp and disc_s1 (EPSSOIL)
if assim_night then begin
 if i eq 0 then begin
print, ' '
print, 'SETTING ASSIMILATION TO ZERO DURING NIGHT'
print, '...AND GET EPSSOIL'
 endif
   if par(i) le par_thresh then begin
;-----------box1
;disc_s1(i) = q1(i) / p1(i)
resp1(i) = p1(i)
grad1(i) = pp1(i) * (H1/MOLVOL)
assim1(i) = 0.
;eps_soil(i) = ((disc_s1(i) - auto_p * (epsstem + (o18equ_stem(i)
- o181(i))))/soil_p) - (o18equ_s(i) - o181(i))
;-----------box2
;disc_s2(i) = q2(i) / p2(i)
resp2(i) = p2(i)
grad2(i) = pp2(i) * (H2/MOLVOL)
assim2(i) = 0.
   endif
endif
;-- end night-time scenario
;-----------------------------------------------------------------------
resass1(i) = assim1(i) + resp1(i)
sumflux1(i) =  assim1(i) + resp1(i) - F12_co2(i) - grad1(i)
resass2(i) = assim2(i) + resp2(i)
sumflux2(i) = assim2(i) + resp2(i) + F12_co2(i) - F23_co2(i) - grad2(i)
assim(i) = assim1(i) + assim2(i)
resp(i) = resp1(i) + resp2(i)
resass(i) = resass1(i) + resass2(i)
totflux(i) = resass1(i) + resass2(i) - grad1(i) - grad2(i)
disc_s1(i)=disc_s1(i) disc_s2(i)=disc_s2(i)
endfor
grad1(ntime-1) = grad1(ntime-2)
grad2(ntime-1) = grad2(ntime-2)
resass1(ntime-1) = resass1(ntime-2)
resass2(ntime-1) = resass2(ntime-2)
resass(ntime-1) = resass(ntime-2)
sumflux1(ntime-1) = sumflux1(ntime-2)
sumflux2(ntime-1) = sumflux2(ntime-2)
sumflux(ntime-1) = sumflux(ntime-2)
assim(ntime-1) = assim(ntime-2)
assim1(ntime-1) = assim1(ntime-2)
assim2(ntime-1) = assim2(ntime-2)
resp(ntime-1) = resp(ntime-2)
resp1(ntime-1) = resp1(ntime-2)
resp2(ntime-1) = resp2(ntime-2)
totflux(ntime-1) = totflux(ntime-2)
disc_s1(ntime-1) = disc_s1(ntime-2)
disc_s2(ntime-1) = disc_s2(ntime-2)
eps_soil(ntime-1) = eps_soil(ntime-2)
disc_l1(ntime-1) = disc_l1(ntime-2)
disc_l2(ntime-1) = disc_l2(ntime-2)
iso_assim1=-assim1*disc_l1 iso_assim2=-assim2*disc_l2
iso_resp1=resp1*disc_s1 iso_resp2=resp2*disc_s2
iso_assim=iso_assim1+iso_assim2 iso_resp=iso_resp1+iso_resp2
iso_net=iso_assim+iso_resp
endelse ; END solving for the co2 fluxes
;;;;;;;;;;;;;;;;;;;;;;;;;;;;;;;;;;;;;;;;;;;;;;;;;;;;;;;;;;;;;;;;;;;;;;;;;;;;;;;;;;;;;;;;;
;-----------compute cumulated fluxes cum_assim=dblarr(ntime)
cum_assim1=dblarr(ntime)
cum_assim2=dblarr(ntime)
cum_ass=dblarr(ntime)
cum_ass1=dblarr(ntime)
cum_ass2=dblarr(ntime)
cum_resp=dblarr(ntime)
cum_resp1=dblarr(ntime)
cum_resp2=dblarr(ntime)
cum_resass=dblarr(ntime)
cum_co2f26m=dblarr(ntime)
cum_f23_co2=dblarr(ntime)
cum_eddy_assim=dblarr(ntime)
cum_eddy_resp=dblarr(ntime)
cum_assim(0)= 0
```

```
cum_assim1(0)= 0
cum_assim2(0)= 0
cum_ass(0)= 0
cum_ass1(0)=0
cum_ass2(0)= 0
cum_resp(0)= 0
cum_resp1(0)= 0
cum_resp2(0)= 0
cum_resass(0)=0
cum_co2f26m(0)=0
cum_f23_co2(0)=0
cum_eddy_assim(0)=0
cum_eddy_resp(0)=0
for i=1,ntime-2 do begin
    cum_assim(i) = cum_assim(i-1) + assim(i)
    cum_assim1(i) = cum_assim1(i-1) + assim1(i)
    cum_assim2(i) = cum_assim2(i-1) + assim2(i)
    cum_resp(i) = cum_resp(i-1) + resp(i)
    cum_resp1(i) = cum_resp1(i-1) + resp1(i)
    cum_resp2(i) = cum_resp2(i-1) + resp2(i)
    cum_resass(i) = cum_resass(i-1) + resass(i)
    cum_co2f26m(i) = cum_co2f26m(i-1) + co2f26m(i)
    cum_f23_co2(i) = cum_f23_co2(i-1) + f23_co2(i)
    cum_eddy_assim(i) = cum_eddy_assim(i-1) + eddy_assim(i)
    cum_eddy_resp(i) = cum_eddy_resp(i-1) + eddy_resp(i)
endfor
cum_assim(ntime-1) = cum_assim(ntime-2)
cum_assim = cum_assim * (timeinc/60.)
cum_assim1(ntime-1) = cum_assim1(ntime-2)
cum_assim1 = cum_assim1 * (timeinc/60.)
cum_assim2(ntime-1) = cum_assim2(ntime-2)
cum_assim2 = cum_assim2 * (timeinc/60.)
cum_ass(ntime-1) = cum_assim(ntime-2)
cum_ass = cum_ass * (timeinc/60.)
cum_ass1(ntime-1) = cum_ass1(ntime-2)
cum_ass1 = cum_ass1 * (timeinc/60.)
cum_ass2(ntime-1) = cum_ass2(ntime-2)
cum_ass2 = cum_ass2 * (timeinc/60.)
cum_resp(ntime-1) = cum_resp(ntime-2)
cum_resp = cum_resp * (timeinc/60.)
cum_resp1(ntime-1) = cum_resp1(ntime-2)
cum_resp1 = cum_resp1 * (timeinc/60.)
cum_resp2(ntime-1) = cum_resp2(ntime-2)
cum_resp2 = cum_resp2 * (timeinc/60.)
cum_resass(ntime-1) = cum_resass(ntime-2)
cum_resass = cum_resass * (timeinc/60.)
cum_co2f26m(ntime-1) = cum_co2f26m(ntime-2)
cum_co2f26m = cum_co2f26m * (timeinc/60.)
cum_f23_co2(ntime-1) = cum_f23_co2(ntime-2)
cum_f23_co2 = cum_f23_co2 * (timeinc/60.)
cum_eddy_assim = cum_eddy_assim * (timeinc/60.)
cum_eddy_assim(ntime-1) = cum_eddy_assim(ntime-2)
cum_eddy_resp = cum_eddy_resp * (timeinc/60.)
cum_eddy_resp(ntime-1) = cum_eddy_resp(ntime-2)
; END solving for the co2 fluxes
;;;;;;;;;;;;;;;;;;;;;;;;;;;;;;;;;;;;;;;;;;;;;;;;;;;;;;;;;;;;;;;;;;;;;;;;;;;;;;;;;;;;;;;;;;;;;;;
;endelse
;;;;;;;;;;;;;;;;;;;;;;;;;;;;;;;;;;;;;;;;;;;;;;;;;;;;;;;;;;;;;;;;;;;;;;;;;;;;;;;;;;;;;;;;;;;;;;;
; CONVERSION OF UNITS
; co2: mol co2 / mol air to ppm
co21 = co21* 1.e6
co22 = co22 * 1.e6
co23 = co23 * 1.e6
co21_o = co21_o * 1.e6
co22_o = co22_o * 1.e6
co21lic_o = co21lic_o * 1.e6
co22lic_o = co22lic_o * 1.e6
if meanboxes then begin
    p0_2m = p0_2m *1.e6
    p1m = p1m * 1.e6
    p2m = p2m * 1.e6
    p4_8m = p4_8m * 1.e6
    p10_8m = p10_8m *1.e6
    p15_6m = p15_6m * 1.e6
    p25_2m = p25_2m * 1.e6
    co21_meanprofile = co21_meanprofile * 1.e6
    co22_meanprofile = co22_meanprofile * 1.e6
endif if only_conc eq 2 then begin
```

```
    cic1 = cic1 * 1.e6
    cic2 = cic2 * 1.e6
    cis1 = cis1 * 1.e6
    cis2 = cis2 * 1.e6
    ciw1 = ciw1 * 1.e6
    ciw2 = ciw2 * 1.e6
    c_sur1 = c_sur1 *1.e6
    c_sur2 = c_sur2 *1.e6
endif if only_conc eq 1 and assume_resp eq 2 then begin
    co2_1 = co2_1 * 1.e6
    co2_2 = co2_2 * 1.e6
endif
; fluxes in mümol m-2s-1
assim1=assim1*(1.e6/3600)
assim2=assim2*(1.e6/3600)
resp1=resp1*(1.e6/3600)
resp2=resp2*(1.e6/3600)
assim=assim*(1.e6/3600)
resp=resp*(1.e6/3600)
co2f26m=co2f26m*(1.e6/3600)
f12_co2=f12_co2*(1.e6/3600)
f23_co2=f23_co2*(1.e6/3600)
eddy_assim=eddy_assim*(1.e6/3600)
eddy_resp=eddy_resp*(1.e6/3600)
totflux=totflux*(1.e6/3600)
; END CONVERSION OF UNITS
;;;;;;;;;;;;;;;;;;;;;;;;;;;;;;;;;;;;;;;;;;;;;;;;;;;;;;;;;;;;;;;;;;;;;;;;;;;
;;;;;;;;;;;;;;;;;;;;;;;;;;;;;;;;;;;;;;;;;;;;;;;;;;;;;;;;;;;;;;;;;;;;;;;;;;;
; PLOTTING AND SAVING
print, ' '
print, 'PLOT times series'
;-- Plot of the co2 biospheric fluxes
;-- Save variables in an column files for other process..
ccg_closedev,dev=dev
; END plotting
;;;;;;;;;;;;;;;;;;;;;;;;;;;;;;;;;;;;;;;;;;;;;;;;;;;;;;;;;;;;;;;;;;;;;;;;;;;;
;;;;;;;;;;;;;;;;;;;;;;;;;;;;;;;;;;;;;;;;;;;;;;;;;;;;;;;;;;;;;;;;;;;;;;;;;;;;
; SAVING all desired data into a column file (define them into the
; var_out string array..
if file_save then begin
 file_out = 'fluxes.txt'
print, ' '
print, 'SAVE DATA TO FILE: '+file_out+' ...'
print, ' ' print, '...AND PRAY TO GOD !!! '
var_out = ['co21_o','co21','co22_o','co22','co23','c131','c132','o181','o182','o183',$
'rn1_o','rn1','rn2_o','rn2','rn3','f12_rn','k12','k23','soil_temp','temp1',$
'temp2','par','H20_conc','o18vap1','o18vap2','o18wat_s','o18wat_stem','o18wat_l1', 'o18wat_l2',$
'c13_l1','c13_l2','o18equ_s','o18equ_stem','o18equ_l1','o18equ_l2','disc_s1', 'disc_s2',$
'disc_l1','disc_l2','cica1','cica2','eps_leaf1','eps_leaf2', 'f12_co2','co2f26m','assim1','resp1',$
'resass1','assim2','resp2','resass2','assim','resp','eddy_assim','eddy_resp','cum_assim',$
'cum_eddy_assim','cum_assim1','cum_assim2','cum_resp', 'cum_eddy_resp','cum_resp1',$
'cum_resp2','cum_f23_co2','cum_co2f26m']
nn = n_elements(var_out) openw,u,file_out,/get_lun,width=10000
spawn,'chmod 777 '+file_out
dd = fltarr(ntime)
printf,u,['date','year','month','day','hour','min',var_out] for
nt=0,ntime-1 do begin
    ccg_dec2date,date(nt),year,month,day,hour,min
    xx = auto_string(date(nt),4)
    xx = [xx, auto_string([year,month,day,hour,min],0) ]
    dd(nt)= (day - 29) * 24 + hour
    for k=0,nn-1 do begin
        res = execute( 'temp =   ' +var_out(k) )
        xx = [xx, auto_string(temp(nt),2) ]
    endfor
    printf,u,xx
endfor free_lun,u
endif
; END SAVING data
;;;;;;;;;;;;;;;;;;;;;;;;;;;;;;;;;;;;;;;;;;;;;;;;;;;;;;;;;;;;;;;;;;;;;;;;;;;;;
!P.MULTI=[0,2,2]
stop END
;;;;;;;;;;;;;;;;;;;;;;;;;;;;;;;;;;;;;;;;;;;;;;;;;;;;;;;;;;;;;;;;;;;;;;;;;;;;;
;;;;;;;;;;;;;;;;;;;;;;;;;;;;;;;;;;;;;;;;;;;;;;;;;;;;;;;;;;;;;;;;;;;;;;;;;;;;;
; End of MAIN program
;;;;;;;;;;;;;;;;;;;;;;;;;;;;;;;;;;;;;;;;;;;;;;;;;;;;;;;;;;;;;;;;;;;;;;;;;;;;;
;;;;;;;;;;;;;;;;;;;;;;;;;;;;;;;;;;;;;;;;;;;;;;;;;;;;;;;;;;;;;;;;;;;;;;;;;;;;;
```

List of Figures

List of Tables

Bibliography

[Allison *et al.*, 1995] Allison, C. E., Francey, R. J. and Meijer, H. A., *Recommandations for the reporting of stable isotope measurements of carbon and oxygen in CO_2 gas*, in *References and Intercomparison Materials for Stable isotopes of Light Elements* (Edited by IAEA-TECDOC-825), pp. 155–162, Vienna, Int. At. Energy Agency, 1995.

[Amthor and Baldocchi, 1998] Amthor, J. S. and Baldocchi, D. D., *Terrestrial higher-plant respiration and net primary production*, in *Terresrial global productivity: past, present and future* (Edited by J. Roy, H. A. Mooney and B. Saugier), San Diego, Academic Press, CA, 1998.

[Andres *et al.*, 1999] Andres, R. J., Marland, G. and Bischof, S., Global and latitudinal estimates of δ^{13}C from fossil-fuel consumption and cement manufacture, Carbon Dioxide Information Center, Oak Ridge National Labaratory, Oak Ridge, Tenn., USA, 1999.

[Andres *et al.*, 1993] Andres, R. J., Marland, G., Boden, T. and Bishoff, S., Carbon dioxide emissions from fossil fuel combustion and cement manufacture 1751-1991 and an estimate of their isotopic composition and latitudinal distribution, Cambridge University Press, New York, 1993.

[Baldocchi *et al.*, 1988] Baldocchi, D., Hicks, B. and Meyers, T., *Measuring biosphere-atmosphere exchanges of biologically related gases with micrometeorological methods*, Ecology, 69, 1331–1340, 1988.

[Ball, 1987] Ball, J. T., *Calculations related to gas exchange*, in *Stomatal Function* (Edited by E. Zeiger, G. D. Farquhar and I. R. Cowan), pp. 445–476, Stanford University Press, Stanford, California, 1987.

[Bariac *et al.*, 1994a] Bariac, T., Gonzalez-Dunia, J., Katerji, N., Béthenod, O., Bertolini, J. M. and Mariotti, A., *Variabilité spatialle de la composition isotopique de l'eau (^{18}O, ^{2}H) dans le continuum sol-plante-atmosphère : 2. approche en conditions naturelles*, Chemical Geology (Isotope Geoscience Section), 115, 317–333, 1994a.

[Bariac *et al.*, 1994b] Bariac, T., Gonzalez-Dunia, J., Tessier, D. and Mariotti, A., *Variabilité spatialle de la composition isotopique de l'eau (^{18}O, ^{2}H) au sein des organes des plantes aériennes : 1. approche en conditions controlées*, Chemical Geology (Isotope Geoscience Section), 15, 307–315, 1994b.

[Bariac *et al.*, 1990] Bariac, T., Jusserand, C. and Mariotti, A., *Evolution spatio-temporelle de la composition isotopique de l'eau dans le continuum sol-plante-atmosphere*, Geochimica et Cosmochimica Acta, 54, 413–424, 1990.

[Battle *et al.*, 2000] Battle, M., Bender, M. L., Tans, P. P., White, J. W. C., Ellis, J. T., Conway, T. and Francey, R. J., *Global carbon sinks and their variability inferred from atmospheric O−2 and $\delta^{13}C$* , Science, 287, 2467–2470, 2000.

[Boaz *et al.*, 1999] Boaz, L., Barkan, E., Bender, M. L., Thiemens, M. H. and Boering, K. A., *Triple-isotopic composition of atmospheric oxygen as a tracer of biospheric productivity*, Nature, 400, 547–550, 1999.

[Boden *et al.*, 1994] Boden, T. A., Kaiser, D. P., Sepanski, R. J. and Stoss, F. W., *Trends'93: A Compendium of Data on Global Change*, CDIAC Oak Ridge ESD publication, 4 195, 1994.

[Boone *et al.*, 1998] Boone, R. D., Nadelhoffer, K. J., Canary, J. D. and Kaye, J. P., *Roots excert a strong influence on the temperature sensitivity of soil respiration*, Nature, 396, 570–572, 1998.

[Bowling *et al.*, 1999] Bowling, D. R., Baldocchi, D. D. and Monson, R. K., *Partitioning net ecosystem exchange in a Tennesse deciduous forest using stable isotopes of CO_2*, Poster presentation, Annual Meeting of the Ecological Society of America, 1999.

[Brenninkmeijer *et al.*, 1983] Brenninkmeijer, C. A. M., Kraft, P. and Mook, W. G., *Oxygen isotope fractionation between CO_2 and H_2O*, Isotope Geoscience, 1, 181–190, 1983.

[Bräunlich, 1996] Bräunlich, M., *Gas chromatographic measurements of atmospheric nitrous oxide in Heidelberg ambient air*, Diploma Thesis, (in German), Institut für Umweltphysik, University of Heidelberg, 1996.

[Buchmann *et al.*, 1998a] Buchmann, N., Brooks, J. R., Flanagan, L. B. and Ehleringer, J. R., *Carbon isotope discrimination of terrestrial ecosystems*, in *Stable Isotopes: integration of biological ecological and geochemical processes* (Edited by H. Griffiths), pp. 203–221, βIOS Scientific Publisher Limited, 1998a.

[Buchmann and Ehleringer, 1998] Buchmann, N. and Ehleringer, J. R., *CO_2 concentration profiles and carbon and oxygen isotopes in C3 and C4 crop canopies*, Agric. For. Meteorol, 89, 45–58, 1998.

[Chen and Black, 1992] Chen, J. M. and Black, T. A., *Defining leaf area index for non-flat leaves*, Plan Cell Environment, 15, 412–429, 1992.

[Ciais *et al.*, 1997a] Ciais, P., Denning, A. S., Tans, P. P., Berry, J. A., Randall, D. A., Collatz, G. J., Sellers, P. J., White, J. W. C., Trolier, M., Meijer, H. A. J., Francey, R. J., Monfray, P. and Heimann, M., *A three dimensional synthesis study of $\delta^{18}O$ in atmospheric CO_2, Part I: Surface fluxes*, J. Geophys. Res., 102, 5 857–5 872, 1997a.

[Ciais *et al.*, 1999] Ciais, P., Friedlingstein, P., Schimel, D. S. and Tans, P. P., *A global calculation of the $\delta^{13}C$ of soil respired carbon: Implications for the biospheric uptake of anthropogenic CO_2*, Global Biogeoch. Cycl., 13, 519–530, 1999.

[Ciais and Meijer, 1998] Ciais, P. and Meijer, H. A. J., *The $^{18}O/^{16}O$ isotope ratio and its role in global carbon cycle research*, in *Stable Isotopes: integration of biological ecological and geochemical processes* (Edited by H. Griffiths), pp. 409–431, βIOS Scientific Publisher Limited, 1998.

[Ciais *et al.*, 1997b] Ciais, P., Tans, P. P., Denning, A. S., Francey, R. J., Trolier, M., Meijer, H. J., White, J. W. C., Berry, J. A., Randall, D. A., Collatz, J. J. G., Sellers, P. J., Monfray, P. and Heimann, M., *A three dimensional synthesis study of $\delta^{18}O$ in atmospheric CO_2, Part II: Simulations with the TM2 transport model*, J. Geophys. Res., 102, 5 873–5 883, 1997b.

[Ciais *et al.*, 1995a] Ciais, P., Tans, P. P., Trolier, M., White, J. W. and Francey, R., *A large Northern Hemisphere terrestrial CO_2 sink indicated by the $^{13}C/^{12}C$ ratio of atmospheric CO_2*, Science, 269, 1 098–1 102, 1995a.

[Ciais *et al.*, 1995b] Ciais, P., Tans, P. P., White, W. C., Trolier, M., Francey, R. J., Berry, J. A., Randall, D. R., Sellers, P. J., Collatz, F. G. and Schimel, D. S., *Partitioning of ocean and land uptake of CO_2 as inferred by $\delta^{13}C$ measurements from the NOAA Climate Monitoring and Diagnostics Laboratory Global Air Sampling*, J. Geophys. Res., 100, 5 051–5 070, 1995b.

[Conway *et al.*, 1994] Conway, T. J., Tans, P. P., Waterman, L. S., Thoning, K. W., Kitzis, D. R., Masarie, K. A. and Zhang, N., *Evidence for interannual variability of the carbon cycle from the National Oceanic and Atmospheric Administration/Climate Monitoring and Diagnostics Laboratory Global Air Sampling Network*, J. Geophys. Res., 99, no. D11, 22 831–22 855, 1994.

[Craig, 1953] Craig, H., *Carbon-13 in plants and the relationships between carbon-13 and carbon-14 vaiations in nature*, The Journal of Geology, 62, 115–149, 1953.

[Craig, 1957] Craig, H., *Isotopic standards for carbon and oxygen and correction factors for mass-spectrometric analysis of carbon dioxide*, Geochimica et Cosmochimica Acta, 12, 133–149, 1957.

[Craig and Gordon, 1965] Craig, H. and Gordon, L. I., Deuterium and oxygen-18 variations in the Ocean and the Marine Atmosphere, Cons. Naz. delle Ric., Lab. di Geol. Nucl., Tries, Italy, 1965.

[Cuntz *et al.*, 2001] Cuntz, M., Ciais, P. and Hoffmann, G., *Modelling the continental effect of oxygen isotopes over Eurasia*, submitted to Tellus, 2001.

[Deacon, 1977] Deacon, E. L., *Gas transfer to and across an air-water interface*, Tellus, 29, 363–374, 1977.

[DKR, 1994] DKR, T. R., Modellbetreuungsgruppe: The ECHAM3 atmospheric general circulation model, Tech. Rep. 6 (ISSN 0940-9327), Deutsches Klimarechenzentrum, Hamburg, 1994.

[Dörr, 1984] Dörr, H., *The study of the gas- and waterbudgets in unsaturated soils via CO_2- and ^{222}Radon measurements*, Dissertation, (in German), Institut für Umweltphysik, University of Heidelberg, 1984.

[Dörr and Münnich, 1980] Dörr, H. and Münnich, K. O., *Carbon-14 and carbon-13 in soil CO_2*, Radiocarbon, 22, 909–918, 1980.

[Dörr and Münnich, 1987] Dörr, H. and Münnich, K. O., *Annual variation in soil respiration in selected areas of the temperature zone*, Tellus, 39, no. B, 114–121, 1987.

[Dörr and Münnich, 1990] Dörr, H. and Münnich, K. O., *^{222}Rn flux and soil air concentration profiles in West-Germany. Soil ^{222}Rn as a tracer for gas transport in the unsaturated soil zone*, Tellus, 42, no. B, 20–28, 1990.

[Edwards *et al.*, 1980] Edwards, N. T., Shugart, H. H., McLaughlin, S. B., Harris, W. F. and Reichle, D. E., *Carbon metabolism in terrestrial ecosystems*, in *Dynamic properties of forest ecosystems* (Edited by D. E. Reichle), pp. 499–536, Camebridge University Press, 1980.

[Enting, 1987] Enting, I. G., *The interannual variations in the seasonal cycle of carbon dioxide concentration at Mauna Loa*, J. Geophys. Res., 92D, 5497–5504, 1987.

[Enting *et al.*, 1995] Enting, I. G., Trudinger, C. M. and Francey, R. J., *A synthesis inversion on the concentration and $\delta^{13}C$ of atmospheric CO_2*, Tellus, 47B, 35–52, 1995.

[Etheridge *et al.*, 1996] Etheridge, D. M., Steele, L. P., Langenfels, R. L., Francey, R. J., Barnola, J.-M. and Morgan, V., *Natural and anthropogenic changes in atmospheric CO_2 over the last 1000 years from air in Antarctic ice and firn*, J. Geophys. Res., 101D, 4115–4128, 1996.

[Etling, 1996] Etling, D., Theoretische Meteorologie, F. Vieweg & Sohn Verlagsgesellschaft mbH, Braunschweig Wiesbaden, 1996.

[Farquhar, 1983] Farquhar, G. D., *On the nature of carbon isotope discrimination in C4 species*, Australian Journal of Plant Physiology, 10, 205–226, 1983.

[Farquhar *et al.*, 1989] Farquhar, G. D., Hubick, K. T., Condon, A. G. and Richards, R. A., *Carbon isotope fractionation and plant water-use efficiency*, in *Stable Isotopes in Ecological Research* (Edited by P. Rundel), Springer-Verlag, New York, 1989.

[Farquhar and Lloyd, 1993] Farquhar, G. D. and Lloyd, J., *Carbon and oxygen isotope effects in the exchange of carbon dioxide between plants and the atmosphere*, in *Stable Isotopes and Plant Carbon-Water Relations* (Edited by J. R. Ehleringer, A. E. Hall and G. D. Farquhar), pp. 47–70, Academic Press, Inc., San Diego, California, 1993.

[Farquhar *et al.*, 1993a] Farquhar, G. D., Lloyd, J., Taylor, J. A., Flanagan, L. B., Syvertsen, J. P., Hubick, K. T., Wong, S. C. and Ehleringer, J. R., *Vegetation effects on the isotope composition of oxygen in atmospheric CO_2*, Nature, 363, 439–443, 1993a.

[Farquhar *et al.*, 1982] Farquhar, G. D., O'Leary, M. H. and Berry, J. A., *On the relationship between carbon isotope discrimination and the intercellular carbon dioxide concentration in leaves*, Australian Journal of Plant Physiology, 9, 121–137, 1982.

[Farquhar and Rashke, 1978] Farquhar, G. D. and Rashke, K., *On the resistance to transpiration of the sites of evoparation within the leaf*, Plant Physiology, 61, 1000–1005, 1978.

[Farquhar *et al.*, 1980] Farquhar, G. D., von Caemmener, S. and Berry, J. A., *A Biochemical model of photosynthesis CO_2 fixation in leaves of C_3 species*, Planta, 149, 78–90, 1980.

[Fischer *et al.*, 1999] Fischer, H., Wahlen, M., Smith, J., Matroanni, D. and Deck, B., *Ice core records of atmospheric CO_2 around the last three glacial terminations*, Science, 283, 1712–1714, 1999.

[Fischer, 1976] Fischer, K., *A slow-pulse ionisation chamber for the measurement of Radon in the air*, Diploma Thesis, (in German), Institut für Umweltphysik, University of Heidelberg, 1976.

[Francey *et al.*, 1999] Francey, R. J., Allison, C. E., Etheridge, D. M., Trudinger, C. M., Enting, I. G., Leuenberger, M., Langenfels, R. L., Michel, E. and Steele, L. P., *A 1000-year high precision record of $\delta^{13}C$ in atmospheric CO_2* , Tellus, 51-B, 170–193, 1999.

[Francey *et al.*, 1990] Francey, R. J., Robbins, F. J., Allison, C. E. and Richards, N. G., *The CSIRO global survey of CO_2 stable isotopes*, in *Baseline Atmospheric Research Program (Australia) 1988* (Edited by S. R. Wilson and G. P. Ayers), Ayers, Department of Administrative Services/Bureau of Meteorology and CSIRO Division of Atmospheric Research, 1990.

[Francey and Tans, 1987] Francey, R. J. and Tans, P., *Latitudinal variation in oxygen-18 of atmospheric CO_2*, Nature, 327, 495–497, 1987.

[Francey *et al.*, 1995] Francey, R. J., Tans, P., Allison, C. E., Enting, I. G., White, J. W. C. and Trolier, M., *Changes in oceanic and terrestrial carbon uptake since 1982*, Nature, 373, 326–330, 1995.

[Förstel *et al.*, 1975] Förstel, H., Putral, A., Schleser, G. and Leith, H., *The world pattern of oxygen-18 in rain water and its importance in understanding the biogeochemical oxygen cycle*, in *Isotope Ratios as Pollutant Source and Behavier Indicators*, pp. 323–344, Int. At. Energy Agency, Vienna, 1975.

[Gamo *et al.*, 1989] Gamo, T., Tsutsumi, M., Sakai, H., Nakazawa, T., Tanaka, M., Honda, H., Kubo, H. and Itoh, T., *Carbon and oxygen isotopic ratios of carbon dioxide of stratospheric profiles over Japan*, Tellus, 41, no. B, 127–133, 1989.

[Gemery *et al.*, 1996] Gemery, P. A., Trolier, M. and White, J. W. C., *Oxygen isotope exchange between carbon dioxide and water following atmospheric sampling using glass flasks*, JGR, 101, 14415–14420, 1996.

[Gillon and Yakir, 2000] Gillon, J. S. and Yakir, D., *Internal Conductance to CO_2 diffusion and $C^{18}OO$ discrimination in C3 leaves*, Plant Physiology, 123, 201–213, 2000.

[Gillon and Yakir, 2001] Gillon, J. S. and Yakir, D., *Influence of carbonic anhydrase activity in terrestrial vegetation on the ^{18}O content of atmospheric CO_2*, SCI, 291, 2584–2587, 2001.

[Gonfiantini *et al.*, 1995] Gonfiantini, R., Stichler, W. and Rozanski, K., *Standards and intercomparison materials distributed by the International Atomic Energy Agency for stable isotope measurements*, in *References and Intercomparison Materials for Stable isotopes of Light Elements* (Edited by IAEA-TECDOC-825), pp. 13–29, Vienna, Int. At. Energy Agency, 1995.

[Greschner, 1995] Greschner, B., *Gaschromatographic measurement of atmospheric carbon dioxide, methane and nitrous oxide in Heidelberg* , Thesis, (in German), Institut für Umweltphysik, University of Heidelberg, 1995.

[Gulledge and Schimel, 2000] Gulledge, J. and Schimel, J. P., *Controls on soil carbon dioxide and methane fluxes in a variety of taiga forest stands in interior Alaska*, Ecosystems, 3, 269–282, 2000.

[Heimann, 1997] Heimann, M., *a review of the contemporary global carbon cycle and as seen a century ago by Arrhenius and Högbom*, Ambio, 26, no. 1, 17–24, 1997.

[Heimann, 2000] Heimann, M., *The Role of the Land Biosphere in the Global Carbon Cycle*, IPCC 2000, TAR, draft, presented within a talk held at the NEBROC special training course on "The Global Carbon Cycle: Present, Past and Future", Bremen, September 14-16, 2000.

[Heimann *et al.*, 1989b] Heimann, M., Keeling, C. D. and Tucker, C. J., *A three-dimentional model of atmospheric CO_2 transport based on observed winds: 3. Seasonal cycle and synoptic time-scale variations*, in *Aspects of climate variability in the Pacific and the Western Americas, Geophysical monograph 55* (Edited by D. H. Peterson), pp. 277–303, AGU, 1989b.

[Houghton *et al.*, 1996] Houghton, J. T., Filho, L. G. M., Callander, B. A., Harris, N., Kattenberg, A. and Maskell, K., Climate Change 1995: The Science of Climate Change, Intergovernmental Panel on Climate Change, Cambridge, UK, 1996.

[Hubbard *et al.*, 1995] Hubbard, R. M., Ryan, M. G. and Lukens, D. L., *A simple, battry operated, temperature-controlled cuvette for respiration measurements*, Tree Physiology, 15, 175–179, 1995.

[IAEA/WMO, 1998] IAEA/WMO, *Global Network for Isotopes in Precipitation*, The GNIP Database, Release 3, October 1999, no. URL: http://www.iaea.org/programs/ri/gnip/gnipmain.htm, 1998.

[Idso and Kimball, 1993] Idso, S. B. and Kimball, B. A., *Tree growth in carbon dioxide enriched air and its implications for the global carbon cycling and maximum levels of CO_2*, Global Biogeoch. Cycl., 7, 537–555, 1993.

[IPCC, 2001] IPCC, W. G. I., *Intergovernmental Panel of Climate Change, Climate Change 2001: The Scientific Basis*, http://www.ipcc.ch, 2001.

[Jacob, 1982] Jacob, H., *Deuterium and oxygen-18 in water vapour, precipitation and leaf water*, Diploma Thesis, (in German), Institut für Umweltphysik, University of Heidelberg, 1982.

[Jähne *et al.*, 1987] Jähne, B., Heinz, G. and Dietrich, W., *Measurement of the diffusion coeficients of sparingly soluble gases in water*, J. Geophys. Res., 92, 10 767–10 776, 1987.

[Jouzel *et al.*, 1993] Jouzel, J., Barkov, N., Barnola, J.-M., Bender, M., Chappellaz, J., Genthon, C., Kotlyakov, V., Lipenkov, V., Lorius, C., Petit, J. R., Raynaud, D., Raisbeck, G., Ritz, C., Sowers, T., Stievenard, M., Yiou, F. and Yiou, P., *Extending the Vostok ice-core record of paleoclimate to the penultimate glacial period*, Nature, 364, 407–412, 1993.

[Kays, 1966] Kays, W. M., Convective heat and mass transfer, McGraw-Hill, New York, USA, 1966.

[Keeling, 1958] Keeling, C. D., *The concentration and isotopic abundances of atmospheric carbon dioxide in rural areas*, Geochimica et Cosmochimica Acta, 13, 322–334, 1958.

[Keeling, 1961] Keeling, C. D., *The concentration and isotopic abundances of atmospheric carbon dioxide in rural and marine air* , Geochimica et Cosmochimica Acta, 24, 277–298, 1961.

[Keeling *et al.*, 1989] Keeling, C. D., Bacastow, R. B., Carter, A. F., Piper, S. C., Whorf, T. P., Heimann, M., Mook, W. G. and Roeloffzen, H., *A three-dimensional model of atmospheric CO_2 transport based on observed winds, 1. Analysis on observational data*, in *Aspects of Climate Variability in the Pacific and the Western Americas, Geophys. Monogr. Ser.* (Edited by D. H. Peterson), vol. 55, pp. 165–236, American Geophysical Union, Washington, D.C., 1989.

[Keeling *et al.*, 1996] Keeling, C. D., Chin, J. F. S. and Whorf, T. P., *Increased activity of northern vegetation inferred from atmospheric CO_2 measurements*, Nature, 382, 146–149, 1996.

[Keeling and Whorf, 2000] Keeling, C. D. and Whorf, T., *Atmospheric CO_2 records from sites in the SIO air sampling network*, in *Trends: A compendium of data of global change*, Carbon Dioxide Information Center, Oak Ridge National Labaratory, U.S. Department of Energy, Oak Ridge, Tenn., USA, 2000.

[Keeling *et al.*, 1995] Keeling, C. D., Whorf, T. P., Wahlen, M. and van der Plicht, J., *Interannual extremes in the rate of rise of atmospheric carbon dioxide since 1980*, Nature, 375, 666–670, 1995.

[Kromer, 1995] Kromer, S., *Respiration during photosynthesis*, Annual Review Plant Physioliology, Plant Molecular Biology, 46, 45–70, 1995.

[Langendörfer *et al.*, 2001] Langendörfer, U., Ciais, P., Cuntz, M., Peylin, P., Bariac, T., Milukova, I., Kolle, O. and Levin, I., *Modeling of biospheric CO_2 gross fluxes via oxygen isotopes in a spruce forest canopy: a ^{222}Radon calibrated box model approach*, submitted to Tellus, 2001.

[Lawlor, 1990] Lawlor, D. W., Photosynthesis: Metabolism, Control and Physiology, Longman Group UK Limited, London, UK, 1990.

[Levin *et al.*, 2001] Levin, I., Born, M., Cuntz, M., Langendörfer, U., Mantsch, S., Naegler, T., Schmidt, M., Varlagin, A., Verclas, S. and Wagenbach, D., *Observation of atmospheric variability and soil exhalation rate of ^{222}Radon at a Russian forest site: Technical approach and deployment for boundary layer studies*, submitted to Tellus, 2001.

[Levin *et al.*, 1995] Levin, I., Graul, R. and Trivett, N. B. A., *Long-term observations of atmospheric CO_2 and carbon isotopes at continental sites in Germany*, Tellus, 47B, 23–34, 1995.

[Lin and Ehleringer, 1997] Lin, G. and Ehleringer, J. R., *Carbon isotopic fractionation does not occur during dark respiration in C3 and C4 plants*, Plant Physiology, 114, 391–394, 1997.

[Lloyd *et al.*, 1996] Lloyd, J., Kruijt, B., Hollinger, D. Y., Grace, J., Francey, R. J., Wong, S. C., Kelliher, F. M., Miranda, A. C., Farquhar, G. D., Gash, J. H. C., Vygodskaya, N. N., Wright, I. R., Miranda, H. S. and Schulze, E. D., *Vegetation Effects on the Isotopic Composition of Atmospheric CO_2 at Local and Regional Scales: Theoretical Aspects and a Comparison between Rain Forest in Amazonia and a Boreal Forest in Siberia*, Australian Journal of Plant Physiology, 23, 371–399, 1996.

[Lloyd *et al.*, 1992] Lloyd, J., Syrversten, J. P., Kiedemann, P. E. and Farquhar, G. D., *Low conductance for CO_2 diffusion from stomata to the sites of carboxylation in leaves of woody species*, Plant Cell Env., 15, 873–899, 1992.

[Lloyd and Taylor, 1994] Lloyd, J. and Taylor, J. A., *On the temperature dependance of soil respiration*, Functional Ecology, 8, 315–323, 1994.

[Majoube, 1971] Majoube, M., *Fractionnement en oxygene-18 et en deuterium entre l'eau et sa vapeur*, Journal de Chimie et Physique, 58, 1 423–1 436, 1971.

[Manning, 1993] Manning, M. R., *Seasonal cycles in atmospheric CO_2 concentrations*, in *The global carbon cycle* (Edited by M. Heimann), pp. 65–94, Springer-Verlag, Heidelberg, 1993.

[Marland and Boden, 1997] Marland, G. and Boden, T. A., *Global, regional and national CO_2 emissions*, in *Trends: A compendium of data of global change*, Carbon Dioxide Information Center, Oak Ridge National Labaratory, Oak Ridge, Tenn., USA, 1997.

[Mauersberger, 1981] Mauersberger, K., *Measurement of heavy ozone in the stratosphere*, Geophysical Research Letters, 8, 935–937, 1981.

[Merlivat, 1978] Merlivat, L., *Molecular diffusivities of $H_2^{18}O$ in gases*, J. Chem. Phys., 69, 2864–2871, 1978.

[Merlivat and Jouzel, 1979] Merlivat, L. and Jouzel, J., *Global climatic interpretation of the deuterium–oxygen 18 relationship for precipitation*, Journal of Geophysical Research, 84, 5 029–5 033, 1979.

[Miller *et al.*, 1999] Miller, J. B., Yakir, D., White, J. W. C. and Tans, P. P., *Measurement of $^{18}O/^{16}O$ in the soil-atmosphere CO_2 flux*, Global Biogeoch. Cycl., 13, 761–774, 1999.

[Milukova *et al.*, 2001] Milukova, I., Kolle, O. *et al.*, *Eddy covariance measurements at the Fyodorovskoje - Forest*, submitted to Tellus, 2001.

[Monin and Obukov, 1954] Monin, A. and Obukov, A., *Dimensionless Characteristics of Turbulence in the Surface Layer*, Akad. Nauk. SSSR, Geofiz. Inst., 24, 1954.

[Mook, 1994] Mook, W. G., Principles of isotope hydrology, Intoductory course on Isotope Hydrology, Department of Hydrogeology and Geographical Hydrology, VU Amsterdam, 1994.

[Mook *et al.*, 1974] Mook, W. G., Bommerson, J. C. and Stavermann, W. H., *Carbon isotope fractionation between dissolved bicarbonate and gaseous carbon dioxide*, Earth and Planetary Science letters, 22, 169–176, 1974.

[Mook *et al.*, 1983] Mook, W. G., Koopmans, M., Carter, A. F. and Keeling, C. D., *Seasonal, latitudinal and secular variations in the abundance and isotopic ratios of atmospheric carbon dioxide. 1. Results from land stations* , JGR, 88, no. C15, 10915–10933, 1983.

[Naegler, 1999] Naegler, T., *Set-up and characterisation of an IR-CO_2monitoring system for the determination of biospheric CO_2 variabilities*, Diploma Thesis, (in German), Institut für Umweltphysik, University of Heidelberg, 1999.

[Naegler *et al.*, 2001] Naegler, T., Kolle, O., Milukova, I., Varlagin, A. and Levin, I., *Comparison of methods to measure nocturnal respirative CO_2 fluxes in a boreal forest in Western Russia*, submitted to Tellus, 2001.

[Nakazawa *et al.*, 1997] Nakazawa, T., Morimoto, S., Aoki, S. and Tanaka, S., *Temporal and spatial variations of the carbon isotopic ratio of atmospheric carbon dioxide in the western Pacific region*, J. Geophys. Res., 102, 1 271–1 285, 1997.

[Neubert, 1998] Neubert, R., *Measurements of the stable isotopomeres of atmospheric carbon dioxide*, Ph.D. Thesis, (in German), Institut für Umweltphysik, University of Heidelberg, 1998.

[Nützmann, 1999] Nützmann, E., *Modeling of the turbulent exchange between the Prandtl-layer and a forest canopy*, Ph.D. Thesis, (in German), University of Göttingen, 1999.

[O'Leary, 1984] O'Leary, M. H., *Measurement of the isotopic fractionation associated with diffusion of carbon dioxide in aqueous solution*, Journal of Physical Chemistry, 88, 823–825, 1984.

[O'Leary, 1993] O'Leary, M. H., *Biochemical Basis of Carbon Isotope Fractionation*, in *Stable Isotopes and Plant Carbon-Water Relations* (Edited by J. R. Ehleringer, A. E. Hall and G. D. Farquhar), pp. 19–26, Academic Press, Inc., San Diego, California, 1993.

[Panofsky and Dutton, 1984] Panofsky, H. A. and Dutton, J. A., Atmospheric Turbulence, Models and Methods for Engineering Applications, J. Wiley, New York, USA, 1984.

[Petit *et al.*, 1999] Petit, J. R., Jouzel, J., Raynaud, D., Barkov, N. I., Barnola, J.-M., Basile, I., Bender, M., Chappellaz, J., Davis, M., Delaygue, G., Delmotte, M., Kotlyakov, V. M., Legrand, M., Lipenkov, V. Y., Loius, C., Pépin, L., Ritz, C., Salzman, E. and Stievenard, M., *Climate and atmospheric history of the past 420,000 years from the Vostok ice core, Antarctica*, Nature, 399, 429–436, 1999.

[Peylin *et al.*, 1999] Peylin, P., Ciais, P., Denning, A. S., Tans, P. P., Berry, J. A. and White, W. C., *A three-dimensional study of $\delta^{18}O$ in atmospheric CO_2: contributin of different land ecosystems*, Tellus, 51, no. B, 642–667, 1999.

[Ramonet *et al.*, 2001] Ramonet, M., Nepomniachii, I., Picard, D., Kazan, V., Kolle, O., Lloyd, J., Sidorov, K. and Ciais, P., *Seasonal and diurnal variability of trace gases above the Fyodorovskoye site - derived from intensive airborne campaigns.*, submitted to Tellus, 2001.

[Raupach *et al.*, 1992] Raupach, M. R., Denmead, T. O. and Dunin, F. X., *Challenges in linking atmospheric CO_2 concentrations to fluxes at local and regional scales*, Australian Journal of Botany, 40, 697–716, 1992.

[Raven and Glidewell, 1981] Raven, J. A. and Glidewell, S. M., *Processes Limiting Photosynthetic Conductance*, chap. Physiological Processes Limiting Plant Productivity, pp. 109–136, Butterworths, London, England, 1981.

[Reich *et al.*, 1991] Reich, J. W., Rastetter, E. B., Melillo, D. W., Kicklighter, D. W., Steudler, P. A., Peterson, B. J., Grace, A. L., Moore, B. and Vorosmarty, C. J., *Potential net primary production in South Africa*, Ecological Applications, 1, 399–429, 1991.

[Reich and Schlesinger, 1992] Reich, J. W. and Schlesinger, W. H., *The global carbon dioxide flux in soil respiration and its relationship to vegetation and climate*, Tellus, 44B, 81–99, 1992.

[Roedel, 1994] Roedel, W., Physik unserer Umwelt: Die Atmosphäre, Springer-Verlag, Berlin Heidelberg New York, 1994.

[Ryan *et al.*, 1997] Ryan, M. G., Lavigne, M. and Gower, S. T., *Annual carbon cost of autotrophic respiration in boeal forest ecosystems in relation to species and climate*, J. Geophys. Res., 102, 28871–28884, 1997.

[Ryan *et al.*, 1994] Ryan, M. G., Lindner, S., Vose, J. M. and Hubbard, R. M., *Dark respiration in pines*, in *Pine ecosystems* (Edited by H. L. Gholz, S. Lindner and R. E. McMurtrie), pp. 50–63, Uppsala, Ecological Bullitins, 1994.

[Schüßler *et al.*, 2000] Schüßler, W., Neubert, R., Levin, I., Fischer, N. and Sonntag, C., *Determination of microbial versus root-produced CO_2 in an agricultural ecosystem by means of $\delta^{13}C$ CO_2 measurements in soil air*, Tellus, 59B, 909–918, 2000.

[Schmidt, 1999] Schmidt, M., *Measurement and balancing anthropogenic greenhousegases in Germany*, Ph.D. Thesis, (in German), Institut für Umweltphysik, University of Heidelberg, 1999.

[Schmidt *et al.*, 2001] Schmidt, M., Neubert, R., Weller, R. and Levin, I., *Variability of CO_2 mixing ratio and its stable isotope ratios at the Schauinsland (Germany) and Neumayer (Antarctica) station*, in preparation, 2001.

[Schulze *et al.*, 1999] Schulze, E.-D., Lloyd, J., Kelliher, F. M., Wirth, C., Rebmann, C., Lühker, B., Mund, M., Knohl, A., Milyukova, I. M., Schulze, W., Ziegler, W., Varlagin, A. B., Sogachev, A. F., Valentini, R., Dore, S., Grigoriev, S., Kolle, O., Panfyorov, M. I., Tchebakova, T. and Vygodskaya, N. N., *Productivity of forests in the Eurosiberian boreal region and their potential to act as a carbon sink - a synthesis*, Global Biogeoch. Cycl., 5, 703–722, 1999.

[Schulze *et al.*, 2000] Schulze, E.-D., Wirth, C. and Heimann, M., *Managing forests after Kyoto*, Science, 289, 2058–2059, 2000.

[Sonntag *et al.*, 1983] Sonntag, C., Münnich, K. O., Jacob, H. and Rozanski, K., *Variations of deuterium and oxygen-18 in continental precipitation and groundwater, and their causes*, in *Variations in the global water budget* (Edited by L. A. Street-Perrot, M. Beran and R. Ratcliffe), pp. 107–124, Reidel, Dordecht, 1983.

[Staufer, 1999] Staufer, B., *Cornucopia of ice core results*, Nature, 399, 412–413, 1999.

[Stryer, 1981] Stryer, L., Biochemistry, W. H. Freeman and Co, San Francisco, 1981.

[Stull, 1988] Stull, R. B., An introduction to boundary-layer meteorology, Kluver Academic Publishers, Dordrecht, 1988.

[Tans, 1998] Tans, P. P., *Oxygen isotopic equilibrium between carbon dioxide and water in soils*, Tellus, 50B, 163–178, 1998.

[Thiemens *et al.*, 1995] Thiemens, M. H., Jackson, T., Zipf, E. C., Erdmann, P. W. and van Egmond, C., *Carbon dioxide and oxygen isotope anomalies in the mesosphere and stratosphere*, Science, 270, 969–972, 1995.

[Thom, 1975] Thom, A. S., *Momentum, mass and heat exchange of vegetation*, in *Vegetation and the atmosphere* (Edited by J. L. Monteith), pp. 57–109, Academic Press, London, 1975.

[Thoning *et al.*, 1989] Thoning, K. W., Tans, P. and Komhyr, W. D., *Atmospheric carbon dioxide at Mauna Loa observatory, 2, Analysis of the NOAA/CMDL data, 1974-1985*, J. Geophys. Res., 94, 8549–8565, 1989.

[Trolier *et al.*, 1996] Trolier, M., White, J. W. C., Tans, P. P., Masarie, K. A. and Gemery, P. A., *Monitoring the isotopic composition of atmospheric CO_2: Measurements from the NOAA global air sampling network*, J. Geophys. Res., 101, 25,897–25,916, 1996.

[Trudinger *et al.*, 1999] Trudinger, C. M., Enting, I. G., Francey, R. J., Etheridge, D. M. and Rayner, P. J., *Long-term varibility in the global carbon cycle inferred from a high-precision CO_2 and $\delta^{13}C$ ice-core record* , Tellus, 51B, 233–248, 1999.

[Trumbore *et al.*, 1995] Trumbore, S. E., Davidson, E. A., Camargo, P. D., Nepstad, D. C. and Martinelli, L. A., *Below-ground cycling of carbon in forests and pastures of Eastern Amazonia*, Global Biogeoch. Cycl., 9, 515–528, 1995.

[Vogel, 1980] Vogel, J. C., *Fractionation of the carbon isotopes during photosynthesis*, Sitzungsberichte der Heidelberger Akademie der Wissenschaften, Mathematisch-naturwissenschaftliche Klasse, 3. Abhandlung, pp. 111–135, 1980.

[Vogel *et al.*, 1970] Vogel, J. C., Grootes, P. M. and Mook, W. G., *Isotopic fractionation between gaseous and dissolved carbon dioxide*, Z. Phys., 230, 225–238, 1970.

[Waring *et al.*, 1998] Waring, R. H., Landsberg, J. J. and Williams, M., *Net primary production of forests: a constant fraction of gross primary production ?*, Tree Physiology, 18, 129–134, 1998.

[White, 1983] White, J. W. C., The climatic significance of D/H ratios in white pine in the north-eastern united states, Ph.D. thesis, Columbia University, New York, 1983.

[Yakir *et al.*, 1994] Yakir, D., Berry, J. A., Giles, L. and Osmond, C. B., *Isotopic heterogeneity of water in transpiring leaves: Identificatiin of the composition that controls $\delta^{18}O$ of atmospheric CO_2 and O_2*, Oecologia, 123, 297–311, 1994.

[Yakir and Sternberg, 2000] Yakir, D. and Sternberg, L., *The use of stable isotopes to study ecosystem gas exchange*, Oecologia, 123, 297–311, 2000.

[Yung *et al.*, 1991] Yung, Y. L., DeMore, W. B. and Pinto, J. P., *Isotopic exchange between carbon dioxide and ozone via $O(^1D)$ in the stratosphere*, Geophysical Research Letters, 18, 13–16, 1991.

Acknowledgements

At the very end of this thesis I deeply hope, that all the energy transformed during these last years was not only boosting entropy, but also increasing the average information content on the $\delta^{18}O$ puzzle. Or is that equivalent ? Anyway, without the help of numerous humans I would be totally hopeless. Therefore I express my sincere thanks.

First of all to my supervisor PD Dr. Ingeborg Levin, for her skillfull introduction into the carbon cycling science field and the possibility itself to perform these studies in Russia. Her permanent attendance to discuss scientific questions as well as her physical help in the field, sometimes simultaneously, was impressive. Summing up the whole spectrum of minor and major break-downs during this "feasibility" project, her open mind helped a lot to keep things moving.

Prof. Dr. Konrad Mauersberger for taking interest in vegetational CO_2 isotopic processes and for revising my thesis.

The Heidelberg carbon group for their assistance in the lab and the enjoyable atmosphere in between high-grade steel and Zarges boxes. Forgiveness for all the flasks. Tobias Naegler for his excellent co-operation during his diploma thesis within the project and all the rest. Dr. Martina Schmidt, the scientific "factotum" of the Heidelberg lab, for her patient introduction into the mysteries of carbon and radon analyses. Thanks to Christian Poss, retaining control over all the tanks and emitting placidity. And, of course, for his poems. The mass spectrometric experience of Christel Facklam and her energetic help with all these flasks is highly appreciated. Renate Heinz for measuring lots of flasks at the GC and fighting with my cold trap construction. Thanks to Jens "the liver" Bader for being a such pleasant and tranquil office neighbor, Stephan Jutzi for only 480 Mbyte, Werner Salewski, Cora Veidt, Hartwig Schröder and Regina Schmidt for not asking too much in the last weeks and their refreshing company during the mensa-breaks.

The measurements performed in Russia would have been unimaginable without the excellent co-operation and the unconventional assistance of our Russian colleagues throughout the project.

Большое спасибо!

to Prof. Dr. Natalja Vygodskaya, Dr. Igor Nepomniachii, Dr. Andrej Varlagin, Irena Milukova, Dr. Andrej Sogachev, Maxim Panfyorov, Konstantin Sidorov, Daniel Kozlov, Michael Puzachenko and Anatoly "Tolja" Bychkov. Their help spanned the whole range of project related tasks and problems: from endless bilateral custom work, visa issue problems, technical support in the field and scientific discussions, via medical assistance (preventing my fingernail from rotting off, thanks to the instructions of Prof. Dr. Natalja Vygodskaya) to the adequate supply with vodka, buckwheat and more than enough of good mood in Fyodorovskoye.

Many thanks also to all the fellows from the other West-European labs in Jena, Paris, Toulouse and Groningen for their assistance, co-operation and the yummy time in the field: Dr. Olaf Kolle, Karl Kübler, Dr. Pierre Friedlingstein, Dr. Philippe Peylin, David Picard, Dr.

Victor Kazan, Matthias "Blondy" Cuntz, Christine Bourg, Dr. Michel Ramonet, Dr. Rolf Neubert, Dr. Jon Lloyd and Sebastien Lafont.

The close collaboration with the Paris group was very productive. Thanks to Dr. T. Bariac for measuring tons of vegetation samples and the fruitful isotopic discussions during my visits in his lab. The exchange with the modelling group of Dr. Philippe Ciais in Paris substantially fertilised my modelling efforts. For the numerous invitations to their lab and their genial hospitality many thanks to Dr. Philippe Peylin, Matthias "Blondy" Cuntz and Dr. Philippe Ciais. The endless discussions with Blondy on this bloody oxygen enlightened the deep swamp - Blondy, you'll kill that cat! Thank you also for carefully reading the manuscript.

As my life and work at the Institut für Umweltphysik in Heidelberg began prior to my contact with isotopes, I would like to thank my colleagues and friends, who contributed to my scientific mindset and made things hearty at the institute: Dr. Eckhard Lehrer, not only for his exceptional company during my diploma thesis, Dr. Dietmar Wagenbach, for skiing prior to meetings and teaching (meta)physical structures, Dr. Hubertus Fischer, even for reading parts of the manuscript, our princesses Dr. Susanne Preunkert, who actually showed me the very first chromatogram and always took care and Dr. Gisela Winckler, the mistress of Doppelkopf, Dr. Kai Hebestreit, the lucky devil of Doppelkopf, Dr. Rainer Weisshaar, responsible for the olfactive design in our office and Dr. Andi Stanzick, for being an excellent non-intoxicated clown.

Without the maintenance of the creative biotope in our Mannheim "Kolmarer Schule" during the days of our studies, I would maybe still be stuck in the basic problems of quantum mechanics. Therefore I would like to thank my friends Rainer "Leo" Schlachter, Dr. Matthew Zepf, Dr. Claus-Georg Lehr, Dr. Jochen Geib, Dr. Hubert Lampeitl, Martin Rösch and Melvin Alfaro Quesada for the vivid disaster we created.

I deeply appreciate my parents laissez-faire education and their ongoing confidence. There was only a minor outcry after my announcement to start the studies of physics, which was fair enough.

Warm thanks are due to Dorothee Langendörfer, the inventor of the sock coffee-cosy, an invaluable engineering set-up to trudge myself over the morning-coma threshold. But basically thanks for being Dorole, preserving the recreative chaos.